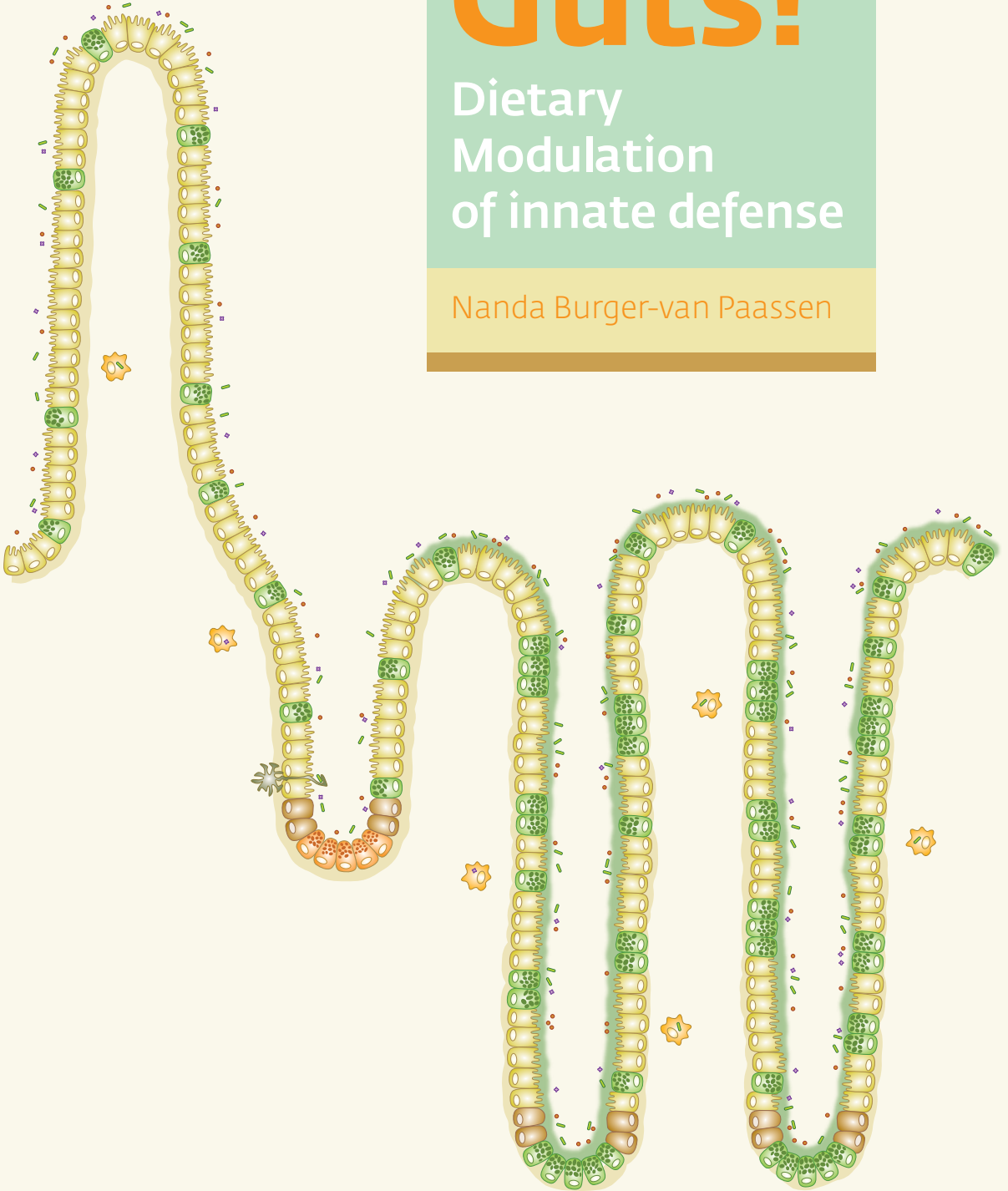


Guts!

Dietary Modulation of innate defense

Nanda Burger-van Paassen



GUTS!

Dietary modulation of innate defense

Nanda Burger-van Paassen

ISBN 978-90-8559-130-6

Printed by: Optima Grafische Communicatie, Rotterdam, The Netherlands

Cover: Ward Mouwen

Part of this study was financially supported by Danone Research, Nederlandse Vereniging voor Gastroenterologie (NVGE) en sectie experimentele gastroenterologie (SEG), Jurriaanse Stichting, Eurotec, Abbott, Sanyo, Nutricia, Nestlé, Yakult.

All rights reserved. No part of this thesis may be reproduced, stored or transmitted in any form, by any means, electronical or mechanical, without prior written permission of the author.

GUTS!

Dietary modulation of innate defense

'GUTS!'

Effect van het dieet op aangeboren afweermechanismen

Proefschrift

ter verkrijging van de graad van doctor
aan de Erasmus Universiteit Rotterdam
op gezag van de rector magnificus
Prof.dr. H.G. Schmidt
en volgens besluit van het College voor Promoties

De openbare verdediging zal plaatsvinden op
woensdag 1 december 2010 om 15:30 uur

door

Nanda van Paassen
geboren te Naaldwijk



PROMOTIECOMMISSIE

Promotoren: Prof.dr. J.B. van Goudoever
Prof.dr. H.J.G. Boehm

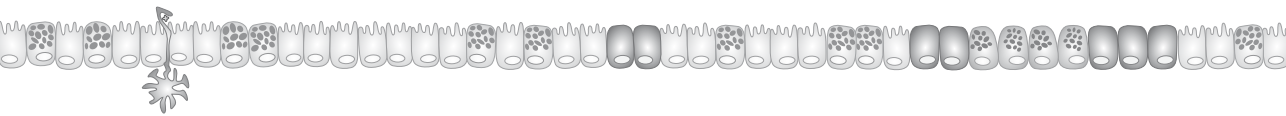
Overige leden: Prof.dr. D. Tibboel
Prof.dr. E.E.S. Nieuwenhuis
Prof.dr. E.H.H.M. Rings

Copromotor: dr. I.B. Renes

Contents

Chapter 1	General Introduction	7
PART I Intestinal epithelial defense mechanisms in early postnatal life		
Chapter 2	Colitis development during the suckling-weaning transition in mucin Muc2-deficient mice	25
Chapter 3	Colonic gene expression patterns of mucin Muc2 knockout mice reveal various phases in colitis development	47
Chapter 4	Absence of the mucin Muc2 leads to increased expression of the bactericidal peptides Reg3 β , Reg3 γ and angiogenin-4	69
Chapter 5	Paneth cell hyperplasia and metaplasia in necrotizing enterocolitis	91
PART II Effect of dietary interventions on intestinal epithelial barrier function		
Chapter 6	Trans-activation of the <i>MUC2</i> promoter by viable and non-viable <i>Lactobacillus</i> GG	111
Chapter 7	The regulation of the intestinal mucin MUC2 expression by short chain fatty acids: implications for epithelial protection.	129
Chapter 8	Dietary influence on colitis-development in Muc2-deficient mice: <i>diet matters!</i>	151
Chapter 9	Intestinal threonine uptake routes for mucin synthesis in preterm pigs and infants	171
PART III Epilogue		
Chapter 10	General discussion	191
Chapter 11	Samenvatting	215
	Dankwoord	225
	Curriculum Vitae	229
	Portfolio	229
	Appendix: Color plates	233

Chapter 1



General Introduction



INTRODUCTION

Necrotizing enterocolitis

Necrotizing enterocolitis (NEC) is the most common gastro-intestinal emergency in the neonatal intensive care. The incidence of NEC ranges from 0.3 to 2.4 infants per 1000 live births, with nearly 70% of cases occurring in infants born at less than 36 weeks of gestation. The incidence of NEC varies, affecting 2-5% of all premature infants.¹ The overall mortality for NEC ranges from 10% to 50%.² Despite optimal medical and surgical management of NEC, infants that recover from the disease suffer from substantial morbidity, such as intestinal obstruction as a consequence of scarring, liver failure due to a prolonged requirement for total parenteral nutrition, short bowel syndrome with intestinal failure and associated nutritional deficiencies, and associated defects in growth and development.³⁻⁴ Length of hospital stay in infants with surgical NEC and medically treated NEC exceeds those of controls by 60 days and 22 days respectively. Based on length of stay, the estimated total hospital charges for infants with surgical NEC in the USA averaged \$186 200 in excess of those for controls and \$73 700 more for infants with medical NEC. The yearly additional hospital charges for NEC were \$216 666 per survivor.⁵ Hence, NEC is a significant and growing health concern for prematurely born infants. The costs in the Netherlands are not exactly known, but will not be very different. As the number of preterm births has almost doubled over the past two decades in the Netherlands (Perinatale Registratie Nederland) and the United States (National Vital Statistics Report 2003), this burden will continue to increase. In addition, recently the national policy has changed into a more liberal approach to the lower limit of viability. More very immature infants (from a gestational age of 24 weeks onwards) will be given a chance to survive, with consequently more risk of developing NEC.

The etiology of NEC is presumed to be multi-factorial and although several potential causes of NEC have been proposed, the only established risk factors are prematurity and a history of enteral feeding.⁶ Associated risk factors are formula feeding⁷⁻⁸, intrauterine growth restriction⁹⁻¹¹, bowel ischemia¹², chorioamnionitis and infection.^{6,13-14} Although the susceptibility to NEC in premature infants is linked to gastrointestinal tract immaturity, the mechanisms whereby these factors cause disease are poorly defined. However, bacterial colonization seems to play a key role in this matter.

NEC and the intestinal microbiota

Thus far, no single microorganism has been identified in cases of NEC. Nevertheless, bacterial colonization in premature infants differs significantly from healthy term subjects. Until recently it was thought that the fetal gut is sterile. However, Mshvildadze et al. showed that meconium contains micro-organisms that are not of postnatal origin.¹⁵ As NEC is not seen during fetal life, postnatal bacterial colonization presumably plays a

role in the disease etiology rather than prenatal colonization. Several determinants can influence colonization patterns in the intestine, for example the mode of delivery, i.e. caesarian section or vaginal delivery.¹⁶ Moreover, the type of feeding, breastfeeding or formula feeding, greatly influences intestinal colonization after birth. In breastfed infants, *Bifidobacterium* is a predominant organism with *Lactobacillus* and *Streptococcus* as minor constituents. In contrast, formula-fed infants develop a more diverse microbiota, consisting of the more pathogenic species *Staphylococcus*, *E. coli*, and *Clostridia*, in addition to *Bifidobacteria*.¹⁷⁻²¹ The intestine of full-term infants is colonized by a large variety of aerobic and anaerobic bacteria at 10 days of age, whereas colonization in premature infants is delayed. In premature infants the number of bacterial species is limited and these species tend to be more virulent compared to full-term infants.²²⁻²³ Moreover, the microbiota shows an increase in abundance of Gamma proteobacteria and a decrease in other bacterial species.²⁴ Common use of broadspectrum antibiotics, increased prevalence of opportunistic pathogens in the hospital environment, instrumentation with nasogastric tubes for feeding and suction catheters to the oropharynx, use of medications such as opioids that delay intestinal transit time and the use of acid neutralizing drugs are all likely to contribute to aberrant bacterial colonization in premature infants. These factors are likely to at least partly explain the difference in vulnerability for developing NEC in premature infants.

Inflammatory bowel diseases and the intestinal microbiota

In adults, inflammatory bowel disease (IBD) consists of Crohn's disease (CD) and ulcerative colitis (UC). Bacteria play an important role in the etiopathogenesis IBD, which is supported by several lines of evidence.²⁵⁻²⁸ First of all, in experimental colitis models, a clear relation between bacterial colonization and the development of colitis has been described, since genetically engineered animal models of IBD, such as Il-10 deficient mice and HLA-B27 transgenic rats, do not develop colitis under germ-free conditions.²⁹⁻³¹ Secondly, the role of luminal bacteria in the pathogenesis of CD is strongly supported by observations showing that clinical symptoms of CD improve when luminal bacterial levels decrease following intestinal washes and antibacterial drug administration.³²⁻³⁴ In addition, postoperative exposure of the terminal ileum to luminal contents is associated with increased inflammation in CD, and diversion of the fecal stream is associated with improvement.³⁵

Intestinal innate defense; the mucin Muc2 and the mucus layer

Defense and tolerance against luminal bacteria are regulated by several factors that collectively constitute the innate immune system, which is defined as: 'The capacity of a normal organism to remain unaffected by microorganisms and their toxins. It results from the presence of naturally occurring anti-infective agents, constitutional factors such as body temperature and immediate acting immune cells such as natural killer cells' (mesh term

PubMed). The innate defense system recognizes pathogens in a non-specific manner, e.g. it responds to pathogens in a generic way, but unlike the adaptive immune system, it does not confer long-lasting or protective immunity to the host. Innate immune systems provide immediate defense against infection, and are found in all classes of plants and animal life. The first line of defense in the intestine is formed by a single layer of epithelial cells, in which several cell types can be distinguished as depicted in Figure 1A. A major component of innate defense in the intestine is the physical barrier that is formed by the intestinal mucus layer, of which the mucin MUC2 is the structural component (Fig. 2). The large MUC2 glycoproteins are secreted into the intestinal lumen by goblet cells (Fig. 1A). Along with small amounts of mucin-associated proteins such as trefoil factor 3 (TFF3), MUC2 polymerizes into a gel of which 80% by weight consists of oligosaccharide side chains, which are added as post-translational modifications to the mucin proteins (Fig. 2). This gel provides an insoluble mucous barrier that protects the intestinal epithelium by trapping bacteria and viruses, which are subsequently expelled by the peristaltic process of the gut, a process called 'non-immune exclusion'. MUC2 is expressed throughout the intestinal epithelium as early as nine weeks of gestation (mRNA), with a developmental switch from a fetal to an adult pattern of MUC2 gene expression at around 23 weeks in the small intestine, and 27 weeks for the colon.³⁶ Post-translational modifications of the MUC2 protein, such as sialylation and glycosylation, contribute to its higher viscosity and acidity.³⁷ A remarkable degree of heterogeneity exists between adult and fetal mucins. In contrast to adult intestinal mucins, the same structures are identified in each part of the fetal intestinal tract and only slight variation in the level of expression of certain glycans is observed.³⁸ This suggests that region-specific glycosylation of intestinal mucins is acquired after birth and likely depends on environmental factors such as nutrition and bacterial colonization. Moreover, significant differences in acidic mucin composition from primarily sulfated to an increase in sialylated sugars at d 4 posthatch were observed in conventionally reared chicks³⁹, again suggesting a role for postnatal bacterial colonization of the intestine. These findings suggest that immature mucins might limit intestinal barrier function in premature neonates. However, further studies are needed to confirm this.

Van der Sluis et al. previously showed that *Muc2* knockout mice (*Muc2*^{-/-}) spontaneously develop clinical and histological signs of colitis.⁴⁰ In humans, decreased numbers of goblet cells and a diminished mucus layer have been related to NEC⁴¹ and IBD.⁴²⁻⁴⁴ The role of an intact intestinal mucus layer is schematically depicted in Figure 1B. Johansson et al⁴⁵ demonstrated that the mouse colonic mucus consists of two layers: the inner layer is densely packed, firmly attached to the epithelium, and devoid of bacteria. In contrast, the outer layer is movable, has an expanded volume due to proteolytic cleavages of the *Muc2* mucin, and is colonized by bacteria (Fig. 1A, B and C). Absence of a protective mucus layer in *Muc2*^{-/-} mice allows direct contact between bacteria/bacterial products with the epithelial cells, causing inflammation. Culture dependent studies of the bacte-

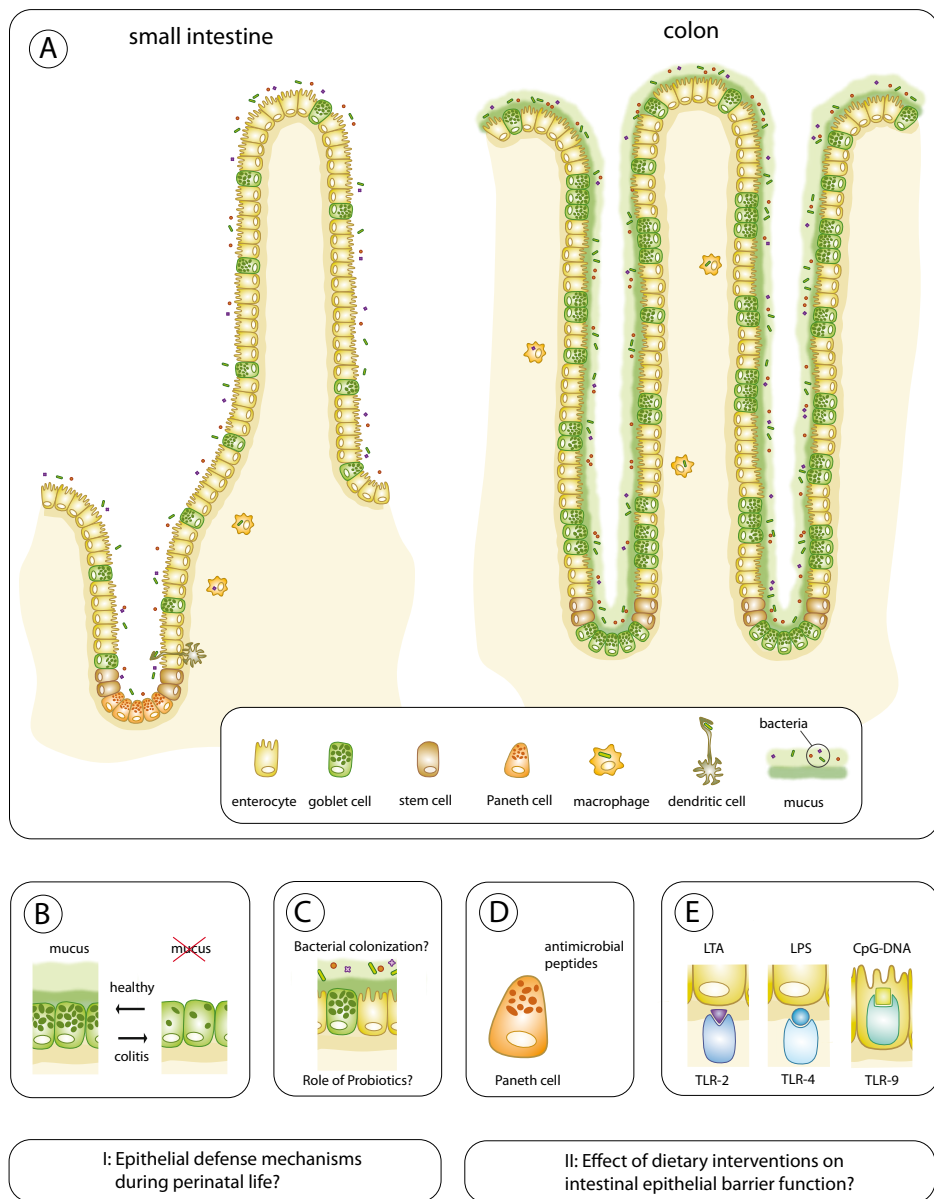


Figure 1. Schematic overview of the small intestinal and colonic epithelium

A schematic overview of a small intestinal left crypt-villus unit (left) and colonic crypts (left) is depicted in (A). (B) The intestinal mucus layer consists of a firm inner layer (dark green) that is devoid of bacteria and a loose outer layer (light green) that contains bacteria. A decreased mucus layer or absence of a functional mucus layer has been related to intestinal diseases i.e. human IBD and NEC and *Muc2*^{-/-} mice. (C) Bacterial colonization and probiotics seem to play an important role in the development, prevention and treatment of IBD and NEC. (D) Antimicrobial peptides are mainly produced in Paneth cells and stored in Paneth cell granules. (E) Detection of intestinal bacteria is mediated via TLRs, such as TLR2 and TLR4 which are located at the basolateral side of enterocytes and TLR9 which is located intra-cellularly.

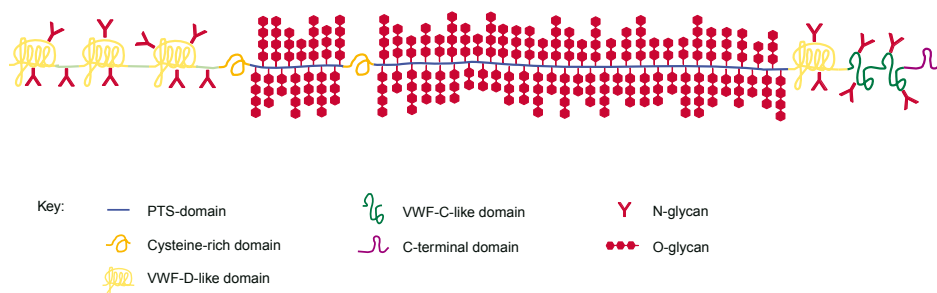


Figure 2. Schematic representation of a MUC2 molecule (adapted from Dekker et al.⁷⁹)

rial populations in the mouse gut have indicated about 10^9 bacteria/g of tissue in the stomach and a gradient of bacterial density along the gut, with numbers changing from 10^7 bacteria/g of tissue in the small intestine to 10^{11} to 10^{12} bacteria/g of tissue in the cecum and colon.⁴⁶⁻⁴⁷

Innate defense; antimicrobial peptides and Toll like receptors

Besides the intestinal mucus layer, an important part of innate defense is formed by a large group of antimicrobial peptides (also called host defense peptides) that function as potent, broad spectrum antibiotics with the ability to kill bacteria and other micro-organisms. Most of the antimicrobial peptides, i.e. lysozyme⁴⁸⁻⁴⁹, secretory phospholipase-A2 (sPLA2)⁵⁰, and human α -defensins (HD5 and -6)⁵¹⁻⁵² are secreted by Paneth cells that are located at the bottom of small intestinal crypt epithelium (Fig. 1A and D). Some antimicrobial proteins such as most α -defensins are expressed constitutively and do not require bacterial signals for their expression.⁵³ However, expression of a subset of antimicrobial proteins is controlled by the recognition of microbe associated molecular patterns by pattern recognition receptors, such as Toll-like receptors (TLRs), NOD1 and NOD2, that are expressed by the epithelial cells.⁵⁴ For example, expression of the antimicrobial C-type lectin regenerating islet-derived protein 3 γ (Reg3 γ), also called HIP/PAP, is up-regulated in the small intestine and colon after bacterial reconstitution of germ-free mice⁵⁵⁻⁵⁶ and expression of angiogenin-4 (Ang4), the orthologue of human ANG, is induced upon colonization with *Bacteroides thetaiotaomicron*, an anaerobe Gram-negative microbe that belongs to the normal mouse and human microbiota.⁵⁷ Furthermore, in conventionally raised mice the expression of Reg3 γ and Ang4 increases substantially after weaning⁵⁶⁻⁵⁷, when the complexity of the microbiota increases as well as the diet and during experimental intestinal infection with *Salmonella* and *Listeria monocytogenes*.⁵⁸⁻⁶⁰ Expression of antimicrobial peptides might be related to specific inhabitants of the microbiota as germ-free mice that were colonized with *Bacteroides thetaiotaomicron* show increased Reg3 γ expression, whereas Reg3 γ expression was lowered by the subsequent introduction of *Bifidobacterium longum*.⁶¹ Therefore, alterations

in the intestinal microbiota are presumably influencing the expression of antimicrobial peptides. On the other hand, antimicrobial peptides also shape the intestinal microbiota suggesting cross-talk between the intestinal microbiota and antimicrobial peptides.

Detection of bacteria in the intestine is mediated by Toll-like receptors (TLRs) (Fig. 1E), which are a family of pattern recognition receptors (PRR). Following bacterial recognition, Toll-like receptors recruit and activate a variety of signal transducing adaptor proteins such as MyD88 that induces Reg3 γ and cytokine expression.⁵⁸ Cytokines are mainly produced by T-cells. Intestinal epithelial cells acquire tolerance following bacterial colonization, presumably to permit colonization without chronic inflammation.⁶² However, aberrant expression levels of TLRs have been related to decreased tolerance and the onset of disease. For example, TLR4 is known to be upregulated in Crohn's disease (CD) and ulcerative colitis (UC) and the expression of TLR4 and TLR2 is upregulated in lamina propria macrophages as well as intestinal epithelial cells in IBD patients.⁶³⁻⁶⁵ Moreover, TLR expression plays a role in the development of NEC. For example, murine and human NEC are associated with increased intestinal TLR2 and TLR4 expression and decreased TLR9 expression.⁶⁶⁻⁶⁸ Additionally, enteral administration of adenovirus expressing mutant TLR4 to neonatal mice reduced the severity of NEC and increased TLR9 expression within the intestine and TLR9 activation with CpG-DNA significantly reduced NEC severity.⁶⁶ On the other hand TLR9-deficient mice exhibited increased NEC severity. Interestingly, Jilling et al showed that TLR mRNA expression is influenced by the type of feeding, i.e. TLR4 mRNA gradually decreases in human milk-fed rats, but increases in rats that were formula-fed during NEC-development.⁶⁹ Together these studies indicate that TLRs play a role in NEC and that modulation of TLR expression, for example by the type of feeding, influences disease severity.

Dietary modulation of innate defense: therapeutic potential for IBD and NEC

Bacterial colonization can be influenced by the diet and thereby forms a promising target for disease treatment and prevention. For example, prebiotics, which are defined as non-digestible food ingredients mostly of a carbohydrate base that improve human health, selectively stimulate the growth and/or activity of existing bacteria in the colon.⁷⁰ Moreover, a Western diet compared to a standard low-fat, plant polysaccharide-rich diet produced a significant increase in adiposity.⁷¹ Mice colonized with a microbiota from the obese Western diet-fed humanized donors gained significantly more weight during the 2 weeks after transplantation than did mice colonized with the humanized microbiota from standard low-fat, plant polysaccharide-rich diet-fed donors, indicating that the microbiota significantly differ between the two dietary groups and subsequently affect the development of adiposity. Strikingly, community composition is dramatically altered over a time scale of hours when animals are switched from mouse chow to a Western diet,

indicating that dietary interventions might have rapid potential in modulating disease processes. As mentioned previously, the microbiota of human milk fed versus formula fed neonates is significantly different. Furthermore, formula fed infants are at increased risk for the development of NEC. Therefore, dietary adaptations and supplementations are suggested to play an important role in the treatment of a variety of diseases including IBD and NEC.

Probiotics and NEC prevention

Probiotics, described as live microbial dietary supplements which beneficially affect the host animal by improving its intestinal microbial balance⁷², seem to form a promising treatment or preventative therapy in this respect. In humans, lactobacilli, *Bifidobacteria* and *Streptococci* are commonly used as probiotics, either as single species or in mixed culture with other bacteria. Numerous randomized, controlled trials (RCTs) have been performed to study the effect of probiotics on prevention of NEC in premature infants. A recent meta-analysis of all these RCTs indicates lower all-cause mortality and necrotizing enterocolitis and shorter time to full feeds after probiotic supplementation in preterm (<34 weeks' gestation) very low birth weight (VLBW; birth weight <1500 g) neonates.⁷³ Issues such as the number of infants studied per strain, dosage, timing of initiation, and long-term safety, however, necessitate more studies before a general conclusion on the use of various probiotics can be made, especially for European neonatal intensive care units, where NEC incidence is relatively low.⁷⁴ Probiotics may prevent NEC by promoting colonization of the gut with beneficial organisms, preventing colonization by pathogens, improving the maturity and function of gut mucosal barrier, and modulating the immune system (e.g., TLR4 receptor, nuclear factor- κ B, inflammatory cytokines) to the advantage of the host.⁷⁵⁻⁷⁶ Probiotic microorganisms are expected to colonize the gut, compete with pathogens, improve the gut barrier function and permeability, and modulate immune function.⁷⁷⁻⁷⁸

THESIS OUTLINE AND AIMS

A better understanding of the innate defense mechanisms that are involved in NEC would enable us to identify preventative strategies and therapeutic targets to prevent or cure this disease. Therefore, the main aims of this thesis are:

1. To study intestinal epithelial defense mechanisms in early postnatal life in mice and humans
2. To study the effect of dietary interventions on intestinal epithelial barrier function *in vitro* and *in vivo*

Part I: Intestinal epithelial defense mechanisms in early postnatal life

In **Part I** we studied the development of colitis during perinatal life and during suckling-weaning transition in *Muc2*^{-/-} mice. In this period there is a major change in the diet, i.e. during weaning mice are transferred from mothers' milk to pelleted food. Moreover, bacterial colonization is altered during this time frame, which makes this model a powerful tool to study innate defense responses during colitis development. We previously demonstrated that *Muc2*^{-/-} mice display clinical and histological signs of colitis from the age of 5 weeks onwards. To study whether absence of *Muc2* already causes development of colitis during fetal life or in the early postnatal period, we investigated the consequences of *Muc2*-deficiency during different phases, e.g., during embryonic development, immediately after birth and during suckling-weaning transition in **Chapter 2**. To identify genes and biological responses that play a pivotal role during colitis development in the pre- and post weaning period of *Muc2*KO mice, intestinal gene expression profiles were studied in **Chapter 3**. In **Chapter 4** we concentrated on a subset of antimicrobial proteins that are controlled by the recognition of microbe associated molecular patterns by pattern recognition receptors expressed by the epithelial cells, namely the regenerating genes *Reg3β* and *Reg3γ* and angiogenin. Finally, innate defense in NEC patients was studied in biopsies from premature infants that underwent surgery for severe NEC in **Chapter 5**. The expression of antimicrobial peptides was studied during the acute and regenerative phase of NEC. Moreover, the effect of human milk feeding versus formula feeding on innate defense capacity was studied by measuring Paneth cell products in ileostomy outflow fluid and subsequently determining the antimicrobial capacity.

Part II: Effect of dietary interventions on intestinal epithelial barrier function

Part II describes the effect of dietary interventions on epithelial barrier function and innate defense. In search for the mechanism through which probiotics exert their beneficial effect, we studied the effect of the probiotic *Lactobacillus rhamnosus* GG on mucin MUC2 synthesis in a goblet-cell like cell culture model and we discuss the mechanisms that are responsible for this effect (**Chapter 6**). Subsequently, we examined the effect of bacterial fermentation products (short chain fatty acids, SCFA) on MUC2 synthesis in **Chapter 7**. Moreover, we investigated the mechanisms that regulate butyrate-mediated effects on MUC2 synthesis. Finally, we studied the effect of a purified diet versus a non-purified diet and probiotic supplementation on disease severity in the *Muc2*^{-/-} colitis model (**Chapter 8**). Finally, we conducted a dual-isotope tracer infusion in preterm piglets and preterm infants. The mucin MUC2 is a glycoprotein that contains high amounts of the amino acid threonine. We studied the preferential site of threonine absorption for *Muc2* synthesis, i.e. basolateral or luminal, in partially enterally fed preterm infants and in colostrum and formula fed preterm pigs in **Chapter 9**.

This thesis will finish with a general discussion and an elaboration on recommended future perspectives in **Chapter 10**. A summary of the results of the studies is given in **Chapter 11**.

REFERENCES

1. Kafetzis DA, Skevaki C, Costalos C. Neonatal necrotizing enterocolitis: an overview. *Curr Opin Infect Dis* 2003;16:349-55.
2. Lin PW, Stoll BJ. Necrotising enterocolitis. *Lancet* 2006;368:1271-83.
3. Blakely ML, Lally KP, McDonald S, Brown RL, Barnhart DC, Ricketts RR, Thompson WR, Scherer LR, Klein MD, Letton RW, Chwals WJ, Touloukian RJ, Kurkchubasche AG, Skinner MA, Moss RL, Hilfiker ML, Network NECSotNNR. Postoperative outcomes of extremely low birth-weight infants with necrotizing enterocolitis or isolated intestinal perforation: a prospective cohort study by the NICHD Neonatal Research Network. *Ann Surg* 2005;241:984-9; discussion 989-94.
4. Henry MC, Moss RL. Neonatal necrotizing enterocolitis. *Semin Pediatr Surg* 2008;17:98-109.
5. Bisquera JA, Cooper TR, Berseth CL. Impact of necrotizing enterocolitis on length of stay and hospital charges in very low birth weight infants. *Pediatrics* 2002;109:423-8.
6. Noerr B. Current controversies in the understanding of necrotizing enterocolitis. Part 1. *Adv Neonatal Care* 2003;3:107-20.
7. Schanler RJ, Lau C, Hurst NM, Smith EO. Randomized trial of donor human milk versus preterm formula as substitutes for mothers' own milk in the feeding of extremely premature infants. *Pediatrics* 2005;116:400-6.
8. Lucas A, Cole TJ. Breast milk and neonatal necrotising enterocolitis. *Lancet* 1990;336:1519-23.
9. Gilbert WM, Danielsen B. Pregnancy outcomes associated with intrauterine growth restriction. *Am J Obstet Gynecol* 2003;188:1596-9; discussion 1599-601.
10. Bernstein IM, Horbar JD, Badger GJ, Ohlsson A, Golan A. Morbidity and mortality among very-low-birth-weight neonates with intrauterine growth restriction. The Vermont Oxford Network. *Am J Obstet Gynecol* 2000;182:198-206.
11. Manogura AC, Turan O, Kush ML, Berg C, Bhide A, Turan S, Moyano D, Bower S, Nicolaides KH, Galan HL, Muller T, Thilaganathan B, Gembruch U, Harman CR, Baschat AA. Predictors of necrotizing enterocolitis in preterm growth-restricted neonates. *Am J Obstet Gynecol* 2008;198:638 e1-5.
12. Nowicki PT. Ischemia and necrotizing enterocolitis: where, when, and how. *Semin Pediatr Surg* 2005;14:152-8.
13. Lee JS, Polin RA. Treatment and prevention of necrotizing enterocolitis. *Semin Neonatol* 2003;8:449-59.
14. Hentschel J, de Veer I, Gastmeier P, Ruden H, Obladen M. Neonatal nosocomial infection surveillance: incidences by site and a cluster of necrotizing enterocolitis. *Infection* 1999;27:234-8.
15. Mshvildadze M, Neu J, Shuster J, Theriaque D, Li N, Mai V. Intestinal microbial ecology in premature infants assessed with non-culture-based techniques. *J Pediatr* 2010;156:20-5.
16. Gronlund MM, Lehtonen OP, Eerola E, Kero P. Fecal microflora in healthy infants born by different methods of delivery: permanent changes in intestinal flora after cesarean delivery. *J Pediatr Gastroenterol Nutr* 1999;28:19-25.
17. Harmsen HJ, Wildeboer-Veloo AC, Raangs GC, Wagendorp AA, Klijn N, Bindels JG, Welling GW. Analysis of intestinal flora development in breast-fed and formula-fed infants by using molecular identification and detection methods. *J Pediatr Gastroenterol Nutr* 2000;30:61-7.
18. Gewolb IH, Schwalbe RS, Taciak VL, Harrison TS, Panigrahi P. Stool microflora in extremely low birthweight infants. *Arch Dis Child Fetal Neonatal Ed* 1999;80:F167-73.

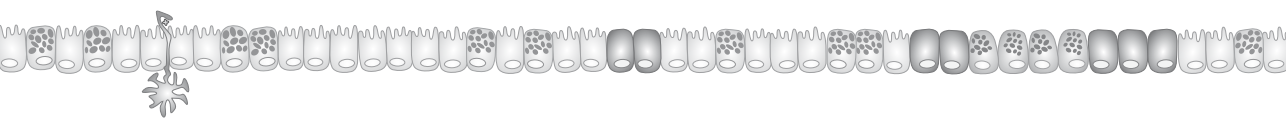
19. Rubaltelli FF, Biadaioli R, Pecile P, Nicoletti P. Intestinal flora in breast- and bottle-fed infants. *J Perinat Med* 1998;26:186-91.
20. Tomkins AM, Bradley AK, Oswald S, Drasar BS. Diet and the faecal microflora of infants, children and adults in rural Nigeria and urban U.K. *J Hyg (Lond)* 1981;86:285-93.
21. Wold AE, Adlerberth I. Breast feeding and the intestinal microflora of the infant--implications for protection against infectious diseases. *Adv Exp Med Biol* 2000;478:77-93.
22. Orrhage K, Nord CE. Factors controlling the bacterial colonization of the intestine in breast-fed infants. *Acta Paediatr Suppl* 1999;88:47-57.
23. Kosloske AM. Epidemiology of necrotizing enterocolitis. *Acta Paediatr Suppl* 1994;396:2-7.
24. Wang Y, Hoenig JD, Malin KJ, Qamar S, Petrof EO, Sun J, Antonopoulos DA, Chang EB, Claud EC. 16S rRNA gene-based analysis of fecal microbiota from preterm infants with and without necrotizing enterocolitis. *Isme J* 2009;3:944-54.
25. Sartor RB. Pathogenesis and immune mechanisms of chronic inflammatory bowel diseases. *Am J Gastroenterol* 1997;92:5S-11S.
26. Sartor RB. Intestinal microflora in human and experimental inflammatory bowel disease. *Curr Opin Gastroenterol* 2001;17:324-30.
27. Farrell RJ, LaMont JT. Microbial factors in inflammatory bowel disease. *Gastroenterol Clin North Am* 2002;31:41-62.
28. Shanahan F. Host-flora interactions in inflammatory bowel disease. *Inflamm Bowel Dis* 2004;10 Suppl 1:S16-24.
29. Sellon RK, Tonkonogy S, Schultz M, Dieleman LA, Grenther W, Balish E, Rennick DM, Sartor RB. Resident enteric bacteria are necessary for development of spontaneous colitis and immune system activation in interleukin-10-deficient mice. *Infect Immun* 1998;66:5224-31.
30. Rath HC, Herfarth HH, Ikeda JS, Grenther WB, Hamm TE, Jr., Balish E, Taurog JD, Hammer RE, Wilson KH, Sartor RB. Normal luminal bacteria, especially *Bacteroides* species, mediate chronic colitis, gastritis, and arthritis in HLA-B27/human beta2 microglobulin transgenic rats. *J Clin Invest* 1996;98:945-53.
31. Dianda L, Hanby AM, Wright NA, Sebesteny A, Hayday AC, Owen MJ. T cell receptor-alpha beta-deficient mice fail to develop colitis in the absence of a microbial environment. *Am J Pathol* 1997;150:91-7.
32. Rutgeerts P, Hiele M, Geboes K, Peeters M, Penninckx F, Aerts R, Kerremans R. Controlled trial of metronidazole treatment for prevention of Crohn's recurrence after ileal resection. *Gastroenterology* 1995;108:1617-21.
33. Sutherland L, Singleton J, Sessions J, Hanauer S, Krawitt E, Rankin G, Summers R, Mekhjian H, Greenberger N, Kelly M, et al. Double blind, placebo controlled trial of metronidazole in Crohn's disease. *Gut* 1991;32:1071-5.
34. Ursing B, Kamme C. Metronidazole for Crohn's disease. *Lancet* 1975;1:775-7.
35. Rutgeerts P, Geboes K, Peeters M, Hiele M, Penninckx F, Aerts R, Kerremans R, Vantrappen G. Effect of faecal stream diversion on recurrence of Crohn's disease in the neoterminal ileum. *Lancet* 1991;338:771-4.
36. Buisine MP, Devisme L, Savidge TC, Gespach C, Gosselin B, Porchet N, Aubert JP. Mucin gene expression in human embryonic and fetal intestine. *Gut* 1998;43:519-24.
37. Allen A, Bell A, Mantle M, Pearson JP. The structure and physiology of gastrointestinal mucus. *Adv Exp Med Biol* 1982;144:115-33.

38. Robbe-Masselot C, Maes E, Rousset M, Michalski JC, Capon C. Glycosylation of human fetal mucins: a similar repertoire of O-glycans along the intestinal tract. *Glycoconj J* 2009;26: 397-413.
39. Forder RE, Howarth GS, Tivey DR, Hughes RJ. Bacterial modulation of small intestinal goblet cells and mucin composition during early posthatch development of poultry. *Poult Sci* 2007; 86:2396-403.
40. Van der Sluis M, De Koning BA, De Bruijn AC, Velcich A, Meijerink JP, Van Goudoever JB, Buller HA, Dekker J, Van Seuningen I, Renes IB, Einerhand AW. Muc2-deficient mice spontaneously develop colitis, indicating that MUC2 is critical for colonic protection. *Gastroenterology* 2006;131:117-29.
41. Schaart MW, de Bruijn AC, Bouwman DM, de Krijger RR, van Goudoever JB, Tibboel D, Renes IB. Epithelial Functions of the Residual Bowel After Surgery for Necrotising Enterocolitis in Human Infants. *J Pediatr Gastroenterol Nutr* 2009.
42. Tytgat KM, van der Wal JW, Einerhand AW, Buller HA, Dekker J. Quantitative analysis of MUC2 synthesis in ulcerative colitis. *Biochem Biophys Res Commun* 1996;224:397-405.
43. Pullan RD, Thomas GA, Rhodes M, Newcombe RG, Williams GT, Allen A, Rhodes J. Thickness of adherent mucus gel on colonic mucosa in humans and its relevance to colitis. *Gut* 1994;35:353-9.
44. Jacobs LR, Huber PW. Regional distribution and alterations of lectin binding to colorectal mucin in mucosal biopsies from controls and subjects with inflammatory bowel diseases. *J Clin Invest* 1985;75:112-8.
45. Johansson ME, Phillipson M, Petersson J, Velcich A, Holm L, Hansson GC. The inner of the two Muc2 mucin-dependent mucus layers in colon is devoid of bacteria. *Proc Natl Acad Sci U S A* 2008;105:15064-9.
46. Savage DC. Microbial ecology of the gastrointestinal tract. *Annu Rev Microbiol* 1977;31: 107-33.
47. Dubos RJ, Savage DC, Schaedler RW. The indigenous flora of the gastrointestinal tract. *Dis Colon Rectum* 1967;10:23-34.
48. Erlandsen SL, Parsons JA, Taylor TD. Ultrastructural immunocytochemical localization of lysozyme in the Paneth cells of man. *J Histochem Cytochem* 1974;22:401-13.
49. Klockars M, Reitamo S. Tissue distribution of lysozyme in man. *J Histochem Cytochem* 1975; 23:932-40.
50. Kiyohara H, Egami H, Shibata Y, Murata K, Ohshima S, Ogawa M. Light microscopic immunohistochemical analysis of the distribution of group II phospholipase A2 in human digestive organs. *J Histochem Cytochem* 1992;40:1659-64.
51. Jones DE, Bevins CL. Defensin-6 mRNA in human Paneth cells: implications for antimicrobial peptides in host defense of the human bowel. *FEBS Lett* 1993;315:187-92.
52. Jones DE, Bevins CL. Paneth cells of the human small intestine express an antimicrobial peptide gene. *J Biol Chem* 1992;267:23216-25.
53. Putsep K, Axelsson LG, Boman A, Midtvedt T, Normark S, Boman HG, Andersson M. Germ-free and colonized mice generate the same products from enteric prodefensins. *J Biol Chem* 2000;275:40478-82.
54. Uehara A, Fujimoto Y, Fukase K, Takada H. Various human epithelial cells express functional Toll-like receptors, NOD1 and NOD2 to produce anti-microbial peptides, but not proinflammatory cytokines. *Mol Immunol* 2007;44:3100-11.

55. Ogawa H, Fukushima K, Naito H, Funayama Y, Unno M, Takahashi K, Kitayama T, Matsuno S, Ohtani H, Takasawa S, Okamoto H, Sasaki I. Increased expression of HIP/PAP and regenerating gene III in human inflammatory bowel disease and a murine bacterial reconstitution model. *Inflamm Bowel Dis* 2003;9:162-70.
56. Cash HL, Whitham CV, Behrendt CL, Hooper LV. Symbiotic bacteria direct expression of an intestinal bactericidal lectin. *Science* 2006;313:1126-30.
57. Hooper LV, Stappenbeck TS, Hong CV, Gordon JI. Angiogenins: a new class of microbicidal proteins involved in innate immunity. *Nat Immunol* 2003;4:269-73.
58. Brandl K, Plitas G, Schnabl B, DeMatteo RP, Pamer EG. MyD88-mediated signals induce the bactericidal lectin RegIII gamma and protect mice against intestinal *Listeria monocytogenes* infection. *J Exp Med* 2007;204:1891-900.
59. Rodenburg W, Keijer J, Kramer E, Roosing S, Vink C, Katan MB, van der Meer R, Bovee-Oudenhoven IM. Salmonella induces prominent gene expression in the rat colon. *BMC Microbiol* 2007;7:84.
60. van Ampting MT, Rodenburg W, Vink C, Kramer E, Schonewille AJ, Keijer J, van der Meer R, Bovee-Oudenhoven IM. Ileal Mucosal and Fecal Pancreatitis Associated Protein Levels Reflect Severity of Salmonella Infection in Rats. *Dig Dis Sci* 2009.
61. Sonnenburg JL, Chen CT, Gordon JI. Genomic and metabolic studies of the impact of probiotics on a model gut symbiont and host. *PLoS Biol* 2006;4:e413.
62. Lotz M, Gutle D, Walther S, Menard S, Bogdan C, Hornef MW. Postnatal acquisition of endotoxin tolerance in intestinal epithelial cells. *J Exp Med* 2006;203:973-84.
63. Cario E, Podolsky DK. Differential alteration in intestinal epithelial cell expression of toll-like receptor 3 (TLR3) and TLR4 in inflammatory bowel disease. *Infect Immun* 2000;68:7010-7.
64. Hausmann M, Kiessling S, Mestermann S, Webb G, Spottl T, Andus T, Scholmerich J, Herfarth H, Ray K, Falk W, Rogler G. Toll-like receptors 2 and 4 are up-regulated during intestinal inflammation. *Gastroenterology* 2002;122:1987-2000.
65. Frolova L, Drastich P, Rossmann P, Klimesova K, Taskalova-Hogenova H. Expression of Toll-like receptor 2 (TLR2), TLR4, and CD14 in biopsy samples of patients with inflammatory bowel diseases: upregulated expression of TLR2 in terminal ileum of patients with ulcerative colitis. *J Histochem Cytochem* 2008;56:267-74.
66. Gribar SC, Sodhi CP, Richardson WM, Anand RJ, Gittes GK, Branca MF, Jakub A, Shi XH, Shah S, Ozolek JA, Hackam DJ. Reciprocal expression and signaling of TLR4 and TLR9 in the pathogenesis and treatment of necrotizing enterocolitis. *J Immunol* 2009;182:636-46.
67. Le Mandat Schultz A, Bonnard A, Barreau F, Aigrain Y, Pierre-Louis C, Berrebi D, Peuchmaur M. Expression of TLR-2, TLR-4, NOD2 and pNF-kappaB in a neonatal rat model of necrotizing enterocolitis. *PLoS ONE* 2007;2:e1102.
68. Leapheart CL, Cavallo J, Gribar SC, Cetin S, Li J, Branca MF, Dubowski TD, Sodhi CP, Hackam DJ. A critical role for TLR4 in the pathogenesis of necrotizing enterocolitis by modulating intestinal injury and repair. *J Immunol* 2007;179:4808-20.
69. Jilling T, Simon D, Lu J, Meng FJ, Li D, Schy R, Thomson RB, Soliman A, Arditi M, Caplan MS. The roles of bacteria and TLR4 in rat and murine models of necrotizing enterocolitis. *J Immunol* 2006;177:3273-82.
70. Saulnier DM, Spinler JK, Gibson GR, Versalovic J. Mechanisms of probiosis and prebiotics: considerations for enhanced functional foods. *Curr Opin Biotechnol* 2009;20:135-41.

71. Turnbaugh PJ, Ridaura VK, Faith JJ, Rey FE, Knight R, Gordon JI. The effect of diet on the human gut microbiome: a metagenomic analysis in humanized gnotobiotic mice. *Sci Transl Med* 2009;1:6ra14.
72. Gibson GR, Roberfroid MB. Dietary modulation of the human colonic microbiota: introducing the concept of prebiotics. *J Nutr* 1995;125:1401-12.
73. Deshpande G, Rao S, Patole S, Bulsara M. Updated meta-analysis of probiotics for preventing necrotizing enterocolitis in preterm neonates. *Pediatrics* 2010;125:921-30.
74. Tarnow-Mordi W, Wilkinson D, Trivedi A, Sinn J, Dutta S, Parikh T, Lin HC. Re: ESPGHAN commentary and education that probiotics substantially reduce all-cause mortality and necrotizing enterocolitis in preterm infants. *J Pediatr Gastroenterol Nutr* 2010;50:694; author reply 694-5.
75. Schanler RJ. Probiotics and necrotising enterocolitis in premature infants. *Arch Dis Child Fetal Neonatal Ed* 2006;91:F395-7.
76. Martin CR, Walker WA. Probiotics: role in pathophysiology and prevention in necrotizing enterocolitis. *Semin Perinatol* 2008;32:127-37.
77. Stratiki Z, Costalos C, Sevastiadou S, Kastanidou O, Skouroliahou M, Giakoumatou A, Petrohilou V. The effect of a bifidobacter supplemented bovine milk on intestinal permeability of preterm infants. *Early Hum Dev* 2007;83:575-9.
78. Indrio F, Riezzo G, Raimondi F, Bisceglia M, Cavallo L, Francavilla R. The effects of probiotics on feeding tolerance, bowel habits, and gastrointestinal motility in preterm newborns. *J Pediatr* 2008;152:801-6.
79. Dekker J, Rossen JW, Buller HA, Einerhand AW. The MUC family: an obituary. *Trends Biochem Sci* 2002;27:126-31.

Chapter 2



Colitis development during the suckling-weaning transition in mucin Muc2-deficient mice

Nanda Burger-van Paassen, Maria van der Sluis, Janneke Bouma, Anita M. Korteland-van Male, Peng Lu, Isabelle Van Seuning, Johannes B. van Goudoever, Ingrid B. Renes

Under Review



ABSTRACT

Background: The mucin Muc2 is the structural component of the colonic mucus layer. Adult Muc2 knockout (Muc2^{-/-}) mice suffer from severe colitis. We hypothesized that Muc2-deficiency induces inflammation before weaning of mother's milk with aggravation of colitis after weaning. **Methods:** Muc2^{-/-} and wild type mice were sacrificed at embryonic day 18.5, and postnatal (P) day 1.5, 7.5, 14, 21, and 28. Colonic morphology, influx of T-cells, and goblet cell-specific protein expression was investigated by (immuno)histochemistry. Cytokine and Toll-like receptor (TLR) profiles in the colon were analyzed by quantitative RT-PCR. **Results:** Muc2^{-/-} mice showed an influx of CD3ε-positive T-cells into the colonic mucosa as of P1.5 and progressive crypt lengthening as of weaning, at P21. Before weaning (P14) the pro-inflammatory immune response (i.e. increased *Il-12 p35*, *Il-12 p40*, and *Tnf-α*, expression) in Muc2^{-/-} mice was accompanied by an immune suppressive response (i.e. increased *Foxp3*, *Tgfb1*, *Il-10*, and *Ebi3* expression). In contrast, after weaning (P28) a pro-inflammatory response remained, whereas the immune suppressive response (i.e. *Foxp3* and *Tgfb1* expression) declined. Interestingly, *Tlr2* and *MyD88* expression levels in Muc2^{-/-} mice also decreased after weaning. Finally, colitis in Muc2^{-/-} mice aggravated after weaning as reflected by decreased body weights, further increase in crypt lengthening, and persistent presence of T-cells in the mucosa. **Conclusions:** In conjunction, our data show that colitis in Muc2^{-/-} mice is limited before weaning and exacerbates after weaning suggesting that mother's milk possesses protective capacities and/or that alterations in the intestinal microbiota, which occur during the suckling-weaning transition, influence colitis development.

Key words: colitis, bacterial colonization, mother's milk, Toll-like receptor

INTRODUCTION

The exact etiology of inflammatory bowel diseases (IBD) such as ulcerative colitis (UC) and Crohn's disease (CD), but also necrotizing enterocolitis (NEC), is still partly unknown. Genetic susceptibility and environmental agents are known to be involved in causing IBD.¹⁻² In NEC, prematurity as well as dysmaturity and formula feeding are the only consistent risk factors associated with the development of this disease.³⁻⁵ However, the intestinal microbiota seems to play a key role in the onset and perpetuation of inflammation in all these disease entities that share the feature of (entero-)colitis. This is supported by the fact that several models for IBD and NEC only develop disease when colonized with bacteria, but not under germ-free conditions.⁶⁻⁷

Detection of bacteria in the intestine is mediated by Toll-like receptors (TLRs), which are a family of pattern recognition receptors. Following bacterial recognition, TLRs recruit and activate a variety of signal transducing adaptor proteins, which trigger a cascade of signaling pathways and ultimately lead to the activation of transcription factors such as NF- κ B and interferon regulatory factors (IRFs). Finally, this results in the transcription of pro-inflammatory cytokines, type I interferons and chemokines. Intestinal epithelial cells acquire tolerance following colonization, presumably to permit colonization without chronic inflammation.⁸ However, aberrant expression levels of TLRs have been related to decreased tolerance and the onset and perpetuation of disease. For example, TLR4 is known to be upregulated in CD and UC and the expression of TLR4 and TLR2 is upregulated in lamina propria macrophages as well as intestinal epithelial cells in IBD patients.⁹⁻¹¹ Additionally, TLR4 which is thought to play an important role in the development of NEC, appears to be up-regulated in several rodent NEC models.¹²⁻¹⁵

Contact between bacteria and TLRs is limited due to the presence of a physical barrier that is formed by the intestinal mucus layer, of which the mucin MUC2 is the structural component. Johansson et al.¹⁶ elegantly showed that the mucus layer exists of two separate layers. The inner colonic mucus layer, which is in contact with the epithelial cells, is devoid of bacteria. Accordingly, the absence of a protective mucus layer, as in *Muc2*^{-/-} mice, allows bacteria to come into direct contact with the epithelial cells, causing intestinal inflammation. Importantly, decreased numbers of goblet cells, the producers of MUC2, and a thinner mucus layer have been related to IBD¹⁷⁻²⁰ and NEC.²¹ Absence of, or breaches in, the mucus layer increase and intensify bacterial-TLR interactions, which in turn might lead to alterations in TLR expression levels.

We previously demonstrated that *Muc2*^{-/-} mice display clinical and histological signs of colitis from the age of 5 weeks on.²² It is unknown whether absence of Muc2 already causes development of colitis in the early postnatal period, more specifically, before weaning of mother's milk. In the present study we investigated the consequences of Muc2-deficiency during different phases, e.g., during embryonic development, im-

mediately after birth and during suckling-weaning transition. We hypothesized that lack of Muc2 induces the development of colitis early after birth, which aggravates during the suckling-weaning transition. We therefore studied morphological changes, influx of immune cells, and expression levels of pro-inflammatory and immune suppressive cytokines as parameters for colitis development. Furthermore, we analyzed the expression profiles of Tlrs, Tlr adaptor proteins and the Tlr activated transcription factor Irf3 during the pre- and post-weaning period in wild type (WT) and Muc2^{-/-} mice.

MATERIALS AND METHODS

Animals

Muc2^{-/-} mice were bred as previously described.²² All mice were generated from Muc2^{+/-} breedings. Mice were housed in the same specific pathogen-free environment with free access to standard rodent pellets (Special Diets Services, Witham, Essex, England) and acidified tap water in a 12-hour light/dark cycle. Animal care and procedures were conducted according to institutional guidelines (Erasmus MC Animal Ethics Committee, Rotterdam) The Netherlands). Wild-type and Muc2^{-/-} mice were tested negative for *Helicobacter hepaticus* and norovirus infection.

Experimental setup

Wild-type (WT) and Muc2^{-/-} littermates were housed together with their birth mother until weaning at the age of 21 days. WT and Muc2^{-/-} mice were sacrificed at the embryonic (E) age of 18.5 days and postnatal (P) ages of 1.5; 7.5; 14; 21, and 28 days. Colonic tissue was excised immediately and either fixed in 4% (wt/vol) paraformaldehyde in phosphate-buffered saline (PBS), stored in RNAlater (Qiagen, Venlo, The Netherlands) at -20°C, or frozen in liquid nitrogen and stored at -80°C.

Histology and histologic grading

Tissue fixed in 4% (wt/vol) paraformaldehyde in PBS was prepared for light microscopy, and 4-μm-thick sections were stained with hematoxylin and eosin (H&E) to study histological changes. To detect differences in mucosal and epithelial thickness in the colon, 10 well-oriented crypts were chosen per intestinal segment and measured using calibrated Leica Application Suite software, version 3.2.0 (Leica Microsystems BV, Rijswijk, The Netherlands). Values are expressed in micrometer (μm) and depicted as box-and-whisker diagrams (maximum value, upper quartile, median, lower quartile and minimal value respectively).

Immunohistochemistry

Four-micrometer-thick sections were cut and prepared for immunohistochemistry (IHC) as described previously²³ using the Vectastain Elite ABC kit (Vector Laboratories, Burlingame, CA) and 3,3'-diaminobenzidine as staining reagent. Antigen unmasking was carried out by heating the sections for 20 min in 0.01 M sodium citrate (pH 6.0; Merck, Darmstadt, Germany) at 100°C. Cd3-positive cells were detected using a mouse monoclonal anti-human Cd3ε antibody, which also cross-reacts with mouse Cd3ε. (DAKO, Heverlee, Belgium; 1:800 diluted in 1% bovine serum albumin, 0.1% Triton X-100 in PBS). To detect Tff3, rabbit-anti-rat TFF3 (1:3000 in PBS; a generous gift from D. K. Podolsky²⁴) was used. Muc4 was stained using an anti-human-MUC4 rabbit-polyclonal antibody (hHA-1) that recognizes the AGYRPPRPAWTFGD amino acid sequence of the C-terminal peptidic region of MUC4a subunit, which is homologous in humans and mice. The antibody was diluted 1:6000 in 1% BSA, 0.1% Triton X-100 in PBS. Irf3 was stained using anti-mouse Irf3 (Abcam, Cambridge, United Kingdom), diluted 1:500 in 1% bovine serum albumin, 0.1% Triton X-100 in PBS.

Quantitative Real-Time RT-PCR (TaqMan Technology)

Total RNA was prepared using the RNeasy midi-kit from Qiagen (Venlo, the Netherlands) and a total of 1.5 µg was used to prepare cDNA. The mRNA expression levels of all

Table 1. Primer sequences for qRT-PCR

Gene	Forward primer	Reverse primer
Tlr2	AAG ATG CGC TTC CTG AAT TTG	TCC AGC GTC TGA GGA ATG C
Tlr4	AAT CCC TGC ATA GAG GTA GTA	ATC CAG CCA CTG AAG TTC T
Tlr9	TCT CCC AAC ATG GTT CTC	AAC GGG GTA CAG ACT TCA
Myd88	CCT GCG GTT CAT CAC TAT	GGC TCC GCA TCA GTC T
Cd3	CCA GCC TCA AAT AAA AAC A	TTG GCC TTC CTA TTC TTG
Cd45	TTT GGG AAC ATT ACT GTG AA	TGG AGC ACA TGA GTC ATT AG
Foxp3	ACA CCC AGG AAA GAC AG	GGC AGT GCT TGA GAA AC
Il-12α (P35 subunit)	GCC TTG GTA GCA TCT ATG AG	TCG GCA TTA TGA TTC AGA GA
Ebi3	CCC GGA CAT CTT CTC TCT	GAG GCT CCA GTC ACT TG
Tgfb1	AAC CAA AGA CAT CTC ACA CA	GCC AGG AAT TGT TGC TAT
Tnfa	TGG CCT CCC TCT CAT C	GGC TGG CAC CAC TAG TT
Ifny	CGG CAC AGT CAT TGA AA	TGC CAG TTC CTC CAG AT
Il-10	CAA GCC TTA TCG GAA ATG	CAT GGC CTT GTA GAC ACC
Tff3	GGC TGC TGC TTT GAC TC	AGC CTG GAC AGC TTC AA
Muc4	CCC GCT CAT CCA CTA TC	TGG CCT CCA TTG TGA C
villin	TCG GCC TCC AGT ATG TAG	CGT CTT CGG GGT AGA ACT
β-actin	GGG ACC TGA CGG ACT AC	TGC CAC AGG ATT CCA TAC

studied genes were quantified using quantitative real-time PCR (qRT-PCR) analysis (TAQman chemistry) based upon the intercalation of SYBR Green on an ABI prism 7900 HT Fast Real Time PCR system (PE Applied Biosystems) as previously described.²⁵ All primer combinations were designed using OLIGO 6.22 software (Molecular Biology Insights) and purchased from Invitrogen. An overview of all primer sequences is given in Table 1.

Statistical analysis

Statistical significance was assessed using the Mann-Whitney U test. (Prism, version 5.00; GraphPad software, San Diego, CA). The data were considered statistically significant at $P < 0.05$.

RESULTS

Significant growth retardation in *Muc2*^{-/-} mice occurs after weaning

Before birth, at P1.5 days and prior to weaning (at P14 and P21), there were no significant differences in body weight between *Muc2*^{-/-} mice and WT mice. However, after weaning, at P28, a significant difference in body weight was observed, as *Muc2*^{-/-} mice were lighter than WT mice (Fig. 1). No additional clinical symptoms of colitis (i.e. diarrhea, occult blood loss, rectal prolapse) were seen before the age of 28 days.

Characteristic changes in colon morphology are present from the age of 28 days

H&E staining was used for morphological analysis. No morphological differences were present before birth between *Muc2*^{-/-} and WT mice, except for the absence of the char-

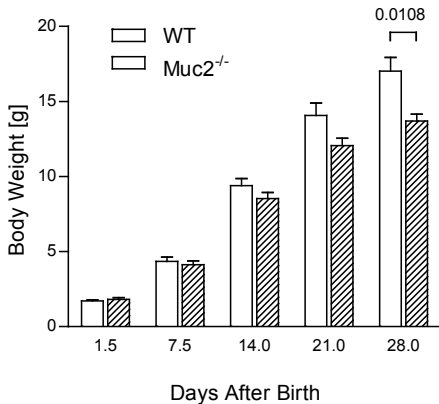


Figure 1. Body weight of WT and *Muc2*^{-/-} mice during postnatal age P1.5 to P28. Body weight of WT (white bars) and *Muc2*^{-/-} (shaded bars) mice in time. No significant differences were observed between WT and *Muc2*^{-/-} mice, except at the age of 28 days. Values are depicted as mean±SEM.

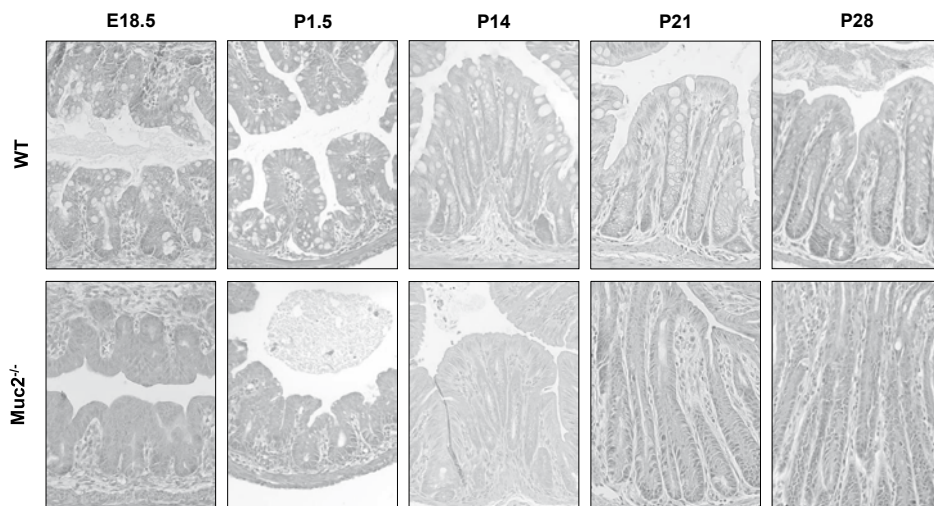


Figure 2. Colonic morphology of WT and *Muc2*^{-/-} mice

Morphology of the distal colon in WT (upper panels) and *Muc2*^{-/-} (lower panels) mice by hematoxylin and eosin staining. Representative sections of the distal colon are depicted at E18.5, P1.5, P14, P21 and P28. The tissue samples are representative of all mice in the studied groups. Note, no evident signs of inflammation or epithelial damage were seen at E18.5, P1.5 and P14. After weaning, at P28, the first signs of colitis (i.e. epithelial flattening and superficial erosion were seen. (See Color Section, p. 233.)

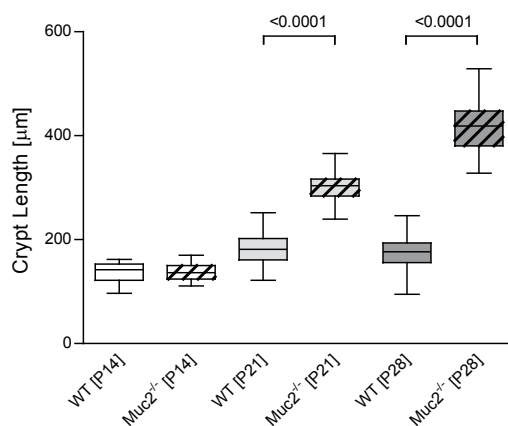


Figure 3. Crypt length is significantly increased in *Muc2*^{-/-} mice at P21 and P28

Crypt length in the distal colon of WT (solid boxes) and *Muc2*^{-/-} (shaded boxes) mice at age 14 days (white), 21 days (light grey) and 28 days (dark grey). Crypt length was significantly different between WT and *Muc2*^{-/-} at the age of 21 and 28 days.

acteristic bell-shaped morphology of the goblet cells. There were no evident signs of inflammation or epithelial damage at E18.5, P1.5 and P14 (Fig. 2). A change in morphology was seen after weaning, with the first signs of colitis, such as epithelial flattening and superficial erosion at P28 (Fig. 2). Crypt length increased during aging and was significantly different between WT and *Muc2*^{-/-} mice at P21 and P28 (Fig. 3).

Lymphocyte Infiltration is increased in *Muc2*^{-/-} mice shortly after birth

Cd3 ϵ was used as a marker for T-cell infiltration and was analyzed by immunohistochemistry (Fig. 4, showing representative stained sections for WT and *Muc2*^{-/-} mice). At P1.5 there was already a marked increase in the amount of Cd3 ϵ -positive T-cells in *Muc2*^{-/-} mice, while in WT mice there were hardly any Cd3 ϵ -positive T-cells visible. Interestingly, the abundance of Cd3 ϵ -positive T-cells slightly increased in WT mice before weaning, whereas a subsequent decrease was observed after weaning. In contrast, in *Muc2*^{-/-} mice a marked increase in the amount of Cd3 ϵ -positive T-cells during aging was seen regardless of weaning. Moreover, the number of infiltrating Cd3 ϵ -positive cells was higher in *Muc2*^{-/-} mice compared to WT mice at each time point investigated.

In addition to the immunohistochemical analysis we determined the presence of immune cells by qRT-PCR (Fig 5A-C). *Cd45* was used as a marker for all differentiated hematopoietic cells except erythrocytes and plasma/B-cells, *Cd3 ϵ* as marker for T-cells, and *Foxp3* as marker for regulatory T-cells (Treg cells). At P14 and P28 *Muc2*^{-/-} mice

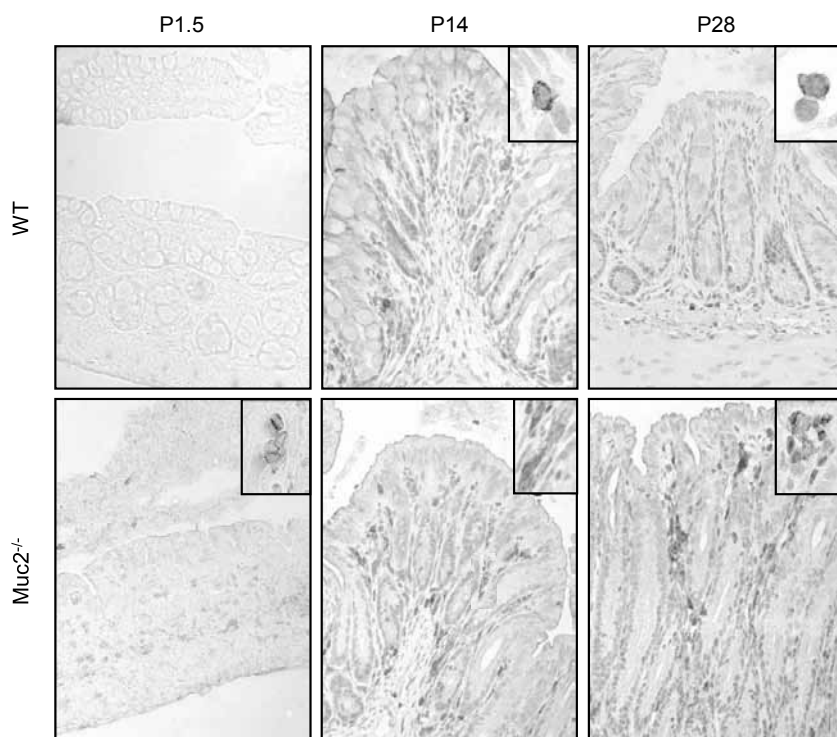


Figure 4. The amount of Cd3-positive T-cells is increased in *Muc2*^{-/-} mice before and after weaning. Infiltration of T-cells determined by Cd3 immunohistochemistry on distal colon sections at different ages (P1.5, P14 and P28). Inserted pictures show higher magnification to point out individual Cd3-positive T-cells. The tissue samples are representative of all mice in the studied groups. Note, the influx of Cd3-positive T-cells, was increased in WT as well as *Muc2*^{-/-} mice before weaning. Weaning from mother's milk resulted in exacerbation of colitis in *Muc2*^{-/-} mice, but not WT mice. (See Color Section, p. 234.)

showed a significant increase in *Cd45* levels and a trend toward increased expression of *Cd3ε*, respectively, indicating increased numbers of immune cells/T-cells in *Muc2*^{-/-} mice compared to WT mice. Gene expression levels of *Foxp3*, the marker for Treg cells, which have immune suppressive functions, were significantly increased in *Muc2*^{-/-} mice compared to WT mice at P14 but not at P28. Moreover, in *Muc2*^{-/-} mice expression levels of *Foxp3* were significantly decreased at P28 compared to P14.

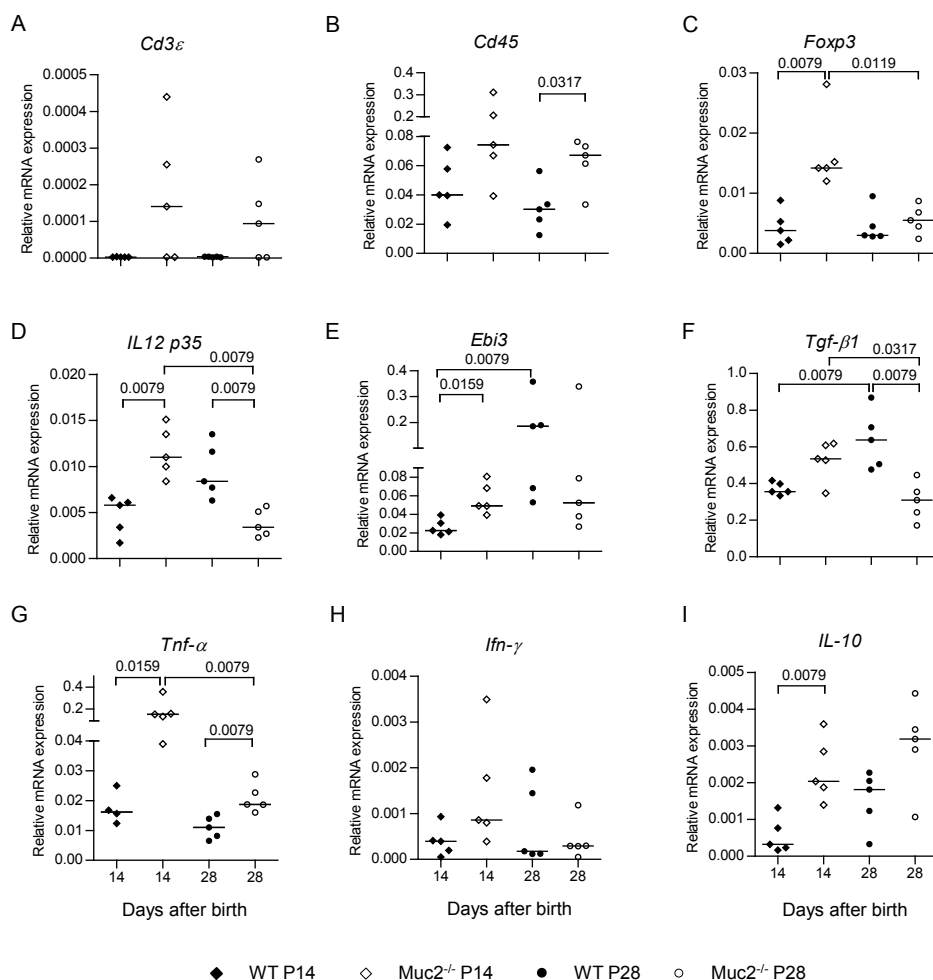


Figure 5. Altered expression of immune response genes in *Muc2*^{-/-} mice before and after weaning. Relative gene expression levels of immune response genes in the distal colon of WT and *Muc2*^{-/-} mice at P14 and P28. Gene expression levels were normalized to β -actin and depicted as median. Groups are depicted as: WT, P14 \blacklozenge ; *Muc2*^{-/-}, P14 \diamond ; WT, P28 \bullet ; and *Muc2*^{-/-}, P28 \circ . Note, a strong immune response was seen before weaning (at P14) with increased expression of *Cd45*, *Cd3ε*, *Foxp3*, *IL-12 p35*, *Ebi3*, *Tgfβ1*, *Tnf-α*, and *IL-10* gene expression levels in the distal colon of *Muc2*^{-/-} mice. After weaning, at P28, *Foxp3*, *IL-12 p35*, *Tgfβ1*, and *Tnf-α* gene expression levels are significantly down-regulated in *Muc2*^{-/-} mice (compared to P14), whereas *IL-10* gene expression levels are maintained.

Altered cytokine gene expression profiles in *Muc2^{-/-}* mice before and after weaning

To assess the development of colitis into further detail, gene expression levels of a subset of cytokines, as mentioned in Table 1, were analyzed. We first focussed on IL-35, a heterodimer of IL-12 p35 and Ebi3, which is produced by Treg cells and inhibits T-cell proliferation and thereby limits inflammation. Both *Il-12 p35* (Fig. 5D) and *Ebi3* (Fig. 5E) were significantly higher in *Muc2^{-/-}* mice compared to WT mice at P14. Interestingly, *Il-12 p35*, which is expressed at much lower levels than *Ebi3* and therefore determines IL-35 levels ²⁶, decreased significantly from P14 till P28 in *Muc2^{-/-}* mice, but not in WT mice. Gene expression levels of *Tgfb1*, another peptide with immune suppressive capacities significantly increased in WT mice from P14 to P28. However, in *Muc2^{-/-}* mice, expression of *Tgfb1* significantly decreased from P14 till P28 (Fig. 5F). Furthermore, at P28, expression of *Tgfb1* was significantly lower in *Muc2^{-/-}* mice compared to WT mice.

Tnf-α, a pro-inflammatory cytokine produced by macrophages, dendritic cells and subsets of T-cells known as Th1 and Th17 cells, is significantly higher in *Muc2^{-/-}* mice compared to WT mice at P14 as well as P28 (Fig. 5G). Yet, in *Muc2^{-/-}* mice *Tnf-α* gene expression levels decreased from P14 till P28, whereas in WT mice *Tnf-α* expression remained stable. *Ifn-γ*, which is also a pro-inflammatory cytokine and generally related to a Th1-type immune response, was not significantly different between WT and *Muc2^{-/-}* mice at P14 and P28, neither were there significant differences from P14 to P28 in WT nor in *Muc2^{-/-}* mice (Fig. 5H). *Il-10*, an immune suppressive cytokine that inhibits the expression of pro-inflammatory cytokines like *Ifn-γ*, *Il-2* and *Tnf-α*, was significantly higher in *Muc2^{-/-}* mice compared to WT mice at P14 (Fig. 5I). Interestingly, in *Muc2^{-/-}* mice *Il-10* gene expression levels remained high as gene expression levels were similar between P14 and P28. Finally, in WT mice *Il-10* expression levels showed a trend toward increased expression from P14 to P28.

Altered mRNA expression of TLRs and TLR signaling molecules correlate with colitis development

Since bacterial colonization plays a pivotal role in the development of colitis, we studied the expression of several Tlrs and Tlr signaling molecules during the suckling-weaning transition, i.e. P14 versus P28, in WT and *Muc2^{-/-}* mice. Gene expression levels of *Tlr2*, a Tlr that recognizes several bacterial ligands such as glycolipids, lipopeptides and lipoproteins, was not significantly different between WT and *Muc2^{-/-}* mice at the age of 14 days. Nevertheless, at P28 there was a significantly lower level of *Tlr2* mRNA in *Muc2^{-/-}* mice compared to WT mice (Fig. 6A). The mRNA expression of *Tlr4*, a receptor for which lipopolysaccharide (LPS) is an important ligand, was significantly increased in *Muc2^{-/-}* mice at P14 compared to WT mice (Fig. 6B). Although not significant, there was still a trend toward increased *Tlr4* mRNA expression in *Muc2^{-/-}* mice at P28. *Tlr9*, the Tlr

for unmethylated CpG DNA (i.e. bacterial DNA), showed increased mRNA expression levels in *Muc2*^{-/-} mice compared to WT mice at P14 ($P = 0.0317$) and P28 (nonsignificant) (Fig. 6C). Finally, Myeloid differentiation factor 88 (*Myd88*), an intracellular signaling adaptor protein that plays a role in Tlr signal transduction, was studied. There were no significant differences in *Myd88* mRNA expression levels between WT and *Muc2*^{-/-} mice at P14 and at P28. However, in *Muc2*^{-/-} mice expression of *Myd88* mRNA was significantly decreased at P28 compared to P14, whereas in WT mice expression levels remained unaltered (Fig. 6D).

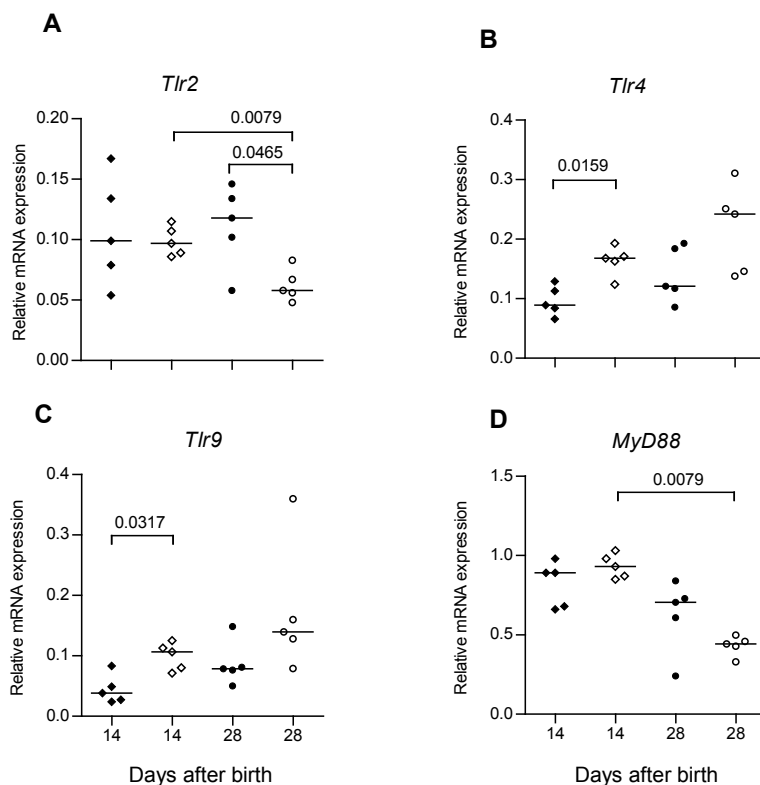


Figure 6. Altered expression of *Tlrs* and *Myd88* before and after weaning

Relative mRNA expression levels of TLRs and TLR signaling molecules in the distal colon of WT and *Muc2*^{-/-} mice at P14 and P28. *Tlr2* mRNA was significantly different between WT and *Muc2*^{-/-} mice at the P28. In *Muc2*^{-/-} mice expression significantly decreased during aging (A). Expression of *Tlr4* was significantly higher in *Muc2*^{-/-} mice compared to WT mice at P14 (B). *Tlr9* expression was significantly higher in *Muc2*^{-/-} mice at P14 compared to WT mice (C). *Myd88* significantly decreased during aging in *Muc2*^{-/-} mice (D). Gene expression levels were normalized to β -actin and depicted as median. Groups are depicted as: WT, P14 ◆; *Muc2*^{-/-}, P14 ◇; WT, P28 ●; and *Muc2*^{-/-}, P28 ○.

Goblet cell differentiation is altered in *Muc2*^{-/-} mice

The mucin *Muc4* and trefoil factor 3 (*Tff3*) were used as goblet cell markers. In both types of mice *Tff3*-positive and *Muc4*-positive goblet cells were localized from the lower crypt till the surface epithelium at E18.5 and P1.5 (Fig. 7A). A similar localization of *Tff3*-positive goblet cells was seen at P14 and P28 (Fig. 7A, upper panel). Interestingly, due to crypt lengthening in *Muc2*^{-/-} mice the total number of *Tff3*-positive goblet cells seemed to increase at P28 compared with WT mice at P28 and with *Muc2*^{-/-} mice at P14. Focusing on *Muc4* expression we observed that *Muc2*^{-/-} mice hardly showed *Muc4*-positive goblet cells at P14 and P28 compared to WT mice (Fig. 7A, lower panel).

Next to the *Tff3* and *Muc4* protein localization studies, qRT-PCR was performed to determine *Tff3* and *Muc4* gene expression levels normalized to villin, which in the colon is mainly expressed by enterocytes (Fig. 7B). In WT mice, *Tff3* gene expression decreased from P14 to P28, whereas *Muc4* gene expression increased. In *Muc2*^{-/-} mice both *Tff3* and *Muc4* gene expression levels did not show any increase or decrease and were thus comparable between P14 and P28. Remarkably, at P14 *Tff3* mRNA levels were significantly lower in *Muc2*^{-/-} mice than in WT mice.

Expression of *Irf3* protein is increased in *Muc2*^{-/-} mice

We were not able to analyze TLR protein expression levels or localization as expression levels were either too low or due to the lack of antibodies suitable for immunohistochemistry on paraffin embedded tissues. Therefore, we determined the localization of interferon regulatory factor 3 (*Irf3*) as a parameter for MyD88-independent TLR4-signaling. Representative stained tissue samples are shown in Figure 8B. In WT mice *IRF3* expression was confined to the nuclei of the epithelial cells of the surface epithelium, whereas in *Muc2*^{-/-} mice, nuclear *Irf3* staining was seen in the epithelial cells along the entire crypts and the surface epithelium, suggesting increased TLR4 signaling in *Muc2*^{-/-} mice. Additionally, in *Muc2*^{-/-} mice *Irf3* expression was also observed in the nuclei of many cells within the lamina propria.

DISCUSSION

In the present study we analyzed the development of colitis during the early post-natal period and suckling-weaning transition. We found that severe signs of colitis in *Muc2*^{-/-} mice develop only after weaning of mother's milk, notwithstanding the fact that subtle signs of colitis were already seen before weaning. Furthermore, expression of pro-inflammatory and immune suppressive cytokines, Tlrs, Tlr-related signaling molecules, and the Tlr activated transcription factor *Irf3* appeared to be altered during the pre- and post weaning period in this colitis model.

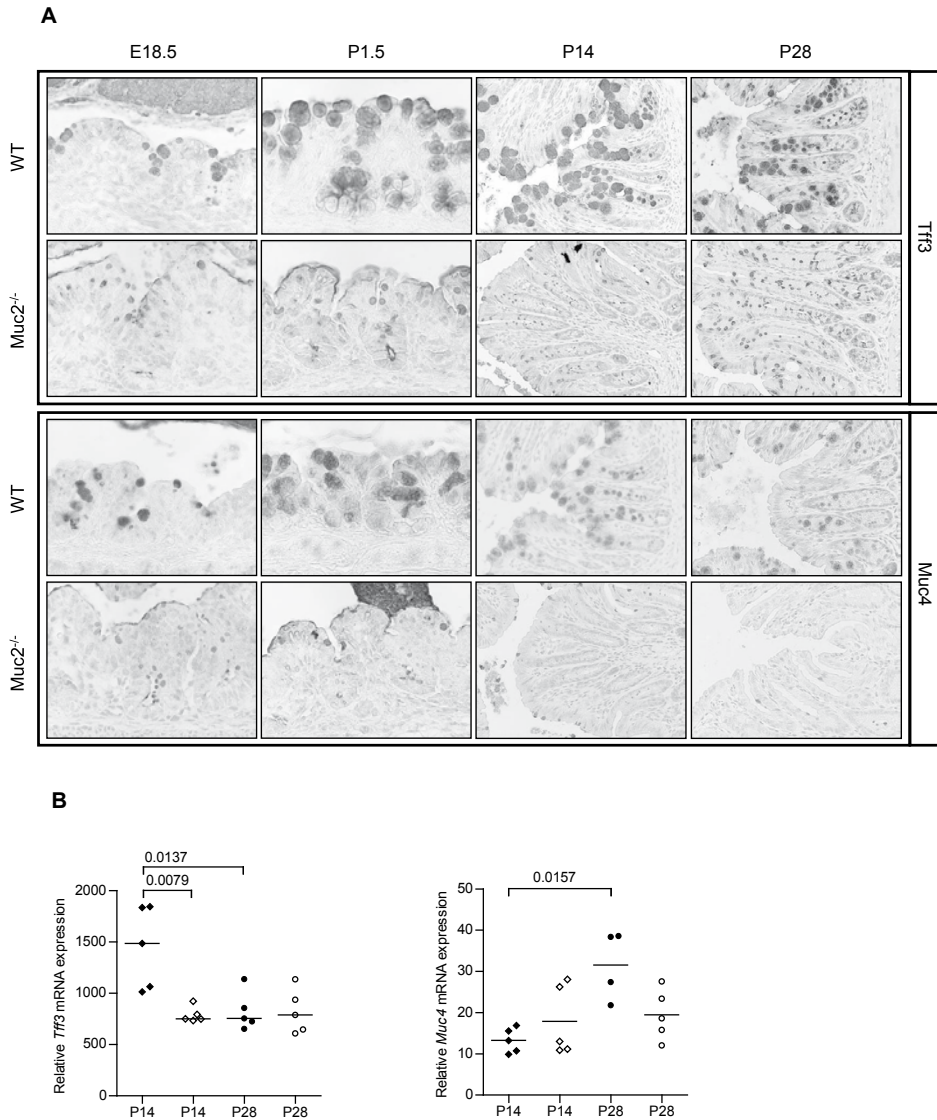


Figure 7. Embryonic and early postnatal expression of intestinal goblet cell markers in the distal colon of WT and *Muc2*^{-/-} mice

(A) Immunohistochemical staining for Tff3 (upper panel) and Muc4 (lower panel) in distal colon of WT and *Muc2*^{-/-} mice at embryonic age 18.5 days (E18.5) and postnatal age of 1.5 (P1.5), 14 (P14) and 28 (P28) days. For each type of staining, upper panels represent WT mice and lower panels represent *Muc2*^{-/-} mice. The tissue samples are representative of all mice in the studied groups. (B) *Tff3* (left) and *Muc4* (right) gene expression levels normalized to villin gene expression and depicted as median. Groups are depicted as: WT, P14 ♦; *Muc2*^{-/-}, P14 ◊; WT, P28 ●; and *Muc2*^{-/-}, P28 ○. Note, *Muc2*^{-/-} mice hardly show Muc4-positive goblet cells at P14 and P28, but *Muc4* gene expression levels in *Muc2*^{-/-} mice are comparable with WT mice. An increase in Tff3-positive goblet cell numbers is seen in *Muc2*^{-/-} mice at P28 compared to WT at P28 and *Muc2*^{-/-} mice at P14. *Tff3* gene expression levels normalized to villin are comparable between *Muc2*^{-/-} mice at P28 and WT at P28 and *Muc2*^{-/-} mice at P14.

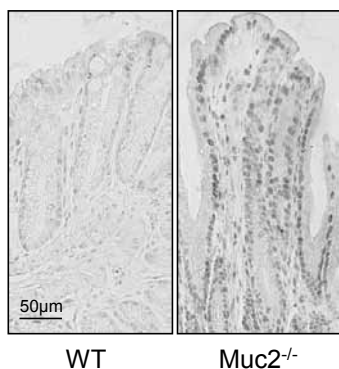


Figure 8. Expression of Irf3 protein in distal colon of WT and *Muc2*^{-/-} mice

Expression and localization of IRF3 in distal colon of WT (left panel) and *Muc2*^{-/-} mice (right panel) at P28 was studied by immunohistochemistry. In WT mice Irf3 expression is confined to the nuclei of the epithelial cells of the surface epithelium, whereas in *Muc2*^{-/-} mice, nuclear Irf3 staining is seen in the epithelial cells along the entire crypts and the surface epithelium. Tissue samples are representative of all mice in the studied groups. (See Color Section, p. 234.)

First of all, our developmental study shows that, except for a significant difference in body weight at the age of 28 days, no clinical symptoms of colitis occur before this age in *Muc2*^{-/-} mice. Secondly, histological examination revealed no morphological alterations in *Muc2*^{-/-} mice before birth or shortly after birth, except for the lack of recognizable goblet cells, which has been described before.²⁷ Crypt lengthening was the first subtle histological sign of colitis in *Muc2*^{-/-} mice and was seen at the age of 21 days. More pronounced histological signs of colitis such as epithelial flattening and superficial erosion were observed from the age of 28 days. In conjunction, these data identify the suckling-weaning transition as an important period during which colitis is initiated in *Muc2*^{-/-} mice. As the transition from breast milk to solid food takes place in this time frame, these data suggest that breast milk might limit the development of colitis in *Muc2*^{-/-} mice. Furthermore, these data might also indicate that the intestinal microbiota is involved in colitis induction in *Muc2*^{-/-} mice, as the suckling weaning transition coincides with dramatic changes in bacterial colonization.²⁸⁻³⁰

One of the most striking so-called 'subtle changes' in *Muc2*^{-/-} mice appears to be the rapid and permanent increase in the number of infiltrating Cd3ε-positive T-cells from P1.5 to P28. The influx of Cd3ε-positive T cells into the colonic mucosa shortly after birth is the first indicator of colitis development in these mice. These data also demonstrate that the inflammatory process in *Muc2*^{-/-} mice is triggered before morphological changes are seen and that *Muc2*^{-/-} mice are predestined to develop colitis. Interestingly, in WT mice an increased influx in Cd3ε-positive T-cells into the colonic mucosa occurred shortly before weaning (P14), which decreased again after weaning (P28). This influx of T-cells might be considered as a physiological phenomenon, as T cells and T cell activity is necessary for intestinal growth during weaning, as reviewed by Cummings et al.³¹

The increase in *Cd45*, *Cd3ε*, *Foxp3* gene expression levels in combination with increased *Il-12 p35*, *Il-12 p40*, *Ebi3*, *Tgfb1*, *Tnfa*, and *Il-10* gene expression levels in the colon of *Muc2*^{-/-} mice before weaning (P14), imply that in *Muc2*^{-/-} mice a vigorous immune response is already developing before weaning. This immune response involves *Cd45*- and *Cd3*-positive T cells and the pro-inflammatory cytokine *Tnf-α* and likely *Il-12* (i.e. a heterodimer of *Il-12 p35* and *Il-12 p40*), and is counter balanced by *Foxp3*-positive Treg cells and the immune suppressive cytokines *Tgfb1*, *Il-10*, and most likely *Il35* (i.e. the heterodimer of *Il12p35* and *Ebi3*). After weaning, at P28, *Foxp3*, *Il-12 p35*, *Tgfb1*, and *Tnf-α* gene expression levels are significantly down-regulated in *Muc2*^{-/-} mice (compared to P14), whereas *Il-10* gene expression levels are maintained. As the immune suppressive cytokine *Il-10* is known as a Th2 cytokine³², these data suggest that after weaning the immune response in *Muc2*^{-/-} mice might be dominated by a Th2 response.

Next, we studied the expression of different Tlrs and Tlr signaling molecules that are involved in recognizing bacterial products in the intestinal lumen. We focused our attention on *Tlr2*, *Tlr4*, and *Tlr9* as these Tlrs enable us to differentiate between responses that are induced by Gram-positive bacteria which mainly induce a TLR2 response, Gram-negative bacteria that signal predominantly through TLR4, and bacterial CpG-DNA motifs which signal via TLR9.³³ Decreased expression of *Tlr2* was seen after weaning, at P28, in *Muc2*^{-/-} mice, correlating with the occurrence of severe signs of colitis. Loss of *Tlr2* has been related to exacerbation of intestinal inflammation.³⁴ Additionally, it has also been demonstrated that *Tlr2* deficiency predisposes to stress-induced injury of tight junction modulated barrier function, leading to perpetuation of mucosal inflammation and apoptosis.³⁵ Thus, besides loss of barrier function due to absence of a protective mucus layer, barrier function might be further impaired in *Muc2*^{-/-} mice by loss of well-functioning tight junctions due to partial *Tlr2* deficiency after weaning.

Although not always significant, expression of *Tlr4* and *Tlr9* was higher in *Muc2*^{-/-} mice before (P14) and after weaning (P28) compared to WT mice. Overexpression of TLR4 is seen in the intestinal mucosa of IBD patients.⁹ In dextran sulfate sodium-induced colitis in mice, *Tlr4* appeared to be involved in the induction of colitis as well as the recovery phase of colitis.³⁶ In *Muc2*^{-/-} mice, increased *Tlr4* mRNA expression and the increased expression of its downstream target IRF3, coincided with aggravation of colitis, suggesting that TLR4 might also play a role in the perpetuation of colitis. Additionally, Obermeier et al. showed that CpG-DNA from endogenous bacteria and thus TLR9 contributes to the perpetuation of chronic intestinal inflammation.³⁷ Therefore, the increased expression of *Tlr9* in *Muc2*^{-/-} mice compared to WT mice might also imply a role for TLR9 in colitis in *Muc2*^{-/-} mice.

Expression levels of *MyD88* mRNA, which forms a signaling complex with the activated Tlrs, were significantly lower in *Muc2*^{-/-} mice at the age 4 weeks compared to 2 weeks. *MyD88* is crucial for the activation of the innate immune defense against

micro-organisms.³⁸⁻⁴⁰ Moreover, it was shown that MyD88^{-/-} mice exhibited increased susceptibility to DSS-induced colitis and that the MyD88-dependent pathway may directly promote the proliferation and survival of colitogenic CD4-positive T cells to sustain chronic colitis, implying a role for MyD88 in colitis.⁴¹⁻⁴² One could speculate that MyD88 expression is down-regulated in 28-day-old Muc2^{-/-} mice to protect the intestinal epithelium from aberrant TLR-signaling due to deviant bacterial colonization, however more studies are necessary to confirm this.

In addition to the molecules involved in the inflammatory response, we studied the function and differentiation of goblet cells during colitis development. Immunohistochemical analysis revealed an increase in Tff3-positive goblet cell numbers in Muc2^{-/-} mice at P28 compared to WT at P28 and Muc2^{-/-} mice at P14. It is highly likely that this increase in goblet cell numbers is due to the observed crypt elongation in Muc2^{-/-} mice, which leads to an increase in epithelial cells in general and thereby also to more goblet cells. The increase in goblet cells is most likely not caused by a predominant differentiation to goblet cells at the expense of other epithelial cell types as *Tff3* gene expression levels normalized to villin (i.e. a gene, which in the colon is mainly expressed by enterocytes) are comparable between Muc2^{-/-} mice and WT at P28 and between Muc2^{-/-} mice at P28 and Muc2^{-/-} mice at P14. Nevertheless, as Tff3 is known to be an important factor that contributes to healing after mucosal injury throughout the gastrointestinal tract⁴³⁻⁴⁶, the increased Tff3-positive goblet cell numbers in Muc2^{-/-} mice at P28, might be a compensatory mechanism stimulating mucosal regeneration.

Finally, Muc2^{-/-} mice hardly show Muc4-positive goblet cells at P14 and P28. Yet, *Muc4* gene expression levels in Muc2^{-/-} mice are comparable with WT mice. In conjunction, these results imply that Muc4 protein secretion is increased in Muc2^{-/-} mice compared to WT mice. This might be caused by a deviant bacterial colonization in Muc2^{-/-} mice compared to WT mice and/or could be caused by inflammatory cytokines that are highly expressed in Muc2^{-/-} mice. Indeed, several *in vitro* and *in vivo* studies confirm that bacterial products and pro-inflammatory cytokines are able to influence mucin synthesis.⁴⁷⁻⁵¹

In conclusion, we demonstrated that diminished epithelial protection due to absence of Muc2, plays a major role in the induction and perpetuation of inflammation in the intestine.

Muc2^{-/-} mice showed an influx of CD3ε⁺-positive T-cells into the colonic mucosa as of P1.5 and progressive crypt lengthening as of weaning, at P21. Before weaning (P14) the pro-inflammatory immune response (i.e. increased *Il-12 p35*, *Il-12 p40*, and *Tnf-α*, expression) in Muc2^{-/-} mice was counter balanced by *Foxp3*-positive Treg cells and the immune suppressive cytokines *Tgfb1*, *Il-10*. In contrast, after weaning (P28) a pro-inflammatory response remained, whereas the immune suppressive response, i.e. *Foxp3* and *Tgfb1* expression, declined. Finally, colitis in Muc2^{-/-} mice aggravated after

weaning as reflected by decreased body weights, further increase in crypt lengthening, and persistent presence of T-cells in the mucosa. Together, these data show that colitis in *Muc2^{-/-}* mice is limited before weaning and exacerbates after weaning suggesting that mother's milk has protective capacities and/or that alterations in the composition of the intestinal microbiota, which occur during the suckling-weaning transition, influence colitis development.

ACKNOWLEDGEMENTS/ GRANTS

This work was supported by the Sophia Foundation for Scientific Research, SSWO Project nr. 559 (Rotterdam, the Netherlands), l'Association François Aupetit (Paris, France) and Danone Research (Friedrichsdorf, Germany).

REFERENCES

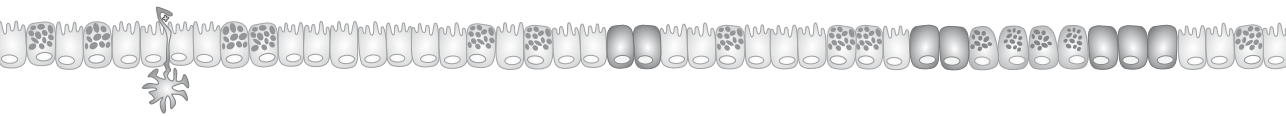
1. Bonen DK, Cho JH. The genetics of inflammatory bowel disease. *Gastroenterology* 2003; 124:521-36.
2. Danese S, Fiocchi C. Etiopathogenesis of inflammatory bowel diseases. *World J Gastroenterol* 2006;12:4807-12.
3. Lin PW, Stoll BJ. Necrotizing enterocolitis. *Lancet* 2006;368:1271-83.
4. Hsueh W, Caplan MS, Qu XW, Tan XD, De Plaen IG, Gonzalez-Crussi F. Neonatal necrotizing enterocolitis: clinical considerations and pathogenetic concepts. *Pediatr Dev Pathol* 2003;6: 6-23.
5. Krediet TG, van Lelyveld N, Vijlbrief DC, Brouwers HA, Kramer WL, Fleer A, Gerards LJ. Microbiological factors associated with neonatal necrotizing enterocolitis: protective effect of early antibiotic treatment. *Acta Paediatr* 2003;92:1180-2.
6. Sangild PT, Siggers RH, Schmidt M, Elnif J, Bjornvad CR, Thymann T, Grondahl ML, Hansen AK, Jensen SK, Boye M, Moelbak L, Buddington RK, Westrom BR, Holst JJ, Burrin DG. Diet- and colonization-dependent intestinal dysfunction predisposes to necrotizing enterocolitis in preterm pigs. *Gastroenterology* 2006;130:1776-92.
7. Sellon RK, Tonkonogy S, Schultz M, Dieleman LA, Grenther W, Balish E, Rennick DM, Sartor RB. Resident enteric bacteria are necessary for development of spontaneous colitis and immune system activation in interleukin-10-deficient mice. *Infect Immun* 1998;66:5224-31.
8. Lotz M, Gutle D, Walther S, Menard S, Bogdan C, Hornef MW. Postnatal acquisition of endotoxin tolerance in intestinal epithelial cells. *J Exp Med* 2006;203:973-84.
9. Cario E, Podolsky DK. Differential alteration in intestinal epithelial cell expression of toll-like receptor 3 (TLR3) and TLR4 in inflammatory bowel disease. *Infect Immun* 2000;68:7010-7.
10. Hausmann M, Kiessling S, Mestermann S, Webb G, Spottl T, Andus T, Scholmerich J, Herfarth H, Ray K, Falk W, Rogler G. Toll-like receptors 2 and 4 are up-regulated during intestinal inflammation. *Gastroenterology* 2002;122:1987-2000.
11. Frolova L, Drastich P, Rossmann P, Klimesova K, Tlaskalova-Hogenova H. Expression of Toll-like receptor 2 (TLR2), TLR4, and CD14 in biopsy samples of patients with inflammatory bowel diseases: upregulated expression of TLR2 in terminal ileum of patients with ulcerative colitis. *J Histochem Cytochem* 2008;56:267-74.
12. Jilling T, Simon D, Lu J, Meng FJ, Li D, Schy R, Thomson RB, Soliman A, Arditi M, Caplan MS. The roles of bacteria and TLR4 in rat and murine models of necrotizing enterocolitis. *J Immunol* 2006;177:3273-82.
13. Leaphart CL, Cavallo J, Gripar SC, Cetin S, Li J, Branca MF, Dubowski TD, Sodhi CP, Hackam DJ. A critical role for TLR4 in the pathogenesis of necrotizing enterocolitis by modulating intestinal injury and repair. *J Immunol* 2007;179:4808-20.
14. Le Mandat Schultz A, Bonnard A, Barreau F, Aigrain Y, Pierre-Louis C, Berrebi D, Peuchmaur M. Expression of TLR-2, TLR-4, NOD2 and pNF-kappaB in a neonatal rat model of necrotizing enterocolitis. *PLoS ONE* 2007;2:e1102.
15. Gripar SC, Sodhi CP, Richardson WM, Anand RJ, Gittes GK, Branca MF, Jakub A, Shi XH, Shah S, Ozolek JA, Hackam DJ. Reciprocal expression and signaling of TLR4 and TLR9 in the pathogenesis and treatment of necrotizing enterocolitis. *J Immunol* 2009;182:636-46.
16. Johansson ME, Phillipson M, Petersson J, Velcich A, Holm L, Hansson GC. The inner of the two Muc2 mucin-dependent mucus layers in colon is devoid of bacteria. *Proc Natl Acad Sci U S A* 2008;105:15064-9.

17. Tytgat KM, van der Wal JW, Einerhand AW, Buller HA, Dekker J. Quantitative analysis of MUC2 synthesis in ulcerative colitis. *Biochem Biophys Res Commun* 1996;224:397-405.
18. Pullan RD, Thomas GA, Rhodes M, Newcombe RG, Williams GT, Allen A, Rhodes J. Thickness of adherent mucus gel on colonic mucosa in humans and its relevance to colitis. *Gut* 1994;35:353-9.
19. Jacobs LR, Huber PW. Regional distribution and alterations of lectin binding to colorectal mucin in mucosal biopsies from controls and subjects with inflammatory bowel diseases. *J Clin Invest* 1985;75:112-8.
20. Renes IB, Van Seuning I. Mucins in intestinal inflammatory diseases: Their expression patterns, regulation, and roles. In: Van Seuning I, ed. *The Epithelial Mucins: Structure/Function. Roles in Cancer and Inflammatory Diseases*. Lille: Research Signpost, 2008:211-232.
21. Schaart MW, de Bruijn AC, Bouwman DM, de Krijger RR, van Goudoever JB, Tibboel D, Renes IB. Epithelial Functions of the Residual Bowel After Surgery for Necrotising Enterocolitis in Human Infants. *J Pediatr Gastroenterol Nutr* 2009.
22. Van der Sluis M, De Koning BA, De Bruijn AC, Velcich A, Meijerink JP, Van Goudoever JB, Buller HA, Dekker J, Van Seuning I, Renes IB, Einerhand AW. Muc2-deficient mice spontaneously develop colitis, indicating that MUC2 is critical for colonic protection. *Gastroenterology* 2006;131:117-29.
23. Verburg M, Renes IB, Meijer HP, Taminiau JA, Buller HA, Einerhand AW, Dekker J. Selective sparing of goblet cells and paneth cells in the intestine of methotrexate-treated rats. *Am J Physiol Gastrointest Liver Physiol* 2000;279:G1037-47.
24. Mashimo H, Wu DC, Podolsky DK, Fishman MC. Impaired defense of intestinal mucosa in mice lacking intestinal trefoil factor. *Science* 1996;274:262-5.
25. Meijerink J, Mandigers C, van de Locht L, Tonnissen E, Goodsaid F, Raemaekers J. A novel method to compensate for different amplification efficiencies between patient DNA samples in quantitative real-time PCR. *J Mol Diagn* 2001;3:55-61.
26. Collison LW, Vignali DA. Interleukin-35: odd one out or part of the family? *Immunol Rev* 2008;226:248-62.
27. Velcich A, Yang W, Heyer J, Fragale A, Nicholas C, Viani S, Kucherlapati R, Lipkin M, Yang K, Augenlicht L. Colorectal cancer in mice genetically deficient in the mucin Muc2. *Science* 2002;295:1726-9.
28. Inoue R, Otsuka M, Ushida K. Development of intestinal microbiota in mice and its possible interaction with the evolution of luminal IgA in the intestine. *Exp Anim* 2005;54:437-45.
29. Davis CP, McAllister JS, Savage DC. Microbial colonization of the intestinal epithelium in suckling mice. *Infect Immun* 1973;7:666-72.
30. Mackie RI, Sghir A, Gaskins HR. Developmental microbial ecology of the neonatal gastrointestinal tract. *Am J Clin Nutr* 1999;69:1035S-1045S.
31. Cummins AG, Thompson FM. Effect of breast milk and weaning on epithelial growth of the small intestine in humans. *Gut* 2002;51:748-54.
32. Laouini D, Alenius H, Bryce P, Oettgen H, Tsitsikov E, Geha RS. IL-10 is critical for Th2 responses in a murine model of allergic dermatitis. *J Clin Invest* 2003;112:1058-66.
33. Takeuchi O, Hoshino K, Kawai T, Sanjo H, Takada H, Ogawa T, Takeda K, Akira S. Differential roles of TLR2 and TLR4 in recognition of gram-negative and gram-positive bacterial cell wall components. *Immunity* 1999;11:443-51.

34. Rakoff-Nahoum S, Paglino J, Eslami-Varzaneh F, Edberg S, Medzhitov R. Recognition of commensal microflora by toll-like receptors is required for intestinal homeostasis. *Cell* 2004;118:229-41.
35. Cario E, Gerken G, Podolsky DK. Toll-like receptor 2 controls mucosal inflammation by regulating epithelial barrier function. *Gastroenterology* 2007;132:1359-74.
36. Ungaro R, Fukata M, Hsu D, Hernandez Y, Breglio K, Chen A, Xu R, Sotolongo J, Espana C, Zaia J, Elson G, Mayer L, Kosco-Vilbois M, Abreu MT. A novel Toll-like receptor 4 antagonist antibody ameliorates inflammation but impairs mucosal healing in murine colitis. *Am J Physiol Gastrointest Liver Physiol* 2009;296:G1167-79.
37. Obermeier F, Dunger N, Strauch UG, Hofmann C, Bleich A, Grunwald N, Hedrich HJ, Aschenbrenner E, Schlegelberger B, Rogler G, Scholmerich J, Falk W. CpG motifs of bacterial DNA essentially contribute to the perpetuation of chronic intestinal inflammation. *Gastroenterology* 2005;129:913-27.
38. Albiger B, Sandgren A, Katsuragi H, Meyer-Hoffert U, Beiter K, Wartha F, Hornef M, Normark S, Normark BH. Myeloid differentiation factor 88-dependent signalling controls bacterial growth during colonization and systemic pneumococcal disease in mice. *Cell Microbiol* 2005;7:1603-15.
39. Park SM, Ko HJ, Shim DH, Yang JY, Park YH, Curtiss R, 3rd, Kweon MN. MyD88 signaling is not essential for induction of antigen-specific B cell responses but is indispensable for protection against *Streptococcus pneumoniae* infection following oral vaccination with attenuated *Salmonella* expressing PspA antigen. *J Immunol* 2008;181:6447-55.
40. Leendertse M, Willems RJ, Giebelen IA, van den Pangaart PS, Wiersinga WJ, de Vos AF, Florquin S, Bonten MJ, van der Poll T. TLR2-dependent MyD88 signaling contributes to early host defense in murine *Enterococcus faecium* peritonitis. *J Immunol* 2008;180:4865-74.
41. Tomita T, Kanai T, Fujii T, Nemoto Y, Okamoto R, Tsuchiya K, Totsuka T, Sakamoto N, Akira S, Watanabe M. MyD88-dependent pathway in T cells directly modulates the expansion of colitogenic CD4⁺ T cells in chronic colitis. *J Immunol* 2008;180:5291-9.
42. Araki A, Kanai T, Ishikura T, Makita S, Uraushihara K, Iiyama R, Totsuka T, Takeda K, Akira S, Watanabe M. MyD88-deficient mice develop severe intestinal inflammation in dextran sodium sulfate colitis. *J Gastroenterol* 2005;40:16-23.
43. Suemori S, Lynch-Devaney K, Podolsky DK. Identification and characterization of rat intestinal trefoil factor: tissue- and cell-specific member of the trefoil protein family. *Proc Natl Acad Sci U S A* 1991;88:11017-21.
44. Thim L, May FE. Structure of mammalian trefoil factors and functional insights. *Cell Mol Life Sci* 2005;62:2956-73.
45. Hoffmann W. Trefoil factors TFF (trefoil factor family) peptide-triggered signals promoting mucosal restitution. *Cell Mol Life Sci* 2005;62:2932-8.
46. Taupin D, Podolsky DK. Trefoil factors: initiators of mucosal healing. *Nat Rev Mol Cell Biol* 2003;4:721-32.
47. Andrianifahanana M, Moniaux N, Batra SK. Regulation of mucin expression: mechanistic aspects and implications for cancer and inflammatory diseases. *Biochim Biophys Acta* 2006;1765:189-222.
48. Enss ML, Schmidt-Wittig U, Muller H, Mai UE, Coenen M, Hedrich HJ. Response of germfree rat colonic mucous cells to peroral endotoxin application. *Eur J Cell Biol* 1996;71:99-104.

49. Mejias-Luque R, Peiro S, Vincent A, Van Seuning I, de Bolos C. IL-6 induces MUC4 expression through gp130/STAT3 pathway in gastric cancer cell lines. *Biochim Biophys Acta* 2008; 1783:1728-36.
50. Iwashita J, Sato Y, Sugaya H, Takahashi N, Sasaki H, Abe T. mRNA of MUC2 is stimulated by IL-4, IL-13 or TNF-alpha through a mitogen-activated protein kinase pathway in human colon cancer cells. *Immunol Cell Biol* 2003;81:275-82.
51. Blanchard C, Durual S, Estienne M, Bouzakri K, Heim MH, Blin N, Cuber JC. IL-4 and IL-13 up-regulate intestinal trefoil factor expression: requirement for STAT6 and de novo protein synthesis. *J Immunol* 2004;172:3775-83.

Chapter 3



Colonic Gene Expression Patterns of Mucin Muc2 Knockout Mice Reveal Various Phases in Colitis Development

Peng Lu, **Nanda Burger-van Paassen**, Maria van der Sluis, Janneke Bouma,
Jean-Pierre Kerckaert, Johannes B. van Goudoever, Isabelle Van Seuningen,
Ingrid B. Renes

Manuscript in preparation



ABSTRACT

Mucin Muc2 knockout (Muc2^{-/-}) mice spontaneously develop colitis. To identify genes, and biological responses which play a pivotal role during colitis development in Muc2^{-/-} mice, gene expression profiles of colonic tissues from 2- and 4-week-old Muc2^{-/-} and wild type (Muc2^{+/+}) mice were determined using microarrays. The majority of highly upregulated genes in both 2-week-old and 4-week-old Muc2^{-/-} mice, were primarily involved in immune responses related to antigen processing/presentation, B-cell and T-cell receptor signaling, leukocyte transendothelial migration, and Jak-STAT signaling. Specifically, Muc2^{-/-} mice expressed high mRNA levels of immunoglobulins, murine histocompatibility-2, pro-inflammatory cytokines, chemokines, and antimicrobial proteins. Additionally, in 4-week-old Muc2^{-/-} mice, expression of genes involved in cell structure related pathways were significantly altered. Particularly, the tight junction-associated gene claudin-10 was up-regulated, whereas claudin-1 and claudin-5 were down-regulated. Furthermore, 4-week-old Muc2^{-/-} mice showed increased expression of genes regulating cell growth together with increased crypt length and increased epithelial proliferation. In conclusion, Muc2-deficiency leads to an active inflammatory response in 2- and 4-week-old Muc2^{-/-} mice, as demonstrated by the altered expression in immune response related genes. In addition, 4-week-old Muc2^{-/-} mice also showed a decrease in epithelial barrier function, and an increase in epithelial proliferation as indicated by, respectively, the altered expression in tight junction related genes and up-regulation of genes stimulating cell growth. Remarkably, up-regulation of genes stimulating cell growth correlated with increased crypt length and increased epithelial proliferation in 4-week-old Muc2^{-/-} mice. Together, these data demonstrate that there are distinct phases in colitis development in Muc2^{-/-} mice.

Key words: Muc2, colitis, microarray, proliferation, immune response, inflammatory response

INTRODUCTION

The intestinal tract constitutes the second largest body surface area, and enormous amounts of food pass through the intestinal tract.¹ The intestinal tract is a thermostable and nutrient rich environment, and comprises approximately 10^{14} bacteria, including both commensal flora and pathogens.² In the small intestine, luminal fluids can kill most ingested microorganisms, and the phasic propulsive motor activity pushes the food together with the unattached bacteria towards the ileal end, so there are only a few species of bacteria in the small intestine. However, the colon contains a high density of living bacteria and the bacteria contribute around 60% of faecal solids.³⁻⁴ The mechanical stress, diet-derived toxins, and pathogens and their products all provide a threat to the integrity of the intestinal tract. In order to cope with these continuous threats, and to maintain mucosal homeostasis, the intestinal epithelium and the underlying mucosa have developed certain defense mechanisms.

Epithelial defense plays an important role and provides protection against inflammatory diseases and cancer. With respect to epithelial defense, the intestinal mucus layer, which forms a physical barrier, is the first defense barrier against luminal substances.⁵⁻⁷ Colonic mucus consists of two layers extending above the epithelial cells; the densely packed inner layer and the expanded outer layer.⁸ The inner layer firmly attaches to the epithelium and forms the physical barrier against bacteria. In contrast, the outer layer is movable and allows the colonization of commensal flora and prevents attachment of pathogens.⁸⁻⁹ Mucins are the principal component of intestinal mucus.¹⁰ The most abundant secretory mucin in the intestinal epithelium of humans and mice is the mucin MUC2¹¹⁻¹³, a high molecular weight glycoprotein expressed by goblet cells.¹⁴

In patients with ulcerative colitis, the number of goblet cells is reduced, and both MUC2 synthesis and secretion are significantly decreased.¹⁵⁻¹⁷ Deficiency of Muc2, as in Muc2^{-/-} mice, results in the absence of recognizable goblet cells along the entire length of the colon and absence of the protective colonic mucus layer.^{8,18} Therefore, bacteria are in direct contact with the intestinal epithelial cells of these mice.⁸ Muc2-deficiency not only affects the protective capacities of the mucus layer, but also leads to colonic inflammation, characterized by mucosal thickening, loss of epithelial integrity, and an increased influx of immune cells. Additionally, the morphological changes in the colon occurred earlier and were more severe in the distal colon than in proximal colon and small intestine.¹⁹

In the present study we aimed to gain insight in the development of colitis in Muc2^{-/-} mice. We hypothesize that biological responses and, therefore, gene expression profiles, are different in 2-week-old versus 4-week-old Muc2^{-/-} mice. To investigate colitis development and biological responses, gene expression profiling was combined with quantitative real-time polymerase chain reaction (qRT-PCR), and (immuno)histochemical

analysis. By using these approaches, in conjunction, we were able to correlate changes in gene expression, with morphological changes and obtained more insight in colitis development in *Muc2*^{-/-} mice.

MATERIALS AND METHODS

Animals

Muc2^{-/-} mice were bred as previously described.¹⁹ All mice were housed in the same specific pathogen-free environment with free access to standard rodent pellets (Special Diets Services, Witham, Essex, England) and acidified tap water in a 12-hour light/dark cycle. All animal care and procedures were conducted according to institutional guidelines (Erasmus MC Animal Ethics Committee, Rotterdam, the Netherlands). Wild-type and *Muc2*^{-/-} mice were tested negative for *Helicobacter hepaticus* and norovirus infection.

Experimental setup

At the ages of 2 and 4 weeks *Muc2*^{-/-} (n=5 per time point) and *Muc2*^{+/+} (n=5 per time point) were sacrificed. Bromodeoxyuridine (BrdU) (Sigma Chemical Co, St Louis, MO) was administered to each animal intraperitoneally (30 mg/kg body weight) one hour before sacrifice to study epithelial proliferation. The distal colon was excised immediately and either fixed in 4% paraformaldehyde in phosphate-buffered saline (PBS) or stored in RNeasy (Qiagen, Venlo, the Netherlands) at -20°C.

RNA isolation and microarray analysis

RNA was isolated using the QIAamp RNA midi-kit (Qiagen, Venlo, the Netherlands) following the manufacturer's protocol. RNA quality was assessed by gel electrophoresis and spectrophotometry. Reverse transcription, cDNA labelling, hybridization of arrays, and scanning were performed by using standard protocols. Individual RNA samples of distal colon from 2- and 4-week-old *Muc2*^{-/-} (n=5 per time point) and *Muc2*^{+/+} mice (n=5 per time point) were analyzed using mouse gene expression microarrays (Mouse GE 4X 44K Microarrays, Agilent Technologies, Palo Alto, CA). GeneSpring GX 10.0.2 software was used to analyze data and perform gene ontology (GO) analysis. Principal component analysis and quality controls metrics plot showed that the quality of data of one of the 4-week-old *Muc2*^{+/+} mice was poor, and therefore data from this mouse was further excluded from analysis. Genes from *Muc2*^{-/-} mice with normalized data values 2-fold above or below the values from *Muc2*^{+/+} mice, were selected to populate the Kyoto encyclopedia of genes and genomes (KEGG) pathways using Pathway Express software.²⁰

Quantitative real-time PCR

Total RNA (1.5 µg) was used to prepare cDNA. Quantitative real-time PCR (qRT-PCR) analysis was performed as previously described.²¹ Briefly, The cDNA from each mouse was used as a template, and SYBR Green was used as intercalation. mRNA expression levels were normalized against β -Actin (*Actb*) expression of each mouse. All primers are given in the *Supplementary Information* (SI Table 1).

Histology and immunohistochemistry

Histological and immunohistochemical analysis were applied as previously described²² using the Vectastain Elite ABC kit (Vector Laboratories, Burlingame, CA) and 3,3'-diaminobenzidine as staining reagent. Briefly, tissue fixed in 4% paraformaldehyde in PBS was embedded in paraffin and cut into 5-µm-thick sections. Antigen unmasking was carried out by heating the sections for 20 min in 0.01 M sodium citrate (pH 6.0; Merck,

Table 1. Gene Ontology Analysis of 2-week-old Muc2^{-/-} vs. Muc2^{+/+} Mice

GO Term	Corrected p-value	Differentially Expressed Genes	GO Accession
Cellular component			
Plasma membrane	1.68E-04	30	GO:0005886
External side of plasma membrane	1.16E-03	14	GO:0009897
Extracellular region part	7.70E-03	68	GO:0044421
Plasma membrane part	9.55E-03	46	GO:0044459
Extracellular region	1.12E-02	71	GO:0005576
Extracellular space	1.65E-02	68	GO:0005615
Biological process			
Immune response	1.16E-24	51	GO:0006955
Immune system process	3.66E-23	56	GO:0002376
Defense response	4.66E-08	32	GO:0006952 GO:0002217 GO:0042829
Antigen processing and presentation	1.19E-03	11	GO:0019882 GO:0030333
Response to stimulus	2.58E-03	76	GO:0050896 GO:0051869
Response to stress	5.23E-03	36	GO:0006950
Humoral immune response	1.35E-02	8	GO:0006959
Response to external stimulus	2.47E-02	20	GO:0009605
Inflammatory response	3.63E-02	14	GO:0006954
Response to wounding	3.76E-02	16	GO:0009611 GO:0002245
Molecular function			
Antigen binding	4.41E-10	12	GO:0003823
Cytokine binding	4.44E-02	7	GO:0019955

Darmstadt, Germany) at 100°C. To detect S100a8 and S100a9, anti-mouse S100a8 and anti-mouse S100a9 antibodies (**R&D Systems Europe Ltd.**, Abingdon, United Kingdom) were used (1:1000 diluted in PBS).

Cell culture and LPS treatment

The murine colonic epithelial cell line CMT-93 was cultured in a 37°C incubator with 5 % CO₂ in Dulbecco's modified Eagle's minimal essential medium supplemented with 10 % foetal calf serum, 50 µg/ml streptomycin, 50 U/ml penicillin and 2 mM L-glutamine. The CMT-93 cells were treated with 10 µg/ml lipopolysaccharides (LPS) from *Escherichia coli* 055:B5 (Sigma Aldrich, the Netherlands). Total RNA was isolated using NucleoSpin® RNA II kit (Macherey-Nagel, the Netherlands). The cDNA synthesis and qRT-PCR were performed as described above.

Statistical analysis

Statistical analysis of microarray results was performed using GeneSpring GX 10.0.2 software. The list of highly regulated genes was narrowed to those genes with statistically significant differences (Asymptotic *p*-value computation, Benjamini-Hochberg correction, *t*-test unpaired, *p*-value cut-off 0.05) and fold change of more than 2 folds. All other data are expressed as mean ± SEM. *P* values were calculated using one-way ANOVA or two-tailed Student's *t*-test. The data were considered statistically significant at *P* < 0.05.

RESULTS

Altered gene expression between *Muc2*^{-/-} and *Muc2*^{+/+} mice

Gene expression profile analysis revealed that in 2-week-old *Muc2*^{-/-} mice, 363 genes (417 probes) were significantly up-regulated and 107 genes (126 probes) were significantly down-regulated more than two fold, compared to 2-week-old *Muc2*^{+/+} mice (SI Table 2). The majority of the up-regulated genes were related to innate and adaptive immune responses. More than 70 genes related to immunoglobulin heavy chain and light chain were up-regulated. Several genes involved in murine histocompatibility 2 (*H2-Aa*, *H2-Ab1*, *H2-DMb1*, *H2-DMb2*, *H2-Q8*, *H2-Q9*, *H2-Q10* and *H2-T24*) were up-regulated. Genes that showed the highest extend of down-regulation were mainly related with plasma triglyceride catabolism and ion transport.

The gene expression profiles of the 4-week-old mice showed that 572 genes (644 probes) were induced and 1130 genes (1274 probes) were repressed more than two fold in *Muc2*^{-/-} mice compared with *Muc2*^{+/+} mice (SI Table 3). In total 166 genes were up-regulated in both 2- and 4-week-old *Muc2*^{-/-} mice (Figure 1A). The majority of the highest up-regulated genes were similar in *Muc2*^{-/-} mice at both ages, and are related

Table 2. Gene Ontology Analysis of 4-week-old Muc2^{-/-} vs. Muc2^{+/+} Mice

GO Term	Corrected p-value	Differentially Expressed Genes	GO Accession
Cellular component			
Extracellular region part	8.34E-23	298	GO:0044421
Extracellular region	6.20E-22	310	GO:0005576
Extracellular space	6.63E-19	275	GO:0005615
Proteinaceous extracellular matrix	2.27E-11	60	GO:0005578
Extracellular matrix	5.09E-11	60	GO:0031012
Extracellular matrix part	1.46E-07	28	GO:0044420
Basement membrane	4.37E-05	18	GO:0005604
Synapse	3.80E-02	24	GO:0045202
Biological process			
Biological adhesion	4.37E-05	82	GO:0022610
Cell adhesion	4.37E-05	82	GO:0007155
Anatomical structure development	5.97E-04	104	GO:0048856
Multicellular organismal development	1.10E-03	137	GO:0007275
Developmental process	1.72E-03	149	GO:0032502
Behavior	7.83E-03	29	GO:0007610
Anatomical structure morphogenesis	4.18E-02	57	GO:0009653
Phosphate transport	4.60E-02	20	GO:0006817
Molecular function			
Calcium ion binding	3.36E-06	118	GO:0005509
Endoribonuclease activity, producing 3'-phosphomonoesters	2.23E-02	10	GO:0016892
Insulin-like growth factor binding	3.57E-02	10	GO:0005520
Pancreatic ribonuclease activity	3.86E-02	9	GO:0004522
Endonuclease activity, active with either ribo- or deoxyribonucleic acids and producing 3'-phosphomonoesters	4.60E-02	10	GO:0016894
Extracellular matrix structural constituent	8.45E-02	17	GO:0005201

to innate and adaptive immune responses (SI Table 3). In contrast, only 47 genes were down-regulated in Muc2^{-/-} mice at both ages (Figure 1B), and highly down-regulated genes of 4-week-old Muc2^{-/-} mice were different from those of 2-week-old Muc2^{-/-} mice (SI Table 3). Moreover, the most down-regulated genes in 4-week-old Muc2^{-/-} mice are associated with a variety of functions, including glucose homeostasis, cation transport, protein targeting, electron transport and fatty acid metabolism.

To further characterize the functional significance of genes expressed in Muc2^{-/-} mice, we performed gene ontology (GO) term analysis with a cut-off *p* value of <0.05

Table 3. Selected KEGG Pathway of Muc2^{-/-} vs. Muc2^{+/+} Mice

Pathway Name	Differentially Expressed Genes	
	2-week-old	4-week-old
Immune/Inflammatory Response		
Antigen processing and presentation	10	4
B cell receptor signaling pathway	5	7
T cell receptor signaling pathway	8	8
Leukocyte transendothelial migration	7	10
Jak-STAT signaling pathway	6	12
MAPK signaling pathway	5	26
Cell Structure		
Adherens junction	0	6
Focal adhesion	3	25
Regulation of actin cytoskeleton	6	23
Gap junction	0	10
Tight junction	2	10
Cell Growth		
Cell cycle	1	10
DNA replication	0	5
Cancer		
Pathways in cancer	5	30
Colorectal cancer	1	6

and KEGG pathway analysis. GO analysis revealed that differentially expressed gene sets in 2-week-old, as well as 4-week-old Muc2^{-/-} mice, were specifically enriched for the GO terms “plasma membrane” and “extracellular region”, which are part of the GO domain “cellular component”. However, in 4-week-old Muc2^{-/-} mice more genes were involved in these GO terms than those in 2-week-old Muc2^{-/-} mice (Tables 1 and 2). In contrast, gene sets associated with the GO domains “biological processes” and “molecular functions” were different between the 2- and 4-week-old Muc2^{-/-} mice. Specifically, within the GO domain “biological processes”, 2-week-old Muc2^{-/-} mice showed genes involved in “immune response”, “immune system response”, and “defense response”, whereas 4-week-old Muc2^{-/-} mice displayed genes associated with “biological adhesion”, “cell adhesion”, and “anatomical structure development”. With respect to the GO domain “molecular functions”, gene sets involved in “antigen binding” were specifically enriched in 2-week-old Muc2^{-/-} mice and genes associated with the GO terms “calcium ion binding” were enriched in 4-week-old Muc2^{-/-} mice. KEGG pathway analysis results corroborate the data obtained by GO term analysis. More specifically, KEGG pathway analysis revealed strong immune and inflammatory responses in both 2- and 4-week-old

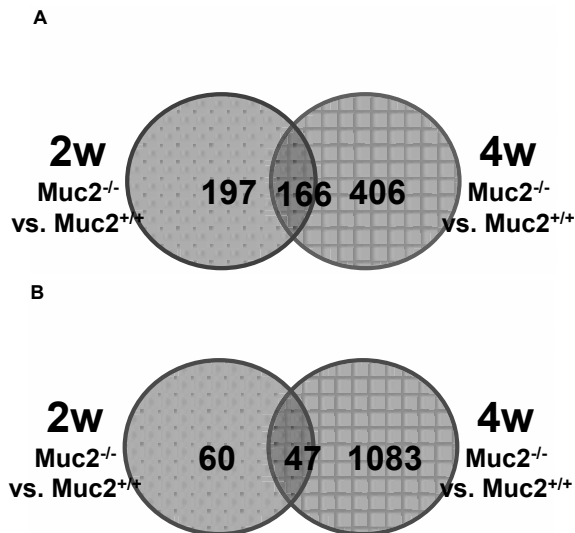


Figure 1. Venn diagram of the number of genes up-regulated (A) and down-regulated (B) in 2-week-old (2w) and 4-week-old (4w) *Muc2*^{-/-} mice compared with *Muc2*^{+/+} mice.

Muc2^{-/-} mice compared with their age related *Muc2*^{+/+} littermates. Similar to GO analysis, KEGG pathway analysis also revealed changes in cell structure and cell growth pathways mainly in 4-week-old *Muc2*^{-/-} mice and to a lesser extent in 2-week-old *Muc2*^{-/-} mice (Table 3).

Changes in inflammatory cytokines and chemokines

Muc2-deficiency significantly modulated the expression of several inflammatory cytokines and chemokines. The pro-inflammatory cytokine tumor necrosis factor α (*Tnf*) was highly up-regulated in *Muc2*^{-/-} mice, which suggests an increased inflammatory response. Further analysis revealed that several *Tnf*-receptor superfamily members (*Tnfrsf1b*, *Tnfrsf13b* and *Tnfrsf17*) were up-regulated as well. QRT-PCR analysis corroborated the microarray results, as *Tnf* transcription was increased in both 2- and 4-week-old *Muc2*^{-/-} mice (Figure 2A). We subsequently analyzed expression levels of genes involved in shedding of *Tnf* (i.e *Tnf* shedding enzymes). There were no significant differences in mRNA levels of a disintegrin and metalloproteinase 17 (*Adam17*), matrix metalloproteinase 10 (*Mmp10*), and matrix metalloproteinase 7 (*Mmp7*) between *Muc2*^{-/-} and *Muc2*^{+/+} mice at both ages (data not shown). However, expression of tissue inhibitor of metalloproteinase 3 (*Timp3*), the inhibitor of *Adam17*, was significantly decreased (Figure 2B). *Tnfrsf1b* transcription was significantly increased in 2-week-old *Muc2*^{-/-} mice compared with age related *Muc2*^{+/+} mice, but there were no differences between *Muc2*^{-/-} mice and *Muc2*^{+/+} mice at the age of 4 weeks (Figure 1C). The induction of *Tnf* transcription by bacterial-epithelial contact was mimicked *in vitro* using the murine colonic epithelial cell line CMT-93 and the bacterial

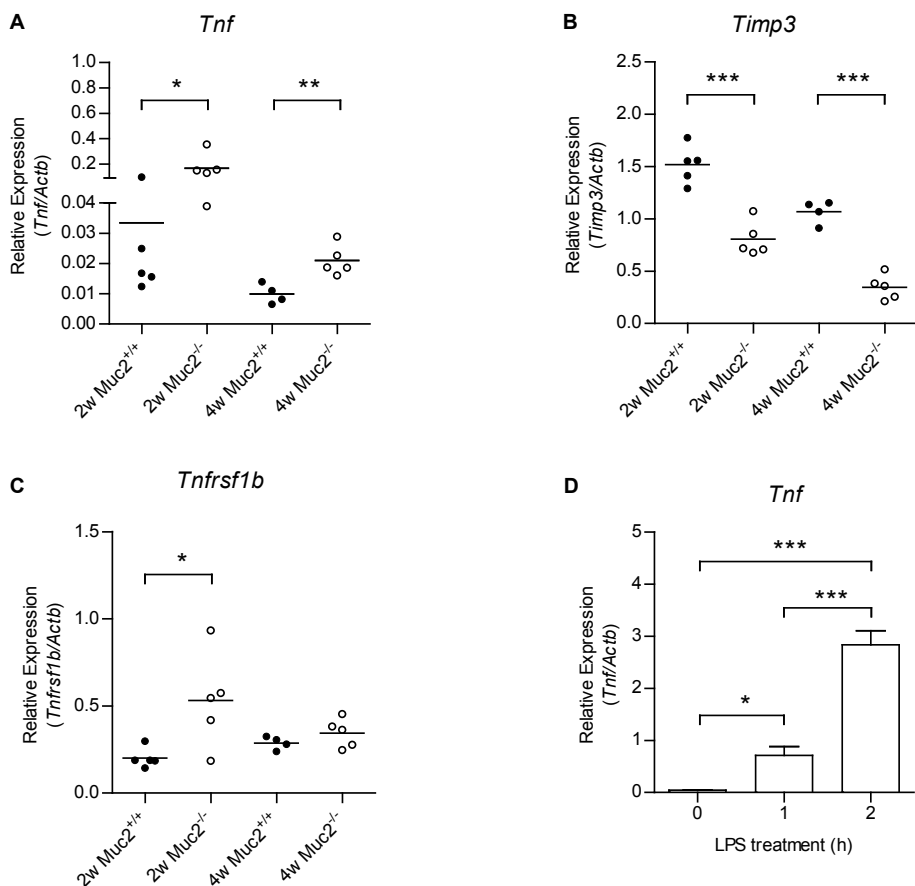


Figure 2. Expression of *Tnf* and *Tnf* related genes in distal colon of *Muc2*^{-/-} mice and LPS-stimulated CMT-93 cells.

Expression of *Tnf* (A), *Timp3* (B) and *Tnfrsf1b* (C) in distal colon of 2- and 4-week-old *Muc2*^{+/+} and *Muc2*^{-/-} mice was quantified with qRT-PCR. (D) CMT-93 cells were treated with 10 μ g/ml LPS for desired time, and the mRNA expression of *Tnf* was quantified with qRT-PCR.

product LPS. Namely, LPS treatment of CMT-93 cells induced a dramatic increase of *Tnf* mRNA (Figure 1D).

In 4-week-old *Muc2*^{-/-} mice, the expression of another pro-inflammatory cytokine interleukin 1 β (*Il1b*) was increased. *Muc2* deficiency also modulated gene expression levels of other cytokines. For example, interleukin 18 binding protein (*Il18bp*) and the receptors for Il-2, Il-12 and Il-20 were induced, whereas Il-15, Il-17D and Il-17F and receptors for Il-5 and Il-17 were repressed in 4-week-old *Muc2*^{-/-} mice. In 2-week-old *Muc2*^{-/-} mice, *Il18bp* and the receptors of Il-2, Il-5, Il-7 and Il-12 was up-regulated.

In addition to altering the expression of cytokines, *Muc2* deficiency induced the expression of several chemokines and chemokine related genes. In 2-week-old *Muc2*^{-/-}

mice, up-regulated genes included chemokine ligands (*Ccl7*, *Ccl8*, *Ccl20*, *Cxcl9* and *Cxcl13*) and chemokine receptors (*Ccr2* and *Ccr10*), whereas the chemokine ligand *Ccl24* was down-regulated. In 4-week-old *Muc2*^{-/-} mice, chemokine ligand 8 (*Ccl8*) and chemokine receptor 10 (*Ccr10*) were up-regulated, and chemokine ligands (*Ccl24* and *Ccl27*) and chemokine receptors (*Ccr1* and *Ccr2*) were down-regulated.

The downstream signaling pathways used by these cytokines and chemokines were also altered in 4-week-old *Muc2*^{-/-} mice. Specifically, dual-specificity phosphatase 9 (*Dusp9*), the inhibitor of the mitogen-activated protein kinase (MAPK) pathway²³, was up-regulated in these mice. Additionally, *Muc2* deficiency altered the mRNA expression of genes in the Jak-STAT signaling pathway, as in 4-week-old *Muc2*^{-/-} mice, *Jak3* was up-regulated along with *Stat1*, and the repressor of Jak-STAT signaling *Socs2* was down-regulated, which all point to an active immune response.

Changes in antimicrobial proteins

As a consequence of *Muc2* deficiency, the gene expression levels of several antimicrobial proteins were up-regulated. The two most highly up-regulated genes, in 2-week-old as

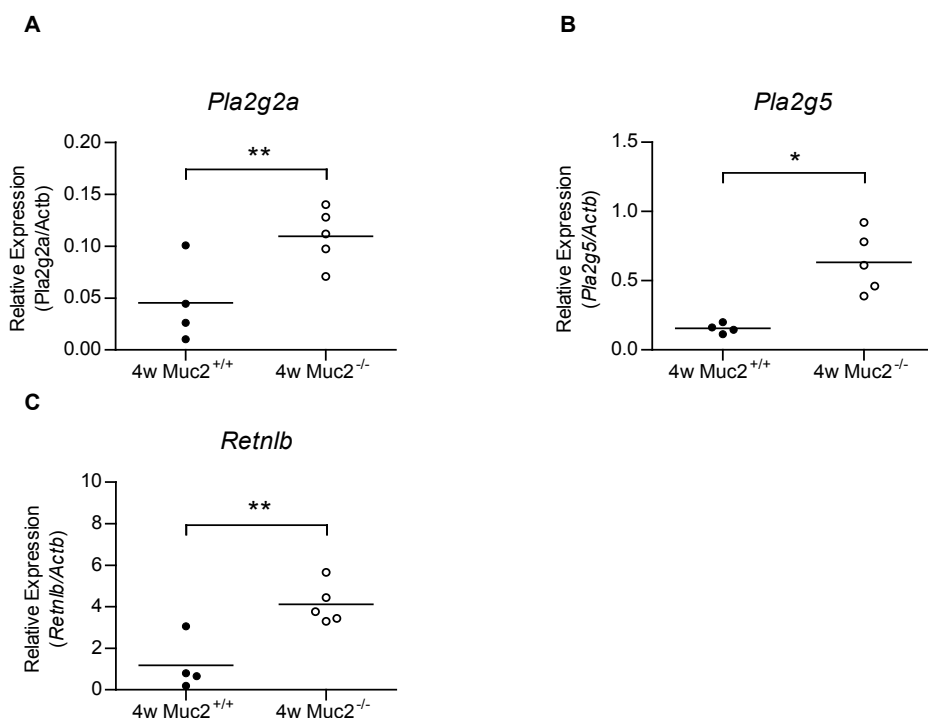


Figure 3. Increased expression of antibacterial peptides in distal colon of *Muc2*^{-/-} mice. Expression of *Pla2g2a* (A), *Pla2g5* (B) and *Retnlb* (C) in distal colon of 4-week-old *Muc2*^{+/+} and *Muc2*^{-/-} mice was quantified with qRT-PCR.

well as 4-week-old *Muc2*^{-/-} mice, were pancreatitis-associated protein (*Pap*) and regenerating islet-derived 3 gamma (*Reg3g*). Both are antimicrobial proteins which directly bind their bacterial targets via interactions with peptidoglycan carbohydrate.²⁴ *Muc2*^{-/-} mice also expressed high levels of other antimicrobial proteins including phospholipase A2 (*Pla2g2a* and *Pla2g5*) and resistin like beta (*Retnlb*). Gene expression levels of *Pla2g2a*, *Pla2g5* and *Retnlb* in 4-week-old mice were confirmed with qRT-PCR (Figure 3).

S100 calcium binding proteins are also important antimicrobial proteins which show altered gene expression patterns in *Muc2*^{-/-} mice. Specifically, in 4-week-old *Muc2*^{-/-} mice,

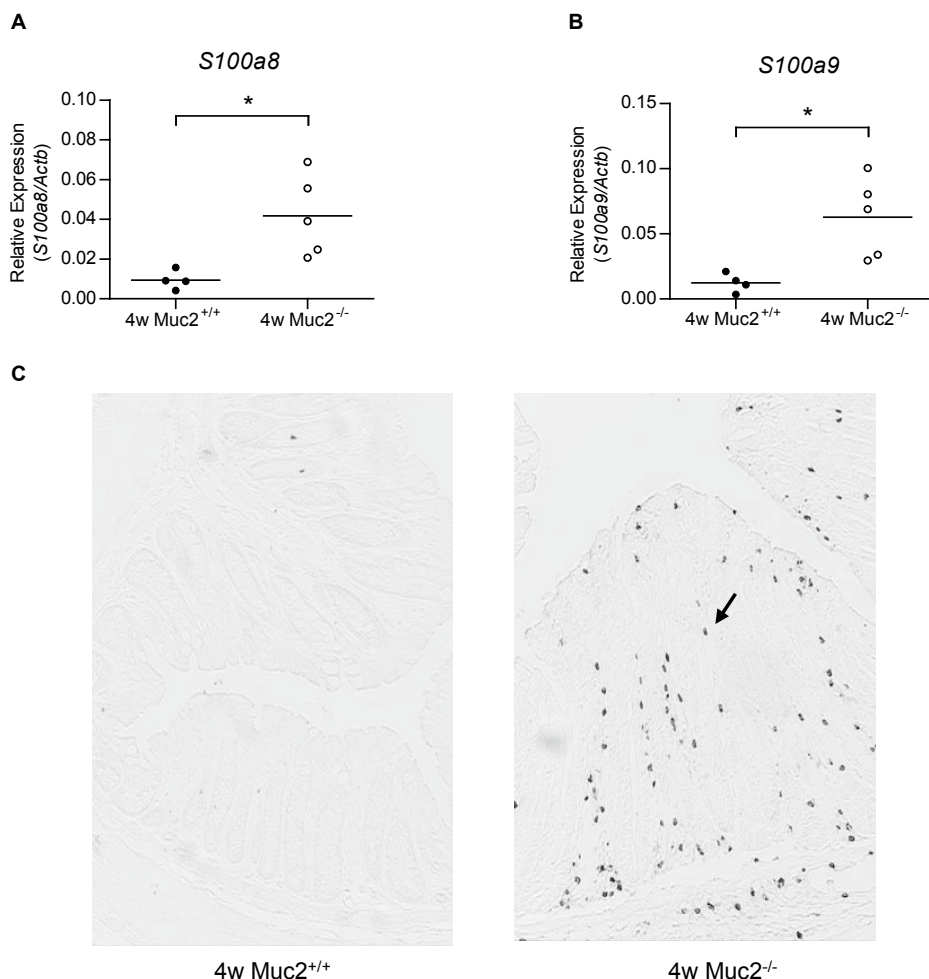


Figure 4. Expression of S100 proteins is up-regulated in distal colon of *Muc2*^{-/-} mice. Expression of *S100a8* (A) and *S100a9* (B) in distal colon of 4-week-old *Muc2*^{+/+} and *Muc2*^{-/-} mice was quantified with qRT-PCR. (C) Representative sections presenting *S100a8* localization in the distal colon of 4-week-old *Muc2*^{+/+} and *Muc2*^{-/-} mice, detected with anti-*S100a8* antibody. The arrow indicates the positive stained cells. (See Color Section, p. 235.)

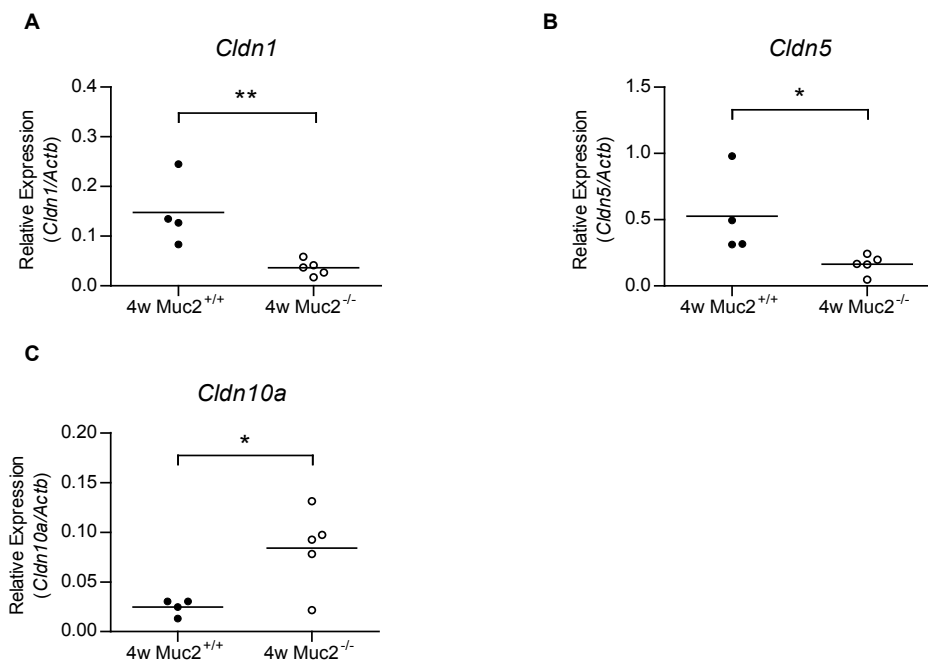


Figure 5. Claudin gene expression is altered in distal colon of Muc2^{-/-} mice. Expression of *Cldn1* (A), *Cldn5* (B) and *Cldn10a* (C) in distal colon of 4-week-old Muc2^{+/+} and Muc2^{-/-} mice was quantified with qRT-PCR

S100a8 and *S100a9* gene expression levels were significantly up-regulated (Figure 4A and 4B). Moreover, immunohistochemical analysis showed that the expression of S100a8 protein in the distal colon of Muc2^{-/-} mice was higher than that of Muc2^{+/+} mice, which hardly showed any S100a8-positive cells (Figure 4C).

Changes in cell structure

As already mentioned above, in 4-week-old Muc2^{-/-} mice, more genes involved in the GO terms related to extracellular changes, compared with 2-week-old Muc2^{-/-} mice (Tables 1 and 2). KEGG pathway analysis supported that Muc2 deficiency leads to an altered expression of genes involved in the cell structure pathways at the age of 4 weeks (Table 3). Among them were genes responsible for adherens junction, actin cytoskeleton, gap junction and tight junction. Moreover, Muc2 deficiency induced the altered expression of 23 cytoskeleton genes. The repression of *Cldn1* and *Cldn5*, which have been shown to increase the transepithelial resistance²⁵⁻²⁷. The altered expression of *Cldn1*, *Cldn5* and *Cldn10a* was confirmed with qRT-PCR (Figure 5).

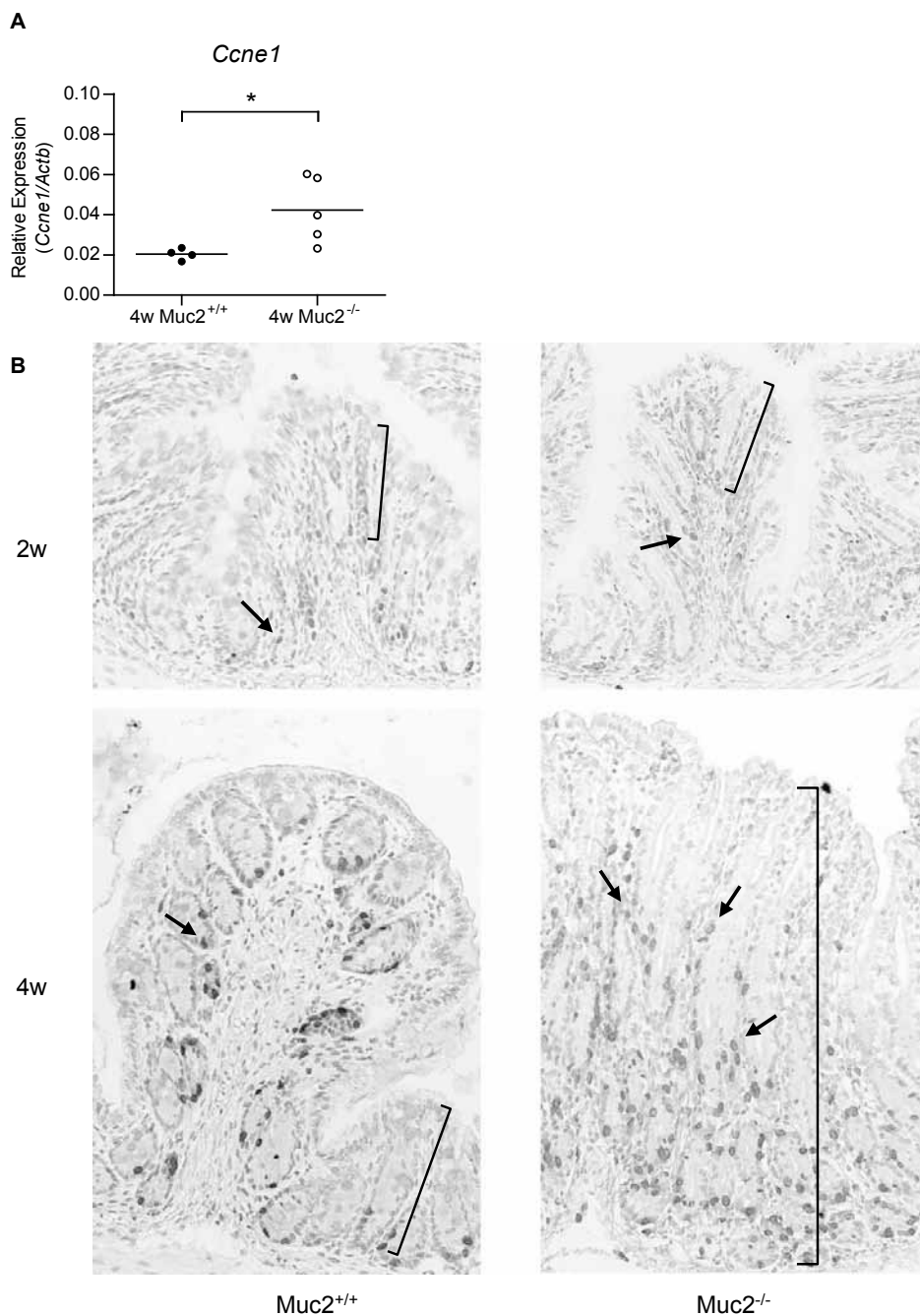


Figure 6. Increased proliferation in the distal colon of *Muc2*^{-/-} mice.
(A) Expression of *Ccne1* in distal colon of 4-week-old *Muc2*^{+/+} and *Muc2*^{-/-} mice was quantified with qRT-PCR. (B) Representative BrdU stained sections of distal colon of 2- and 4-week-old *Muc2*^{+/+} and *Muc2*^{-/-} mice. The arrow indicates the positive stained cells, and the square bracket shows the crypt region. (See Color Section, p. 236.)

Changes in cell proliferation

KEGG pathway analysis revealed that 10 genes involved in the cell cycle pathway and 5 genes related to DNA replication pathway were regulated in 4-week-old *Muc2*^{-/-} mice (Table 3). DNA helicase HCM complex (*Mcm2*, *Mcm3* and *Mcm5*), DNA polymerase *Pola2* and endonuclease *Fen1* were up-regulated, which indicate increased DNA replication and thus proliferation. Detailed examination of the genes involved in cell cycle pathways also revealed accelerated transition from G1 to S phase, as E2F transcription factor 1 (*E2f1*) and cyclin E1 (*Ccne1*) were significantly up-regulated. The increased expression of *Ccne1* was confirmed with qRT-PCR (Figure 6A). Cell division cycle 6 homolog (*Cdc6*) was also up-regulated in 4-week-old *Muc2*^{-/-} mice, which supports the enhanced DNA replication. In contrast to 4-week-old *Muc2*^{-/-} mice, in 2-week-old *Muc2*^{-/-} mice only one gene involved in the cell cycle pathway was altered (Table 3), which supports the hypothesis of increased proliferation in 4-week-old *Muc2*^{-/-} mice, and most likely not in 2-week-old *Muc2*^{-/-} mice. To confirm this we performed (immuno)histochemical analyses, which showed that 2-week-old *Muc2*^{-/-} and *Muc2*^{+/+} mice had comparable crypt lengths and comparable numbers of BrdU-positive epithelial cells, whereas 4-week-old *Muc2*^{-/-} mice showed increased crypt lengths and increased numbers of BrdU-positive epithelial cells compared with age related *Muc2*^{+/+} mice (Figure 6B). Finally, KEGG pathway analysis demonstrated that 30 cancer-related genes were differentially expressed in 4-week-old *Muc2*^{-/-} mice compared with only 5 genes in 2-week-old *Muc2*^{-/-} mice (Table 3).

DISCUSSION

Intestinal mucins are important in epithelial defense against external stimulation including mechanical stress, commensal flora and pathogens.⁵⁻⁷ In patients with ulcerative colitis, deficiency of MUC2, the major component of intestinal mucins, was significantly correlated with the activity of the mucosal inflammation.¹⁵⁻¹⁷ In the colon of mice lacking *Muc2*, there is direct contact of bacteria with epithelial cells and bacteria even appear to invade the colonic crypts.⁸ *Muc2*^{-/-} mice spontaneously developed colitis and colorectal cancer, which implies an important role of *Muc2* in intestinal protection and defense.^{18-19,28} To more specifically address the protective function of *Muc2* in the suppression of ulcerative colitis and to identify genes and biological responses which play a pivotal role during colitis in *Muc2*^{-/-} mice, we performed gene profiling studies with distal colonic tissue of *Muc2*^{-/-} mice at 2 and 4 weeks of age.

In *Muc2*^{-/-} mice, the mucus layer is absent due to the lack of *Muc2*, and bacteria can directly interact with epithelial cells⁸, thereby activating immune responses. The influx of CD3-positive cells was induced in 2-week-old *Muc2*^{-/-} mice, and showed a further increase in 4-week-old *Muc2*^{-/-} mice (unpublished data) compared to *Muc2*^{+/+} mice.

Gene expression profile analysis showed that large amounts of immunoglobulin and murine histocompatibility 2 were synthesized, suggesting that the antigen presentation pathway was significantly up-regulated in *Muc2*^{-/-} mice at both ages. Besides, the B cell receptor signaling pathway, T cell receptor signaling pathway and leukocyte trans-endothelial migration pathway were altered in *Muc2*^{-/-} mice. Changes in neutrophils, macrophages, mast cells, eosinophils, natural killer cell and dendritic cell related genes were also observed in *Muc2*^{-/-} mice, indicating an active innate immune response against external stress. In accordance with our previous study¹⁹, direct interaction with bacteria significantly modulated the expression of several inflammatory cytokines and immune related pathways. Bacteria can stimulate the production of proinflammatory cytokines such as *Tnf*, which plays a crucial role in the induction of colitis.²⁹⁻³¹ The gene expression of *Tnf* receptor *Tnfrsf1b* expression was also up-regulated in *Muc2*^{-/-} mice, and high levels of *Tnfrsf1b* can mediate inflammation in a ligand-independent fashion.³² *Tnf* can also upregulate other proinflammatory cytokines such as *Il-1β*, thus amplifying the inflammatory signals.^{31,33} In *Muc2*^{-/-} mice, *Tnf* was up-regulated with age and *Il1b* was found to be induced in both 2- and 4-week-old *Muc2*^{-/-} mice. *Il-12* is another important cytokine in the initiation of inflammatory response.³⁴⁻³⁵ Microarray analysis did not show altered *Il12* expression, however, the expression of *Il12r* was induced in *Muc2*^{-/-} mice at both ages, which supports the fact that *Muc2*^{-/-} mice show an increased inflammatory response. Bacterial stimulation and *Il-12* can also induce the expression of interferon- γ .^{29,36} Although there is no direct evidence of increased interferon- γ in *Muc2*^{-/-} mice, several interferon- γ induced genes were up-regulated. *Muc2* deficiency also altered the expression of genes in the Jak-STAT signaling pathway and MAPK pathway.

Responding to the enhanced invasion of bacteria, *Muc2*^{-/-} mice expressed high mRNA levels of antimicrobial proteins including pancreatitis-associated protein²⁴, regenerating islet-derived 3 gamma²⁴, S100 calcium binding proteins³⁷ and phospholipase A2.³⁸⁻³⁹ Resistin like beta, which most likely influences the microbial environment of the colon⁴⁰, was also significantly up-regulated in 4-week-old *Muc2*^{-/-} mice.

GO analysis revealed that the genes which are distributed in the plasma membrane and extracellular region were significantly altered in *Muc2*^{-/-} mice at both ages. However, much more genes were regulated and the *p*-value was more significant in 4-week-old *Muc2*^{-/-} mice, which indicates that *Muc2*-deficiency altered the epithelial structure in those mice. Furthermore, the biological processes were differently changed in 2-week-old compared with 4-week-old *Muc2*^{-/-} mice. The altered biological processes were restricted to immune and inflammatory responses in 2-week-old *Muc2*^{-/-} mice, whereas the 4-week-old *Muc2*^{-/-} mice showed significant changes in cell structure related biological processes including cell adhesion, anatomical structure development and developmental processes. KEGG pathway analysis also revealed that genes associated with adherens junction, actin cytoskeleton, gap junction and tight junction pathways

were significantly altered in 4-week-old Muc2^{-/-} mice, and to a lesser extent in 2-week-old Muc2^{-/-} mice. In fact, the down-regulation of *Cldn1* and *Cldn5* combined with the up-regulation of *Cldn10a* strongly suggests a diminished epithelial barrier function in 4-week-old Muc2^{-/-} mice, since those claudins can alter the epithelial structure and lead to altered transepithelial resistance.^{25-27,41-42} Furthermore, Tnf can also cause barrier loss in cultured intestinal epithelial monolayers⁴³⁻⁴⁴ and intestinal epithelial barrier dysfunction via interaction with Tnfrsf1b.⁴⁵ Finally, more genes involved in DNA replication, G1 to S transition and cancer were up-regulated in 4-week-old Muc2^{-/-} mice, which can also lead the changes in epithelial cell structure. Indeed, we previously demonstrated that Muc2^{-/-} mice showed epithelial cell flattening, lamina propria distortion, and crypt lengthening within the colon.¹⁹

With respect to the colonic morphology, 2-week-old Muc2^{-/-} mice showed normal colonic crypt lengths and cell dividing rate. In contrast, 4-week-old Muc2^{-/-} mice showed, increased crypt lengths and accelerated cell dividing rate of epithelial cells as measured by BrdU incorporation. Interestingly, the changes in crypt lengths and epithelial cell proliferation in 4-week-old Muc2^{-/-} mice was accompanied by up-regulation of genes involved in cell cycle regulation as demonstrated by microarray analysis. Lastly, 30 cancer-related genes were differentially expressed in 4-week-old Muc2^{-/-} mice compared with only 5 genes in 2-week-old Muc2^{-/-} mice. Taken together, the development of colitis and possibly cancer development is highly associated with the differentially expressed genes in Muc2^{-/-} mice at different ages. In fact, our data strongly imply that during aging of Muc2^{-/-} mice colitis exacerbates and the risk to develop cancer significantly increases.

In summary, Muc2-deficiency leads to an active inflammatory response in 2- and 4-week-old mice as demonstrated by the altered expression in immune response related genes. Additionally, 4-week-old Muc2^{-/-} mice show a decrease in epithelial barrier function and an increase in epithelial proliferation as indicated by, respectively, the altered expression in tight junction related genes and up-regulation of genes stimulating cell growth. Finally, up-regulation of genes stimulating cell growth in 4-week-old Muc2^{-/-} mice correlated with increased crypt length and increased epithelial proliferation.

Together, these data demonstrate that there are distinct phases in colitis development in 2-week-old to 4-week-old Muc2^{-/-} mice.

ACKNOWLEDGMENTS

We thank Anita M. Korteland-van Male and Adrianus C.J.M. De Bruijn for the excellent technical assistance.



FUNDING

This work was supported by Sophia Foundation for Scientific Research (SSWO Projects nr. 559 and 629), Erasmus MC, Rotterdam, the Netherlands.

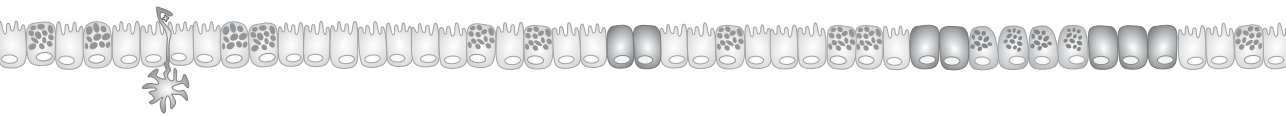
REFERENCES

1. Bengmark S. Ecological control of the gastrointestinal tract. The role of probiotic flora. *Gut* 1998;42:2-7.
2. Steinhoff U. Who controls the crowd? New findings and old questions about the intestinal microflora. *Immunol Lett* 2005;99:12-6.
3. Guarner F, Malagelada JR. Gut flora in health and disease. *Lancet* 2003;361:512-9.
4. Stephen AM, Cummings JH. The microbial contribution to human faecal mass. *J Med Microbiol* 1980;13:45-56.
5. Dharmani P, Srivastava V, Kissoon-Singh V, Chadee K. Role of Intestinal Mucins in Innate Host Defense Mechanisms against Pathogens. *J Innate Immun* 2009;1:123-35.
6. Hecht G. Innate mechanisms of epithelial host defense: spotlight on intestine. *Am J Physiol* 1999;277:C351-8.
7. Hollingsworth MA, Swanson BJ. Mucins in cancer: protection and control of the cell surface. *Nat Rev Cancer* 2004;4:45-60.
8. Johansson ME, Phillipson M, Petersson J, Velcich A, Holm L, Hansson GC. The inner of the two Muc2 mucin-dependent mucus layers in colon is devoid of bacteria. *Proc Natl Acad Sci U S A* 2008;105:15064-9.
9. Belley A, Keller K, Gottke M, Chadee K. Intestinal mucins in colonization and host defense against pathogens. *Am J Trop Med Hyg* 1999;60:10-5.
10. Velcich A, Palumbo L, Selleri L, Evans G, Augenlicht L. Organization and regulatory aspects of the human intestinal mucin gene (MUC2) locus. *J Biol Chem* 1997;272:7968-76.
11. Van Klinken BJ, Dekker J, Buller HA, de Bolos C, Einerhand AW. Biosynthesis of mucins (MUC2-6) along the longitudinal axis of the human gastrointestinal tract. *Am J Physiol* 1997; 273:G296-302.
12. Tytgat KM, Buller HA, Opdam FJ, Kim YS, Einerhand AW, Dekker J. Biosynthesis of human colonic mucin: Muc2 is the prominent secretory mucin. *Gastroenterology* 1994;107:1352-63.
13. van Klinken BJ, Einerhand AW, Duits LA, Makkink MK, Tytgat KM, Renes IB, Verburg M, Buller HA, Dekker J. Gastrointestinal expression and partial cDNA cloning of murine Muc2. *Am J Physiol* 1999;276:G115-24.
14. Gum JR, Jr., Hicks JW, Gillespie AM, Carlson EJ, Komuves L, Karnik S, Hong JC, Epstein CJ, Kim YS. Goblet cell-specific expression mediated by the MUC2 mucin gene promoter in the intestine of transgenic mice. *Am J Physiol* 1999;276:G666-76.
15. Tytgat KM, van der Wal JW, Einerhand AW, Buller HA, Dekker J. Quantitative analysis of MUC2 synthesis in ulcerative colitis. *Biochem Biophys Res Commun* 1996;224:397-405.
16. Van Klinken BJ, Van der Wal JW, Einerhand AW, Buller HA, Dekker J. Sulphation and secretion of the predominant secretory human colonic mucin MUC2 in ulcerative colitis. *Gut* 1999; 44:387-93.
17. Gersemann M, Becker S, Kubler I, Koslowski M, Wang G, Herrlinger KR, Griger J, Fritz P, Fellermann K, Schwab M, Wehkamp J, Stange EF. Differences in goblet cell differentiation between Crohn's disease and ulcerative colitis. *Differentiation* 2009;77:84-94.
18. Velcich A, Yang W, Heyer J, Fragale A, Nicholas C, Viani S, Kucherlapati R, Lipkin M, Yang K, Augenlicht L. Colorectal cancer in mice genetically deficient in the mucin Muc2. *Science* 2002;295:1726-9.
19. Van der Sluis M, De Koning BA, De Bruijn AC, Velcich A, Meijerink JP, Van Goudoever JB, Buller HA, Dekker J, Van Seuning I, Renes IB, Einerhand AW. Muc2-deficient mice sponta-

- neously develop colitis, indicating that MUC2 is critical for colonic protection. *Gastroenterology* 2006;131:117-29.
20. Draghici S, Khatri P, Tarca AL, Amin K, Done A, Voichita C, Georgescu C, Romero R. A systems biology approach for pathway level analysis. *Genome Res* 2007;17:1537-45.
 21. Meijerink J, Mandigers C, van de Locht L, Tonnissen E, Goodsaid F, Raemaekers J. A novel method to compensate for different amplification efficiencies between patient DNA samples in quantitative real-time PCR. *J Mol Diagn* 2001;3:55-61.
 22. Verburg M, Renes IB, Meijer HP, Taminau JA, Buller HA, Einerhand AW, Dekker J. Selective sparing of goblet cells and paneth cells in the intestine of methotrexate-treated rats. *Am J Physiol Gastrointest Liver Physiol* 2000;279:G1037-47.
 23. Emanuelli B, Eberle D, Suzuki R, Kahn CR. Overexpression of the dual-specificity phosphatase MKP-4/DUSP-9 protects against stress-induced insulin resistance. *Proc Natl Acad Sci U S A* 2008;105:3545-50.
 24. Cash HL, Whitham CV, Behrendt CL, Hooper LV. Symbiotic bacteria direct expression of an intestinal bactericidal lectin. *Science* 2006;313:1126-30.
 25. Inai T, Kobayashi J, Shibata Y. Claudin-1 contributes to the epithelial barrier function in MDCK cells. *Eur J Cell Biol* 1999;78:849-55.
 26. Furuse M, Hata M, Furuse K, Yoshida Y, Haratake A, Sugitani Y, Noda T, Kubo A, Tsukita S. Claudin-based tight junctions are crucial for the mammalian epidermal barrier: a lesson from claudin-1-deficient mice. *J Cell Biol* 2002;156:1099-111.
 27. Wen H, Watry DD, Marcondes MC, Fox HS. Selective decrease in paracellular conductance of tight junctions: role of the first extracellular domain of claudin-5. *Mol Cell Biol* 2004;24:8408-17.
 28. Yang K, Popova NV, Yang WC, Lozonchi I, Tadesse S, Kent S, Bancroft L, Matise I, Cormier RT, Scherer SJ, Edelmann W, Lipkin M, Augenlicht L, Velcich A. Interaction of Muc2 and Apc on Wnt signaling and in intestinal tumorigenesis: potential role of chronic inflammation. *Cancer Res* 2008;68:7313-22.
 29. Sohn EJ, Paape MJ, Connor EE, Bannerman DD, Fetterer RH, Peters RR. Bacterial lipopolysaccharide stimulates bovine neutrophil production of TNF-alpha, IL-1beta, IL-12 and IFN-gamma. *Vet Res* 2007;38:809-18.
 30. Corazza N, Brunner T, Buri C, Rihs S, Imboden MA, Seibold I, Mueller C. Transmembrane tumor necrosis factor is a potent inducer of colitis even in the absence of its secreted form. *Gastroenterology* 2004;127:816-25.
 31. Sands BE, Kaplan GG. The role of TNFalpha in ulcerative colitis. *J Clin Pharmacol* 2007;47:930-41.
 32. Douni E, Kollias G. A critical role of the p75 tumor necrosis factor receptor (p75TNF-R) in organ inflammation independent of TNF, lymphotoxin alpha, or the p55TNF-R. *J Exp Med* 1998;188:1343-52.
 33. Louis E. The immuno-inflammatory reaction in Crohn's disease and ulcerative colitis: characterisation, genetics and clinical application. Focus on TNF alpha. *Acta Gastroenterol Belg* 2001;64:1-5.
 34. Zhang S, Wang Q. Factors determining the formation and release of bioactive IL-12: regulatory mechanisms for IL-12p70 synthesis and inhibition. *Biochem Biophys Res Commun* 2008;372:509-12.

35. Chikano S, Sawada K, Shimoyama T, Kashiwamura SI, Sugihara A, Sekikawa K, Terada N, Nakanishi K, Okamura H. IL-18 and IL-12 induce intestinal inflammation and fatty liver in mice in an IFN-gamma dependent manner. *Gut* 2000;47:779-86.
36. Kobayashi K, Kai M, Gidoh M, Nakata N, Endoh M, Singh RP, Kasama T, Saito H. The possible role of interleukin (IL)-12 and interferon-gamma-inducing factor/IL-18 in protection against experimental *Mycobacterium leprae* infection in mice. *Clin Immunol Immunopathol* 1998;88: 226-31.
37. Corbin BD, Seeley EH, Raab A, Feldmann J, Miller MR, Torres VJ, Anderson KL, Dattilo BM, Dunman PM, Gerads R, Caprioli RM, Nacken W, Chazin WJ, Skaar EP. Metal chelation and inhibition of bacterial growth in tissue abscesses. *Science* 2008;319:962-5.
38. Harwig SS, Tan L, Qu XD, Cho Y, Eisenhauer PB, Lehrer RI. Bactericidal properties of murine intestinal phospholipase A2. *J Clin Invest* 1995;95:603-10.
39. Haapamaki MM, Gronroos JM, Nurmi H, Alanen K, Kallajoki M, Nevalainen TJ. Gene expression of group II phospholipase A2 in intestine in ulcerative colitis. *Gut* 1997;40:95-101.
40. He W, Wang ML, Jiang HQ, Steppan CM, Shin ME, Thurnheer MC, Cebra JJ, Lazar MA, Wu GD. Bacterial colonization leads to the colonic secretion of RELMbeta/FIZZ2, a novel goblet cell-specific protein. *Gastroenterology* 2003;125:1388-97.
41. Van Itallie CM, Rogan S, Yu A, Vidal LS, Holmes J, Anderson JM. Two splice variants of claudin-10 in the kidney create paracellular pores with different ion selectivities. *Am J Physiol Renal Physiol* 2006;291:F1288-99.
42. Angelow S, Ahlstrom R, Yu AS. Biology of claudins. *Am J Physiol Renal Physiol* 2008;295: F867-76.
43. Taylor CT, Dzus AL, Colgan SP. Autocrine regulation of epithelial permeability by hypoxia: role for polarized release of tumor necrosis factor alpha. *Gastroenterology* 1998;114:657-68.
44. Wang F, Graham WV, Wang Y, Witkowski ED, Schwarz BT, Turner JR. Interferon-gamma and tumor necrosis factor-alpha synergize to induce intestinal epithelial barrier dysfunction by up-regulating myosin light chain kinase expression. *Am J Pathol* 2005;166:409-19.
45. Wang F, Schwarz BT, Graham WV, Wang Y, Su L, Clayburgh DR, Abraham C, Turner JR. IFN-gamma-induced TNFR2 expression is required for TNF-dependent intestinal epithelial barrier dysfunction. *Gastroenterology* 2006;131:1153-63.

Chapter 4



Absence of the mucin Muc2 leads to increased expression of the bactericidal peptides Reg3 β , Reg3 γ and angiogenin-4

Nanda Burger-van Paassen, Linda Loonen, Janneke Bouma, A.M. Korteland-van Male, Adrianus CJM de Bruijn, Maria van der Sluis, Johannes B Van Goudoever, Jerry M. Wells, Jan Dekker, Isabelle Van Seuning, Ingrid B Renes

Manuscript in preparation



ABSTRACT

Background: The mucin Muc2 is the structural component of the intestinal mucus layer. Absence of Muc2 leads to loss of this mucus layer allowing direct bacterial-epithelial interactions. We hypothesized that absence of the protective mucus layer leads to increased expression of anti-bacterial proteins, which are controlled by bacterial signals through activation of epithelial pattern recognition receptors. Specifically, we aimed to study the consequence of Muc2 deficiency on the expression of the anti-bacterial proteins Reg3 β , Reg3 γ , and angiogenin-4 (Ang4) in the intestine. **Methods:** Small intestinal and colonic tissue of Muc2^{-/-} and wild-type mice was collected at postnatal day 14 (P14) and P28. Expression of Reg3 β , Reg3 γ , and Ang4 was studied by quantitative RT-PCR, Western blot, *in situ* hybridization, and immunohistochemistry. **Results:** Absence of Muc2 strongly increased Reg3 β and Reg3 γ expression in the small intestine and colon. Expression of Reg3 β , Reg3 γ , and Ang4 was higher in the small intestine and proximal colon compared to the distal colon. Moreover, in the distal colon of Muc2^{-/-} mice Reg3 β , Reg3 γ , and Ang4 levels decreased at P28 compared to P14. Interestingly, morphological signs of colitis were only seen in the distal colon of Muc2^{-/-} mice at P28. **Conclusions:** Absence of Muc2 results in up-regulation of Reg3 β and Reg3 γ expression, suggesting altered bacterial-epithelial signaling in Muc2^{-/-} mice, leading to increased innate defense capacity. Morphological signs of colitis were only seen in the distal colon of Muc2^{-/-} mice at P28, where and when expression levels of Reg3 β , Reg3 γ , and Ang4 were the lowest. These data imply that Reg3 proteins and/or Ang4 limit intestinal inflammation/damage.

Key words: Regenerating genes, Reg3 β , Reg3 γ , Angiogenin, Ang4, Muc2, colitis, suckling-weaning transition, bacterial colonization, mother's milk, innate defense

INTRODUCTION

The mucus layer that covers the intestinal epithelium forms a physical barrier against bacteria and is thereby an important component of the innate defense. The mucin MUC2 is the structural component of the colonic mucus layer. Interestingly, bacteria use the glycosyl-chains of mucins as a nutrient source. Johansson et al. previously demonstrated that the intestinal mucus layer exists of two separate layers.¹ The inner layer is densely packed, firmly attached to the epithelium, and devoid of bacteria. In contrast, the outer layer is colonized by bacteria. Breaches in this protective mucus layer allow direct contact between bacteria and the epithelial cells, which leads to an inflammatory response. Muc2^{-/-} mice lacking the mucus layer develop spontaneous colitis.¹⁻²

In human intestinal diseases such as ulcerative colitis (UC) and necrotizing enterocolitis (NEC), the synthesis of MUC2 mucin is decreased³⁻⁷, which might lead to increased bacterial-epithelial interaction. Bacteria are known to play a key role in the development of colitis as the development of colitis in genetically engineered rodent models of inflammatory bowel diseases (IBD) such as Il-10 deficient mice and HLA-B27 transgenic rats is not observed when these animals are maintained under germ-free conditions.⁸⁻¹⁰ However, colonization of Il-10 deficient mice and HLA-B27 transgenic rats with the normal enteric microbiota leads to severe and chronic colitis. IBD and NEC are not caused by specific intestinal bacterial species, but a disordered intestinal microbiota or altered microbial profiles might be involved in the pathogenesis of these diseases. In IBD and NEC a dysbiosis of the microbiota is strongly implicated in the pathophysiology of the disease.¹¹⁻¹²

The composition of the microbiota is partly shaped by specific antimicrobial proteins, e.g. defensins and antimicrobial C-type lectins.¹³ Some antimicrobial proteins such as most α -defensins are expressed constitutively and do not require bacterial signals for their expression.¹⁴ However, expression of a subset of antimicrobial proteins is controlled by the recognition of microbe associated molecular patterns by pattern recognition receptors expressed by the epithelial cells.¹⁵ For example, expression of the antimicrobial C-type lectin regenerating islet-derived protein 3g (Reg3 γ), also called HIP/PAP in humans, is up-regulated in the small intestine and colon after bacterial reconstitution of germ-free mice.¹⁶⁻¹⁷ Expression of angiogenin-4 (Ang4), the orthologue of human ANG, is induced upon colonization with *Bacteroides thetaiotaomicron*, an anaerobe Gram-negative microbe that belongs to the normal mouse and human microbiota.¹⁸ Furthermore, in conventionally raised mice the expression of Reg3 γ and Ang4 increases substantially after weaning¹⁷⁻¹⁸, when the complexity of the microbiota increases and during experimental intestinal infection.¹⁹⁻²¹ Additionally, Reg3 $\gamma\beta$, Reg3 γ and HIP/PAP appear to be important in inflammatory diseases and intestinal injury as their expression is increased in IBD patients and in DSS models of mouse colitis.¹⁶

The aim of this study was to investigate the effect of the mucus layer on Reg3 γ , Reg3 β , and Ang4 expression and localization in the colon and small intestine using the Muc2^{-/-} mouse as a model. With this approach we aimed to i) study the consequence of Muc2 deficiency, i.e. absence of a protective mucus layer and, ii) analyze the effect of weaning (i.e., transfer from breast milk to pelleted food), when the density and complexity of the microbiota increases significantly.

MATERIALS AND METHODS

Animals

Muc2^{-/-} mice were bred as previously described.² All mice were housed in the same specific pathogen-free environment with free access to standard rodent pellets (Special Diets Services, Witham, Essex, England) and acidified tap water in a 12-hour light/dark cycle. All animal care and procedures were conducted according to institutional guidelines (Erasmus MC Animal Ethics Committee, Rotterdam, the Netherlands). Wild-type and Muc2^{-/-} mice were tested negative for *Helicobacter hepaticus* and norovirus infection.

Experimental setup

Wild-type (WT) and Muc2^{-/-} littermates were housed together with their birth mother until weaning at the age of 21 days. WT and Muc2^{-/-} mice were sacrificed at the postnatal ages of 14 days (P14) and 28 days (P28). Colonic tissue was excised and either fixed in 4% (wt/vol) paraformaldehyde in phosphate-buffered saline (PBS), stored in RNAlater (Sigma-Aldrich Chemie, Zwijndrecht, the Netherlands) at -20°C, or frozen in liquid nitrogen and stored at -80°C.

Quantitative Real-Time PCR

Total RNA was prepared using the RNeasy midi-kit (Qiagen, Venlo, the Netherlands). Total RNA (1.5 μ g) was used to prepare cDNA. The mRNA expression levels of Reg3 β , Reg3 γ , Ang4 and Lysozyme type P (lysozyme-P), as well as the 'housekeeping' gene actin were quantified using real-time PCR analysis based upon the intercalation of SYBR® Green on an ABI prism 7900 HT Fast Real Time PCR system (PE Applied Biosystems) as previously described.² All primer combinations were designed using OLIGO 6.22 software (Molecular Biology Insights) and purchased from Invitrogen. An overview of all primer sequences is given in Table 1.

Western blot analysis

Distal colonic tissue samples were homogenized in 500 μ l HIS buffer (50 mM Tris/HCl pH 7.5, 5 mM EDTA pH 8.0, 1% Triton X-100, 10 mM iodoacetamide, 100 μ g/ml soy bean

Table 1: Primer sequences for Quantitative Real-time PCR

gene	Forward primer	Reverse primer
Reg3β	TGG GAA TGG AGT AAC AAT G	GGC AAC TTC ACC TCA CAT
Reg3γ	CCA TCT TCA CGT AGC AGC	CAA GAT GTC CTG AGG GC
Ang4	TTG GCT TGG CAT CAT AGT	CCA GCT TTG GAA TCA CTG
Lysozyme-P	CAG GGT GGT GAG AGA TCC	AAG CGA GGA AGT GTG ACC
β-actin	GGG ACC TGA CGG ACT AC	TGC CAC AGG ATT CCA TAC

trypsin inhibitor, 10 μ g/ml pepstatine A, 10 μ g/ml leupeptine, 1% (w/v) aprotinine and 5 μ l 100 mM PMSF). Total protein concentration was quantified using the bicinchoninic acid assay (Pierce assay, Perbio Science, Etten-Leur, the Netherlands). Twenty μ g of total protein was denatured at 95°C for 5 min in laemmli loading buffer and subjected to 12% (w/v) SDS-polyacrylamide gel electrophoresis (SDS-PAGE). The separated proteins were transferred to nitrocellulose membranes (Protran BA 83, 0.2 μ m) and the blots were blocked for 1 h at room temperature in 5% (w/v) non-fat dry milk (NFDM, Campina Melkunie, Eindhoven, the Netherlands) dissolved in phosphate buffered saline containing 0.1% (v/v) Tween-20 (PBST). Blots were incubated overnight at 4°C with β -actin (Abcam, ab6276 1:10,000) in PBST or with the custom made primary antibodies against Reg3 β (1:20,000) and Reg3 γ (1:20,000) (Eurogentec, Seraing, Belgium). These antibodies were generated in rabbits against the synthetically produced peptides, using the peptide sequences GEDSLKNIPSARISC (Reg3 β) and MIKSSGNSGQYVC (Reg3 γ). The chosen peptide sequences correspond to unique sequences within the Reg3 protein and allow differentiation between the Reg3 β and Reg3 γ proteins. Serum from immunized rabbits was affinity purified using the same peptides. Selectivity and cross reactivity of the generated antibodies for the Reg3 proteins were checked by ELISA. Finally, blots were incubated with the secondary antibody goat-anti-rabbit IRDye® 800CW (1:20,000, Li-cor) for Reg3 β and Reg3 γ , and goat-anti-mouse IRDye®680CW (1:20,000, Li-cor) for β -actin. Signals were detected with the Odyssey scanner (Li-cor, Westburg, Leusden, the Netherlands). Serial dilution series of the protein samples were analyzed to ensure that the quantification of each protein by its cognate antibody was performed in the linear range of this technique.

Histology and histologic grading

Tissue fixed in 4% (wt/vol) paraformaldehyde in PBS was prepared for light microscopy, and 4- μ m-thick sections were stained with hematoxylin and eosin (H&E) to study morphological changes. To detect differences in mucosal thickness in the colon, 10 well-oriented crypts were chosen per intestinal segment and measured using calibrated Leica Application Suite software, version 3.2.0 (Leica Microsystems BV, Rijswijk, the Netherlands).

Immunohistochemistry

Four-micrometer-thick sections were prepared for immunohistochemistry as described previously²² using the Vectastain Elite ABC kit (Vector Laboratories, Burlingame, CA) and the staining reagent 3,3'-diaminobenzidine. The antigens were unmasked by heating the sections for 20 min in 0.01 M sodium citrate (pH 6.0; Merck) supplemented with 0.1% v/v Tween-20 at 100°C. Expression of Reg3 β was detected using an anti-mouse Reg3 β antibody (1:500 diluted in 1% bovine serum albumin, 0.1% Triton X-100 in phosphate buffered saline (PBS)), R&D Systems Europe Ltd., Abingdon, United Kingdom, AF5110) and with the previously described custom made antibody against Reg3 β (1:25,000 in PBS). Reg3 γ was detected using the previously described custom made antibody against Reg3 γ (1:25,000 in PBS). Expression of angiogenin-4 was detected using an anti-human-angiogenin antibody (1:50 diluted in 1% bovine serum albumin, 0.1% Triton X-100 in PBS, R&D Systems Europe Ltd., Abingdon, United Kingdom, AF265).

In Situ Hybridization (ISH)

Non-radioactive *in situ* hybridization (ISH) was performed according to a previously described method with slight modifications.²³ Briefly, sections were deparaffinized, hydrated, and incubated in the following solutions: 0.2 M HCl, distilled water, 0.1% (w/v) pepsin in 0.01 M HCl, 0.2% (w/v) glycine in PBS, PBS, 4% paraformaldehyde in PBS, PBS, and finally in twice in 2 \times SSC (0.03 M Na₃-citrate in 0.3 M NaCl). Until hybridization, sections were stored in a solution of 50% (v/v) formamide in 2 \times SSC at 37°C. For hybridization probes were diluted to a concentration of approximately 100 ng/ml in hybridization solution [50% (v/v) deionized formamide, 10% (w/v) dextran sulphate, 4 \times SSC, 1 \times Denhardt's solution (0.02% w/v ficoll 400, 0.02% w/v polyvinylpyrrolidone and 0.02% w/v bovine serum albumin), 1 mg/ml tRNA, 250 μ g/ml herring sperm DNA] to incubated at 68°C for 15 min, and layered onto the sections. Sections were hybridized overnight at 52°C in a humid chamber. Post-hybridization washes were performed at 45°C using the following steps: 50% (v/v) formamide in 2 \times SSC, 50% (v/v) formamide in 1 \times SSC, and 0.1 \times SSC. A 15 min incubation with RNase T1 (2 U/ml in 1 mM EDTA in 2 \times SSC) at 37°C was followed by washes of 0.1 \times SSC at 45°C and 2 \times SSC at room temperature. The digoxigenin-labelled hybrids were detected by incubation with anti-digoxigenin (Fab, 1:1000 in TBS/1%BA + 1% v/v sheep serum, Roche) conjugated to alkaline phosphatase for 2.5 h at room temperature. Thereafter, sections were washed in 0.025% (v/v) Tween in Tris-buffered saline (pH 7.5). For staining, sections were layered with detection buffer (0.1 M Tris-HCl, 0.1 M NaCl, 0.05 M MgCl₂, pH 9.5) containing 0.33 mg/ml 4-nitroblue tetrazolium chloride, 0.16 mg/ml 5-bromo-4-chloro-3-indolyl-phosphate, 8% (v/v) polyvinyl alcohol (Mw 31 000–50 000, Aldrich Chemical, Milwaukee, WI, USA), and 1 mM levamisole (Sigma).

The colour reaction was performed overnight in the dark and was stopped when the desired intensity of the resulting blue precipitate was reached. Finally, sections were washed in 10 mM Tris–HCl pH 9.5 containing 1 mM EDTA, distilled water, and mounted with Aquamount improved (Gurr, Brunswick, Amsterdam, The Netherlands).

Probe preparation for ISH

Digoxigenin-11-UTP-labelled RNA probes were prepared according to the manufacturer’s instructions (Boehringer Mannheim GmbH, Biochemica, Mannheim, Germany) using T3 and T7 RNA polymerase. Gene fragments for Ang4, Reg3β and Reg3γ were amplified, using the primers listed in Table 2, and cloned in pBluescript II SK.

Table 2: Primer sequences for probe preparation for *In situ* hybridization

Gene	Forward primer	Reverse primer	Amplified product (bp)
Reg3β	TGGGA ATGGA GTAAC AATG	AT GTGAG GTGAA GTTGC C	146
Reg3γ	CAATC ACTGT GGTAC CCTG	GATTT TCTCC TTCTC TGGC	229
Ang4	CCAGC TTTGG AATCA CTGT	CT ATGAT GCCAA GCCAA	151

Statistical analysis

All data are expressed as median. Statistical significance was assessed using the Mann-Whitney U test (Prism, version 5.00; GraphPad software, San Diego, CA). The data were considered statistically significant at *P* < 0.05.

RESULTS

Clinical Symptoms and intestinal morphology

At P14, when the mice received breast milk, there were no significant differences in body weights between Muc2^{-/-} and WT mice, nor were there any clinical or morphological signs of colitis. However, at P28, when mice had been transferred from breast milk to pelleted food, the body weights of Muc2^{-/-} mice were significantly lower than that of WT mice (*P* = 0.0108) (Fig 1A). Additionally, the colonic tissue from Muc2^{-/-} mice showed increased crypt lengths (Fig 1B) and flattening of the epithelial cells (Fig. 1C) compared to WT mice. In the proximal colon and small intestine no differences in morphology were observed between Muc2^{-/-} and WT mice at each time point investigated.

Quantitative analysis of Reg3β, Reg3γ, and Ang4 mRNA levels

A comparison of Reg3β, Reg3γ and Ang4 mRNA levels within colonic tissue of WT mice and Muc2^{-/-} mice revealed five remarkable findings. First, in WT as well as Muc2^{-/-} mice

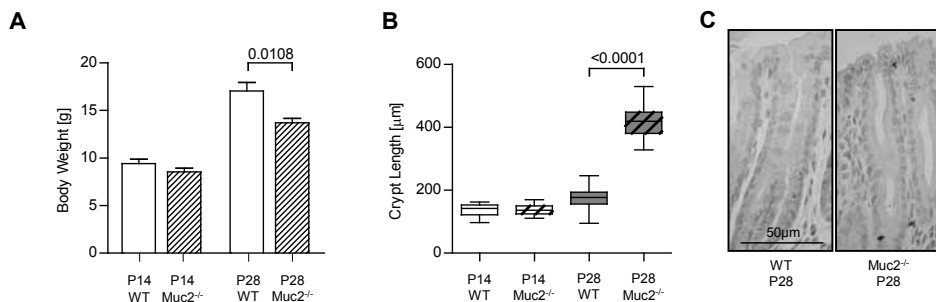


Figure 1. Clinical Symptoms and intestinal morphology

(A) Body weight of WT and Muc2^{-/-} mice are depicted at P14 and P28. Body weight was significantly lower in Muc2^{-/-} compared to WT mice at P28. (B) Crypt lengths of WT and Muc2^{-/-} mice at P14 and P28 in distal colonic tissue sections. Values are depicted as box-and-whisker diagrams (maximum value, upper quartile, median, lower quartile and minimal value respectively). (C) Hematoxylin and eosin staining in WT and Muc2^{-/-} mice at P28 are displayed. (See Color Section, p. 237.)

higher *Reg3β*, *Reg3γ*, and *Ang4* mRNA levels were found in the proximal colon compared to the distal colon at P14 and P28 (Fig. 2). Second, Muc2^{-/-} mice had significantly increased *Reg3β* and *Reg3γ* mRNA levels in the distal colon at P14 and P28 compared to WT mice, a trend that was also observed in the proximal colon. Third, during aging from P14 to P28, *Reg3β*, *Reg3γ*, and *Ang4* mRNA levels in the proximal colon increased in WT as well as Muc2^{-/-} mice. Fourth, in the distal colon *Ang4* levels also increased during aging in WT mice, however in Muc2^{-/-} mice the expression levels decreased. Fifth, in the distal colon, *Reg3β* and *Reg3γ* mRNA expression levels were hardly detectable in WT mice, but significantly increased in Muc2^{-/-} mice.

In the small intestine *Reg3β* and *Reg3γ* mRNA levels were comparable between WT and Muc2^{-/-} mice at P14 (Fig. 3A and B). In contrast, at P28 *Reg3β*, and *Reg3γ* mRNA levels significantly increased in the Muc2^{-/-} mice, but remained stable in the WT mice. Focussing on two Paneth cell-specific products, we found that *Ang4* and *Lysozyme-P* mRNA levels were comparable between WT and Muc2^{-/-} mice at P14 as well as P28 (Fig. 3C and D). Remarkably, from P14 to P28 mRNA levels of *Ang4* as well as *lysozyme-P* were significantly increased in both types of mice.

Quantitative analysis of *Reg3β* and *Reg3γ* protein levels in the small intestine

Expression of *Reg3β* and *Reg3γ* protein in the jejunum was studied by Western blot analysis. At P14 protein expression levels were below the detection limit in WT as well as Muc2^{-/-} mice (data not shown). At P28, expression of both *Reg3β* (Fig. 4A) and *Reg3γ* (Fig. 4B) was significantly increased in Muc2^{-/-} mice compared to WT mice, in which *Reg3β* and *Reg3γ* protein levels remained undetectable. This difference in *Reg3β* and *Reg3γ* protein expression levels at P28 corresponded to the observed difference in mRNA levels.

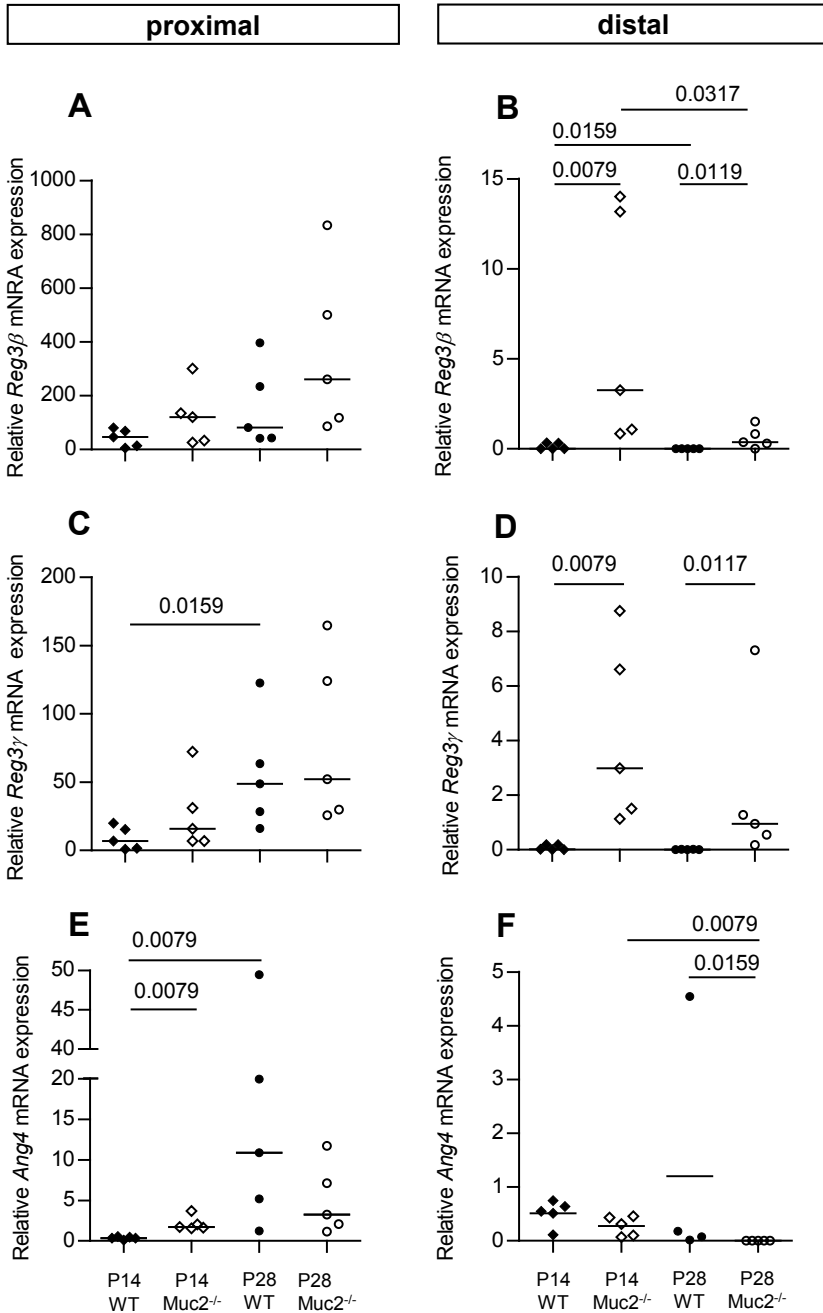


Figure 2. Expression of *Reg3β*, *Reg3γ* and *Ang4* mRNA in the colon
Expression of *Reg3β* (A,B), *Reg3γ* (C,D), *Ang4* (E,F) mRNA relative to β -actin expression in colonic tissue of WT and *Muc2*^{-/-} are depicted. Proximal and distal colonic expression levels are shown in the left and right panels respectively (* $P < .05$, ** $P < .01$). Values are expressed as median. Groups are depicted as: WT, P14 \blacklozenge ; *Muc2*^{-/-}, P14 \diamond ; WT, P28 \bullet ; and *Muc2*^{-/-}, P28 \circ .

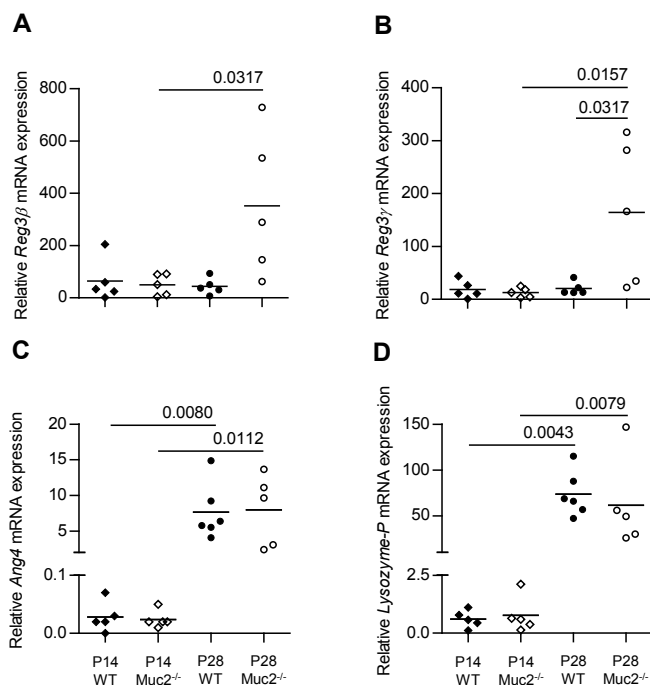


Figure 3. Expression *Reg3β*, *Reg3γ*, *Ang4* and *lysozyme-P* mRNA in the small intestine
Small intestinal expression of *Reg3β* (A), *Reg3γ* (B), *Ang4* (C) and *lysozyme-P* (D) mRNA expression relative to β -actin expression. Values are expressed as median. Groups are depicted as: WT, P14 \blacklozenge ; *Muc2*^{-/-}, P14 \diamond ; WT, P28 \bullet ; and *Muc2*^{-/-}, P28 \circ .

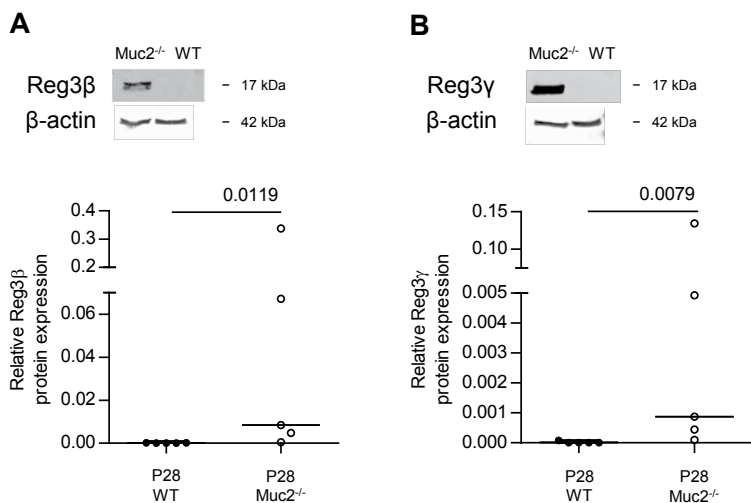


Figure 4. Expression of *Reg3β* and *Reg3γ* protein in the small intestine
Small intestinal expression of *Reg3β* (A) and *Reg3γ* (B) protein relative to β -actin expression. Photomicrographs depict examples of *Reg3β* and *Reg3γ* expression in WT and *Muc2*^{-/-} mice and corresponding β -actin expression. Values are expressed as median. Groups are depicted as: WT, P28 \bullet ; and *Muc2*^{-/-}, P28 \circ .

Localization of *Reg3 β* , *Reg3 γ* , and *Ang4* mRNA and protein in the colon

We next determined the localization of these markers within the colonic tissue of WT and *Muc2*^{-/-} mice by ISH and immunohistochemistry. ISH revealed that expression of both *Reg3 β* mRNA (Fig. 5A, *Muc2*^{-/-} P28) and *Reg3 γ* mRNA (data not shown) is localized at the basolateral side of goblet cells and within enterocytes in the proximal colon of WT and *Muc2*^{-/-} mice at P14 and P28.

Reg3 β protein was localized in goblet cells and enterocytes in the middle and lower part of the crypt in WT and *Muc2*^{-/-} mice at P14 and P28 (data not shown). There were no differences between WT and *Muc2*^{-/-} mice at both ages studied. Colonic *Reg3 γ* protein expression was undetectable in WT animals at P14 and P28 (Fig. 5B) and in *Muc2*^{-/-} mice at P14. However, in *Muc2*^{-/-} mice at P28, *Reg3 γ* protein could be localized at

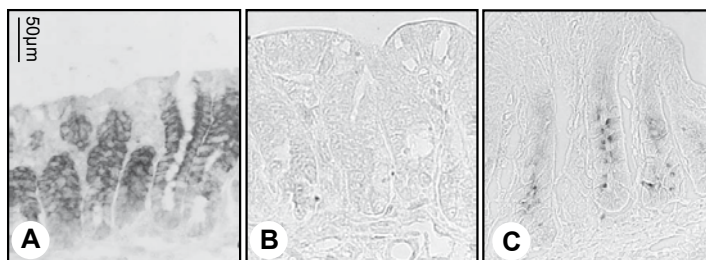


Figure 5. Localization of *Reg3 β* mRNA and *Reg3 γ* protein in the proximal colon. Localization of *Reg3 β* mRNA in *Muc2*^{-/-} by ISH (A), and localization of *Reg3 γ* protein by immunohistochemistry in (B) WT and (C) *Muc2*^{-/-} mice at P28. (See Color Section, p. 237.)

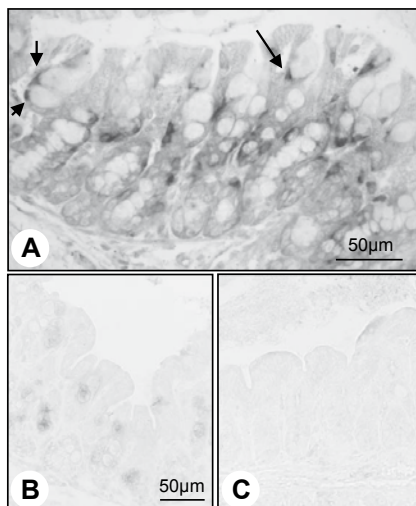


Figure 6. Localization of *Ang4* mRNA and *Ang4* protein in the proximal colon. Localization of *Ang4* mRNA in *Muc2*^{-/-} mice by ISH (A) (arrows depict *Ang4* mRNA at the basolateral side of goblet cells), and localization of *Ang4* protein by immunohistochemistry in (B) WT and (C) *Muc2*^{-/-} mice at P28. (See Color Section, p. 238.)

the apical side of crypt epithelial cells (Fig. 5 C). Like *Reg3 β* , *Reg3 γ* protein was localized mainly at the middle and lower areas of the crypt in these animals.

Ang4 mRNA was detected at the basolateral side of goblet cells in the proximal colon of WT mice at P14 (not shown) and P28 (Fig. 6A). Goblet cells are not clearly visible in *Muc2^{-/-}* mice but as the localization of *Ang4* mRNA in *Muc2^{-/-}* mice was similar to WT we predict that it is also located in goblet cells (not shown). Immunohistochemical staining showed that *Ang4* protein was clearly visible in goblet cells of WT mice at P14 and P28 (Fig 6B). In *Muc2^{-/-}* mice, goblet cells contained *Ang4* protein at P14 (not shown), but not at P28 (Fig. 6C). We could not detect the *in situ* expression of *Reg3 β* , *Reg3 γ* , and *Ang4* mRNA and protein in the distal colon, most likely because expression levels were too low. Remarkably, expression levels of *Reg3 β* , *Reg3 γ* , and *Ang4* mRNA and protein showed considerable mouse to mouse variation.

Localization of *Reg3 β* , *Reg3 γ* , and *Ang4* mRNA and protein in the small intestine

Reg3 β mRNA was localized in goblet cells and enterocytes in the small intestine of WT and *Muc2^{-/-}* mice at P14 and P28 (Fig. 7). Additionally, *Reg3 β* mRNA was observed in some Paneth cells of *Muc2^{-/-}* mice at P28 (Fig. 7D), but not in WT mice. In WT mice, *Reg3 β* mRNA was seen at the base of the villi at P14 (Fig. 7A) and P28 (Fig. 7C). A similar pattern was seen in *Muc2^{-/-}* mice at P14 (Fig. 7B). In contrast, at P28 the expression pattern of *Reg3 β* mRNA in *Muc2^{-/-}* mice spread from the base of the villi to the tip (Fig. 7D), while in WT mice *Reg3 β* mRNA expression remained restricted to the villus base.

As for *Reg3 β* mRNA, the *Reg3 γ* mRNA was also seen in goblet cells and enterocytes at P14 and P28 (data not shown). At P14 and P28, *Reg3 γ* mRNA expression was observed in Paneth cells in WT mice as well as *Muc2^{-/-}* mice (data not shown). There was no evidence for a different localization of *Reg3 γ* in WT and *Muc2^{-/-}* mice.

Immunohistochemical analysis of *Reg3 β* and *Reg3 γ* protein showed similar results compared to the mRNA localization described above (Fig. 7). More specifically, at P14 *Reg3 β* protein was localized in enterocytes, displayed by a typical Golgi-staining and in goblet cells of WT as well as *Muc2^{-/-}* mice (Fig. 7E and F). *Reg3 β* -positive Paneth cells were only observed in *Muc2^{-/-}* mice at P28 (Fig. 7H). *Reg3 β* protein was seen from crypt-villus junction till halfway up the villi in enterocytes and within goblet cells along the entire villi at P14 in WT and *Muc2^{-/-}* mice. At P28 goblet cells of WT mice did not show expression of *Reg3 β* protein, whereas goblet cells of *Muc2^{-/-}* mice were still *Reg3 β* -positive (Fig. 7G and H). Moreover, expression of *Reg3 β* protein in *Muc2^{-/-}* mice was seen along the complete crypt-villus units, whereas expression was limited to the lower part of the villi in WT mice.

Reg3 γ protein was localized in Paneth cells and goblet cells of WT and *Muc2^{-/-}* mice at P14 (Fig. 7I and J). *Reg3 γ* -positive goblet cells were still present at P28 in *Muc2^{-/-}* mice,

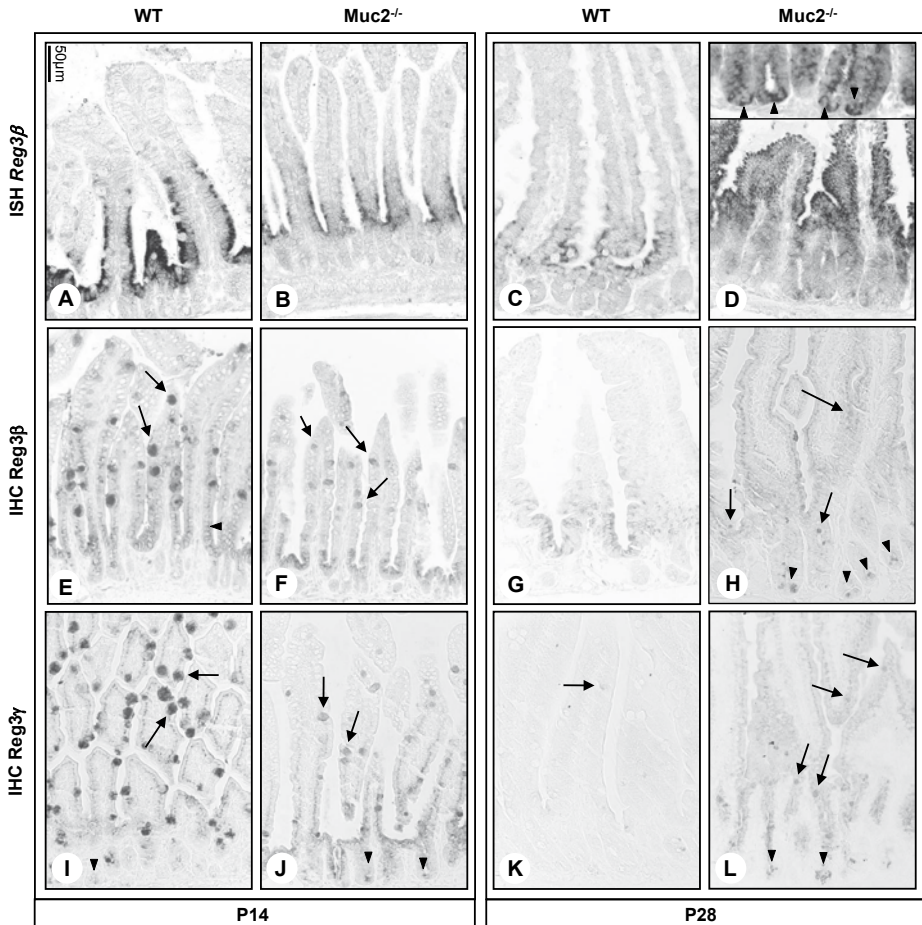


Figure 7. Localization of *Reg3β* mRNA and *Reg3β* and *Reg3γ* protein in the small intestine. ISH for *Reg3β* mRNA in WT and *Muc2*^{-/-} mice at P14 (A,B) and P28 (C,D)(arrowheads in zoom in indicate *Reg3β*-positive Paneth cell in *Muc2*^{-/-} at P28). Immunohistochemical staining for *Reg3β* in WT and *Muc2*^{-/-} mice at P14 (E,F) (arrowhead indicates Golgi-staining in enterocytes in WT at P14) and P28 (G,H)(arrows indicate *Reg3γ*-positive goblet cells in WT and *Muc2*^{-/-} mice at P14, arrowheads indicate *Reg3β*-positive Paneth cells in *Muc2*^{-/-} at P28). Immunohistochemical staining for *Reg3γ* is depicted in the lower panel in WT and *Muc2*^{-/-} mice at P14 (I,J)(arrows indicate *Reg3γ*-positive goblet cells, arrowheads indicate *Reg3γ*-positive Paneth cells) and P28 (K,L)(arrows indicate *Reg3γ*-positive goblet cells, arrowheads indicate *Reg3γ*-positive Paneth cells). (See Color Section, p. 239.)

but only faint staining was seen in WT mice (Fig. 7K and L). *Reg3γ*-positive Paneth cells were not visible in WT mice at P28 (Fig 7K). In *Muc2*^{-/-} mice, however, *Reg3γ*-positive Paneth cells were clearly visible at P28 and the abundance of *Reg3γ*-positive Paneth cells in these mice even seemed to increase from P14 to P28.

Finally, small intestinal *Ang4* mRNA was localized in Paneth cells of both WT and *Muc2*^{-/-} mice at both ages studied (*Suppl. Information* Fig.1, showing *Ang4* mRNA in *Muc2*^{-/-} mice at P14). At P14, *Ang4* mRNA was not only observed in the Paneth cells



Figure 8. Localization of Ang4 protein in the small intestine

Localization of Ang4 protein in small intestine of WT and *Muc2*^{-/-} mice at P14 (left panel) and P28 (right panel)(arrowheads indicate Ang4-positive Paneth cells). (See Color Section, p. 240.)

but also at the apical side of the villus enterocytes in both types of mice. Ang4 protein expression patterns were similar to the *Ang4* mRNA expression patterns with expression localized to Paneth cells at P14 and P28 (Fig. 8) and to enterocytes along the villi at P14 in WT and *Muc2*^{-/-} mice. Similar to *Reg3γ*, the number of Ang4-positive Paneth cells increased from P14 to P28.

DISCUSSION

In the present study we examined the expression and localization of *Reg3β*, *Reg3γ* and *Ang4* in intestinal tissue of WT and *Muc2*^{-/-} mice at the age of 14 days and post weaning at 28 days. We demonstrated that the expression of these genes, that are related to innate defense, differ between *Muc2*^{-/-} and WT mice before and after weaning, a time frame during which changes in intestinal morphology are described. These changes might be related to a different microbiota or to an altered interaction between bacteria and the intestinal epithelial cells in the absence of a mucus layer.

Expression levels of *Reg3β*, *Reg3γ*, and *Ang4* mRNA in the proximal colon were considerably higher compared to expression levels in the distal colon of WT and *Muc2*^{-/-} mice at both time points. An explanation for the observed differences in the expression levels of these genes between the proximal and distal colon might be that an intrinsic program encoded in the epithelial cells determines the segmental expression of the studied innate defense molecules. On the other hand, altered expression of *Reg3γ* might be related to the composition of the microbiota as demonstrated in a simplified model where germ-free mice are sequentially colonised with *Bacteroides thetaiotaomicron* and then *Bifidobacterium longum*.²⁴ As expected from previous studies colonization of germ-free mice with *Bacteroides thetaiotaomicron* induced *Reg3γ* expression but this was

lowered by the subsequent introduction of *Bifidobacterium longum*. Thus the observed differences in *Reg3β*, *Reg3γ*, and *Ang4* gene expression between the proximal and distal colon might be related to differences in the composition of the microbiota in these parts of the intestine. Indeed, it was shown by Lepage et al. and Zoetendal et al. that there is approximately 4% difference in mucosa-associated bacterial communities between the right colon (i.e. proximal colon) and left colon (i.e. distal colon).²⁵⁻²⁶

Regardless of the mechanisms of *Reg3* gene and *Ang-4* gene regulation, there seems to be a correlation between *Reg3β*, *Reg3γ*, and *Ang4* gene expression levels and the location of colitis in *Muc2^{-/-}* mice. Colitis is only seen in the distal colon of *Muc2^{-/-}* mice at P28, where the expression levels of *Reg3β*, *Reg3γ*, and *Ang4* were the lowest. This finding implies that *Reg3* proteins and/or *Ang4* can limit intestinal inflammation or damage directly or indirectly. Interestingly, studies from Folch-Puy et al. indicate that PAP I, also known as HIP, p23, or *Reg2* protein, directly inhibits the inflammatory response by blocking NF-κB activation through a STAT3-dependent mechanism.²⁷ As *Reg3β* mRNA levels are higher in the proximal colon than distal colon of *Muc2^{-/-}* mice, together with the fact that colitis is only seen in the distal colon, *Reg3β* may play an anti-inflammatory role in *Muc2^{-/-}* mice. Additionally, one might speculate that the distal colon is more prone to develop colitis than the proximal colon as *Reg3β* mRNA levels are also higher in the proximal colon than in the distal colon of WT mice.

Expression levels of *Reg3β* and *Reg3γ* mRNAs were consistently higher in *Muc2^{-/-}* mice compared to WT mice in both the proximal and distal colon. This is most likely due to increased commensal bacterial-epithelial interaction in *Muc2^{-/-}* mice. Given that the glycosyl-chains of mucins are a nutrient source for bacteria, the absence of *Muc2* is likely to influence the composition of the microbiota. Thus differences in the composition of the colonic microbiota between WT and *Muc2^{-/-}* mice might therefore also influence *Reg3* and *Ang4* protein expression. Furthermore, Pochart et al. showed that in healthy subjects dominant bacterial species differ between the mucosa-associated microbiota and the fecal microbiota.²⁸ In patients with active Crohn's disease, the fecal microbiota was more similar to the mucosal microbiota, suggesting that the microbiota plays an important role in this disease. The absence of a functional mucus layer in *Muc2^{-/-}* mice would allow the fecal bacteria to come into contact with the mucosal epithelium which might influence the expression of *Reg3β* and *Reg3γ* in *Muc2^{-/-}* mice.

After weaning, expression levels of *Reg3β*, *Reg3γ*, and *Ang4* mRNAs in the proximal colon were increased in WT and *Muc2^{-/-}* mice. Cash et al. showed that *Reg3γ* mRNA expression increased during the weaning period in the small intestine of conventionally raised mice, but not germ-free mice.¹⁷ The same accounts for *Ang4* expression in the small intestine.¹⁸ It is known that weaning changes the composition of the intestinal microbiota. This can be explained by the food source itself that forms a substrate for specific bacteria, but also by the abrogation of protective factors that are present in

mother's milk, such as sCD14, sTLR2, TGF β , IL-10, and lactoferrin.²⁹⁻³² Therefore, increased expression of Reg3 β and Reg3 γ at P28 in WT as well as Muc2^{-/-} mice might be regarded as a host innate response to the absence of protective factors in the mother's milk and an altered intestinal microbiota.

Like Reg3 β and Reg3 γ , Ang4 mRNA levels in the distal colon also turned out to be increased after weaning in WT mice. Contrastingly, in Muc2^{-/-} mice, expression levels of Ang4 decreased after weaning. Hooper et al. previously described that Ang4 displays species-selective, bactericidal activity.¹⁸ However, high ANG levels were also reported to be cytotoxic for eukaryotic cells.³³ In this respect the decreased expression of Ang4 in the distal colon of Muc2^{-/-} mice might be regarded as a protective mechanism to limit aggravation of damage in this model.

Focussing on the small intestine, next to crypt lengthening as from the age of 16 weeks, no signs of inflammation were seen in the Muc2^{-/-} colitis model.² Yet, in the present paper, we demonstrate that small intestinal expression of Reg3 β and Reg3 γ mRNAs were increased in Muc2^{-/-} mice compared to WT mice at P28. Since these differences became apparent after weaning, this suggests an important role for bacterial colonization, which is supported by the findings of other authors.¹⁶⁻¹⁷ Besides the aspect of weaning, the absence of Muc2 is likely to influence the intestinal microbiota since mucins form a nutrient source for certain groups of bacteria.³⁴ Small intestinal expression levels of Ang4 mRNA were increased after weaning in WT as well as Muc2^{-/-} mice. Furthermore, we showed that expression of Ang4 in the small intestine resembles the expression of lysozyme-P over time. It is known that Paneth cell development occurs after birth in mice, with a complete constitution of the Paneth-cell lineage from the age of 3 to 4 weeks.³⁵ Therefore, increased expression of lysozyme-P and Ang4 mRNAs at P28 compared to P14 is most likely due to an increase in Paneth cell numbers during development from P14 to P28.

With *in situ* hybridization we showed that both Reg3 β and Reg3 γ mRNAs in the proximal colon are localized at the basolateral side of the goblet cells at P14 and P28 in WT mice. In Muc2^{-/-} mice we cannot distinguish between enterocytes and goblet cells based on their morphology. However, expression seemed to be similar in WT and KO mice. It was previously shown that Reg3 γ and Ang4 are expressed in small intestine and localized exclusively in Paneth cells¹⁷⁻¹⁸ and Reg3 β mRNA was shown in colonic goblet cells and columnar cells.¹⁶ Besides secreting Relm β , which is suggested to have an immune effector function³⁶⁻³⁸, goblet cells were until now not known to play a role in innate defense response via the secretion of anti-bacterial proteins. Our demonstration that Reg3 β , Reg3 γ , and Ang4 are expressed in colonic goblet cells highlights a new and important role for goblet cells in innate defense.

By immunohistochemistry, we could not detect clear differences in Reg3 β protein expression in the proximal colon between WT and Muc2^{-/-} mice, nor were there any clear

differences between P14 and P28. Additionally, Reg3 γ protein expression was only seen in the proximal colon of Muc2^{-/-} mice at P28. This might be due to the fact that protein expression levels of Reg3 genes are below detection levels. However, as Reg3 γ protein expression was only seen in the proximal colon of Muc2^{-/-} mice at P28, we suggest that the bactericidal activity in the proximal colon of Muc2^{-/-} mice increases after weaning. In the small intestine, Reg3 β protein was seen in goblet cells, enterocytes, and Paneth cells at P14. In WT mice, goblet cells did not express Reg3 β protein any more at P28, whereas Muc2^{-/-} mice still showed Reg3 β mRNA expression in goblet cells. The latter could indicate increased Reg3 β secretion by goblet cells after weaning. Furthermore, Reg3 β mRNA and protein expression by Paneth cells and by enterocytes in the lower villus and crypt suggests a stem cell protective function for Reg3 β against bacterial invasion.

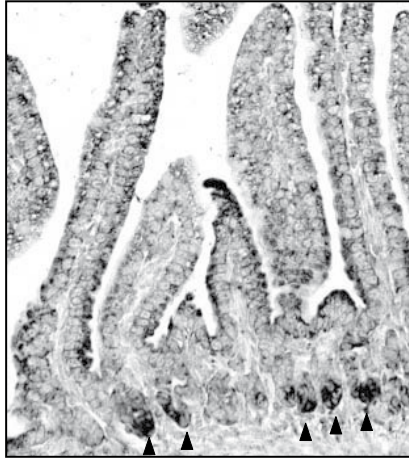
In summary, absence of Muc2 results in strong up-regulation of Reg3 β and Reg3 γ mRNAs in the small intestine and colon, suggesting altered bacterial-epithelial signaling in Muc2^{-/-} mice, leading to increased innate defense capacity. Alterations in Reg3 and Ang4 gene expression were related to weaning from mother's milk, which is known to alter the composition of the microbiota. Therefore an important role for bacteria in regulation of Reg3 and Ang4 gene expression is suggested. Furthermore, colitis is only seen in the distal colon of Muc2^{-/-} mice at P28, where and when expression levels of Reg3 β , Reg3 γ , and Ang4 mRNAs were the lowest. This finding implies that Reg3 proteins and/or Ang4 limit the induction of intestinal inflammation and/or damage. Additionally, down-regulation of Ang4 in Muc2^{-/-} mice with colitis might be a protective mechanism to limit Ang4-induced cell damage in these mice, as ANG is known to be cytotoxic for host cells. This study also highlights a new role for goblet cells in host innate immunity by demonstrating that they produce the antimicrobial peptides Reg3 β , Reg3 γ , and Ang4.

REFERENCES

1. Johansson ME, Phillipson M, Petersson J, Velcich A, Holm L, Hansson GC. The inner of the two Muc2 mucin-dependent mucus layers in colon is devoid of bacteria. *Proc Natl Acad Sci U S A* 2008;105:15064-9.
2. Meijerink J, Mandigers C, van de Locht L, Tonnissen E, Goodsaid F, Raemaekers J. A novel method to compensate for different amplification efficiencies between patient DNA samples in quantitative real-time PCR. *J Mol Diagn* 2001;3:55-6.
3. Tytgat KM, van der Wal JW, Einerhand AW, Buller HA, Dekker J. Quantitative analysis of MUC2 synthesis in ulcerative colitis. *Biochem Biophys Res Commun* 1996;224:397-405.
4. Pullan RD, Thomas GA, Rhodes M, Newcombe RG, Williams GT, Allen A, Rhodes J. Thickness of adherent mucus gel on colonic mucosa in humans and its relevance to colitis. *Gut* 1994;35:353-9.
5. Jacobs LR, Huber PW. Regional distribution and alterations of lectin binding to colorectal mucin in mucosal biopsies from controls and subjects with inflammatory bowel diseases. *J Clin Invest* 1985;75:112-8.
6. Schaart MW, de Bruijn AC, Bouwman DM, de Krijger RR, van Goudoever JB, Tibboel D, Renes IB. Epithelial Functions of the Residual Bowel After Surgery for Necrotising Enterocolitis in Human Infants. *J Pediatr Gastroenterol Nutr* 2009.
7. Lin PW, Stoll BJ. Necrotising enterocolitis. *Lancet* 2006;368:1271-83.
8. Kuhn R, Lohler J, Rennick D, Rajewsky K, Muller W. Interleukin-10-deficient mice develop chronic enterocolitis. *Cell* 1993;75:263-74.
9. Sellon RK, Tonkonogy S, Schultz M, Dieleman LA, Grenther W, Balish E, Rennick DM, Sartor RB. Resident enteric bacteria are necessary for development of spontaneous colitis and immune system activation in interleukin-10-deficient mice. *Infect Immun* 1998;66:5224-31.
10. Taurog JD, Richardson JA, Croft JT, Simmons WA, Zhou M, Fernandez-Sueiro JL, Balish E, Hammer RE. The germfree state prevents development of gut and joint inflammatory disease in HLA-B27 transgenic rats. *J Exp Med* 1994;180:2359-64.
11. Takaishi H, Matsuki T, Nakazawa A, Takada T, Kado S, Asahara T, Kamada N, Sakuraba A, Yajima T, Higuchi H, Inoue N, Ogata H, Iwao Y, Nomoto K, Tanaka R, Hibi T. Imbalance in intestinal microflora constitution could be involved in the pathogenesis of inflammatory bowel disease. *Int J Med Microbiol* 2008;298:463-72.
12. Wang Y, Hoenig JD, Malin KJ, Qamar S, Petrof EO, Sun J, Antonopoulos DA, Chang EB, Claud EC. 16S rRNA gene-based analysis of fecal microbiota from preterm infants with and without necrotizing enterocolitis. *Isme J* 2009;3:944-54.
13. Vaishnava S, Behrendt CL, Ismail AS, Eckmann L, Hooper LV. Paneth cells directly sense gut commensals and maintain homeostasis at the intestinal host-microbial interface. *Proc Natl Acad Sci U S A* 2008;105:20858-63.
14. Putsep K, Axelsson LG, Boman A, Midtvedt T, Normark S, Boman HG, Andersson M. Germ-free and colonized mice generate the same products from enteric prodefensins. *J Biol Chem* 2000;275:40478-82.
15. Uehara A, Fujimoto Y, Fukase K, Takada H. Various human epithelial cells express functional Toll-like receptors, NOD1 and NOD2 to produce anti-microbial peptides, but not proinflammatory cytokines. *Mol Immunol* 2007;44:3100-11.
16. Ogawa H, Fukushima K, Naito H, Funayama Y, Unno M, Takahashi K, Kitayama T, Matsuno S, Ohtani H, Takasawa S, Okamoto H, Sasaki I. Increased expression of HIP/PAP and regen-

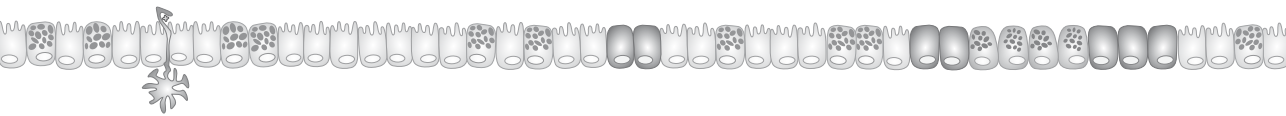
- erating gene III in human inflammatory bowel disease and a murine bacterial reconstitution model. *Inflamm Bowel Dis* 2003;9:162-70.
17. Cash HL, Whitham CV, Behrendt CL, Hooper LV. Symbiotic bacteria direct expression of an intestinal bactericidal lectin. *Science* 2006;313:1126-30.
 18. Hooper LV, Stappenbeck TS, Hong CV, Gordon JI. Angiogenins: a new class of microbicidal proteins involved in innate immunity. *Nat Immunol* 2003;4:269-73.
 19. Brandl K, Plitas G, Schnabl B, DeMatteo RP, Pamer EG. MyD88-mediated signals induce the bactericidal lectin RegIII gamma and protect mice against intestinal *Listeria monocytogenes* infection. *J Exp Med* 2007;204:1891-900.
 20. Rodenburg W, Keijer J, Kramer E, Roosing S, Vink C, Katan MB, van der Meer R, Bovee-Oudenhoven IM. Salmonella induces prominent gene expression in the rat colon. *BMC Microbiol* 2007;7:84.
 21. van Ampting MT, Rodenburg W, Vink C, Kramer E, Schonewille AJ, Keijer J, van der Meer R, Bovee-Oudenhoven IM. Ileal Mucosal and Fecal Pancreatitis Associated Protein Levels Reflect Severity of Salmonella Infection in Rats. *Dig Dis Sci* 2009.
 22. Verburg M, Renes IB, Meijer HP, Taminiau JA, Buller HA, Einerhand AW, Dekker J. Selective sparing of goblet cells and paneth cells in the intestine of methotrexate-treated rats. *Am J Physiol Gastrointest Liver Physiol* 2000;279:G1037-47.
 23. Lindenbergh-Kortleve DJ, Rosato RR, van Neck JW, Nauta J, van Kleffens M, Groffen C, Zwarthoff EC, Drop SL. Gene expression of the insulin-like growth factor system during mouse kidney development. *Mol Cell Endocrinol* 1997;132:81-91.
 24. Sonnenburg JL, Chen CT, Gordon JI. Genomic and metabolic studies of the impact of probiotics on a model gut symbiont and host. *PLoS Biol* 2006;4:e413.
 25. Lepage P, Seksik P, Sutren M, de la Cochetiere MF, Jian R, Marteau P, Dore J. Biodiversity of the mucosa-associated microbiota is stable along the distal digestive tract in healthy individuals and patients with IBD. *Inflamm Bowel Dis* 2005;11:473-80.
 26. Zoetendal EG, von Wright A, Vilpponen-Salmela T, Ben-Amor K, Akkermans AD, de Vos WM. Mucosa-associated bacteria in the human gastrointestinal tract are uniformly distributed along the colon and differ from the community recovered from feces. *Appl Environ Microbiol* 2002;68:3401-7.
 27. Folch-Puy E, Granell S, Dagorn JC, Iovanna JL, Closa D. Pancreatitis-associated protein I suppresses NF-kappa B activation through a JAK/STAT-mediated mechanism in epithelial cells. *J Immunol* 2006;176:3774-9.
 28. Pochart P, Lemann F, Flourie B, Pellier P, Goderel I, Rambaud JC. Pyxigraphic sampling to enumerate methanogens and anaerobes in the right colon of healthy humans. *Gastroenterology* 1993;105:1281-5.
 29. LeBouder E, Rey-Nores JE, Rushmere NK, Grigorov M, Lawn SD, Affolter M, Griffin GE, Ferrara P, Schiffrin EJ, Morgan BP, Labeta MO. Soluble forms of Toll-like receptor (TLR)2 capable of modulating TLR2 signaling are present in human plasma and breast milk. *J Immunol* 2003;171:6680-9.
 30. Labeta MO, Vidal K, Nores JE, Arias M, Vita N, Morgan BP, Guillemot JC, Loyaux D, Ferrara P, Schmid D, Affolter M, Borysiewicz LK, Donnet-Hughes A, Schiffrin EJ. Innate recognition of bacteria in human milk is mediated by a milk-derived highly expressed pattern recognition receptor, soluble CD14. *J Exp Med* 2000;191:1807-12.

31. Filipp D, Alizadeh-Khiavi K, Richardson C, Palma A, Paredes N, Takeuchi O, Akira S, Julius M. Soluble CD14 enriched in colostrum and milk induces B cell growth and differentiation. *Proc Natl Acad Sci U S A* 2001;98:603-8.
32. Claud EC, Savidge T, Walker WA. Modulation of human intestinal epithelial cell IL-8 secretion by human milk factors. *Pediatr Res* 2003;53:419-25.
33. Saxena SK, Rybak SM, Davey RT, Jr., Youle RJ, Ackerman EJ. Angiogenin is a cytotoxic, tRNA-specific ribonuclease in the RNase A superfamily. *J Biol Chem* 1992;267:21982-6.
34. Sonnenburg JL, Angenent LT, Gordon JI. Getting a grip on things: how do communities of bacterial symbionts become established in our intestine? *Nat Immunol* 2004;5:569-73.
35. Garabedian EM, Roberts LJ, McNevin MS, Gordon JI. Examining the role of Paneth cells in the small intestine by lineage ablation in transgenic mice. *J Biol Chem* 1997;272:23729-40.
36. Artis D, Wang ML, Keilbaugh SA, He W, Brenes M, Swain GP, Knight PA, Donaldson DD, Lazar MA, Miller HR, Schad GA, Scott P, Wu GD. RELMbeta/FIZZ2 is a goblet cell-specific immune-effector molecule in the gastrointestinal tract. *Proc Natl Acad Sci U S A* 2004;101:13596-600.
37. Krimi RB, Kotelevets L, Dubuquoy L, Plaisancie P, Walker F, Lehy T, Desreumaux P, Van Seuningen I, Chastre E, Forgue-Lafitte ME, Marie JC. Resistin-like molecule beta regulates intestinal mucous secretion and curtails TNBS-induced colitis in mice. *Inflamm Bowel Dis* 2008;14:931-41.
38. Steppan CM, Brown EJ, Wright CM, Bhat S, Banerjee RR, Dai CY, Enders GH, Silberg DG, Wen X, Wu GD, Lazar MA. A family of tissue-specific resistin-like molecules. *Proc Natl Acad Sci U S A* 2001;98:502-6.



Suppl Information Figure 1. Localization of *Ang4* mRNA small intestine
 Localization of *Ang4* mRNA at P14 in small intestine of *Muc2*^{-/-} mice (arrowheads indicate *Ang4*-positive Paneth cells).

Chapter 5



Paneth cell hyperplasia and metaplasia in necrotizing enterocolitis

Patrycja J. Puiman, **Nanda Burger-van Paassen**, Maaïke W. Schaart, Adrianus C.J.M. de Bruijn, Ronald R. de Krijger, Dick Tibboel, Johannes B. van Goudoever, Ingrid B. Renes

Accepted for publication, Pediatric Research



ABSTRACT

Paneth cell dysfunction has been suggested in necrotizing enterocolitis (NEC). The aim of the present study was to: i) study Paneth cell presence, protein expression, and developmental changes in preterm infants with NEC; ii) determine Paneth cell products and antimicrobial capacity in ileostomy outflow fluid. Intestinal tissue from NEC patients (n=55), preterm control infants (n=22), and term controls (n=7) was obtained during surgical resection and at stoma closure after recovery. Paneth cell abundance and protein expression were analyzed by immunohistochemistry. RNA levels of Paneth cell proteins were determined by quantitative real-time RT-PCR. In ileostomy outflow fluid, Paneth cell products were quantified and antimicrobial activity was measured *in vitro*. In acute NEC, Paneth cell abundance in small intestinal tissue was not significantly different from preterm controls. After recovery from NEC, Paneth cell hyperplasia was observed in the small intestine concomitant with elevated human alpha-defensin 5 (HD5) mRNA levels. In the colon, metaplastic Paneth cells were observed. Ileostomy fluid contained Paneth cell proteins and inhibited bacterial growth. In conjunction, these data suggest an important role of Paneth cells and their products in various phases of NEC.

INTRODUCTION

Paneth cells, named after Joseph Paneth¹, play a significant role in the innate immune response. Localized at the base of the crypts of Lieberkühn, Paneth cells are abundant in the ileum and only occasionally found in the proximal colon.² Paneth cells have defensive functions including: 1) protection of stem cells in response to invading microbes³⁻⁴; 2) eradication of ingested pathogens⁵⁻⁷; 3) regulation of the composition, distribution, and number of commensal bacteria in the intestinal lumen⁸⁻⁹; 4) induction of cytokine secretion, immune cell recruitment, and chloride secretion to flush the intestinal crypts of pathogens.¹⁰⁻¹¹

Paneth cells execute their functions by production of antimicrobial proteins/peptides such as lysozyme¹²⁻¹³, secretory phospholipase-A2 (sPLA2)¹⁴, and human α -defensins (HD5 and -6).¹⁵⁻¹⁶ In the human fetal intestine, Paneth cells are present from 20 weeks of gestation, however HD5 and -6 mRNAs are expressed from 13.5 weeks onwards.¹⁷⁻¹⁸ Both Paneth cell numbers and HD5 and -6 mRNA expression are lower in premature infants at 24 weeks of gestation compared to term infants, and up to 200-fold lower than in adults.¹⁸ In the premature infant, who is often exposed to nosocomial pathogens and has delayed colonization with beneficial commensals, this phenomenon could result in higher susceptibility to bacterial infection and inflammation.

Although Paneth cell dysfunction in necrotizing enterocolitis (NEC) has been suggested¹⁹, little is known about Paneth cell abundance and function in preterm infants at risk for NEC. NEC is the most common gastrointestinal disease in premature infants with mortality rates up to 50% for infants needing surgery.²⁰⁻²¹ Risk factors for NEC are prematurity, very low birth weight, enteral formula feeding, and bacterial colonization.²²⁻²⁴ However, the underlying etiology and the impact of the innate immune system on the development of NEC require further investigation.

We hypothesized that preterm infants with acute NEC have fewer Paneth cells compared to control patients, and that Paneth cell numbers are up-regulated during recovery from NEC, thereby enhancing the innate immune response. Our aim was to i) study Paneth cell presence, Paneth cell protein expression, and disease-related changes in Paneth cell numbers over time in premature infants with NEC compared to control patients, and ii) to measure Paneth cell products in ileostomy outflow fluid during NEC recovery and to determine the bactericidal activity of ileal outflow fluid.

METHODS

Study population

Premature infants, who underwent bowel resection for NEC between August 2003 and September 2009, were eligible for the study. NEC was diagnosed and staged according to Bell's criteria.²⁵ Diagnosis was confirmed during surgery and by histopathological evaluation of resected intestinal tissue. Samples of both ends of the resected intestine represented macroscopically vital tissue and were collected for histology and quantitative real-time RT-PCR (qRT-PCR). Approximately 3-5 weeks after surgery, when infants received an enteral intake of at least 100 ml·kg·d, enterostomy outflow fluid was collected every 3h for 24h and immediately stored at -20°C. After full recovery, patients underwent a second surgical procedure when eligible for reanastomosis (i.e. stoma closure). To allow proper reanastomosis tissue was resected, which was collected for histology. Patients who underwent surgery for resection of post-NEC strictures, as a result of obstructive fibrotic intestinal tissue that developed during non-surgical therapy for NEC, were also included. These samples were not subjected to surgical manipulation or exposed to the extra-abdominal environment, and are thus representative for the effects of NEC only. Again, samples were taken from both the proximal and distal part of the resected intestine. Finally, both preterm and term neonates who underwent resection for developmental defects or diseases other than NEC were included as control patients, and intestinal tissue was collected as described above. Infants diagnosed with cystic fibrosis were excluded. The study protocol was approved by the 'Central Committee on Research involving Human Subjects' (The Hague, the Netherlands) and written informed consent was obtained from the parents.

Histology and Immunohistochemistry

Intestinal tissues were fixed in 4% (wt/vol) paraformaldehyde in phosphate buffered saline for 24h at 4°C and processed for light microscopy. Five micrometer-thick sections were cut and deparaffinized through a graded series of xylol-ethanol. For histology, tissue samples were stained with hematoxylin and eosin. To determine Paneth cell-specific expression of lysozyme, trypsin and HD5, immunohistochemistry was performed as described previously.²⁶⁻²⁷ Antibodies used were anti-human lysozyme (Dako, Glostrup, Denmark), anti-human trypsin (MAB 1482; Millipore, Billerica, MA, USA) and anti-human HD5 (HyCult Biotechnology, Uden, the Netherlands). Secondary antibodies applied were biotinylated horse anti-mouse IgG diluted (Vector Laboratories, Burlingame, England) and biotinylated goat anti-rabbit IgG (Vector Laboratories). Detection was performed using the ABC-PO complex (Vectastain Elite Kit, Vector Laboratories). Staining was developed using diaminobenzidine.

Collected tissue samples were assigned to intestinal segments according to their origin: jejunum, ileum, cecum, colon ascendens, colon transversum, colon descendens, and rectosigmoid. When samples originated from the same intestinal segment, only one sample per segment was analyzed. Samples from NEC and control infants were matched and analyzed according to their segment of origin. Tissue morphology was qualitatively assessed by 2 trained observers (PJP&IBR). A semi-quantitative assessment of Paneth cell abundance based on lysozyme and HD5 positive cells was performed. Paneth cells within 10 crypts per tissue sample were scored blinded as follows: 0: no Paneth cells; 1: 0-1 Paneth cells per crypt and at least 1 Paneth cell per 10 crypts; 2: 1-4 Paneth cells per crypt; 3: more than 4 Paneth cells per crypt. Scores were given by one observer and validated by the second observer.

Quantitative real-time RT-PCR

RNA was isolated from snap-frozen ileal tissue (RNeasy Midi kit; Qiagen Benelux, Venlo, the Netherlands) and used for cDNA synthesis. Expression levels of *DEFA5* (HD5), *LYZ* (lysozyme), *TRY2* (anionic trypsin), and *PLA2G2A* (sPLA2) were quantified using qRT-PCR analysis based upon the intercalation of SYBR Green on an ABI prism 7900HT Fast Real-Time PCR system (PE Applied Biosystems, Foster City, CA, USA) as described previously.²⁸ Messenger RNA levels were expressed relative to the epithelial-specific housekeeping gene *VIL1* (Villin). Primer combinations are given in Table 1.

Table 1. Primer sequences used for quantitative real time RT-PCR

Gene	Forward primer	Reverse primer
<i>LYZ</i>	5'- TTT GCT GCA AGA TAA CAT C -3'	5'- GAC GGA CAT CTC TGT TTT G -3'
<i>DEFA5</i>	5'- TGC AGG AAA TGG ACT CTC -3'	5'- GCC ACT GAT TTC ACA CAC -3'
<i>PLA2G2A</i>	5'- TGG CAC CAA ATT TCT GA -3'	5'- GCA GCC TTA TCA CAC TCA -3'
<i>TRY2</i>	5'- GCT CCA AGG AAT TGT CTC -3'	5'- GGG GCT TTA GCT GTT G -3'
<i>VIL1</i>	5'- CTG CCT TCT CTG CTC TG -3'	5'- ATC GGT GAG AAA ATG AGA C -3'

Primers for *DEFA5* (HD5), *LYZ* (lysozyme), *TRY2* (anionic trypsin), and *PLA2G2A* (secretory phospholipase A2) were designed using OLIGO 6.22 software (Molecular Biology Insights, Cascade, CO, USA).

Protein isolation and Western blot analyses

To isolate proteins from the small intestinal outflow fluid, cesium-chloride density gradient ultracentrifugation was performed as described previously.²⁹⁻³⁰ Fractions with a buoyant density >1.35 g/ml, containing high density proteins, were discarded. Fractions with a buoyant density <1.35 g/ml were pooled, dialyzed, and used to quantify lysozyme, trypsin, and sPLA2 by Western-blot. The used dialysis membrane had a cut-off size of 10 kD and therefore did not allow analysis of HD5 as HD5 is smaller than 10 kD. Primary antibodies used were rabbit anti-lysozyme (Dako), rabbit anti-sPLA2 (H-74) (Santa Cruz

Biotechnology, Santa Cruz, CA, USA), and mouse anti- α -trypsin (MAB 1482, Chemicon International). Bound antibodies were detected using HRP-conjugated goat anti-rabbit or anti-mouse antibodies and Luminol Enhancer (Pierce, Thermo Fisher Scientific Inc., Rockford, IL, USA). Western-blots were analyzed using densitometry.

Antimicrobial assay

Escherichia coli (*E. coli*), *Lactococcus lactis* (*L. lactis*), and *Lactobacillus rhamnosus* (LGG) were grown overnight in LB medium, GM17 medium, and MRS medium (BD, Franklin Lakes, NJ, USA) respectively, at 37°C. The pooled antimicrobial protein fractions (100 μ g) were added to 200 μ l of bacterial cultures of 2×10^7 colony forming units (CFU)/ml and incubated for 1 h at 37°C. A 10^{-4} dilution was prepared and 100 μ l of the suspension was plated. After overnight incubation at 37°C, CFUs were counted. Bacterial growth inhibition was analyzed by calculating the number of CFUs in comparison to untreated bacteria.

Statistical analysis

Comparisons between patient groups were made using ANOVA with a post-hoc Tukey T-test for normally distributed data or the Kruskal-Wallis Test followed by Dunn's Multiple Comparison Test for not-normally distributed data. Protein and mRNA levels of antimicrobial proteins were determined using the Mann Whitney test. Analyses were performed using GraphPad Prism version 5.0 (GraphPad Software, San Diego, CA, USA). Significance was defined at $P < .05$.

RESULTS

Study population

A total of 84 infants were included in the study. Patient characteristics are shown in table 2. Forty-nine preterm infants underwent bowel resection for stage III acute NEC, further referred to as A-NEC. After resection of necrotic tissue, primary anastomosis was performed in 4 patients, an enterostomy was created in 40 infants, and in 5 patients NEC lesions were too extensive to allow further surgical treatment compatible with life. In total 13 infants (27%) died of complications of NEC. After recovery, 31 out of the 40 enterostomy patients were eligible for reanastomosis (further referred to as NEC-R), allowing repeated tissue collection. Additionally, six premature infants were included, who had received non-surgical treatment for NEC, but developed post-NEC strictures requiring surgery (Post-NEC Stricture).

Twenty-two premature infants were included as control (Preterm CO). These patients were diagnosed with small intestinal atresia ($n=8$), milk curd obstruction ($n=3$),

Table 2. Patient Demographics

	NEC	Post-NEC Stricture	Preterm CO	Term CO	P-value
No. of patients	49	6	22	7	
Demographics					
Sex, % male	61	67	50	57	
Gestational age (wk)	29.5 ± 3	31.8 ± 3.7	32.9 ± 3.9	38.2 ± 1.2	a,c,i,k
Birth weight (g)	1239 ± 501.8	1618 ± 507.5	2051 ± 874.8	2946 ± 738.9*	a,c,h,j
Apgar score 1 min	7 (4 - 9)	7.5 (2.9 - 9)	8 (5 - 9)*	9 (8 - 9)†	NS
Apgar score 5 min	9 (8 - 10)	9.5 (8.3 - 10)	9 (8 - 9)*	9 (9 - 10)†	NS
Clinical and surgical outcome					
Postnatal age at 1 st surgery (d)	11 (7 - 17.5)	40 (35.8 - 51)	1.5 (0 - 16)	2 (0 - 3)	b,d,e,g,h
Gestational age at 1 st surgery (wk)	31.7 (29.2 - 34)	38 (35.8 - 40.5)	34.4 (31 - 36.1)	38 (37.6 - 40.3)	b,c,f
Primary anastomosis, %	8	100	27	42.3	
Jejunostomy, %	12	-	23	14.3	
Ileostomy, %	61	-	45	42.3	
Colostomy, %	8	-	4	-	
Deaths, %	27	-	4	-	
Patients eligible for reanastomosis, %	63	-	59	-	
Postnatal age at reanastomosis (d)	95 (57 - 125)	-	55 (44 - 102)	-	NS
Gestational age at reanastomosis (wk)	43 (40.1 - 46.6)	-	41 (39.5 - 46.4)	-	NS

Data provided are percentages or means ± SD. Medians (interquartile range) are provided for variables that are not normally distributed.

a $P < .001$ for comparisons between NEC and Preterm controls.

b $P < .05$ for comparisons between NEC and Preterm controls.

c $P < .001$ for comparisons between NEC and Term Controls.

d $P < .05$ for comparisons between NEC and Term Controls.

e $P < .05$ for comparisons between NEC and Post-NEC Strictures.

f $P < .001$ for comparisons between NEC and Post-NEC Strictures.

g $P < .001$ for comparisons between Post-NEC Strictures and Preterm Controls.

h $P < .001$ for comparisons between Post-NEC Strictures and Term controls.

i $P < .01$ for comparisons between Post-NEC Strictures and Term controls.

j $P < .05$ for comparisons between Preterm controls and Term controls.

k $P < .01$ for comparisons between Preterm controls and Term controls.

ns. not significant.

*Data on 1 patient was not recorded. † Data on 2 patients was not recorded.

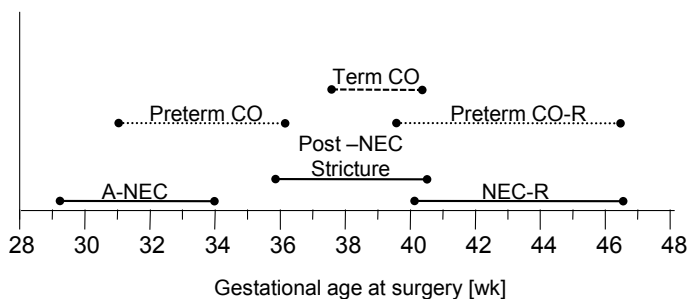


Figure 1. Time-frame representing an overview of intestinal tissue sampling according to gestational age. Bars represent interquartile ranges. A-NEC patients are significantly younger than Preterm CO (Mann-Whitney $P < .01$), but corrected gestational age is comparable during reanastomosis. Corrected gestational age during reanastomosis is in both groups not different from patients with Post-NEC strictures and Term Controls during surgery.

perforation due to herniation ($n=2$), solitary perforation ($n=1$), ileus ($n=1$), meckel's diverticulum ($n=1$), volvulus ($n=2$), gastroschisis ($n=3$) and cloacal malformation ($n=1$). After intestinal resection, 6 infants received a primary anastomosis and 16 an enterostomy. Post-surgically 1 patient died of additional clinical complications. After full recovery, 13 infants were eligible for stoma closure (Preterm CO-R), allowing repeated tissue collection.

Seven term infants who were resected for small intestinal atresia ($n=3$), intestinal perforation ($n=3$), and volvulus ($n=1$), were included as term controls (Term CO).

Figure 1 depicts the corrected gestational age at the time of tissue sampling during surgery for all patient groups.

Sample evaluation

In most infants the resected intestine covered multiple intestinal segments. Samples were cut from both ends of the resected material and therefore sample numbers do not correlate with the number of patients included. Samples from jejunum, ileum, and colon were used for morphological analysis ($n=157$). Samples that showed complete mucosal erosion were excluded from further analyses ($n=36$). The remaining samples were stained for lysozyme, HD5, and trypsin to analyze Paneth cell-specific protein expression. Scoring was based upon both lysozyme and HD5 staining. Table 3 demonstrates the number of samples that were obtained and evaluated for each patient group.

Paneth cell hyperplasia during NEC recovery

Paneth cells were present in small intestinal tissue of NEC patients and Preterm CO, and were positive for lysozyme (Figure 2A-D), HD5 (Figure 2E-H), and trypsin (not shown). Abundance of Paneth cells, determined by lysozyme and HD5 staining, was not significantly different between A-NEC and Preterm CO (Figure 3). In reanastomosis

Table 3. Sample evaluation of intestinal tissue obtained during acute surgery (A) and reanastomosis (B)

A. Acute surgery		Small Intestine		Colon		
Patient Groups	Total	Excluded	Evaluated	Total	Excluded	Evaluated
NEC	46	16	30	18	8	10
Post-NEC Stricture	0	0	0	5	0	5
Preterm CO	21	4	17	2	1	1
Term CO	7	1	6	1	0	1
B. Reanastomosis		Small Intestine		Colon		
Patient Groups	Total	Excluded	Evaluated	Total	Excluded	Evaluated
NEC	29	3	26	13	2	11
Preterm CO	12	1	11	3	0	3

Note: Tissue samples were obtained from both ends of resected intestine and might originate from multiple intestinal segments. Therefore patient numbers do not correlate with sample numbers.

ILEUM

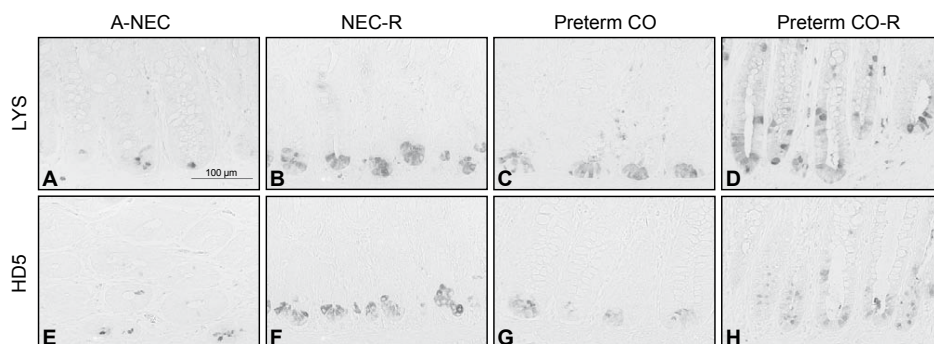


Figure 2. Immunohistochemistry for lysozyme- (LYS) (A-D) and HD5-positive (E-H) Paneth cells in ileal tissue from NEC patients and Preterm CO. (A, E) A-NEC; (B, F) NEC-R; (C, G) Preterm CO; (D, H) Preterm CO-R. Images are representative of 19 A-NEC, 21 NEC-R, 9 Preterm CO, and 6 Preterm CO-R specimens derived from the ileum. (See Color Section, p. 240.)

samples, no differences in Paneth cell abundance between NEC-R and Preterm CO-R were observed (Figure 3). However, small intestinal samples in both NEC-R and Preterm CO-R showed increased numbers of Paneth cells, determined by lysozyme and HD5 staining, when compared to A-NEC and Preterm CO samples, respectively (Figure 3). To determine whether this increase in Paneth cell numbers was age- or disease-related, we compared Term CO samples to NEC-R and Preterm CO-R samples, as the corrected gestational age at time of surgery was not significantly different between these groups (Figure 1). Interestingly, Paneth cell abundance in small intestinal NEC-R and Preterm CO-R tissue was increased compared to Term CO indicating a disease-related effect.

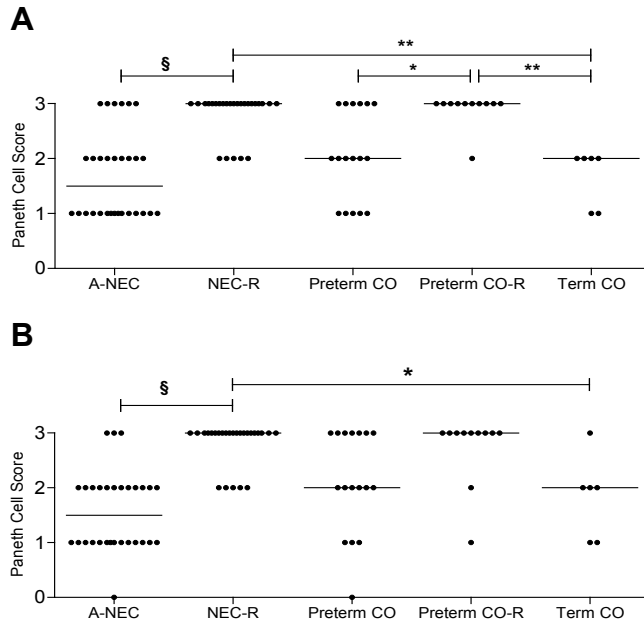


Figure 3. Paneth cell abundance in small intestinal tissue from A-NEC and NEC-R patients, Preterm CO and Preterm CO- R, and Term CO obtained during acute surgery and reanastomosis. Scoring of HD5-positive (A) and lysozyme-positive (B) Paneth cells, based upon the number of stained cells per crypt from an average of 10 crypts (see methods). Lines represent medians. Statistics were performed using the Kruskal-Wallis - Dunn's Multiple Comparison test. * $P < .05$; ** $P < .01$; § $P < .001$.

COLON

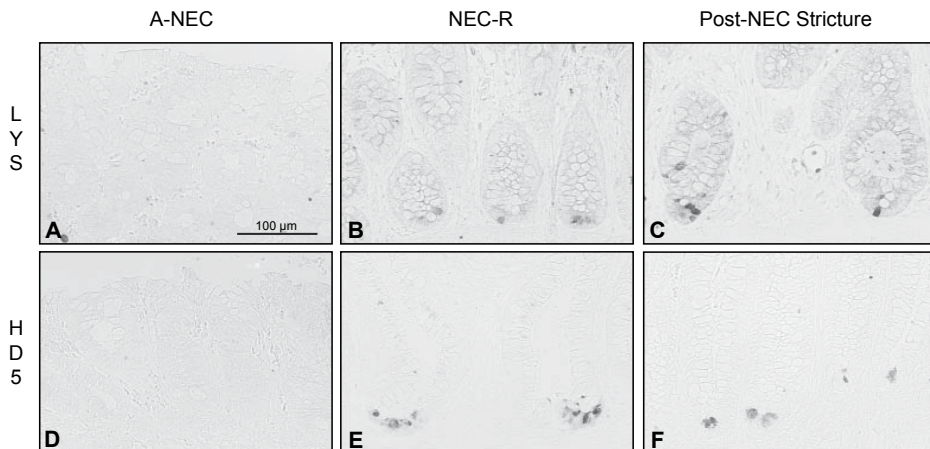
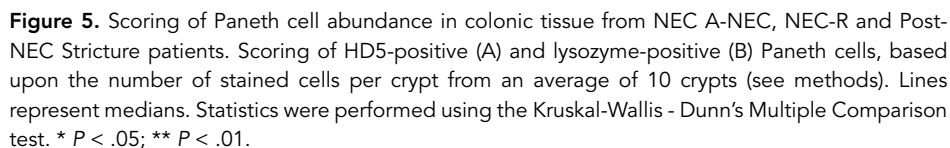


Figure 4. Representative immunohistochemistry for lysozyme (LYS; A-C) and HD5 (D-F) in metaplastic Paneth cells in colonic tissue from NEC patients. (A, D) A-NEC. (B, E) NEC-R. (C, F) Post-NEC Stricture. Images are representative of 10 A-NEC, 11 NEC-R, and 5 Post-NEC Stricture specimens. (See Color Section, p. 241.)



In 9 out of 10 samples, no Paneth cells were found in colonic tissue from A-NEC patients (Figure 4 and 5). Unexpectedly, at the time of reanastomosis nearly all proximal and distal colon samples showed metaplastic Paneth cells, determined by lysozyme and HD5 staining (Figure 4). This finding was confirmed by the Post-NEC Stricture colon samples which all displayed metaplastic Paneth cells (Figure 4). Figure 5 presents the scoring of Paneth cell-abundance in the colon and demonstrates the induction of metaplastic Paneth cells, assessed by staining for HD5 (Figure 5A) and lysozyme (Figure 5B), in NEC-R and Post-NEC Stricture. In Preterm CO-R, only few colon samples (n=3) were obtained, nevertheless all samples showed Paneth cell metaplasia (not shown).

Analyses of ileal samples from 21 NEC patients by qRT-PCR showed that *LYZ*, *TRY2*, and *PLA2G2A* mRNA levels were not different in tissue from A-NEC (n=8) vs. NEC-R (n=13) (Figure 6). However, expression of *DEFA5* was significantly higher in NEC-R compared to A-NEC (Figure 6A-D). Although sample numbers obtained from preterm control infants were limited, expression of *LYZ*, *TRY2*, *PLA2G2A*, and *DEFA5* tended to be higher in Preterm CO-R samples (n=5) compared to Preterm CO (n=4) (Figure 6E-H).

leostomy outflow fluid from 12 patients was collected during the regenerative phase of NEC (Table 4). Isolates of the outflow fluid samples contained lysozyme, trypsin, and sPLA2. As lysozyme and trypsin are present in breast milk, we analyzed whether levels of these antimicrobial products would differ between infants receiving breast milk (n=6) or

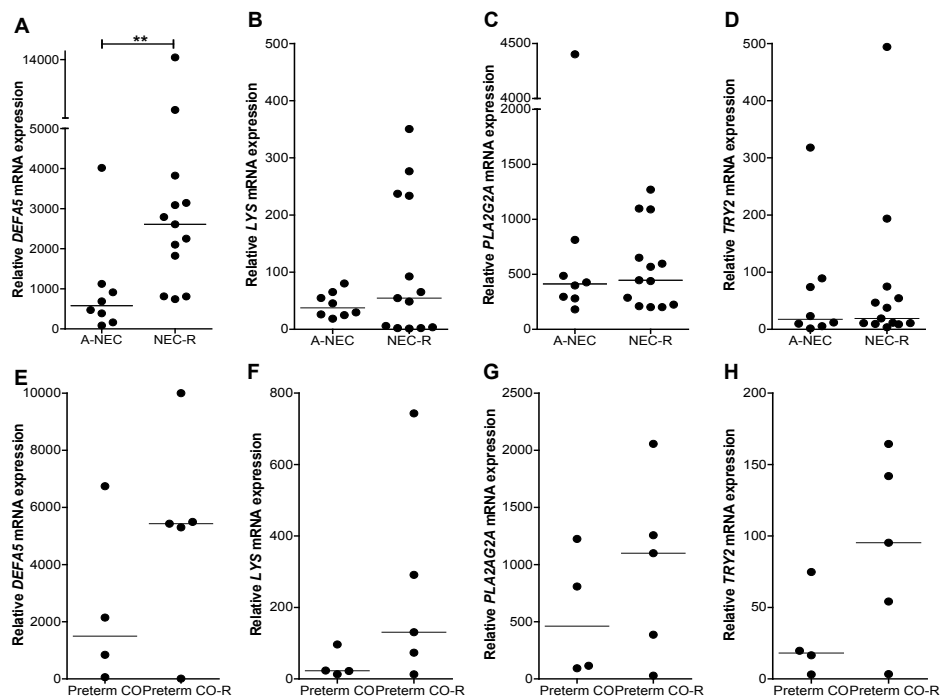


Figure 6. Expression of anti-bacterial peptide genes in A-NEC and NEC-R (A-D) and Preterm CO and Preterm CO-R (E-H): (A, E) *DEFA5*, (B, F) *LYS*, (C, G) *PLA2G2A*, and (D, H) *TRY2*. *DEFA5* expression was upregulated in NEC Reanastomosis; Mann Whitney test $P = .013$. Lines represent medians.

Table 4. Baseline characteristics of NEC patients sampled for ileostomy outflow fluid

No. of patients	12
Demographics	
Sex, % male	92
Gestational age (wk)	29.1 \pm 3.1
Birth weight (g)	1210 \pm 524
Postnatal age at 1 st surgery (d)	11.5 (7.8 - 13.5)
Time of enterostomy outflow collection post-surgery (d)	22 (18.3 - 25)
Patients receiving breast milk, %	50
Patients receiving antibiotic treatment during sampling, %	33

Data provided are percentages or means \pm SD. Medians (interquartile range) are provided for variables that are not normally distributed.

formula ($n=6$). There was no statistically significant difference between the groups (data not shown).

Bactericidal activity of the outflow fluid isolates was demonstrated by growth inhibition of *E. coli* with 52% ($\pm 18\%$), *L. lactis* with 81% ($\pm 20\%$) and *LGG* with 43% ($\pm 17\%$) (Figure 7A). Increasing concentrations of protein isolates ($n=7$) were used to determine

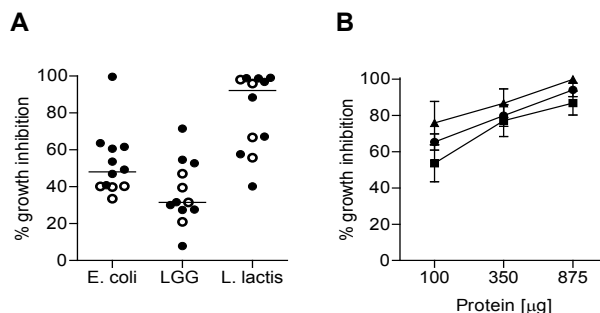


Figure 7. (A) Antimicrobial assay showing bactericidal activity of protein isolates from ileostomy outflow fluid samples ($n=12$) on *E. coli*, LGG and *L. lactis*. Bactericidal activity is expressed as % growth inhibition compared to non-treated controls. Open symbols denote antibiotic-treated patients. Lines represent means. (B) Bacterial challenge assay showing up to 100 % growth inhibition of *E. coli*—●—, LGG—■— and *L. Lactis*—▲— with increasing doses of protein isolates ($n=7$). Bars represent means \pm SEM.

bacterial growth inhibition capacity. Growth inhibition up to 100% was reached as presented in figure 7B. To evaluate whether antibiotic treatment influenced the observed effect, we compared bacterial growth inhibition from isolates of antibiotic-treated patients ($n=4$) to isolates from patients without antibiotics, but no difference was observed (Figure 7).

DISCUSSION

Paneth cells play a key role in the innate immune response and host defense. Although Paneth cell dysfunction has been suggested, little is known about Paneth cell presence and function in the immature gut and gastrointestinal complications of prematurity such as NEC. In the present study we analyzed Paneth cell-presence, function, and disease-related changes in Paneth cell abundance over time in preterm infants with NEC. Our results show Paneth cell hyperplasia and metaplasia in premature infants recovering from NEC. Furthermore, Paneth cell-products from ileostomy outflow fluid of NEC patients exhibited strong bactericidal activity.

First, Paneth cell presence and protein expression in small intestinal samples of A-NEC patients vs. Preterm CO was investigated. We found that Paneth cells were present in A-NEC both A-NEC and Preterm CO.

Coutinho and colleagues observed an absence of lysozyme-positive Paneth cells in acute NEC, and suggested a developmental defect in Paneth cells, i.e. delayed maturation of Paneth cells, leading to lack of antimicrobial agents such as lysozyme and defensins.¹⁹ Besides the fact that 40% of their NEC-patients were term newborns in whom the disease is thought to be different from premature infants³¹⁻³³, the absence of

lysozyme-positive Paneth cells might be explained by enhanced secretion of lysozyme. Nevertheless, our study demonstrates Paneth cell-specific lysozyme and HD5 mRNA and protein in A-NEC contradicting Paneth cell deficiency in preterm infants.

Similarly to our results, Salzman *et al.* showed presence of Paneth cells in acute NEC patients.³⁴ Semi-quantitative analysis of the 6 preterm acute NEC infants investigated in that study revealed an increase in Paneth cell numbers and *HD5* mRNA levels in infants with NEC compared to (near) term control infants. In our study we did not observe a difference between A-NEC and Term CO with respect to Paneth cell abundance; however we did when we compared NEC-R infants to Term CO. Another point of interest is that in the study of Salzman, intracellular peptide levels in NEC did not coincide with the observed rise in mRNA. Although we did not quantify intracellular peptide levels per Paneth cell, low *HD5* mRNA levels coincided with low numbers of HD5-positive Paneth cells, whereas high *HD5* mRNA levels correlated with the hyperplasia of HD5-positive Paneth cells during reanastomosis. Therefore, our study is the first to report small intestinal Paneth cell hyperplasia after recovery from NEC and strongly implies an up-regulation of Paneth cell abundance. We did not detect differences in lysozyme, sPLA2, and trypsin mRNA levels in A-NEC vs. NEC-R. However, in contrast to HD5, these products are not restricted to Paneth cells for their production and therefore don't necessarily reflect changes in Paneth cell abundance.

In concordance to the hyperplasia observed in NEC, Paneth cell numbers in Preterm CO-R were also up-regulated compared to Preterm CO. Moreover, both Preterm CO-R and NEC-R tissue showed higher numbers of Paneth cells compared to Term CO. Most likely severe or prolonged intestinal inflammation, which to a lesser extend was also seen in preterm control infants, might explain the observed hyperplasia. However, the effect of increased postnatal age in this preterm population compared to Term CO cannot be excluded.

A novel finding in our study is the occurrence of Paneth cell metaplasia in colon samples during NEC-recovery. The expression of lysozyme, trypsin, and HD5 indicated the presence of well-differentiated cells able to exert Paneth cell-defensive functions. Although Paneth cell metaplasia has not been described in NEC, this phenomenon has been reported in inflammatory bowel disease.³⁵ Metaplasia can occur through restitution or regeneration of tissue after intestinal mucosal surface loss, either due to resection, and/or inflammation.³⁶ However, as our Post-NEC stricture patients had not undergone resection during acute NEC, but did show Paneth cell metaplasia, we suggest that inflammation caused Paneth cell-metaplasia.

During recovery, lysozyme, trypsin, and sPLA2 were present in intestinal outflow fluid and outflow fluid inhibited bacterial growth *in vitro*. Similar outcomes were found in *in vitro* studies performed with human and mouse peptide isolates.³⁷⁻³⁹ A caveat is that these antibacterial products are not Paneth cell specific. However, the presence

of Paneth cells in A-NEC and the presence of these peptides in the ileal outflow fluid, imply that Paneth cells in preterm infants are present and at least partially functional by secreting antimicrobial products. Therefore, Paneth cell deficiency, i.e. a lack of Paneth cells, in preterm infants with NEC seems unlikely. However, we cannot exclude that there are abnormalities in Paneth cells that limit their functioning in infants with NEC.

A limitation of the present study is that interpretation of our findings is difficult since preterm controls also exhibit signs of inflammation, numbers of age-matched control patients are limited, and collecting material from a healthy control group is not feasible. Nevertheless, our results indicate the presence of Paneth cells in preterm infants with NEC, and imply that Paneth cell hyperplasia and metaplasia is most likely caused by inflammation. Subsequently, increased Paneth cell numbers suggests enhanced secretion of active antimicrobial products and might be indicative of an enhanced innate defense response during prolonged inflammation which might contribute to NEC-recovery. However, it still remains to be elucidated which possible cell signaling and regulatory pathways are involved in these processes to target improvement of therapy and clinical outcome.

ACKNOWLEDGEMENTS

The author's thank J. Bouma for excellent technical assistance.


FUNDING

Partly supported by Danone. The study sponsor had no role in the study design, analysis of data, or writing of the manuscript.

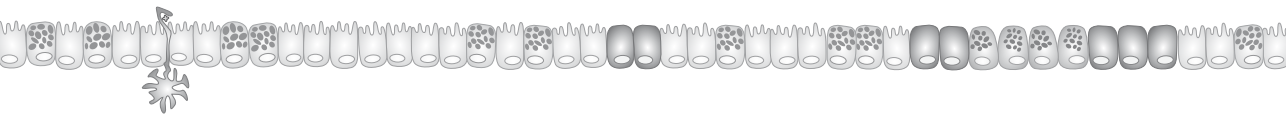
REFERENCES


1. Paneth J. Ueber die secernirenden Zellen des Dünndarm-Epithels. *Arch. Mikroskop. Anat.* 1888;113-191.
2. Sandow MJ, Whitehead R. The Paneth cell. *Gut* 1979;20:420-31.
3. Ganz T. Defensins: antimicrobial peptides of innate immunity. *Nat Rev Immunol* 2003;3:710-20.
4. Salzman NH, Underwood MA, Bevins CL. Paneth cells, defensins, and the commensal microbiota: a hypothesis on intimate interplay at the intestinal mucosa. *Semin Immunol* 2007;19:70-83.
5. Ayabe T, Satchell DP, Wilson CL, Parks WC, Selsted ME, Ouellette AJ. Secretion of microbicidal alpha-defensins by intestinal Paneth cells in response to bacteria. *Nat Immunol* 2000;1:113-8.
6. Salzman NH, Ghosh D, Huttner KM, Paterson Y, Bevins CL. Protection against enteric salmonellosis in transgenic mice expressing a human intestinal defensin. *Nature* 2003;422:522-6.
7. Fernandez MI, Regnault B, Mulet C, Tanguy M, Jay P, Sansonetti PJ, Pedron T. Maturation of paneth cells induces the refractory state of newborn mice to *Shigella* infection. *J Immunol* 2008;180:4924-30.
8. Wilson CL, Ouellette AJ, Satchell DP, Ayabe T, Lopez-Boado YS, Stratman JL, Hultgren SJ, Matrisian LM, Parks WC. Regulation of intestinal alpha-defensin activation by the metalloproteinase matrilysin in innate host defense. *Science* 1999;286:113-7.
9. Salzman NH, Hung K, Haribhai D, Chu H, Karlsson-Sjoberg J, Amir E, Teggatz P, Barman M, Hayward M, Eastwood D, Stoel M, Zhou Y, Sodergren E, Weinstock GM, Bevins CL, Williams CB, Bos NA. Enteric defensins are essential regulators of intestinal microbial ecology. *Nat Immunol* 2010;11:76-83.
10. Lin PW, Simon PO, Jr., Gewirtz AT, Neish AS, Ouellette AJ, Madara JL, Lencer WI. Paneth cell cryptdins act in vitro as apical paracrine regulators of the innate inflammatory response. *J Biol Chem* 2004;279:19902-7.
11. Lencer WI, Cheung G, Strohmeier GR, Currie MG, Ouellette AJ, Selsted ME, Madara JL. Induction of epithelial chloride secretion by channel-forming cryptdins 2 and 3. *Proc Natl Acad Sci U S A* 1997;94:8585-9.
12. Erlandsen SL, Parsons JA, Taylor TD. Ultrastructural immunocytochemical localization of lysozyme in the Paneth cells of man. *J Histochem Cytochem* 1974;22:401-13.
13. Klockars M, Reitamo S. Tissue distribution of lysozyme in man. *J Histochem Cytochem* 1975;23:932-40.
14. Kiyohara H, Egami H, Shibata Y, Murata K, Ohshima S, Ogawa M. Light microscopic immunohistochemical analysis of the distribution of group II phospholipase A2 in human digestive organs. *J Histochem Cytochem* 1992;40:1659-64.
15. Jones DE, Bevins CL. Paneth cells of the human small intestine express an antimicrobial peptide gene. *J Biol Chem* 1992;267:23216-25.
16. Jones DE, Bevins CL. Defensin-6 mRNA in human Paneth cells: implications for antimicrobial peptides in host defense of the human bowel. *FEBS Lett* 1993;315:187-92.
17. Klockars M, Reitamo S, Adinolfi M. Ontogeny of human lysozyme. Distribution in fetal tissues. *Biol Neonate* 1977;32:243-9.

18. Mallow EB, Harris A, Salzman N, Russell JP, DeBerardinis RJ, Ruchelli E, Bevins CL. Human enteric defensins. Gene structure and developmental expression. *J Biol Chem* 1996;271: 4038-45.
19. Coutinho HB, da Mota HC, Coutinho VB, Robalinho TI, Furtado AF, Walker E, King G, Mahida YR, Sewell HF, Wakelin D. Absence of lysozyme (muramidase) in the intestinal Paneth cells of newborn infants with necrotising enterocolitis. *J Clin Pathol* 1998;51:512-4.
20. Sharma R, Tepas JJ, 3rd, Hudak ML, Wludyka PS, Mollitt DL, Garrison RD, Bradshaw JA, Sharma M. Portal venous gas and surgical outcome of neonatal necrotizing enterocolitis. *J Pediatr Surg* 2005;40:371-6.
21. Blakely ML, Lally KP, McDonald S, Brown RL, Barnhart DC, Ricketts RR, Thompson WR, Scherer LR, Klein MD, Letton RW, Chwals WJ, Touloukian RJ, Kurkchubasche AG, Skinner MA, Moss RL, Hilfiker ML. Postoperative outcomes of extremely low birth-weight infants with necrotizing enterocolitis or isolated intestinal perforation: a prospective cohort study by the NICHD Neonatal Research Network. *Ann Surg* 2005;241:984-9; discussion 989-94.
22. Lin PW, Stoll BJ. Necrotising enterocolitis. *Lancet* 2006;368:1271-83.
23. Lucas A, Cole TJ. Breast milk and neonatal necrotising enterocolitis. *Lancet* 1990;336:1519-23.
24. Claud EC, Walker WA. Hypothesis: inappropriate colonization of the premature intestine can cause neonatal necrotizing enterocolitis. *Faseb J* 2001;15:1398-403.
25. Bell MJ, Ternberg JL, Feigin RD, Keating JP, Marshall R, Barton L, Brotherton T. Neonatal necrotizing enterocolitis. Therapeutic decisions based upon clinical staging. *Ann Surg* 1978; 187:1-7.
26. Renes IB, Verburg M, Bulsing NP, Ferdinandusse S, Buller HA, Dekker J, Einerhand AW. Protection of the Peyer's patch-associated crypt and villus epithelium against methotrexate-induced damage is based on its distinct regulation of proliferation. *J Pathol* 2002;198:60-8.
27. Schaart MW, Yamanouchi T, van Nispen DJ, Raatgeep RH, van Goudoever JB, de Krijger RR, Tibboel D, Einerhand AW, Renes IB. Does small intestinal atresia affect epithelial protein expression in human newborns? *J Pediatr Gastroenterol Nutr* 2006;43:576-83.
28. Meijerink J, Mandigers C, van de Locht L, Tonnissen E, Goodsaid F, Raemaekers J. A novel method to compensate for different amplification efficiencies between patient DNA samples in quantitative real-time PCR. *J Mol Diagn* 2001;3:55-61.
29. Schaart MW, Schierbeek H, de Bruijn AC, Tibboel D, van Goudoever JB, Renes IB. A novel method to determine small intestinal barrier function in human neonates in vivo. *Gut* 2006; 55:1366-7.
30. Tytgat KM, Klomp LW, Bovelandt FJ, Opdam FJ, Van der Wurff A, Einerhand AW, Buller HA, Strous GJ, Dekker J. Preparation of anti-mucin polypeptide antisera to study mucin biosynthesis. *Anal Biochem* 1995;226:331-41.
31. Holman RC, Stoll BJ, Clarke MJ, Glass RI. The epidemiology of necrotizing enterocolitis infant mortality in the United States. *Am J Public Health* 1997;87:2026-31.
32. Maayan-Metzger A, Itzhak A, Mazkereth R, Kuint J. Necrotizing enterocolitis in full-term infants: case-control study and review of the literature. *J Perinatol* 2004;24:494-9.
33. The Canadian Neonatal N. Variations in Incidence of Necrotizing Enterocolitis in Canadian Neonatal Intensive Care Units. *J Pediatr Gastroenterol Nutr* 2004;39:366-372.
34. Salzman NH, Polin RA, Harris MC, Ruchelli E, Hebra A, Zirin-Butler S, Jawad A, Martin Porter E, Bevins CL. Enteric defensin expression in necrotizing enterocolitis. *Pediatr Res* 1998;44: 20-6.

- 
35. Tanaka M, Saito H, Kusumi T, Fukuda S, Shimoyama T, Sasaki Y, Suto K, Munakata A, Kudo H. Spatial distribution and histogenesis of colorectal Paneth cell metaplasia in idiopathic inflammatory bowel disease. *J Gastroenterol Hepatol* 2001;16:1353-9.
 36. Helmrath MA, Fong JJ, Dekaney CM, Henning SJ. Rapid expansion of intestinal secretory lineages following a massive small bowel resection in mice. *Am J Physiol Gastrointest Liver Physiol* 2007;292:G215-22.
 37. Eisenhauer PB, Harwig SS, Lehrer RI. Cryptdins: antimicrobial defensins of the murine small intestine. *Infect Immun* 1992;60:3556-65.
 38. Ouellette AJ, Hsieh MM, Nosek MT, Cano-Gauci DF, Huttner KM, Buick RN, Selsted ME. Mouse Paneth cell defensins: primary structures and antibacterial activities of numerous cryptdin isoforms. *Infect Immun* 1994;62:5040-7.
 39. Porter EM, van Dam E, Valore EV, Ganz T. Broad-spectrum antimicrobial activity of human intestinal defensin 5. *Infect Immun* 1997;65:2396-401.

Chapter 6





Trans-activation of the *MUC2* promoter by viable and non-viable *Lactobacillus* GG

Nanda Burger-van Paassen, Janneke Bouma, Günther Boehm, Johannes B. van Goudoever, Isabelle Van Seuning, Ingrid B. Renes

Submitted



ABSTRACT

Beneficial effects have been addressed to the use of probiotics in health and disease. However, the mechanisms of action are largely unknown. The mucin MUC2 is the structural component of the intestinal mucus layer that forms a physical barrier against bacteria and harmful substances. We hypothesize that probiotics increase MUC2 synthesis. We aimed to study the effect of probiotic bacterium *Lactobacillus* GG (LGG) on MUC2 synthesis in LS174T, a human goblet cell-like cancer cell line. LGG treatment resulted in a dose dependent increase in MUC2 mRNA levels and MUC2 promoter transactivation in LS174T cells. A higher amount of nonviable LGG was required to increase MUC2 mRNA expression and MUC2 promoter activation compared to viable LGG. Moreover, stimulation of LS174T cells with viable LGG resulted in increased MUC2 protein expression. Treatment of cells with LGG-conditioned medium (LGG-CM) also resulted in increased MUC2 mRNA levels and MUC2 promoter transactivation. Subjecting LGG-CM to proteases, DNases or heat did not result in diminished MUC2 RNA levels or loss of MUC2 promoter transactivation. Furthermore, an AP-1 binding site responsible for the LGG-induced MUC2 promoter transactivation was identified. In conclusion, LGGs stimulate MUC2 synthesis in the LS174T cell line. As viable bacteria are able to activate the MUC2 promoter in lower dosages compared to nonviable bacteria, secreted bacterial products also seem to be able to stimulate MUC2 promoter transactivation. Proteins and DNA are ruled out as actors in this matter because transactivation of the MUC2 promoter was maintained after pretreatment of LGG-CM with DNase, proteases, or heat. Bacterial fermentation products are considered as possible candidates. In conjunction, these data imply that LGG can stimulate MUC2 synthesis directly and also indirectly via LGG secreted products.

Key words: MUC2, *Lactobacillus* GG (LGG), short chain fatty acids, viable, nonviable

INTRODUCTION

Probiotics are defined as 'live microbial dietary supplements which beneficially affect the host animal by improving its intestinal microbial balance'.¹ There is a growing interest in the use of probiotic bacteria for their suggested positive influence on human and animal health. Numerous probiotics have been introduced for general use whereas clinical applications of probiotics include treatment or prevention of a variety of intestinal and extra-intestinal diseases. The exact mechanism through which probiotics exert their beneficial effects is largely unknown.

Lactic acid bacteria and Bifidobacteria are both well known probiotics. Different species are thought to have specific properties, including competition for nutrients and adhesion sites with pathogenic bacteria, production of bacteriocins, inhibition of bacterial translocation, effects on immunoglobulins and antimicrobial peptide secretion.²⁻⁹ *Lactobacillus rhamnosus* GG (LGG) is a natural occurring bacterium originally isolated from the healthy human intestine. In contrast to many bacterial strains, LGG was shown to survive the acidic environment of the stomach as well as bile acids in the duodenum and proximal jejunum.¹⁰ LGG is one of the best-studied probiotic bacteria in clinical trials. It is effective in preventing and treating diarrhea¹¹⁻¹⁶, primary rotavirus infections^{14,17-18}, and atopic dermatitis in children.¹⁹⁻²⁰

Nevertheless, data demonstrating how LGG induces its beneficial effects are limited. The intestinal mucus layer forms a physical barrier between bacteria and potential toxic and noxious agents present in the gut lumen and the underlying tissues. The secretory mucin MUC2 is the predominant mucin in the colon²¹ and MUC2 synthesis is diminished in UC²²⁻²³ and presumably also in NEC.²⁴ Interestingly, in a number of studies it has been demonstrated that probiotics are able to alter mucin synthesis.²⁵⁻²⁶ For example, *Lactobacillus plantarum* 299v and LGG appeared to inhibit the adherence of an enteropathogenic *Escherichia coli* to intestinal epithelial cells.²⁷ These probiotic bacteria appeared to up-regulate MUC2 and MUC3 mRNA expression by intestinal epithelial cells. Furthermore, media containing MUC2 and MUC3 protein was shown to inhibit binding of *E. coli* to these epithelial cells. Therefore, it can be hypothesized that these probiotics increase epithelial barrier function by inducing increased synthesis of intestinal mucines. Furthermore, the stimulating effect of LGG on MUC2 mRNA synthesis has recently been studied in a 2,4,6-trinitrobenzenesulfonic acid (TNBS) colitis model.²⁸ However, the mechanisms via which LGG affects MUC2 synthesis has not been studied in detail before. For example, it is currently unknown whether non-viable LGGs or LGG conditioned culture medium is able to affect MUC2 promoter activation and thereby MUC2 protein levels.

Therefore, our objective was to study the effect of viable, nonviable LGG, and LGG conditioned culture media on MUC2 synthesis at the mRNA and promoter level.

Moreover, we identified a LGG-responsive region within the *MUC2* promoter. By studying all these parameters in conjunction we aimed to obtain more information on the mechanisms of LGG-induced effects on mucin *MUC2* synthesis.

MATERIALS AND METHODS

Cell culture

The LS174T colonic cancer cell line was cultured in a 37°C incubator with 5% CO₂ in Dulbecco's modified Eagle's minimal essential medium (DMEM) supplemented with non-essential amino acids and 10% fetal calf serum (Boehringer, Mannheim, Germany) as before.²⁹

Culture of LGG and preparation of LGG conditioned culture medium

Lactobacillus rhamnosus GG (LGG) was cultured in Mann Rogosa Sharp (MRS) medium and grown overnight at 37°C in an oxygen-deprived atmosphere. The density of the overnight culture was measured at 600nm. Reference values for optical density as a measure for the amount of colony forming units were produced previously. Bacteria were harvested by centrifugation at 4000 rpm for 15 minutes at 4°C, washed five times in ice-cold PBS, and reconstituted at 10¹⁰ CFU/ml PBS. Serial dilutions were made in complete DMEM before adding to LS174T cells.

To prepare LGG conditioned culture medium (LGG-CM), LGG was grown overnight in MRS medium at 37°C in an oxygen-deprived atmosphere. The bacterial preparation was diluted to approximately 10⁶–10⁷ CFU/ml in complete DMEM and incubated for 24h at 37°C. The LGG-CM was centrifuged twice at 4,000 rpm for 15 min to separate the bacteria, and the resulting supernatant was filtered through a 0.45-μm membrane (Millex; Millipore, Bedford, MA) to remove any insoluble particles and diluted to a final concentration of 25% and 50% in complete DMEM before use.

Quantitative real-time RT-PCR

LS174T cells were seeded in 6-well plates at 0.5×10⁶ cells/well. Cells were incubated 16 hours after seeding with viable LGG, nonviable LGG or LGG-CM. After 4 hours of stimulation, cells were washed, lysed, and harvested. Total RNA was prepared using the Nucleospin RNA II-kit from Macherey-Nagel (Düren, Germany). Total RNA (1.5 μg) was used to prepare cDNA. The mRNA expression levels of *MUC2* as well as the house-keeping gene *GAPDH* were quantified using real-time PCR (qRT-PCR) analysis (TAQman chemistry) based upon the intercalation of SYBR Green on an ABI prism 7900 HT Fast Real Time PCR system (PE Applied Biosystems) as previously described.³⁰ The primer combinations for *MUC2* (5'-CTC CGC ATG AGT GTG AGT -3', and 5'-TAG CAG CCA

CAC TTG TCT G -3') and *GAPDH* (5'-GTC GGA GTC AAC GGA TT -3', and 5'-AAG CTT CCC GTT CTC AG -3') were designed using OLIGO 6.22 software (Molecular Biology Insights) and purchased from Invitrogen. The effect of (non)viable LGG and LGG-CM on *MUC2* transcription was studied by co-incubating cells with (non)viable LGG or LGG-CM and actinomycin D (0.5 µg/ml) (Sigma-Aldrich, Zwijndrecht, the Netherlands). Quantitative real-time RT-PCR was performed as described above.

Immunocytochemistry

LS174T cells were grown on poly-L-lysine-coated microscope glass slides 24 h prior to treatment with LGG. Cells were nontreated or treated with or 10⁶ cfu/ml LGG for 24 h. Cells were fixed in ice-cold methanol at -20°C for 10 min and rinsed in PBS. *MUC2* mucin expression was determined by immunocytochemistry. Cells were incubated for 60 min at room temperature with the monoclonal *MUC2* antibody (WE9)³¹ diluted in phosphate buffered saline (PBS)(1:100), rinsed four times with PBS, and incubated at room temperature for 60 min with the biotinylated horse-antimouse antibody (Vector) diluted in PBS (1:1000), followed by 1 h incubation with ABC-PO complex (Vectastain Elite Kit; Vector Laboratories), each component diluted 1:400 in PBS. After incubation, binding was visualized using 0.5 mg/ml DAB (diaminobenzidine), 0.02% v/v H₂O₂ in 30 mM imidazole and 1 mM EDTA (pH 7.0). The slides were counterstained with hematoxylin.

Cell transfections

Previously described *pGL3-MUC2* promoter constructs covering the -2627/-1, -2096/+27, -947/-1 and -371/+27 region of *MUC2* promoter were used.²⁹ LS174T cells were seeded at 2.0 x 10⁵/well in 24-well plates. Transfections and co-transfections were performed the next day by adding 0.25 µg of the *pGL3* construct of interest and 0.15 µg of phRG-B as an internal control. Transfection and co-transfection experiments were performed using Effectene reagent (Qiagen, Venlo, The Netherlands) as described previously.²⁹ Cells were incubated with the transfection mixture for 24 h at 37°C. Stimulation with variable dosage of viable LGG, nonviable LGG or LGG-CM was performed during 24 h. Total cell extracts were prepared using 1x passive lysis buffer (Promega), as described in the manufacturer's instruction manual. Cell extract (10 µl) was mixed with 100 µl of luciferase assay reagent (Promega, Leiden, the Netherlands) to determine luciferase activity in a Glomax luminescence counter (Promega, Leiden, the Netherlands). Luciferase activity is expressed as fold induction of the nonstimulated sample compared with that of the LGG-stimulated samples, after correction for transfection efficiency as measured by the Renilla luciferase-activity. All experiments were performed in triplicate in at least three separate experiments.

Site-directed mutagenesis

A previously found consensus AP-1 site (ATGAGTCAGA) in the *MUC2* promoter at -817/-808³² was mutated using the QuickChange® site-directed mutagenesis kit (Stratagene, Amsterdam, the Netherlands) according to the manufacturer's instructions. The sequences of the oligonucleotides used to mutate the AP-1 site are depicted in table I. The mutation was confirmed by DNA sequencing.

LC/IRMS analysis

High performance liquid chromatography (HPLC) analysis of the VFAs was carried out on a Knauer pump system (Berlin, Germany) and a Midas auto sampler (Spark, Emmen, Netherlands), fitted with a ICSep ION-300 analytical column (7.8 x 300mm; Transgenomic, Achrom, Zulte, Belgium) and eluted at 300 $\mu\text{L min}^{-1}$ isocratically at 35°C with 0.0085 N H_2SO_4 . Injection volume was 10 μL . The HPLC system was coupled to a Delta XP isotope ratio mass spectrometer (IRMS) by a LC Isolink interface (Thermo Fisher, Bremen, Germany). The technique of the Isolink interface is based on wet oxidation of organic components with peroxodisulfate under acidic conditions. The CO_2 produced is subsequently separated from the mobile phase in a capillary gas exchanger flushed with helium gas, dried and led into the ion source of the mass spectrometer in a helium stream via the open split interface. The temperature of the oxidation reactor was set at 99.9°C. The flow rates of the acid (1.5 M H_3PO_4) and oxidant reagents (0.7 M $\text{Na}_2\text{S}_2\text{O}_8$) were 30 $\mu\text{L min}^{-1}$ each. Peak identification was based on retention times. Concentration measurements were based on the peak areas of the m/z 44 signals of the separated compound, using external standards for calibration. Samples were analyzed in duplicate.

Statistical analysis

All values in this article are mean values \pm standard deviation (SD).

RESULTS

LGG increases *MUC2* mRNA expression

LS174T cells were stimulated with variable dosages of viable and nonviable LGG. Stimulation with viable LGG already showed an increase in *MUC2* mRNA expression at a concentration of 10^6 CFU/ml (Fig. 1A). To determine whether metabolic activity of the LGG is required for this increase, viable LGG was heat-inactivated. Stimulation with 10^6 CFU/ml hardly showed any effect, while *MUC2* mRNA levels increased upon stimulation with 10^8 CFU/ml nonviable LGG (Fig. 1A).

As LGG also increased *MUC2* mRNA levels in a nonviable state, we aimed to study the effect metabolic products secreted by LGG on *MUC2* mRNA synthesis by means

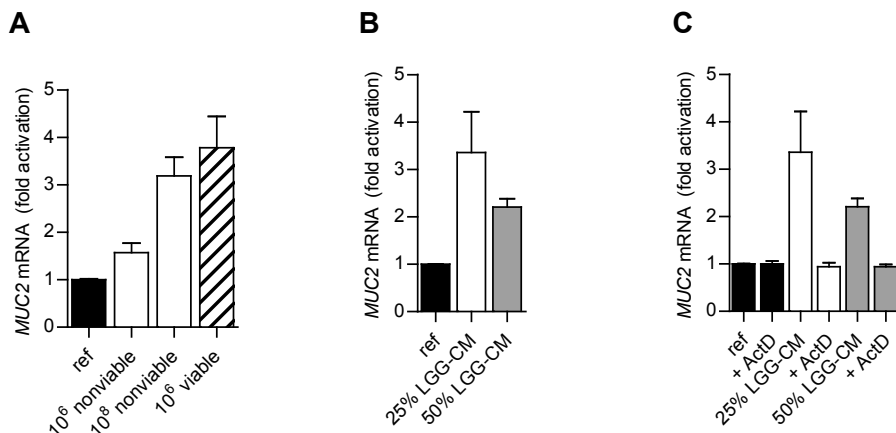


Figure 1. Effect of LGG on *MUC2* mRNA expression

Relative *MUC2* mRNA expression in LS174T cells upon stimulation with viable LGG and nonviable LGG (A) and LGG conditioned Culture Medium (LGG-CM) (B). To determine whether LGG stimulation influences *MUC2* synthesis at the transcriptional level, LS174T cells were stimulated with LGG-CM and co-incubated with actinomycin D (ActD) (C). Expressed values are depicted as mean \pm SD, relative to control values (ref), which were arbitrarily set on 1.

of LGG conditioned culture medium (LGG-CM). Nondiluted LGG-CM turned out to be acidic and toxic to the LS174T cells as determined by pH measurement, determination of floating cells in each well, and trypan blue staining. Therefore, the LGG-CM was diluted to concentrations of 25% and 50%, which were proven not to be cytotoxic. Increased mRNA expression was seen when LS174T cells were stimulated with 25% CM, whereas 50% CM only showed a slight increase (Fig. 1B).

To determine whether the activating effect of LGG on *MUC2* expression occurred at the transcriptional level, cells were pretreated with actinomycin D, which inhibits transcription. The results indicate that activation of *MUC2* gene expression by LGG indeed occurred at the transcriptional level, as *MUC2* mRNA levels returned to basal levels when cells were pretreated with actinomycin D (Fig. 1C).

LGG stimulates *MUC2* protein synthesis

To determine whether LGG also affected *MUC2* protein synthesis, the effect of viable LGG on *MUC2* protein expression was analyzed by immunocytochemistry (Fig. 2). In non-stimulated LS174T cells *MUC2* staining was hardly visible. Stimulation with viable LGG clearly results in an increased amount of *MUC2*-positive cells.

MUC2 promoter transactivation by LGG

Transfections with *MUC2* promoter constructs were performed to study the effect of LGG on *MUC2* promoter transactivation via luciferase assays. LS174T cells transfected with

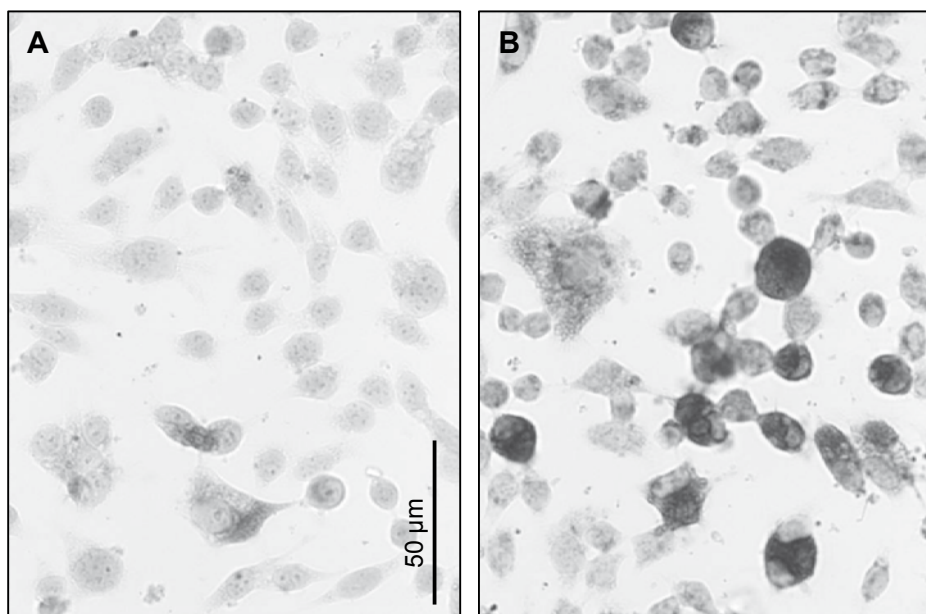


Figure 2. LGG increases MUC2 protein expression

LS174 T cells were stimulated with 10^6 viable LGG. Nonstimulated LS174T cells (A) are compared with LS174T cells stimulated with viable LGG (B). (See Color Section, p. 241.)

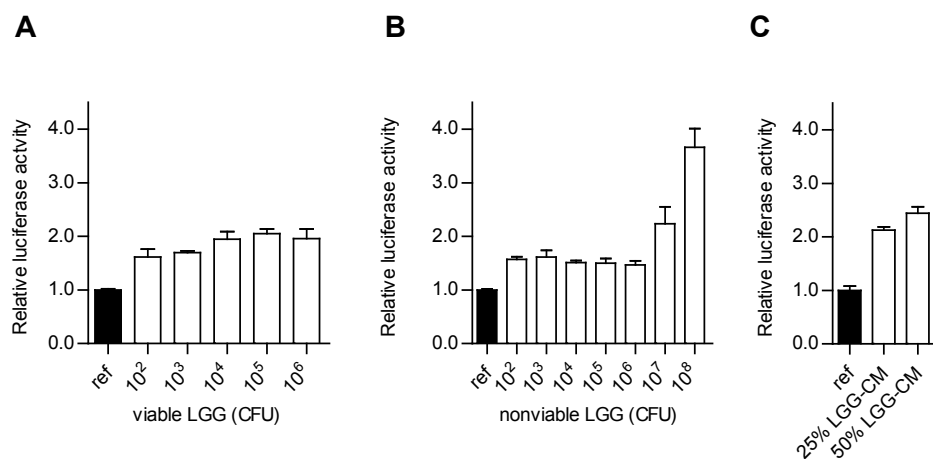


Figure 3. MUC2 promoter transactivation by LGG and LGG-CM

Relative luciferase activity showing the effect of (non)viable LGGs or LGG conditioned culture medium (LGG-CM) on MUC2 promoter transactivation. Cells were transfected with the -947/-1 MUC2 promoter construct before being stimulated with viable LGGs (A), nonviable LGGs (B) or LGG-CM (C) as described in experimental procedures. Results are expressed as fold activation compared to non-stimulated cells (ref). Results represent mean \pm SD obtained in triplicate in three separate experiments.

various *MUC2* promoter constructs were stimulated with viable LGG in concentrations ranging from 10² to 10⁸ CFU/ml. As the construct covering the -947/-1 region showed the most marked induction of luciferase activity, we used this promoter construct in subsequent experiments. Viable and nonviable bacteria in concentrations ranging from 10² to 10⁸ CFU/ml were used for stimulation of transfected LS174T cells. Both preparations showed a dose dependent increase in *MUC2* promoter activity. However, higher concentrations of nonviable LGG were needed to reach an effect comparable to the effect obtained with viable LGG. Specifically viable LGG already showed a two-fold increase in *MUC2* promoter activity upon stimulation with 10⁵ CFU/ml (Fig. 3A), whereas 10⁷ non-viable LGG/ml was needed to induce *MUC2* promoter transactivation (Fig. 3B). Finally, LGG-CM also resulted in transactivation of the *MUC2* promoter (Fig. 3C).

Identification of LGG-responsive regions in the *MUC2* promoter

Previous studies already revealed a consensus putative binding site (ATGAGTCAGA) for the transcription factor AP-1, a transcription factor known to mediate butyrate-induced *MUC2* promoter activation³², at -817/-808. To determine whether this putative AP-1 binding site was responsible for the LGG-induced *MUC2* promoter transactivation, specific nucleotides within the *MUC2* promoter sequence were mutated (Table 1). This mutation resulted in a marked reduction of the LGG-induced *MUC2* transactivation (Fig. 4).

Heat, protease and DNase treatment do not influence luciferase activity during LGG conditioned CM treatment

In search for the active biological substance that is responsible for *MUC2* promoter transactivation, LGG-CM was exposed to various treatments, namely heat, DNase or protease (proteinase K, trypsin and papain) (Fig. 5). Regardless of the pre-treatment, the stimulatory effect of LGG-CM on *MUC2* promoter transactivation was maintained.

Short chain fatty acids from LGG-CM stimulate *MUC2* synthesis

Short chain fatty acids (SCFAs) are produced by bacterial fermentation of undigested carbohydrates. As we previously showed that SCFAs can affect *MUC2* synthesis³², we

Table 1. Sequences of the sense oligonucleotides used for site-directed mutagenesis. AP-1 consensus sequence is italicized. Mutated nucleotides are bold and underlined. Antisense oligonucleotides were also synthesized and annealed to the sense oligonucleotide to produce double-stranded DNA.

Mutations	Sequence 5'-3'
Site directed mutagenesis	
WT 114 (-830/-795)	CAG GAT CCC CAC CAT GAG TCA GAG GTA GTT CTG GGG
Mutated T114	CAG GAT CCC CAC <u>CAG</u> GAG <u>CCA</u> GAG GTA GTT CTG GGG

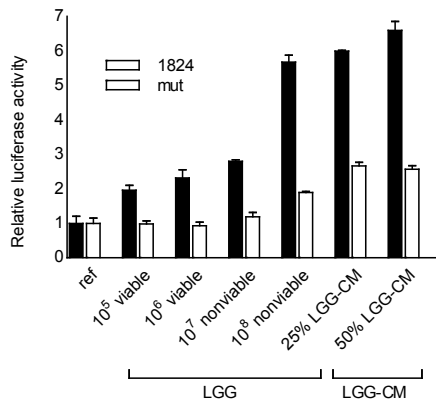


Figure 4. AP-1 binding site is responsible for LGG-induced *MUC2* promoter transactivation. Relative luciferase activity diagram showing the effect of site-directed mutagenesis on *MUC2* promoter activation by viable LGG, nonviable LGG or LGG-CM. Cells were transfected either with the wild-type -947/-1 construct (WT, black bars) or with the AP-1 mutated construct (mut, white bars) before being stimulated with LGG or LGG-CM as described in experimental procedures. Results are expressed as fold activation compared to non-stimulated cells (ref). Results represent mean \pm SD obtained in triplicate in three separate experiments.

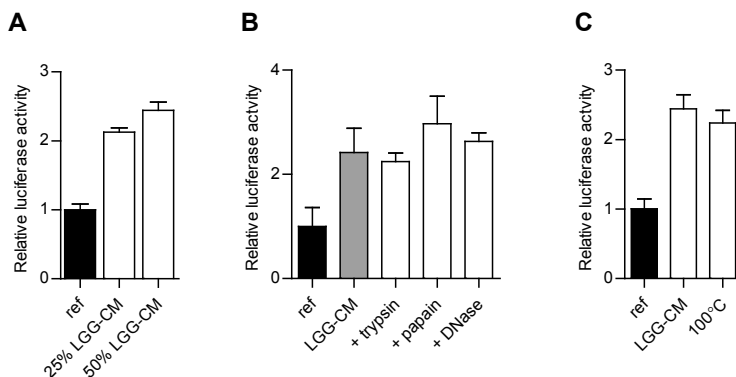


Figure 5. Exposing LGG-CM to heat, protease and DNase treatment does not influence LGG-CM-induced *MUC2* promoter activation. Relative luciferase activity showing the effect of proteases or DNase (B) or heat treatment (C) on *MUC2* promoter transactivation by LGG-conditioned culture medium (LGG-CM). LS174T cells were transfected with the -947/-1 construct *MUC2* promoter construct before being stimulated with protease-, DNase-, or heat-treated LGG-CM as described in experimental procedures. Results are expressed as fold-activation in the treated cells compared to non-stimulated cells (ref). Results represent mean \pm SD obtained in triplicate in three separate experiments.

hypothesized that SCFAs produced by LGG caused the transactivation of the *MUC2* promoter upon stimulation of the cells with LGG-CM. To test this, we analyzed the concentrations of acetate, propionate and butyrate in LGG-CM. LGG-CM appeared to contain 5.8 mM acetate, 0.8 mM propionate, and 0.5 mM butyrate. Next, LS174T cells transfected with the *MUC2* promoter construct were exposed to these concentrations

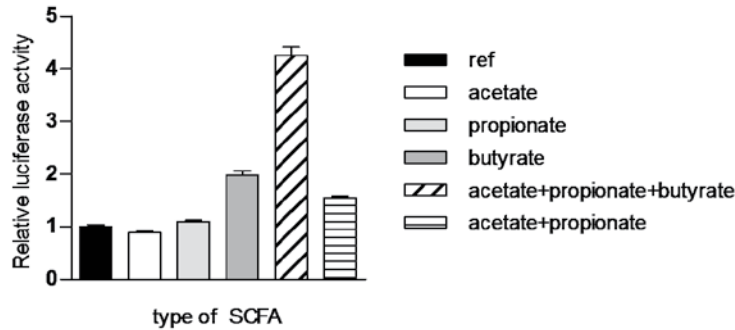


Figure 6. SCFAs induce MUC2 promoter activation in LS174T cells

Relative luciferase activity showing the effect of SCFAs on MUC2 promoter transactivation. LS174T cells were transfected with the -947/-1 construct MUC2 promoter construct before being stimulated with acetate (5.8 mM), propionate (0.8 mM), butyrate (0.5 mM) or a combination of these SCFAs as described in experimental procedures. Expressed values are depicted as mean \pm SD, relative to control values (ref) which were arbitrarily set on 1.

of SCFAs. As shown in Figure 6, stimulation with 5.8 mM acetate or 0.8 mM propionate and the combination of acetate and propionate did not result in increased MUC2 promoter activity. However, treatment of transfected cells with 0.5 mM butyrate resulted in increased MUC2 promoter transactivation. Interestingly, the combination of acetate, propionate and butyrate showed a synergistic effect on MUC2 promoter activity.

DISCUSSION

In the present study the effect of the probiotic bacterium LGG on MUC2 synthesis, an important marker for epithelial protection, was investigated. We demonstrate that a variety of LGG preparations induce MUC2 synthesis in the LS174T cell line, revealing a mechanism through which probiotics might exert their beneficial effects in the human host.

First of all, our study shows that LGG stimulates MUC2 mRNA synthesis. This is in line with studies performed with the intestinal epithelial cell lines Caco-2 and HT29, in which LGG appeared to increase MUC2 mRNA expression.²⁶⁻²⁷ Interestingly, our studies show distinct differences between the stimulatory effect of viable LGG on MUC2 gene expression compared to nonviable LGG. More specifically, viable LGG stimulate MUC2 synthesis in lower dosages, i.e. were more potent in low concentrations, compared to nonviable LGG. Van Baarlen et al.³³ demonstrated a differential effect of viable versus nonviable bacteria on small intestinal gene expression. Gene expression profiles in human duodenal biopsy samples after ingestion of dead, stationary or midlogphase *L. plantarum* respectively, showed that consumption of *L. plantarum* leads to regulation of hundreds

of duodenal mucosal genes that modulate immune responses, cellular metabolism and biogenesis. Interestingly, human mucosa responded differentially to various preparations of the same bacterial strain. For example, nuclear factor kappa-B (NFkB) signaling and its downstream or antagonizing pathways can be differentially induced by various preparations of the same bacterial species. Differential immune responses toward living and dead *L. plantarum* were also described by Bloksma and co-workers who showed that subcutaneous injections with preparations of viable *L. plantarum* induced mild inflammatory responses, whereas dead bacteria induced antibody formation by plasma cells and infiltration of polymorph nuclear cells in mice.³⁴ Although viable and nonviable LGG were both able to increase MUC2 expression in our experiments, it is likely that different pathways regulate this common final effect, namely increased MUC2 synthesis.

Secondly, our promoter studies revealed that *MUC2* promoter transactivation is already seen at low dosages of viable LGG. For nonviable LGG higher dosages are needed for initial *MUC2* promoter transactivation. However, when high dosages of nonviable LGG were added an even higher activation of the *MUC2* promoter was observed. LGG conditioned CM showed an 'intermediate' effect on *MUC2* promoter trans activation since its effect was lower than the effect of viable, but higher than that of nonviable LGG. We identified an LGG-responsive region in the *MUC2* promoter, namely an AP-1 binding site. Lin et al.³⁵ already showed that AP-1 represents a primary target for probiotic-mediated suppression of TNF transcription. Furthermore, lactobacilli and the VSL#3 bacterial mixture strengthen intestinal barrier function through the upregulation of human beta-defensin-2 via induction of pro-inflammatory pathways including NF-κB and AP-1 as well as MAPKs.⁸ However, to our knowledge, this is the first study that reveals AP-1 as a stimulatory transcription factor that is responsible for *MUC2* promoter transactivation after stimulation with LGG. Altogether, these studies suggest that stimulation of the transcription factor AP-1 by probiotics influences intestinal barrier function at different levels.

Next, LGG conditioned CM was tested in search for the biological active substance that explains the stimulatory effect of LGG on MUC2 synthesis. Therefore several treatments, i.e. heat inactivation, DNase and protease, were applied. However, none of these substances were able to diminish the stimulatory effect of LGG conditioned CM on MUC2 synthesis, implying that bacterial DNA and secreted proteins are not the active substances in this matter. These data are supported by several other studies in which CM was tested. For example, Caballero-Franco et al.²⁵ demonstrated that CM derived from VSL#3, a mixture of 8 probiotic bacteria, induced mucin secretion in LS174T cells, but not *MUC2* mRNA. They speculate that, during the first hours of exposure, VSL#3 CM acts like a secretagogue inducing only the discharge of mucins from goblet cell vesicles without necessarily influencing mucin gene expression. However, our data show that LGG indeed affects *MUC2* mRNA synthesis. We speculate that both mechanisms,

both immediate release of MUC2 from goblet cells storages as well as mRNA synthesis, might be activated by probiotic bacteria. As these authors already mentioned, proteins cannot be fully ruled out as the biological active substance since short peptides and highly glycosylated proteins are typically resistant to protease treatment or lipids, which are resistant to heat.²⁵

Concentrations of SCFA in the LGG conditioned CM were measured as these substances are metabolites produced by LGGs, which might cause the stimulatory effect on MUC2 synthesis. Interestingly, stimulation with a combination of SCFAs was more effective compared to single SCFA stimulation. These data suggest that manipulation of the intestinal SCFA profile and thereby optimizing intestinal innate defense appears to be a potent effect of probiotic supplementation. Production of SCFAs by bacteria, which may be a key mechanism by which probiotics exert their beneficial effects, has been reviewed by Wong et al.³⁶ However, the production of SCFAs has also been related to intestinal diseases. Lin et al. demonstrated that luminal administration of SCFAs causes concentration-dependent intestinal mucosal injury in newborn rats at pH 4.0, a pH chosen to resemble the acidic milieu encountered in NEC.³⁷⁻³⁸ Furthermore, intraluminal administration of 3–5% (340–567 mmol/L) acetic acid has been widely used for over 20 years to create a very reliable colitis model in rodents³⁹ and other animal species.⁴⁰ Propionic acid has also been shown to induce intestinal injury in newborn piglets.⁴¹ Therefore, the optimal probiotic strain(s) with subsequent SCFA profiles are still to be found and harmful concentrations obviously need to be avoided.

Finally, in most definitions of probiotics, viability throughout the gastrointestinal tract is a requirement. In this study however, we show that nonviable bacteria also increase MUC2 synthesis and therefore the beneficial effect by means of increasing intestinal barrier function through stimulation of MUC2 synthesis can be accomplished by both viable and nonviable LGG, as well as LGG-CM. This feature can be of utmost importance for the use of probiotics in clinical trials, since safety of probiotics remains an issue.

In summary, in the present study we showed that the probiotic bacterium LGG is able to stimulate MUC2 mRNA synthesis in a dose dependent manner. Secondly, we demonstrated that transactivation of the MUC2 promoter by LGG is, at least partly, induced via the transcription factor AP-1. Finally, we showed that bacterial viability is not a prerequisite for stimulating MUC2 synthesis. Taken together our data demonstrate that nonviable 'probiotics' and probiotic metabolites might be promising as prophylaxis to prevent NEC, as both can up-regulate MUC2 synthesis and thereby improve intestinal barrier function.

FUNDING

This work was partly supported by Danone Research (Friedrichsdorf, Germany).

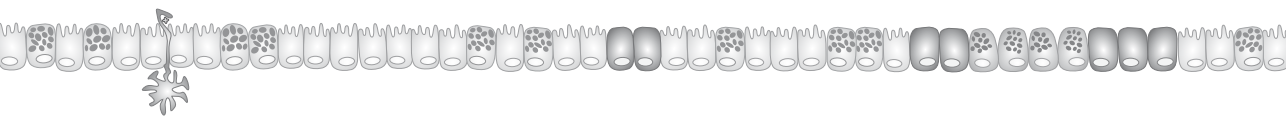
REFERENCES

1. Gibson GR, Roberfroid MB. Dietary modulation of the human colonic microbiota: introducing the concept of prebiotics. *J Nutr* 1995;125:1401-12.
2. Lee YK, Puong KY. Competition for adhesion between probiotics and human gastrointestinal pathogens in the presence of carbohydrate. *Br J Nutr* 2002;88 Suppl 1:S101-8.
3. Candela M, Perna F, Carnevali P, Vitali B, Ciati R, Gionchetti P, Rizzello F, Campieri M, Brigidi P. Interaction of probiotic *Lactobacillus* and *Bifidobacterium* strains with human intestinal epithelial cells: adhesion properties, competition against enteropathogens and modulation of IL-8 production. *Int J Food Microbiol* 2008;125:286-92.
4. Gillor O, Etzion A, Riley MA. The dual role of bacteriocins as anti- and probiotics. *Appl Microbiol Biotechnol* 2008;81:591-606.
5. Mattar AF, Drongowski RA, Coran AG, Harmon CM. Effect of probiotics on enterocyte bacterial translocation in vitro. *Pediatr Surg Int* 2001;17:265-8.
6. Fukushima Y, Kawata Y, Hara H, Terada A, Mitsuoka T. Effect of a probiotic formula on intestinal immunoglobulin A production in healthy children. *Int J Food Microbiol* 1998;42:39-44.
7. Mondel M, Schroeder BO, Zimmermann K, Huber H, Nuding S, Beisner J, Fellermann K, Stange EF, Wehkamp J. Probiotic *E. coli* treatment mediates antimicrobial human beta-defensin synthesis and fecal excretion in humans. *Mucosal Immunol* 2009;2:166-72.
8. Schlee M, Harder J, Koten B, Stange EF, Wehkamp J, Fellermann K. Probiotic lactobacilli and VSL#3 induce enterocyte beta-defensin 2. *Clin Exp Immunol* 2008;151:528-35.
9. Wehkamp J, Harder J, Wehkamp K, Wehkamp-von Meissner B, Schlee M, Enders C, Sonnenborn U, Nuding S, Bengmark S, Fellermann K, Schroder JM, Stange EF. NF-kappaB- and AP-1-mediated induction of human beta defensin-2 in intestinal epithelial cells by *Escherichia coli* Nissle 1917: a novel effect of a probiotic bacterium. *Infect Immun* 2004;72:5750-8.
10. Charteris WP, Kelly PM, Morelli L, Collins JK. Development and application of an in vitro methodology to determine the transit tolerance of potentially probiotic *Lactobacillus* and *Bifidobacterium* species in the upper human gastrointestinal tract. *J Appl Microbiol* 1998;84:759-68.
11. Basu S, Paul DK, Ganguly S, Chatterjee M, Chandra PK. Efficacy of high-dose *Lactobacillus rhamnosus* GG in controlling acute watery diarrhea in Indian children: a randomized controlled trial. *J Clin Gastroenterol* 2009;43:208-13.
12. Basu S, Chatterjee M, Ganguly S, Chandra PK. Effect of *Lactobacillus rhamnosus* GG in persistent diarrhea in Indian children: a randomized controlled trial. *J Clin Gastroenterol* 2007;41:756-60.
13. Szajewska H, Skorka A, Ruszczynski M, Gieruszczak-Bialek D. Meta-analysis: *Lactobacillus* GG for treating acute diarrhoea in children. *Aliment Pharmacol Ther* 2007;25:871-81.
14. Szajewska H, Kotowska M, Mrukowicz JZ, Armanska M, Mikolajczyk W. Efficacy of *Lactobacillus* GG in prevention of nosocomial diarrhea in infants. *J Pediatr* 2001;138:361-5.
15. Pant AR, Graham SM, Allen SJ, Harikul S, Sabchareon A, Cuevas L, Hart CA. *Lactobacillus* GG and acute diarrhoea in young children in the tropics. *J Trop Pediatr* 1996;42:162-5.
16. Vanderhoof JA, Whitney DB, Antonson DL, Hanner TL, Lupo JV, Young RJ. *Lactobacillus* GG in the prevention of antibiotic-associated diarrhea in children. *J Pediatr* 1999;135:564-8.
17. Shornikova AV, Isolauri E, Burkanova L, Lukovnikova S, Vesikari T. A trial in the Karelian Republic of oral rehydration and *Lactobacillus* GG for treatment of acute diarrhoea. *Acta Paediatr* 1997;86:460-5.

18. Majamaa H, Isolauri E, Saxelin M, Vesikari T. Lactic acid bacteria in the treatment of acute rotavirus gastroenteritis. *J Pediatr Gastroenterol Nutr* 1995;20:333-8.
19. Kalliomaki M, Salminen S, Arvilommi H, Kero P, Koskinen P, Isolauri E. Probiotics in primary prevention of atopic disease: a randomised placebo-controlled trial. *Lancet* 2001;357:1076-9.
20. Kirjavainen PV, Salminen SJ, Isolauri E. Probiotic bacteria in the management of atopic disease: underscoring the importance of viability. *J Pediatr Gastroenterol Nutr* 2003;36:223-7.
21. Tytgat KM, Buller HA, Opdam FJ, Kim YS, Einerhand AW, Dekker J. Biosynthesis of human colonic mucin: Muc2 is the prominent secretory mucin. *Gastroenterology* 1994;107:1352-63.
22. Pullan RD, Thomas GA, Rhodes M, Newcombe RG, Williams GT, Allen A, Rhodes J. Thickness of adherent mucus gel on colonic mucosa in humans and its relevance to colitis. *Gut* 1994;35:353-9.
23. Tytgat KM, van der Wal JW, Einerhand AW, Buller HA, Dekker J. Quantitative analysis of MUC2 synthesis in ulcerative colitis. *Biochem Biophys Res Commun* 1996;224:397-405.
24. Schaart MW, de Bruijn AC, Bouwman DM, de Krijger RR, van Goudoever JB, Tibboel D, Renes IB. Epithelial functions of the residual bowel after surgery for necrotising enterocolitis in human infants. *J Pediatr Gastroenterol Nutr* 2009;49:31-41.
25. Caballero-Franco C, Keller K, De Simone C, Chadee K. The VSL#3 probiotic formula induces mucin gene expression and secretion in colonic epithelial cells. *Am J Physiol Gastrointest Liver Physiol* 2007;292:G315-22.
26. Mattar AF, Teitelbaum DH, Drongowski RA, Yongyi F, Harmon CM, Coran AG. Probiotics up-regulate MUC-2 mucin gene expression in a Caco-2 cell-culture model. *Pediatr Surg Int* 2002;18:586-90.
27. Mack DR, Michail S, Wei S, McDougall L, Hollingsworth MA. Probiotics inhibit enteropathogenic *E. coli* adherence in vitro by inducing intestinal mucin gene expression. *Am J Physiol* 1999;276:G941-50.
28. Amit-Romach E, Uni Z, Reifen R. Multistep mechanism of probiotic bacterium, the effect on innate immune system. *Mol Nutr Food Res* 2009.
29. Perrais M, Pigny P, Copin MC, Aubert JP, Van Seuningen I. Induction of MUC2 and MUC5AC mucins by factors of the epidermal growth factor (EGF) family is mediated by EGF receptor/Ras/Raf/extracellular signal-regulated kinase cascade and Sp1. *J Biol Chem* 2002;277:32258-67.
30. Meijerink J, Mandigers C, van de Locht L, Tonnissen E, Goodsaid F, Raemaekers J. A novel method to compensate for different amplification efficiencies between patient DNA samples in quantitative real-time PCR. *J Mol Diagn* 2001;3:55-61.
31. Tytgat KM, Bovelandt FJ, Opdam FJ, Einerhand AW, Buller HA, Dekker J. Biosynthesis of rat MUC2 in colon and its analogy with human MUC2. *Biochem J* 1995;309 (Pt 1):221-9.
32. Burger-van Paassen N, Vincent A, Puiman PJ, van der Sluis M, Bouma J, Boehm G, van Goudoever JB, van Seuningen I, Renes IB. The regulation of intestinal mucin MUC2 expression by short-chain fatty acids: implications for epithelial protection. *Biochem J* 2009;420:211-9.
33. van Baarlen P, Troost FJ, van Hemert S, van der Meer C, de Vos WM, de Groot PJ, Hooiveld GJ, Brummer RJ, Kleerebezem M. Differential NF-kappaB pathways induction by *Lactobacillus plantarum* in the duodenum of healthy humans correlating with immune tolerance. *Proc Natl Acad Sci U S A* 2009;106:2371-6.

34. Bloksma N, de Heer E, van Dijk H, Willers JM. Adjuvanticity of lactobacilli. I. Differential effects of viable and killed bacteria. *Clin Exp Immunol* 1979;37:367-75.
35. Lin YP, Thibodeaux CH, Pena JA, Ferry GD, Versalovic J. Probiotic *Lactobacillus reuteri* suppress proinflammatory cytokines via c-Jun. *Inflamm Bowel Dis* 2008;14:1068-83.
36. Wong JM, de Souza R, Kendall CW, Emam A, Jenkins DJ. Colonic health: fermentation and short chain fatty acids. *J Clin Gastroenterol* 2006;40:235-43.
37. Lin J, Nafday SM, Chauvin SN, Magid MS, Pabbatireddy S, Holzman IR, Babyatsky MW. Variable effects of short chain fatty acids and lactic acid in inducing intestinal mucosal injury in newborn rats. *J Pediatr Gastroenterol Nutr* 2002;35:545-50.
38. Nafday SM, Green RS, Chauvin SN, Holzman IR, Magid MS, Lin J. Vitamin A supplementation ameliorates butyric acid-induced intestinal mucosal injury in newborn rats. *J Perinat Med* 2002;30:121-7.
39. MacPherson BR, Pfeiffer CJ. Experimental production of diffuse colitis in rats. *Digestion* 1978;17:135-50.
40. Kim HS, Berstad A. Experimental colitis in animal models. *Scand J Gastroenterol* 1992;27: 529-37.
41. Di Lorenzo M, Bass J, Krantis A. An intraluminal model of necrotizing enterocolitis in the developing neonatal piglet. *J Pediatr Surg* 1995;30:1138-42.

Chapter 7



The regulation of the intestinal mucin MUC2 expression by short chain fatty acids: implications for epithelial protection.

Nanda Burger-van Paassen*, Audrey Vincent*, Patrycja J. Puiman, Maria van der Sluis, Janneke Bouma, Günther Boehm, Johannes B. van Goudoever, Isabelle Van Seuningen, Ingrid B. Renes

Biochemical Journal 2009 May 13;420(2):211-9.



ABSTRACT

SCFAs (short-chain fatty acids), fermentation products of bacteria, influence epithelial-specific gene expression. We hypothesize that SCFAs affect goblet-cell-specific mucin MUC2 expression and thereby alter epithelial protection. In the present study, our aim was to investigate the mechanisms that regulate butyrate-mediated effects on MUC2 synthesis. Human goblet cell-like LS174T cells were treated with SCFAs, after which MUC2 mRNA levels and stability, and MUC2 protein expression were analysed. SCFA-responsive regions and *cis*-elements within the MUC2 promoter were identified by transfection and gel-shift assays. The effects of butyrate on histone H3/H4 status at the MUC2 promoter were established by chromatin immunoprecipitation. Butyrate (at 1 mM), as well as propionate, induced an increase in MUC2 mRNA levels. MUC2 mRNA levels returned to basal levels after incubation with 5–15 mM butyrate. Interestingly, this decrease was not due to loss of RNA stability. In contrast, at concentrations of 5–15 mM propionate, MUC2 mRNA levels remained increased. Promoter-regulation studies revealed an active butyrate-responsive region at –947/–371 within the MUC2 promoter. In this region we identified an active AP1 (c- Fos/c-Jun) *cis*-element at –818/–808 that mediates butyrate-induced activation of the promoter. Finally, MUC2 regulation by butyrate at 10–15 mM was associated with increased acetylation of histone H3 and H4 and methylation of H3 at the MUC2 promoter. In conclusion, 1 mM butyrate and 1–15 mM propionate increase MUC2 expression. The effects of butyrate on MUC2 mRNA are mediated via AP-1 and acetylation/methylation of histones at the MUC2 promoter.

Key words: histone acetylation, histone methylation, human milk feeding, MUC2, necrotizing enterocolitis, short-chain fatty acid

INTRODUCTION

Short chain fatty acids (SCFAs) are produced by fermentation of undigested carbohydrates. SCFAs, and more specifically acetate, propionate and butyrate, are the major anions in the lumen of the large intestine. Several functions of SCFAs have been described, i.e. lowering intestinal pH, energy-source for colonocytes, stimulation of colonic blood flow, smooth muscle contraction, transepithelial chloride secretion and exertion of proliferative stimuli of colonic epithelial cells.¹ It is known that dietary fibers and SCFA have beneficial effects in inflammatory bowel disease (IBD), e.g. by inhibition of pro-inflammatory cytokine-induced NFκB activation and absorption of sodium and water.²⁻⁴ In addition, SCFAs and especially butyrate are known to influence intestinal specific gene expression, thereby influencing immune responses and oxidative and metabolic stress.⁵⁻⁹

The composition of SCFAs in the intestine is determined by the composition of the microbiota, which in its turn is influenced by the diet. For example, prebiotics selectively stimulate the growth, and or, activity of Bifidobacteria and thereby influence the SCFA composition.¹⁰ Moreover, in human milk-fed infants the large bowel is generally dominated by Bifidobacteria and lactic acid bacteria. The microbiota of formula-fed infants on the other hand, is more diverse, less stable and often contains more Bacteroides, Clostridium and Enterobacteriaceae.¹¹⁻¹⁴ This difference in the composition of the microbiota results in a different SCFA composition between human milk-fed and formula-fed infants. It is well known that the ratio between the SCFAs butyrate, propionate, and acetate differ in breast-fed infants compared to formula-fed infants (i.e. 2:6:90 in human milk fed infants versus 5:20:70 in formula fed infants).¹⁵ Based on the fact that more than 90% of the infants who develop necrotizing enterocolitis (NEC), which is the most common gastro-intestinal emergency in premature infants, have received formula feeding, as opposed to human milk solely, one could suggest that the production of SCFAs by bacteria and the composition of SCFAs in the intestine might play a role in the pathogenesis of NEC. Altered fecal concentrations of butyrate have also been reported in patients with ulcerative colitis (UC). In addition, a diminished capacity of the intestinal mucosa to oxidize butyrate has been reported in patients with active UC.¹⁶⁻¹⁸

Both UC and NEC share the feature of an impaired intestinal barrier function. Mucins are required for the maintenance of an adequate mucus layer that covers the intestinal epithelium and thereby forms a physical barrier that protects the intestinal epithelium against toxic agents. The mucin MUC2 is the predominant mucin in the colon and MUC2 synthesis is diminished in UC¹⁹⁻²⁰ and presumably also NEC.

It has been shown in cell line studies, experimental animal models and fresh human intestinal tissue specimens, that butyrate alters *MUC2* expression in a dose dependent manner.²¹⁻²⁵ However, the mechanisms that are responsible for these alterations have not been studied in detail so far.

In the present study, we investigated the role of increasing concentrations of butyrate, as well as acetate and propionate on *MUC2* expression in LS174T cells, a human goblet cell-like cell line. Furthermore, The effects of butyrate on *MUC2* expression were respectively studied at the promoter, mRNA and protein level. We identified butyrate-responsive regions and *cis*-elements within the *MUC2* promoter and determined the effects of butyrate treatment on histone H3 and H4 status at the *MUC2* promoter.

EXPERIMENTAL

Cell culture

The LS174T colonic cancer cell line was cultured in a 37°C incubator with 10% CO₂ in Dulbecco's modified Eagle's minimal essential medium supplemented with non-essential amino acids and 10% foetal calf serum (Boehringer Mannheim) as before.²⁶

Cell proliferation assay and morphological alterations

LS174T cells (2×10^5) were pre-cultured in 24-well plates overnight to allow them to adhere. Subsequently cells were stimulated with physiological concentrations of butyrate (0, 1, 5, or 10 mM) (sodium butyrate, Sigma-Aldrich, Steinheim, Germany) diluted in cell culture medium for 24 h. After removal of the culture medium, cells were treated with trypsin-EDTA solution and counted. All experiments were performed in triplicate in at least three separate experiments. In addition, cell proliferation and cell death were determined using the WST-I (WST-I proliferation agent, Roche Molecular Biochemicals, Germany) and trypan blue exclusion assays, respectively. Further, butyrate-induced morphological changes were studied microscopically.

Quantitative real- time PCR

LS174T cells were seeded in 6-well plates at 0.5×10^6 cells/well. Cells were incubated 16 hours after seeding with either a low (1mM), moderate (5 mM) or high (10 and 15 mM) concentration of butyrate, acetate or propionate (Sigma-Aldrich, Steinheim, Germany). After 24 hours of stimulation, cells were lysed and harvested. Total RNA was prepared using the Nucleospin RNA II-kit from Macherey-Nagel. 1.5 µg of total RNA was used to prepare cDNA. The mRNA expression levels of *MUC2* as well as the housekeeping gene *GAPDH* were quantified using real-time PCR (qRT-PCR) analysis (TAQman chemistry) based upon the intercalation of SYBR Green on an ABI prism 7900 HT Fast Real Time PCR system (PE Applied Biosystems) as previously described.²⁷ The primer combinations for *MUC2* (5'-CTC CGC ATG AGT GTG AGT -3', and 5'-TAG CAG CCA CAC TTG TCT G -3') and *GAPDH* (5'-GTC GGA GTC AAC GGA TT -3', and 5'-AAG CTT CCC GTT CTC AG -3') were designed using OLIGO 6.22 software (Molecular Biology Insights)

and purchased from Invitrogen. The effect of butyrate on MUC2 transcription and *de novo* protein synthesis was respectively studied by co-incubating cells with butyrate and either actinomycin D (0.5 µg/ml) or cycloheximide (10 µg/ml) (Sigma-Aldrich, Steinheim, Germany). qRT-PCR was performed as described above.

RNA stability assay

LS174T cells were seeded at 1×10^6 cells/well in a 6-well cluster 24h prior to the experiment. At $t=0$, the cells were treated with either 0 mM or 5 mM butyrate in combination with 4 µg/ml actinomycin D (Sigma-Aldrich, Steinheim, Germany). Cells were harvested after 0, 4, 6, 8, 10 and 24 h of butyrate/actinomycin D treatment. RNA isolation, cDNA synthesis and qRT-PCR were performed as mentioned above. To verify the amplification efficiency as well as the amount of mRNA present in the treated cells, a serial dilution of cDNA derived from non-treated LS174T cells was amplified in duplicate on each plate.

Cell transfections

pGL3-MUC2 promoter constructs covering the -371/+27, -947/-1, -2096/+27 and -2627/-1 regions of MUC2 promoter were previously described.²⁶ The AP-1-Luc reporter construct was a kind gift from Dr Avery (Pennsylvania State University, USA). LS174T cells were seeded at 2.0×10^5 /well in 24-well plates. Transfections and co-transfections were performed the next day by adding 0.25 µg of the pGL3 construct of interest and 0.15 µg of phRG-B as an internal control. Transfection and co-transfection experiments were performed using Effectene® reagent (Qiagen) as described previously.²⁶ Cells were incubated with the transfection mixture for 24 h at 37°C. Stimulation with variable dosage of butyrate was performed during 24 h. Total cell extracts were prepared using 1x passive lysis buffer (Promega), as described in the manufacturer's instruction manual. 10 µl of cell extract was used to determine luciferase activity in a Glomax luminescence counter (Promega) using the dual luciferase assay system (Promega). The luciferase activity is expressed as fold induction of the nonstimulated sample compared with that of the SCFA-stimulated samples, after correction for transfection efficiency as measured by the Renilla luciferase activity. All experiments were performed in triplicate in at least three separate experiments.

Site-directed mutagenesis

The consensus AP-1 site (ATGAGTCAGA) found in the MUC2 promoter at -817/-808 was mutated using the QuickChange site-directed mutagenesis kit (Stratagene) according to the manufacturer's instructions. The sequence of the oligonucleotides used to mutate the AP-1 site are depicted in table I. The mutation was confirmed by DNA sequencing.

Electrophoretic mobility shift assay (EMSA)

Nuclear extracts from LS174T cells, untreated or treated with butyrate were prepared as described before²⁸, quantified using the bicinchoninic acid assay (Pierce, Perbio Science, Brebières, France) and stored at -80°C. Oligonucleotides were synthesized by MWG-Biotech (Germany), sequences are shown in Table 1. Annealed oligonucleotides were radiolabeled using T4 polynucleotide kinase (Promega) and [$\gamma^{32}\text{P}$]-dATP (GE Healthcare) and purified by chromatography on a Bio-Gel P-6 column (Bio-Rad, Marnes-la-Coquette, France). Nuclear protein incubation with radiolabeled probes and competitions with unlabeled probes were as described in Perrais et al.²⁶ For super-shift analyses, 2 μl of the antibody of interest [anti-c-fos (K-25, SC-253X) and anti-c-jun (SC-44X), Santa-Cruz laboratories, Tebu-Bio, Le-Perray-en-Yvelines, France, were added to the proteins and left for 1 h at room temperature (22°C) before adding the radiolabeled probe. Electrophoresis conditions and gel processing were as described before.²⁶

Table 1. Sequences of the sense oligonucleotides used for site-directed mutagenesis and EMSA. AP-1 consensus sequence is italicized. Mutated nucleotides are bold and underlined. Antisense oligonucleotides were also synthesized and annealed to the sense oligonucleotide to produce double-stranded DNA.

Mutations	Sequence 5'-3'
Site directed mutagenesis	
WT 114 (-830/-795)	CAG GAT CCC CAC CAT GAG TCA GAG GTA GTT CTG GGG
Mutated T114	CAG GAT CCC CAC <u>CAG</u> GAG <u>CCA</u> GAG GTA GTT CTG GGG
EMSA	
T282 (-822/-804)	CCA CCA TGA GTC AGA GGT A
Mutated T282	CCA CCA <u>TTA</u> GTG AGA GGT A

Western Blotting

Nuclear proteins (10 μg) were separated by running a 10% SDS-polyacrylamide gel electrophoresis, followed by electrotransfer onto a 0.45 μm PVDF membrane (Millipore, Saint-Quentin en Yvelines, France). The membranes were incubated either with specific antibodies against c-fos (sc-253, 1:10,000) or c-jun (sc-44, 1:5,000) (Santa Cruz laboratories) for 1 h at room temperature, or with specific antibodies against histone H3 (anti-acetylated lysine, mono-/di-/trimethylated lysine 4) and histone H4 (anti-acetylated lysine) (Upstate #06-599 (1:10,000 dilution), #05-791 (1:10,000 dilution) and #06-598 (1:1,000 dilution), respectively for 2 h at room temperature. Secondary antibodies used were horseradish peroxidase-conjugated anti-rabbit IgGs (Pierce). For detection, blots were processed with West® Pico chemiluminescent substrate (Pierce) and the signal was detected by exposing the processed blots to Hyperfilm™ ECL® (enhanced chemiluminescence; Amersham Biosciences). For Sp1 detection, the membranes were incubated 1 h at room temperature with anti-Sp1 antibody (sc-59, 1:10,000, Santa Cruz laboratories)

and alkaline phosphatase-conjugated anti-goat IgGs (Promega) as secondary antibody. For detection, the membrane was incubated with Nitro Blue Tetrazolium Chloride and 5-bromo-4-chloro-3-indolyl phosphate substrate (Life Technologies, Cergy-Pontoise, France).²⁹

Immunocytochemistry

LS174T cells were grown on poly-L-Lysine coated microscope glass slides 24 h prior to butyrate treatment. Cells were treated with 0, 1, 2, 5 and 10 mM butyrate for 24h. Cells were fixed in ice-cold methanol at -20°C for 10 min and rinsed in phosphate-buffered saline (PBS). The MUC2 mucin expression was determined by immunocytochemistry. For this purpose, cells were incubated for 60 min at room temperature with the monoclonal MUC2 antibody (WE9)³⁰ diluted in PBS (1:200), rinsed four times with PBS, and incubated at room temperature for 60 min with the biotinylated horse-anti-mouse antibody (Vector) diluted in PBS (1:1000), followed by 1h incubation with ABC-PO complex (Vectastain Elite Kit, Vector laboratories), each component diluted 1:400 in PBS. After incubation, binding was visualized using 0.5mg/ml 3,3'-diaminobenzidine (DAB), 0.02% v/v H_2O_2 in 30mM Imidazole, 1 mM EDTA (pH7.0). The slides were counterstained with hematoxylin.

Chromatin Immunoprecipitation (ChIP)

Cells untreated or treated with butyrate (10×10^6) were fixed in 1% (v/v) formaldehyde and chromatin was sonicated and immunoprecipitated as described in Piessen et al.³¹ with either 5 μg of specific antibodies against histone H3 (anti-acetylated lysine, mono-/di-/trimethylated lysine 4, methylated lysine 9 and trimethylated lysine 27) and histone H4 (anti-acetylated lysine) (Upstate) or with normal rabbit IgGs (Upstate) at 4°C . Immunoprecipitated chromatin (50 ng) was then used as a template for PCR using the following pairs of primers: forward primer1: 5'-TTGGCATT CAGGCTACAGGG-3' and reverse primer1: 5' GGCTGGCAGGGGCGGTG-3', covering the -236/+24 region of *MUC2* promoter. PCR was performed using AmpliTaq Gold polymerase as described by Piessen et al.³¹ PCR products (15 μl) were separated on a 2% (w/v) agarose gel containing ethidium bromide run in 1X TBE [Tris/borate/EDTA ($1 \times \text{TBE} = 45 \text{ mM Tris/borate and } 1 \text{ mM EDTA}$)] buffer.

Statistical analysis

All values in this article are mean values \pm standard deviation (SD).

RESULTS

Butyrate affects cell morphology and proliferation

SCFAs are known to affect epithelial proliferation, differentiation, apoptosis, and gene expression. Butyrate is, compared to acetate and propionate, the most effective SCFA in inducing alterations in these processes. Therefore, we first analyzed the effects of various concentrations of butyrate on morphology, proliferation and apoptosis of LS174T cells. Butyrate induced marked changes in morphology, which are characterized by elongation/stretching of the cells (Fig. 1A). Furthermore, butyrate treatment inhibited the proliferation of the LS174T cells in a dose-dependent manner, as reflected by a decrease in cell number upon butyrate treatment (Fig. 1B). These data were confirmed by WST-1 cell proliferation assays (data not shown). Finally, none of the butyrate concentrations (1-10 mM) used in this study induced cell death of LS174T cells, as determined by trypan-blue exclusion assays and analysis of cell morphology.

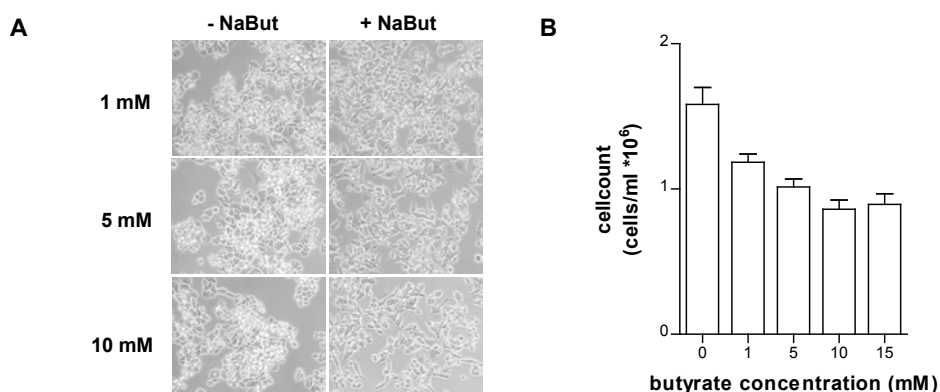


Figure 1. Butyrate affects cell morphology and proliferation

(A) LS174T cells stimulated with 1, 5 or 10 mM butyrate (right panel) demonstrate stretching/ elongation and flattening compared to untreated cells (left panel). (B) Cell counts before and after butyrate stimulation show a dose-dependent decrease in cell number after butyrate stimulation.

SCFAs alter MUC2 mRNA expression

LS174T cells were stimulated with increasing concentrations, from 1 mM to 15 mM, of butyrate, propionate, or acetate to determine the effects of the different SCFAs on MUC2 mRNA expression (Fig. 2A). One mM butyrate induced a 2.5-fold increase in MUC2 mRNA levels compared to untreated cells. In contrast, stimulation with higher concentrations, i.e. 5-15 mM butyrate, did not induce an increase in MUC2 mRNA levels, as at these concentrations MUC2 mRNA levels were comparable with control levels. Similar to butyrate, 1 mM propionate induced a 2.5 fold increase in MUC2 mRNA levels. Furthermore, at 5 mM propionate, MUC2 mRNA levels increased 4.2 fold, whereas at higher concentrations MUC2 mRNA levels decreased again. Acetate treatment resulted

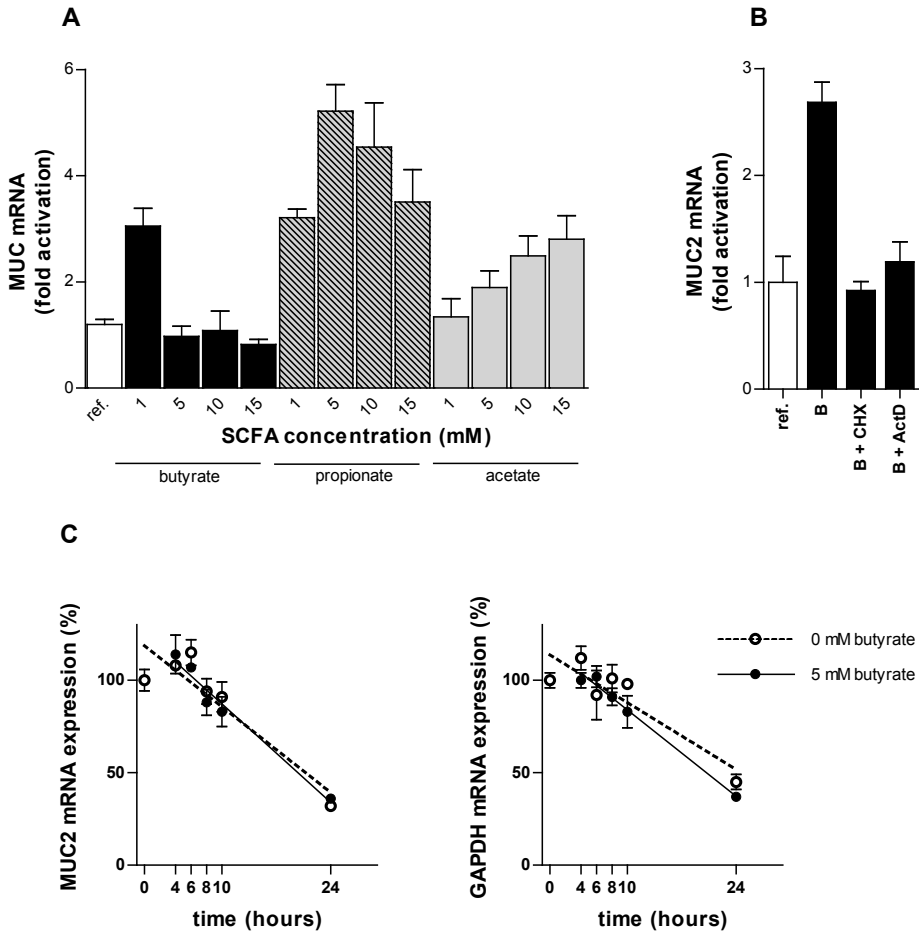


Figure 2. SCFAs alter *MUC2* mRNA expression

(A) *MUC2* mRNA fold activation in LS174T cells upon stimulation with SCFAs (butyrate, propionate and acetate) compared to untreated cells (ref.). (B) To determine whether butyrate stimulation influences *MUC2* synthesis on transcriptional or translational level, LS174T cells were stimulated with butyrate (B) (1 mM) in the presence of cycloheximide (CHX) or actinomycin D (ActD). (C) Stability of *MUC2* mRNA (left panel) and GAPDH mRNA (right panel) over time was measured by RT-PCR. LS174T cells were stimulated with butyrate (5 mM) after which mRNA synthesis was ceased through addition of actinomycin D. Relative mRNA expression was determined at the given time points (0, 4, 6, 8, 10 and 24 hours after addition of actinomycin D). All results represent means \pm SD obtained in triplicate in three separate experiments

in a dose-dependent increase in *MUC2* mRNA levels as of 5 mM reaching a 2.2 fold induction at 15 mM. To determine whether the activating effect of SCFAs on *MUC2* expression occurred at the transcriptional level, cells were pretreated with actinomycin D, which inhibits transcription. The results indicate that activation of *MUC2* expression by 1 mM butyrate occurred at the transcriptional level, as *MUC2* mRNA levels returned to basal levels when cells were pretreated with actinomycin D (Fig. 2B). This process also requires de novo protein synthesis as pretreatment of LS174T cells with cycloheximide,

an inhibitor of mRNA translation, decreased MUC2 mRNA levels to basal levels as well (Fig. 2B). Similar results were obtained when cells were stimulated with propionate or acetate instead of butyrate (data not shown). Since butyrate increased MUC2 mRNA levels at low concentrations (1 mM) in contrast to no effect at moderate (5 mM) and high (10 and 15 mM) concentrations, we studied whether this decrease was due to a decrease in MUC2 RNA stability. For that we pre-treated cells with actinomycin D over a 24h period of time, and then incubated cells with 5 mM butyrate before measuring MUC2 mRNA amount by qRT-PCR. The results show no differences in MUC2 mRNA stability between butyrate-stimulated and non-stimulated cells (Fig. 2C).

Effect of butyrate on MUC2 protein expression

To determine whether butyrate also induced an increase in MUC2 protein expression in LS174T cells, immunocytochemistry was performed with an antibody specific for MUC2. In non-stimulated cells MUC2 staining was hardly visible (Fig. 3). Stimulation with 1 mM of butyrate clearly shows an increase in MUC2 staining. This effect was even more pronounced in cells stimulated with 2 mM of butyrate (Fig. 3).

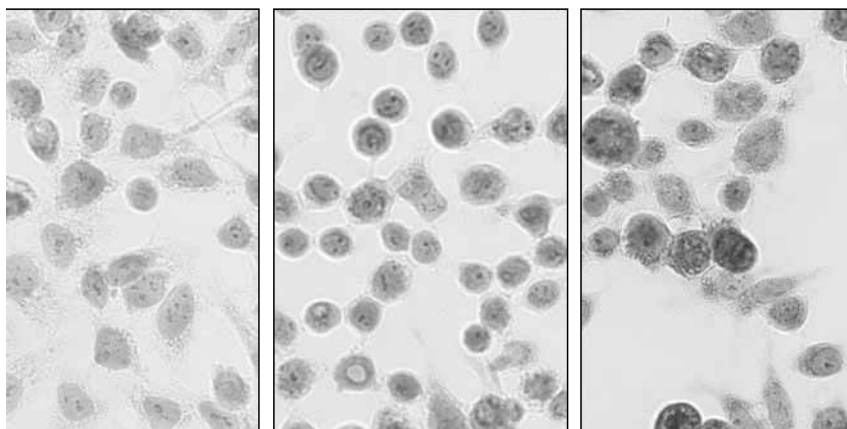


Figure 3. Effect of butyrate on MUC2 protein expression
MUC2 apomucin expression by immunocytochemistry in non-stimulated (0 mM) and butyrate (1 and 2 mM) stimulated LS174T cells. (Magnification x40) (See Color Section, p. 242.)

Identification of butyrate responsive regions in the *MUC2* promoter

Transfections with *MUC2* promoter constructs were performed to identify butyrate-responsive regions. The *MUC2* promoter constructs used are indicated in Figure 4A. Stimulation of LS174T cells with low (0.5-2 mM) concentrations of butyrate demonstrated a dose-dependent increase in luciferase-activity after transfection with each of the promoter construct used (Fig. 4B). The highest transactivation was seen using *MUC2* promoter construct -947/-1 indicating a possible butyrate-responsive element within the -947/-372 region. Analysis of the *MUC2* promoter sequence indeed revealed the presence

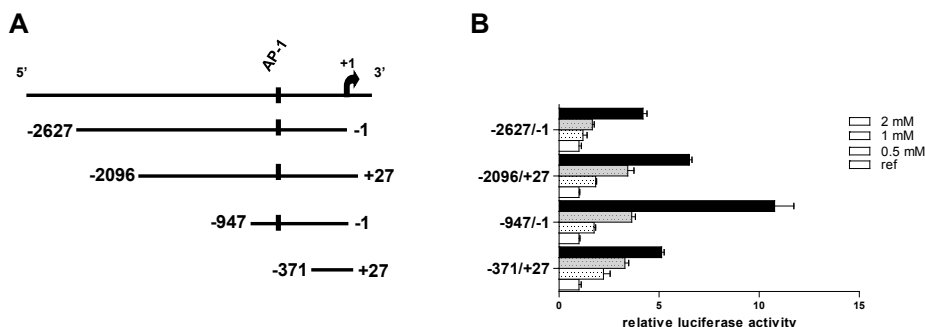


Figure 4. Identification of butyrate responsive regions in the *MUC2* promoter

Schematic representation of *MUC2* promoter and the different constructs used to study *MUC2* promoter activity (A). Numbering refers to transcription initiation site designated +1. (B) Transfected cells were stimulated with butyrate as described in experimental procedures. Results are expressed as fold activity in the butyrate-stimulated cells compared to non-stimulated cells. Results represent means \pm SD obtained in triplicate in three separate experiments.

of a consensus putative binding site (ATGAGTCAGA) for the transcription factor AP-1 at -817/-808, a transcription factor known to mediate butyrate-induced transcriptional effects. To determine whether this putative AP-1 binding site was responsible for the butyrate-induced *MUC2* promoter transactivation, specific nucleotides within the sequence were mutated (Table 1). The mutation resulted in a 50% reduction of the butyrate-induced *MUC2* promoter transactivation (Fig. 5A). Activation of AP-1 by butyrate in LS174T cells was confirmed by treating AP-1-Luc-transfected cells with butyrate. The stimulation was dose-dependent with a maximal 13.3-fold induction at 2 mM butyrate (Fig. 5B).

C-fos and c-jun bind to the AP-1 element in *MUC2* promoter

As the transcription factors c-fos and c-jun are known to bind as a complex to AP-1 binding elements within promoters, EMSAs were carried out to show the binding of these two transcription factors to the AP-1 element found at -817/-808. When incubated with nuclear extract from untreated and butyrate-stimulated (1 mM and 10 mM) LS174T cells, the radiolabeled probe T282 (containing the putative AP-1 binding site, see table I) produced one retarded band (Fig. 6, lane 2). Specificity of the protein-DNA complex was confirmed by strong decrease of the shifted band when unlabeled competition was performed with a 50 times excess of unlabeled T282 probe (lane 3), whereas competition with a 50 times excess of unlabeled mutated T282 probe (lane 4) did not affect the shifted band. Involvement of c-jun and c-fos in the complex formation was then proven in supershift experiments carried out with antibodies specific for c-jun (lane 5) and c-fos (lane 6), respectively. Addition of the two antibodies indeed resulted in a supershift that was observed both in untreated cells and butyrate-stimulated cells. This was well-correlated with the amount of c-fos and c-jun found in the cells (Fig. 7). Altogether, this suggests that the decreased *MUC2* mRNA levels after stimulation of cells with 5 mM or

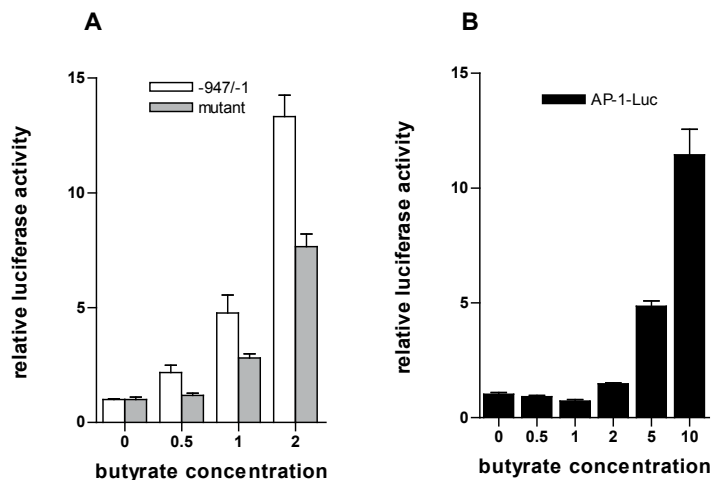


Figure 5. The effect of site directed mutagenesis on *MUC2* promoter activation by butyrate (A) Relative luciferase activity diagram showing the effect of site-directed mutagenesis on *MUC2* promoter activation by butyrate. Cells were transfected either with the wild-type -947/-1 construct (WT, white bars) or with the AP-1 mutated construct (mut, grey bars) before being stimulated with butyrate as described in experimental procedures. (B) Luciferase activity in cells transfected with AP-1-Luc reporter construct and stimulated with butyrate. Results are expressed as fold activity of the butyrate-stimulated compared to non-stimulated cells. Results represent means \pm SD obtained in triplicate in three separate experiments.

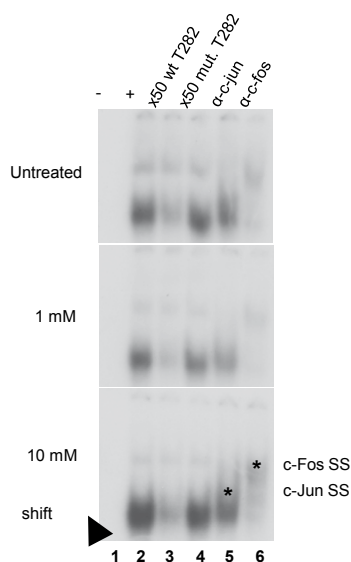


Figure 6. C-fos and c-jun bind to the AP-1 element in *MUC2* promoter Identification of an AP-1 *cis*-element in *MUC2* promoter by EMSA. Nuclear extracts from untreated cells or cells treated with either 1 or 10 mM butyrate. Radiolabeled probe T282 alone (lane 1), radiolabeled T282 with nuclear extract (lane 2), cold competition with 50x excess of unlabeled wt T282 probe (lane 3), cold competition with 50x excess of unlabeled mutated T282 (lane 4). Supershift analysis was performed by pre-incubating the nuclear extract with 1 μ l of anti-c-jun (lane 5) and anti-c-fos (lane 6) antibodies, respectively. Arrows and stars indicate positions of the shifted and supershifted (ss) protein-DNA complexes.

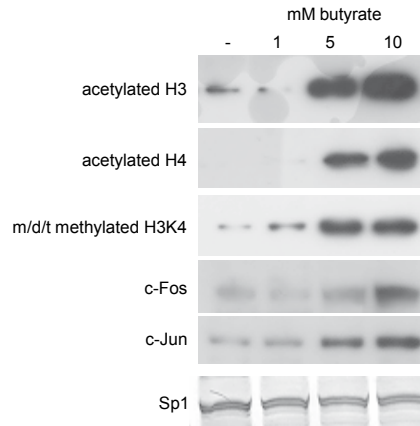


Figure 7. Expression of acetylated histones upon butyrate stimulation
Study of the expression of acetylated histones H3 and H4, m/d/t methylated H3K4, c-Fos, c-Jun and Sp1 in untreated (-) and butyrate-treated (1, 5 and 10 mM) LS174T cells by western-blotting.

10 mM butyrate compared to 1 mM butyrate stimulation (see Fig. 2), are not caused by a decreased binding capacity of AP-1 (i.e. the c-fos/c-jun complex) to its *cis*-element within the *MUC2* promoter.

Butyrate alters histone status at the *MUC2* promoter in a dose-dependent manner

Since butyrate is known to affect histone deacetylase (HDAC) activity, and that the *MUC2* promoter is known to be regulated by HDAC³², we hypothesized that histone status at *MUC2* promoter may be involved in *MUC2* regulation by butyrate. To determine whether alterations in *MUC2* expression correlated to changes in histone acetylation and/or methylation we first examined the effect of butyrate on the levels of acetylated H3 and H4 histones as well as m/d/t methylated H3K4 in LS174T cells by Western blotting (Fig. 7). Acetylated histone H3 and H4 and mono-/di-/tri-methylated H3 on lysine (K) 4, which correlate with activation of transcription, were strongly increased after stimulation with both moderate (5 mM) and high (10 mM) concentrations of butyrate.

To establish the effects of butyrate on histone H3 and H4 status at the *MUC2* promoter, ChIP assays were performed with chromatin from non-stimulated and butyrate-stimulated LS174T cells (Fig. 8). In untreated and 1 mM butyrate-treated cells, *MUC2* promoter covering the -236/+24 region was mainly associated with mono-/di-/tri-methylated K4H3 as well as to a lower extent with acetylated histone H3 and H4, which correlate with activation of transcription. At 5 mM butyrate this status of chromatin activation was confirmed with a stronger association with acetylated H3. At these two concentrations we also observed an increase of 3mK27H3, which is usually indicative of transcription inhibition. At 10 mM butyrate, histone modifications at the *MUC2* promoter

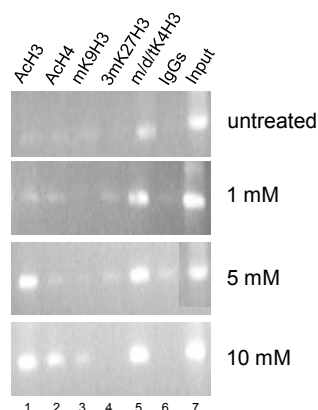


Figure 8. Butyrate alters histone status at the MUC2 promoter in a dose-dependent manner. Study of the histone status at the MUC2 promoter by ChIP. Acetylated histone H3 (AcH3, lane 1), acetylated histone H4 (AcH4, lane 2), and m/d/tK4H3 (lane 5) are representative of activation of transcription whereas histone H3 methylated on lysine 9 (mK9H3, lane 3) and histone H3 trimethylated on lysine 27 (3mK27H3, lane 4) are representative of inhibition of transcription. Lane 6: negative control with IgGs. Lane 7: Input.

were characterized by modifications inducing active chromatin (AcH3, AcH4 and m/d/tK4H3) and usually indicative of inactive chromatin (mK9H3).

DISCUSSION

In the present study we analyzed the effect of SCFAs on epithelial cell morphology, proliferation, and, as marker for epithelial protection, MUC2 expression. Moreover, we identified the mechanisms responsible for the butyrate-induced changes in MUC2 expression. By studying these parameters in conjunction we aimed to gain more insight in the effects of SCFAs on epithelial protection.

The present study revealed that butyrate altered the morphology of LS174T cells by inducing cell elongation/stretching. This suggests that butyrate affects LS174T cell differentiation. Additionally, butyrate caused a dose-dependent decrease in cell number. As this SCFA did not induce apoptosis at the concentrations used in this study, we conclude that butyrate inhibits epithelial proliferation. Several *in vitro* studies support our finding that butyrate inhibits proliferation.³³⁻³⁷ For example, butyrate inhibited the proliferation of non-confluent and sub-confluent HT-29 cells in a dose-dependent manner (1-8 mM).³⁶ Furthermore, Siavoshian et al. demonstrated that the mechanism through which butyrate inhibits proliferation in HT-29 cells is exerted via the induction of cyclin D3, an inhibitor of cell cycle progression and p21, a stimulator of cell differentiation.³³

Next, we studied the effect of SCFAs on MUC2 synthesis in the LS174T cell line. Butyrate, propionate, as well as acetate, were able to increased MUC2 mRNA synthesis.

Specifically, butyrate increased MUC2 mRNA levels at low concentrations and had no effect at moderate and high concentrations. Both low and moderate propionate concentrations increased MUC2 mRNA levels, whereas at higher concentrations, MUC2 mRNA levels were still increased but to a lesser extent. Finally, a dose-dependent increase in MUC2 mRNA levels was seen after stimulation with acetate, with the smallest increase at low concentrations and highest increase at high concentrations.

Of the SCFAs studied in this paper, only the effects of butyrate on mucin expression have been described extensively. Hatayama et al. also showed that concentrations of 1-2 mM butyrate increased MUC2 expression in LS174T cells.²² Barcelo et al.²³ demonstrated a significant discharge of mucins at concentrations of 5 mM of butyrate, while increasing the concentration to 100 mM decreased this mucus response in mice. Highly relevant, *ex vivo* stimulation of macroscopically normal fresh colon tissue with 0.05-1 mM butyrate stimulates MUC2 synthesis, whereas at stimulation with 10 mM butyrate MUC2 synthesis levels returned to basal levels.²⁴ These studies correlate with our data with respect to the effects of butyrate on MUC2 expression (i.e. increase in MUC2 at low concentration and no effect at high concentrations).

Despite previous studies showing induction of MUC2 by butyrate, no precise analysis of the molecular mechanisms has been performed.²¹⁻²⁵ Since butyrate is known to mediate its effects via the AP-1 transcription factor, and because we found a putative consensus binding site (ATGAGTCAGA) for AP-1 at -817/-808 in the *MUC2* promoter, we studied its regulation by AP-1. AP-1 is a multiprotein complex, composed of the products of c-Jun and c-Fos proto-oncogenes. Growth factors, neurotransmitters, polypeptide hormones, bacterial and viral infections as well as a variety of physical and chemical stresses, employ AP-1 to translate external stimuli, both into short-term and long-term changes of gene expression. Interestingly, we found that butyrate was able to activate an AP-1 reporter construct and to induce c-Fos and c-Jun protein expression in the LS174T cell line, indicating that butyrate-induced MUC2 transcription might occur via AP-1 binding to the *MUC2* promoter. That is what we indeed demonstrated by mutating the consensus AP-1 binding site, which abolished both binding of AP-1 and inhibited butyrate-induced MUC2 activation. As butyrate only increased MUC2 mRNA and protein levels at low concentrations (1-2 mM), but not at high concentrations (5-10 mM), this suggested that activation of the *MUC2* promoter, and up-regulation of MUC2 RNA and protein levels, at low concentration of butyrate was, at least partly, regulated by AP-1.

Since butyrate is a well-known HDAC inhibitor, butyrate-induced alterations in gene expression can also reflect changes in histone modification status and chromatin marks. To assess whether the increase of *MUC2* expression following butyrate treatment was associated with chromatin status, we performed ChIP experiments. As expected, our data indicate that butyrate treatment is associated with dose-dependent increased of both global histone acetylation levels and histone H3 and H4 acetylation at *MUC2* promoter

region. Since cross talk between histone post-translational modifications are important in establishing the histone code, increased mono-/di-/trimethylation of K4H3 observed at *MUC2* promoter after butyrate treatment may be directly linked to increased histone H3 acetylation, as previously shown by Nightingale et al.³⁸ For a long time methylation of K9H3 has been considered as a chromatin mark associated with heterochromatin and gene silencing. However, a recent study showed that higher H3K9 monomethylation levels are detected in active promoters surrounding gene transcription start sites, suggesting that this modification may be associated with transcription activation.³⁹ These data are concordant with our present results, showing that in LS174T cells, the proximal region of *MUC2* promoter is associated with monomethylation of K9H3. However, to our knowledge, this is the first time that a positive effect of high concentrations of butyrate on K9H3 methylation is shown. Strikingly, we found that treatment with low concentration of butyrate induced an increase of H3K27 trimethylation at *MUC2* promoter, which therefore adopted a bivalent chromatin pattern. This bivalent profile has already been described for embryonic stem cell genes as well as DNA-hypermethylated genes which were reexpressed by demethylation.⁴⁰ We previously showed that *MUC2* is regulated by a complex combination of DNA (de)methylation and establishment of a (de)repressive histone code.⁴¹ The changes of global epigenetic profile stated at *MUC2* promoter may thus be partly responsible for the increase in *MUC2* expression level induced by low concentration of butyrate.

Surprisingly, treatment with moderate and high concentrations of butyrate, yet associated with active chromatin marks at the *MUC2* promoter, did not induce increased *MUC2* expression. Dual effects of HDAC inhibitors on gene expression have already been shown for numerous genes⁴², including mucin genes. In particular, Augenlicht et al.⁴³ demonstrated that cell treatment with butyrate induce an inhibition of *MUC2* expression, correlated with repression of secretory functions of colonic cells. This repression may be due to changes in histone modification patterns, since trichostatin A, another HDAC inhibitor, has the same inhibiting effect on *MUC2* expression in LS174T cells.⁴¹ However, our results clearly show that *MUC2* promoter is associated with active chromatin marks at high concentrations of butyrate. Therefore, the dual effect observed at high concentrations, is most likely due to dramatic butyrate-induced changes in the global chromatin landscape⁴², rather than direct histone modifications at *MUC2* promoter. Numerous studies showing that expression and post-translational modifications of factors known to positively or negatively regulate *MUC2* transcription (including, among others, Sp3, CDX-2 or p53 transcription factors⁴⁴⁻⁴⁶) is dramatically affected by butyrate, support this hypothesis.

Taken together, we have shown that butyrate stimulates *MUC2* expression at low concentrations, but has no effect on *MUC2* expression at moderate and high concentrations. We therefore hypothesize that low concentrations of butyrate could have a

protective effect on intestinal barrier function by increasing mucus production, whereas moderate to high concentrations may decrease intestinal barrier function by decreasing MUC2 production. This effect might partially explain the difference in incidence of NEC between the formula-fed and human milkfed newborn infants. Manipulation of the SCFA profile can be established by influencing the composition of microbiota, for instance by treatment with prebiotics, probiotics and/or human milk. This approach seems to be promising in the treatment of IBD and NEC. In summary, the *in vitro* results in the present study indicate that low concentrations of butyrate stimulate MUC2 expression, which *in vivo* would lead to an increased intestinal epithelial barrier function. In contrast, high concentrations of butyrate decrease MUC2 expression which might diminish intestinal barrier function. Moreover, identification of AP-1 and histone modifications as mechanisms involved in MUC2 regulation by butyrate may represent pathways to target prevention of IBD and NEC by influencing SCFA production by the intestinal flora.

ACKNOWLEDGEMENTS

We thank Dr Avery (Pennsylvania State University, University Park, PA, U.S.A.) for the gift of the AP-1-Luc construct.

FUNDING

This work was supported by unrestricted grants from The Nutricia Research Foundation and The Association François Aupetit (to I. V. S.). A. V. is the recipient of an Inserm-région Nord-Pas de Calais PhD fellowship.

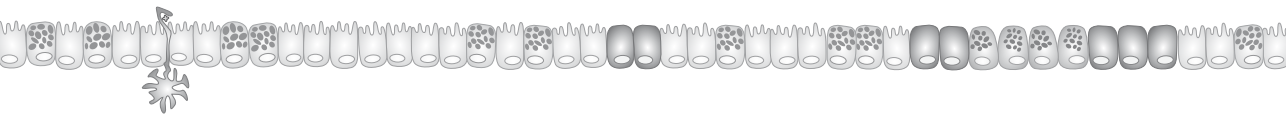
REFERENCES

1. Cummings JH RJ, Sakata T Physiological and clinical aspects of short-chain fatty acids. Cambridge University Press, Cambridge 1995.
2. Andoh A, Tsujikawa T, Fujiyama Y. Role of dietary fiber and short-chain fatty acids in the colon. *Curr Pharm Des* 2003;9:347-58.
3. Galvez J, Rodriguez-Cabezas ME, Zarzuelo A. Effects of dietary fiber on inflammatory bowel disease. *Mol Nutr Food Res* 2005;49:601-8.
4. Tedelind S, Westberg F, Kjerrulf M, Vidal A. Anti-inflammatory properties of the short-chain fatty acids acetate and propionate: a study with relevance to inflammatory bowel disease. *World J Gastroenterol* 2007;13:2826-32.
5. Alvaro A, Sola R, Rosales R, Ribalta J, Anguera A, Masana L, Vallve JC. Gene expression analysis of a human enterocyte cell line reveals downregulation of cholesterol biosynthesis in response to short-chain fatty acids. *IUBMB Life* 2008.
6. Sauer J, Richter KK, Pool-Zobel BL. Physiological concentrations of butyrate favorably modulate genes of oxidative and metabolic stress in primary human colon cells. *J Nutr Biochem* 2007;18:736-45.
7. Welter H, Claus R. Expression of the monocarboxylate transporter 1 (MCT1) in cells of the porcine intestine. *Cell Biol Int* 2008;32:638-45.
8. Kiela PR, Kuscuglu N, Midura AJ, Midura-Kiela MT, Larmonier CB, Lipko M, Ghishan FK. Molecular mechanism of rat NHE3 gene promoter regulation by sodium butyrate. *Am J Physiol Cell Physiol* 2007;293:C64-74.
9. Daly K, Shirazi-Beechey SP. Microarray analysis of butyrate regulated genes in colonic epithelial cells. *DNA Cell Biol* 2006;25:49-62.
10. Gibson GR, Roberfroid MB. Dietary modulation of the human colonic microbiota: introducing the concept of prebiotics. *J Nutr* 1995;125:1401-12.
11. Harmsen HJ, Wildeboer-Veloo AC, Raangs GC, Wagendorp AA, Klijn N, Bindels JG, Welling GW. Analysis of intestinal flora development in breast-fed and formula-fed infants by using molecular identification and detection methods. *J Pediatr Gastroenterol Nutr* 2000;30:61-7.
12. Balmer SE, Wharton BA. Diet and faecal flora in the newborn: breast milk and infant formula. *Arch Dis Child* 1989;64:1672-7.
13. Stark PL, Lee A. The microbial ecology of the large bowel of breast-fed and formula-fed infants during the first year of life. *J Med Microbiol* 1982;15:189-203.
14. Kleessen B, Bunke H, Tovar K, Noack J, Sawatzki G. Influence of two infant formulas and human milk on the development of the faecal flora in newborn infants. *Acta Paediatr* 1995; 84:1347-56.
15. Knol J, Scholtens P, Kafka C, Steenbakkers J, Gro S, Helm K, Klarczyk M, Schopfer H, Bockler HM, Wells J. Colon microflora in infants fed formula with galacto- and fructo-oligosaccharides: more like breast-fed infants. *J Pediatr Gastroenterol Nutr* 2005;40:36-42.
16. Den Hond E, Hiele M, Evenepoel P, Peeters M, Ghoos Y, Rutgeerts P. In vivo butyrate metabolism and colonic permeability in extensive ulcerative colitis. *Gastroenterology* 1998;115: 584-90.
17. Roediger WE. The colonic epithelium in ulcerative colitis: an energy-deficiency disease? *Lancet* 1980;2:712-5.
18. Kato K, Ishii Y, Mizuno S, Sugitani M, Asai S, Kohno T, Takahashi K, Komuro S, Iwamoto M, Miyamoto S, Takayama T, Arakawa Y. Usefulness of rectally administering [1-(13)C]-butyrate

- for breath test in patients with active and quiescent ulcerative colitis. *Scand J Gastroenterol* 2007;42:207-14.
19. Pullan RD, Thomas GA, Rhodes M, Newcombe RG, Williams GT, Allen A, Rhodes J. Thickness of adherent mucus gel on colonic mucosa in humans and its relevance to colitis. *Gut* 1994;35:353-9.
 20. Tytgat KM, van der Wal JW, Einerhand AW, Buller HA, Dekker J. Quantitative analysis of MUC2 synthesis in ulcerative colitis. *Biochem Biophys Res Commun* 1996;224:397-405.
 21. Shimotoyodome A, Meguro S, Hase T, Tokimitsu I, Sakata T. Short chain fatty acids but not lactate or succinate stimulate mucus release in the rat colon. *Comp Biochem Physiol A Mol Integr Physiol* 2000;125:525-31.
 22. Hatayama H, Iwashita J, Kuwajima A, Abe T. The short chain fatty acid, butyrate, stimulates MUC2 mucin production in the human colon cancer cell line, LS174T. *Biochem Biophys Res Commun* 2007;356:599-603.
 23. Barcelo A, Claustre J, Moro F, Chayvialle JA, Cuber JC, Plaisancie P. Mucin secretion is modulated by luminal factors in the isolated vascularly perfused rat colon. *Gut* 2000;46:218-24.
 24. Finnie IA, Dwarakanath AD, Taylor BA, Rhodes JM. Colonic mucin synthesis is increased by sodium butyrate. *Gut* 1995;36:93-9.
 25. Sakata T, Setoyama H. Local stimulatory effect of short-chain fatty acids on the mucus release from the hindgut mucosa of rats (*Rattus norvegicus*). *Comp Biochem Physiol A Physiol* 1995;111:429-32.
 26. Perrais M, Pigny P, Copin MC, Aubert JP, Van Seuning I. Induction of MUC2 and MUC5AC mucins by factors of the epidermal growth factor (EGF) family is mediated by EGF receptor/Ras/Raf/extracellular signal-regulated kinase cascade and Sp1. *J Biol Chem* 2002;277:32258-67.
 27. Meijerink J, Mandigers C, van de Locht L, Tonnissen E, Goodsaid F, Raemaekers J. A novel method to compensate for different amplification efficiencies between patient DNA samples in quantitative real-time PCR. *J Mol Diagn* 2001;3:55-61.
 28. Van Seuning I, Ostrowski J, Bomszyk K. Description of an IL-1-responsive kinase that phosphorylates the K protein. Enhancement of phosphorylation by selective DNA and RNA motifs. *Biochemistry* 1995;34:5644-50.
 29. Jonckheere N, Van Der Sluis M, Velghe A, Buisine MP, Suttmuller M, Ducourouble MP, Pigny P, Buller HA, Aubert JP, Einerhand AW, Van Seuning I. Transcriptional activation of the murine *Muc5ac* mucin gene in epithelial cancer cells by TGF-beta/Smad4 signalling pathway is potentiated by Sp1. *Biochem J* 2004;377:797-808.
 30. Tytgat KM, Boveland FJ, Opdam FJ, Einerhand AW, Buller HA, Dekker J. Biosynthesis of rat MUC2 in colon and its analogy with human MUC2. *Biochem J* 1995;309 (Pt 1):221-9.
 31. Piessen G, Jonckheere N, Vincent A, Hemon B, Ducourouble MP, Copin MC, Mariette C, Van Seuning I. Regulation of the human mucin MUC4 by taurodeoxycholic and taurochenodeoxycholic bile acids in oesophageal cancer cells is mediated by hepatocyte nuclear factor 1alpha. *Biochem J* 2007;402:81-91.
 32. Vincent A, Ducourouble MP, Van Seuning I. Epigenetic regulation of the human mucin gene MUC4 in epithelial cancer cell lines involves both DNA methylation and histone modifications mediated by DNA methyltransferases and histone deacetylases. *Faseb J* 2008.
 33. Siavoshian S, Segain JP, Kornprobst M, Bonnet C, Cherbut C, Galmiche JP, Blottiere HM. Butyrate and trichostatin A effects on the proliferation/differentiation of human intestinal epithelial cells: induction of cyclin D3 and p21 expression. *Gut* 2000;46:507-14.

34. Whitehead RH, Young GP, Bhathal PS. Effects of short chain fatty acids on a new human colon carcinoma cell line (LIM1215). *Gut* 1986;27:1457-63.
35. Barnard JA, Warwick G. Butyrate rapidly induces growth inhibition and differentiation in HT-29 cells. *Cell Growth Differ* 1993;4:495-501.
36. Comalada M, Bailon E, de Haro O, Lara-Villoslada F, Xaus J, Zarzuelo A, Galvez J. The effects of short-chain fatty acids on colon epithelial proliferation and survival depend on the cellular phenotype. *J Cancer Res Clin Oncol* 2006;132:487-97.
37. Archer S, Meng S, Wu J, Johnson J, Tang R, Hodin R. Butyrate inhibits colon carcinoma cell growth through two distinct pathways. *Surgery* 1998;124:248-53.
38. Nightingale KP, Gendreizig S, White DA, Bradbury C, Hollfelder F, Turner BM. Cross-talk between histone modifications in response to histone deacetylase inhibitors: MLL4 links histone H3 acetylation and histone H3K4 methylation. *J Biol Chem* 2007;282:4408-16.
39. Barski A, Cuddapah S, Cui K, Roh TY, Schones DE, Wang Z, Wei G, Chepelev I, Zhao K. High-resolution profiling of histone methylations in the human genome. *Cell* 2007;129:823-37.
40. McGarvey KM, Van Neste L, Cope L, Ohm JE, Herman JG, Van Criekinge W, Schuebel KE, Baylin SB. Defining a chromatin pattern that characterizes DNA-hypermethylated genes in colon cancer cells. *Cancer Res* 2008;68:5753-9.
41. Vincent A, Perrais M, Desseyn JL, Aubert JP, Pigny P, Van Seuning I. Epigenetic regulation (DNA methylation, histone modifications) of the 11p15 mucin genes (MUC2, MUC5AC, MUC5B, MUC6) in epithelial cancer cells. *Oncogene* 2007;26:6566-76.
42. Reczek PR, Weissman D, Huvos PE, Fasman GD. Sodium butyrate induced structural changes in HeLa cell chromatin. *Biochemistry* 1982;21:993-1002.
43. Augenlicht L, Shi L, Mariadason J, Laboisie C, Velcich A. Repression of MUC2 gene expression by butyrate, a physiological regulator of intestinal cell maturation. *Oncogene* 2003;22:4983-92.
44. White NR, Mulligan P, King PJ, Sanderson IR. Sodium butyrate-mediated Sp3 acetylation represses human insulin-like growth factor binding protein-3 expression in intestinal epithelial cells. *J Pediatr Gastroenterol Nutr* 2006;42:134-41.
45. Domon-Dell C, Wang Q, Kim S, Keding M, Evers BM, Freund JN. Stimulation of the intestinal Cdx2 homeobox gene by butyrate in colon cancer cells. *Gut* 2002;50:525-9.
46. Palmer DG, Paraskeva C, Williams AC. Modulation of p53 expression in cultured colonic adenoma cell lines by the naturally occurring luminal factors butyrate and deoxycholate. *Int J Cancer* 1997;73:702-6.

Chapter 8



Dietary influence on colitis-development in Muc2-deficient mice: *diet matters!*

Nanda Burger-van Paassen, Patrycja J. Puiman, Peng Lu, Nicolas Le Polles, Janneke Bouma, Anita M. Korteland-van Male, Günther Boehm, Johannes B. van Goudoever, Ingrid B. Renes

Manuscript in preparation



ABSTRACT

Background: Muc2 knockout (Muc2^{-/-}) mice do not have a protective mucus layer and spontaneously develop colitis. **Objective:** To study the effects of a purified diet and probiotic supplementation on growth and disease severity in Muc2^{-/-} mice. **Methods:** Muc2^{-/-} and wildtype (WT) mice were fed a non-purified (NP, i.e., standard chow) diet, a NP-diet with daily administration of *Bifidobacterium breve* and *Bifidobacterium animalis subsp. lactis* (NP+PRO), or a purified (P) diet during 5 weeks, starting directly after weaning. The purified diet contains 60% less fibers, and milk-casein proteins instead of plant proteins. Clinical symptoms and colonic morphological changes were monitored. Inflammation was studied by immunohistochemistry and determination of cytokine gene expression. **Results:** In Muc2^{-/-} mice, the P-diet significantly increased bodyweight compared to the NP and NP+PRO diet. Bodyweights of Muc2^{-/-} mice fed P-diet were similar to WT mice. Crypt length was increased in Muc2^{-/-} mice compared to WT mice regardless the type of diet. In Muc2^{-/-} mice the P diet limited the increase in crypt length compared to NP or NP+PRO diet. In Muc2^{-/-} mice the NP+PRO diet reduced the crypt lengthening compared to NP diet. Muc2^{-/-} mice that were fed the P-diet showed a limited influx of Cd3ε-positive T cells, increased expression of *Ebi3* and *Il12p35*, which as protein dimer is known as the immune suppressive cytokine IL35, decreased abundance of S100a8 and S100a9-positive cells and increased abundance of Muc4-positive cells compared to Muc2^{-/-} mice fed NP or NP+PRO diet. **Conclusions:** Type of diet and, to a lesser extent probiotic supplementation affect colitis severity in Muc2^{-/-} mice. The type of protein and amount of insoluble fibers modulate disease activity in mice prone to develop colitis. Moreover, probiotics might have beneficial effects in Muc2^{-/-} mice as NP+PRO diet reduced crypt lengthening compared to NP diet. Together these data imply that feeding strategy in subjects with colitis might have considerable implications for disease severity.

Key words: Muc2, Muc2-deficiency, colitis, nutrition, probiotics

INTRODUCTION

Innate defense in the gut consists of several components that together prevent bacteria and other micro-organisms from invasion into the intestinal epithelium. Mucus produced by goblet cells is a key component of the physical barrier that covers the intestinal epithelium. The structural component of this mucus layer is the mucin MUC2. We previously showed that deficiency of Muc2, as in Muc2 knockout (Muc2^{-/-}) mice, leads to the development of clinical and histological signs of colitis.¹ As the synthesis of the mucin MUC2 is decreased in human intestinal diseases such as ulcerative colitis (UC)²⁻⁴ and necrotizing enterocolitis (NEC)⁵, the Muc2^{-/-} mouse model is a powerful tool, enabling us to study the physiologic role of the epithelial barrier in many aspects.

Nutrition plays an important role in human inflammatory bowel disease (IBD), i.e. enteral nutrition is an effective therapy for the induction of clinical remission in adult Crohn's disease (CD) and is the primary treatment for pediatric CD.⁶⁻⁷ The exact mechanisms through which enteral nutrition exert these beneficial effects is unknown, but most likely consists of direct anti-inflammatory effects on enterocytes, a suppressive effect on mucosal inflammatory cytokine levels, promotion of the integrity of the epithelium and modulation of the intestinal microbiota.⁸⁻¹³ Necrotizing enterocolitis (NEC) is an acquired intestinal disease that predominantly occurs in premature infants. It is known by a very high morbidity and mortality and currently only supportive therapy is available. Besides prematurity, enteral feeding, more specifically formula feeding versus human milk feeding, is a risk factor for the development of NEC.¹⁴⁻¹⁵ Although NEC probably develops due to a combination of risk factors, dietary interventions have shown to play an important role in disease prevention.

One of the big advantages of nutritional therapy is the relatively low cost and minimal risk of side effects. Therefore nutritional therapy forms an interesting target for prevention of NEC and treatment in IBD. Probiotics are described as 'live microbial dietary supplements which beneficially affect the host animal by improving its intestinal microbial balance'.¹⁶ Although data concerning the effect of probiotics in IBD are conflicting¹⁷⁻¹⁸, enteral supplementation of probiotics significantly reduced the risk of severe necrotizing enterocolitis (NEC) in preterm infants.¹⁹ Moreover, colitis was attenuated or prevented in a variety of experimental colitis models that were treated with probiotics.²⁰⁻²¹

The phenotype of Muc2^{-/-} mice is variable and might depend on the genotypic background, a phenomenon that was also described for IL-10-deficient mice.²² More specifically, Velcich et al. used Muc2^{-/-} mice on a mixed genotypic background (C57/Bl6-129Sv), which hardly displayed intestinal inflammation, whereas we used Muc2^{-/-} mice on a 129Sv background that showed severe colitis.^{1,23} However, differences in the diet might also be responsible as animals that developed colitis were fed a standard, non-purified

rodent diet, whereas animals that did not show a clear colitis phenotype were fed a purified, AIN-based diet (AIN-76A).

In the present study, we investigated the effect of a purified diet, i.e. semi synthetic AIN based diet, relative to a non-purified diet, i.e. standard rodent chow, and supplementation with probiotics on growth and disease severity in *Muc2*^{-/-} mice. We hypothesized that a purified diet or supplementation with probiotics would decrease disease severity in *Muc2*^{-/-} mice. Besides clinical disease markers, we studied colonic inflammation markers, serum cytokine profiles and cytokine gene expression profiles in colonic tissue. Together these studies indicate that disease severity is affected by the type of diet.

MATERIAL AND METHODS

Animals

Wild type (WT) and *Muc2*^{-/-} mice were bred as previously described.¹ All mice were generated from *Muc2*^{+/-} breedings. Mice were housed in the same specific pathogen-free environment in a 12-hour light/dark cycle with free access to acidified tap water. Animal care and procedures were conducted according to institutional guidelines (Erasmus MC Animal Ethics Committee, Rotterdam, the Netherlands). Mice were maintained in a barrier facility. Wild-type and *Muc2*^{-/-} mice were tested negative for *Helicobacter hepaticus* and norovirus infection.

Experimental Setup

The experiment was divided into three groups. Group 1 received a non-purified (NP) diet, consisting of standard rodent pellets (Special Diets Services, Witham, Essex, England), group 2 received a purified (P), semi-synthetic diet (AIN93G pellets, Research Diet Services BV, Wijk bij Duurstede, the Netherlands) and group 3 received the NP diet supplemented with probiotics (NP+PRO). Animals were weaned from mother's milk at the age of approximately 21 days. Supplementation of probiotics was started immediately thereafter. The probiotic mixture consisted of two probiotic strains: *Bifidobacterium breve* and *Bifidobacterium animalis subsp. lactis* (Danone Research, Wageningen, the Netherlands) in a final concentration of 1x10⁹CFU/animal/day. The probiotic freeze-dried powder was dissolved in NaCl 0,9%. Finally, the mixture was dissolved in sterilized Dutch custard (Stabilac, Campina, the Netherlands). The control suspension existed of maltodextrin dissolved according to the same method as the probiotic suspension. A daily amount of 200µl per animal was inserted into a custom made spoon. To guarantee the administration of a well-defined amount of probiotics, animals were separated by a cage divider during the consumption of the probiotic suspension. Average consumption time

was less than 15 minutes, after which the aforementioned cage divider was removed. Body weight, dietary intake and clinical symptoms were determined thrice weekly. Animals were sacrificed at the age of 8 weeks. Colonic tissue samples were excised immediately and either fixed in 4% (wt/vol) paraformaldehyde in phosphate-buffered saline (PBS), stored in RNAlater (Qiagen, Venlo, The Netherlands), at -20°C , or frozen in liquid nitrogen and stored at -80°C .

The animals in the three experimental groups will be referred to as WT NP and Muc2^{-/-} NP for animals that were fed the NP diet, WT P and Muc2^{-/-} P for animals that were fed the P diet and WT NP+PRO and Muc2^{-/-} NP+PRO for animals that were fed the NP diet supplemented with probiotics.

Histology

Tissue fixed in 4% (wt/vol) paraformaldehyde in PBS was prepared for light microscopy, and 4- μm -thick sections were stained with H&E. To detect differences in crypt length in the colon, 10 well-oriented crypts were chosen per intestinal segment and measured using calibrated Leica Application Suite software, version 3.2.0 (Leica Microsystems BV, Rijswijk, The Netherlands).

Immunohistochemistry

Sections were cut and prepared for immunohistochemistry as described previously²⁴ using the Vectastain Elite ABC kit (Vector Laboratories, Burlingame, CA) and 3,3'-diaminobenzidine as staining reagent. Antigen unmasking was carried out by heating the sections for 20 min in 0.01 M sodium citrate (pH 6.0; Merck, Darmstadt, Germany) at 100°C . CD3 ϵ -positive cells were detected using an anti-human CD3 ϵ antibody (DAKO, Heverlee, Belgium; 1:800 diluted in 1% bovine serum albumin, 0.1% Triton X-100 in PBS). As demonstrated by immunocytochemistry, this antibody cross-reacts with the CD3 ϵ -equivalent protein in mouse²⁵. Additionally, nonspecific binding was reduced by blocking with TENG-T (10 mmol/L Tris-HCl, 5 mmol/L EDTA, 150 mmol/L NaCl, 0.25% [wt/vol] gelatin, 0.05% [wt/vol] Tween 20). To detect S100a8 and S100a9, both known as cytosolic granulocyte proteins expressed in neutrophils and macrophages, anti-mouse S100a8 and anti-mouse S100a9 antibodies (R&D Systems Europe Ltd., Abingdon, United Kingdom) were used (1:1000 diluted in PBS). Muc4 was stained using an anti-human MUC4 rabbit-polyclonal antibody (hHA-1) that recognizes the AGYRPPRPAWTFGD amino acid sequence of the C-terminal peptidic region of MUC4 α subunit, which is homologous in humans and mice. The antibody was diluted 1:6000 in 1% BSA, 0.1% Triton X-100 in PBS.

Serum Cytokine Levels

Serum was obtained from coagulated blood collected by heart puncture and stored at -80°C until further analysis. The concentrations of several cytokines (Il-12p70, Tnf- α , interferon gamma (Ifn- γ), monocyte chemoattractant protein-1 (Mcp-1), Il-10 and Il-6) in serum were determined with a BD Cytometric Bead Array mouse inflammation kit (BD-Pharmingen, San Diego, CA, USA).

Quantitative Real-Time PCR (TaqMan Technology)

Total RNA was prepared using the RNeasy midi-kit (Qiagen, Venlo, the Netherlands) and 1.5 μ g was used to prepare cDNA. Cytokine mRNA expression levels as well as the housekeeping gene actin were quantified using real-time PCR (qRT-PCR) analysis (TaqMan chemistry) based upon the intercalation of SYBR Green on an ABI prism 7900 HT Fast Real Time PCR system (PE Applied Biosystems) as previously described.¹ All primer combinations were designed using OLIGO 6.22 software (Molecular Biology Insights) and purchased from Invitrogen. An overview of the primer sequences used is given in Table 1.

Table 1: primer sequences for quantitative real time PCR

gene	Forward primer	Reverse primer
Il-1 β	CCCCAACTGGTACATCA	AGAATGTGCCATGGTTTC
IL-6	CCCAACAGACCTGTCTAT	GGCAAATTCCTGATTAT
IL-10	CAA GCC TTA TCG GAA ATG	CAT GGC CTT GTA GAC ACC
Il-12 α (P35 subunit)	GCC TTG GTA GCA TCT ATG AG	TCG GCA TTA TGA TTC AGA GA
Il-12 β (P40 subunit)	CAC GGC AGC AGA ATA AAT A	GAG GGA GAA GTA GGA ATG G
Il-35 β (Ebi3 subunit)	CCC GGA CAT CTT CTC TCT	GAG GCT CCA GTC ACT TG
Tnf- α	TGGCCTCCCTCTCATC	GGCTGGCACCACCTAGTT
Ifn- γ	CGG CAC AGT CAT TGA AA	TGC CAG TTC CTC CAG AT
MCP-1	TGG GTC CAG ACA TAC ATT AAA A	GGG TCA ACT TCA CAT TCA AA
β -actin	GGG ACC TGA CGG ACT AC	TGC CAC AGG ATT CCA TAC

Statistical analysis

All data are expressed as median \pm SEM or median values. Statistical significance was assessed using the Mann-Whitney U test. (Prism, version 5.00; GraphPad software, San Diego, CA). The data were considered statistically significant at $P < 0.05$.

RESULTS

Type of diet and probiotic supplementation influence disease severity in *Muc2*^{-/-} mice.

Weight loss or growth retardation can be considered as one of the major clinical symptoms of colitis. At the age of 8 weeks, there was a significant difference in body weight between *Muc2*^{-/-} NP and WT NP mice (Figure 1A). Contrastingly, in mice that were fed the P diet, there was no difference between *Muc2*^{-/-} and WT mice. Probiotic supplementation

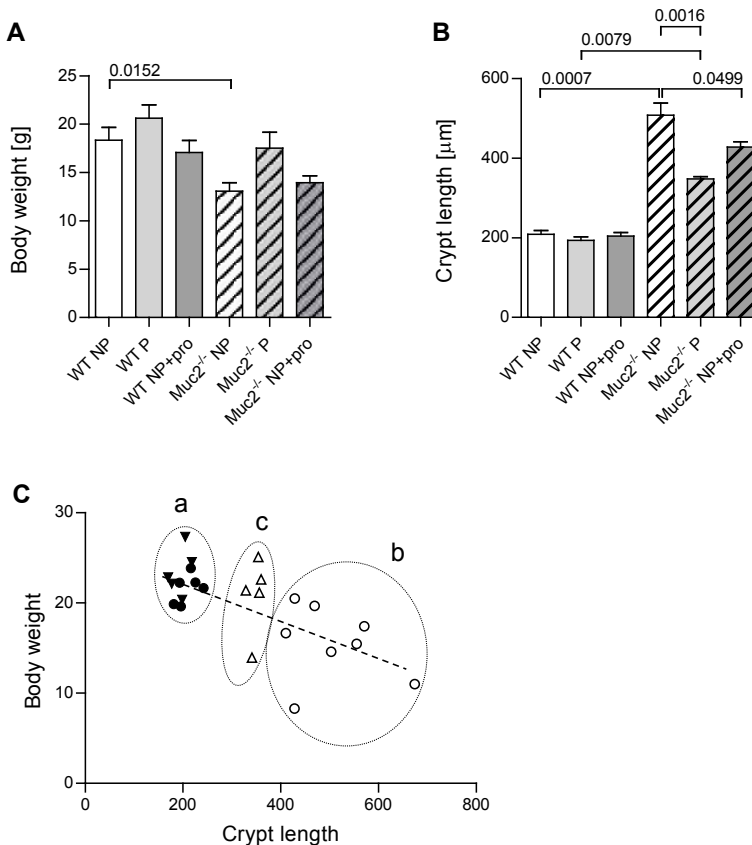


Figure 1. Effect of the type of diet and probiotic supplementation on growth and disease severity. Body weight (A) and crypt length (B) of wild type (WT) and *Muc2*^{-/-} mice in dietary subgroups are depicted as mean \pm SEM. (C) Crypt length (x-axis) significantly correlates with body weight (y-axis) ($R^2 = 0.4517$, $P = .0003$). Three subgroups can be distinguished: (a) all WT animals in which bodyweight and crypt length are not affected by the type of diet, (b) *Muc2*^{-/-} NP mice that displayed the highest disease severity reflected in the highest crypt length combined with the lowest bodyweight and (c) *Muc2*^{-/-} P mice that form an intermediate group displaying increased crypt length but bodyweights comparable with WT mice. Groups are depicted as \blacktriangledown : WT mice that were fed purified (P) diet, \triangle : *Muc2*^{-/-} mice that were fed the P diet, \bullet : WT that were fed the non-purified (NP) diet, \circ : *Muc2*^{-/-} mice that were fed the NP diet. (* $P < .05$, ** $P < .01$, # $P < .001$)

did not influence body weight in WT mice nor *Muc2*^{-/-} mice. Total daily consumption of pelleted food did not differ between WT and *Muc2*^{-/-} mice, nor between mice fed NP diet compared to P diet (data not shown).

As bodyweight is a non-specific, general disease marker, we measured crypt length as a site-specific marker for colitis severity. Similar to body weights, which were different between *Muc2*^{-/-} NP and WT NP mice, crypt lengths also differed significantly between *Muc2*^{-/-} NP and WT NP mice (Fig 1B). Specifically, *Muc2*^{-/-} NP mice showed increased crypt lengths compared with WT NP mice. Crypt lengths were also significantly increased in *Muc2*^{-/-} mice fed P diet in comparison with WT mice fed P diet. Furthermore, crypt length was significantly increased in *Muc2*^{-/-} NP mice compared to *Muc2*^{-/-} P mice. Finally, supplementation with probiotics significantly decreased crypt length in *Muc2*^{-/-} NP+PRO mice compared to *Muc2*^{-/-} NP mice. Linear regression analysis showed that there is a negative correlation between crypt length and body weight ($P < .0003$) (Figure 1C). Three subgroups can be distinguished: a) all WT animals in which bodyweight and crypt length are not affected by the type of diet, (b) *Muc2*^{-/-} NP mice that displayed the highest disease severity reflected in the highest crypt length combined with the lowest bodyweight and (c) *Muc2*^{-/-} P mice that form an intermediate group as these mice displayed increased crypt length but had bodyweights comparable with WT mice.

Increased Lymphocyte Infiltration and altered cytokine expression in *Muc2*^{-/-} NP mice

The observed differences between the previously described groups might be explained by an altered inflammatory status of the intestinal mucosa. Therefore, the influx of CD3ε-positive T-cells was studied as a marker for inflammation. In mice that were fed the NP diet, the amount of CD3ε-positive T-cells was increased in *Muc2*^{-/-} mice compared with WT mice (Fig. 2). Interestingly, NP-fed *Muc2*^{-/-} mice showed an increased influx of CD3ε-positive T cells compared to P-fed *Muc2*^{-/-} mice.

No differences in *Cd3ε* mRNA expression were seen upon treatment with probiotics (not shown). To study the increase of CD3ε-positive T-cells into further detail, gene expression levels of the pro-inflammatory cytokines *Tnf-α*, *Il1-β*, *Il-6*, *Ifn-γ*, and *Il-12* (heterodimer of p35 and p40), chemokine *Mcp-1* and anti-inflammatory cytokines *Il-10* and *Il-35* (heterodimer of p35 and *Ebi3*), were determined in the distal colon of *Muc2*^{-/-} mice (Fig. 3). The pro-inflammatory cytokines *Tnf-α*, *Il1β*, *Il-6*, and *Ifn-γ* and the chemokine *Mcp-1* were not differentially expressed in *Muc2*^{-/-} NP compared with *Muc2*^{-/-} P mice. Expression levels of the *Il-12* p35 subunit and *Ebi3* were significantly increased in *Muc2*^{-/-} P mice compared to *Muc2*^{-/-} NP mice. In contrast, expression of the *Il-12* p40 subunit was not significantly different between WT and *Muc2*^{-/-} mice.

Serum cytokine levels only showed significantly increased expression of *Tnf-α* protein in *Muc2*^{-/-} NP mice compared to *Muc2*^{-/-} P mice. All other serum cytokine levels

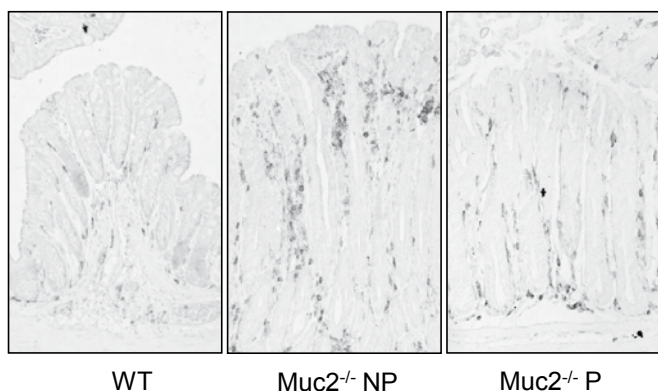


Figure 2. Influx of Cd3ε-positive T-cells

The extent of inflammation in the distal colon was assessed by immunohistochemistry for Cd3ε. Representative stained tissue samples for all groups are shown. Normal WT mice hardly show any Cd3ε-positive T-cells (left panel), whereas Muc2^{-/-} mice that were fed the non-purified (NP) diet show an increased amount of Cd3ε-positive T-cells that are localized along the complete crypt length, but also cluster together at the luminal side of the epithelium (middle panel). Muc2^{-/-} mice that were fed the purified (P) diet showed a decreased amount of Cd3ε-positive T-cells compared to Muc2^{-/-} NP mice, that was still increased compared to WT mice (right panel). Crypt lengthening in Muc2^{-/-} mice, as quantified in Fig. 2B, is evident when WT are compared with Muc2^{-/-} NP or Muc2^{-/-} P mice. (See Color Section, p. 242.)

(Il-12-p70, Mcp-1, Tnf-α, Ifn-γ and Il-6, Il-10) showed variable expression levels that were not significantly different between the different study groups (Figure 4).

Purified diet reduces expression of S100a8 and S100a9 and increases expression of Muc4 in Muc2^{-/-} mice

To assess the amount of mucosal damage, we performed immunohistochemistry for two S100 proteins, which are produced by neutrophils and macrophages, and are related to inflammation of the intestine, namely S100a8 and S100a9. Moreover, we studied the expression of Muc4 as a marker for epithelial damage. First, the numbers of both S100a8-positive cells (Fig. 5) and S100a9-positive cells (not shown) were increased in Muc2^{-/-} NP mice compared to Muc2^{-/-} P mice. No difference was observed in the number of S100a8-positive and S100a9-positive cells between Muc2^{-/-} mice that received probiotics and control mice. Contrastingly, the expression of Muc4 was decreased in Muc2^{-/-} NP mice compared to Muc2^{-/-} P mice. Like the S100 proteins, Muc4 expression was not different between Muc2^{-/-} NP+PRO and Muc2^{-/-} NP mice. Increased S100 protein expression and decreased Muc4 expression were seen in the areas where inflammation was the most severe.

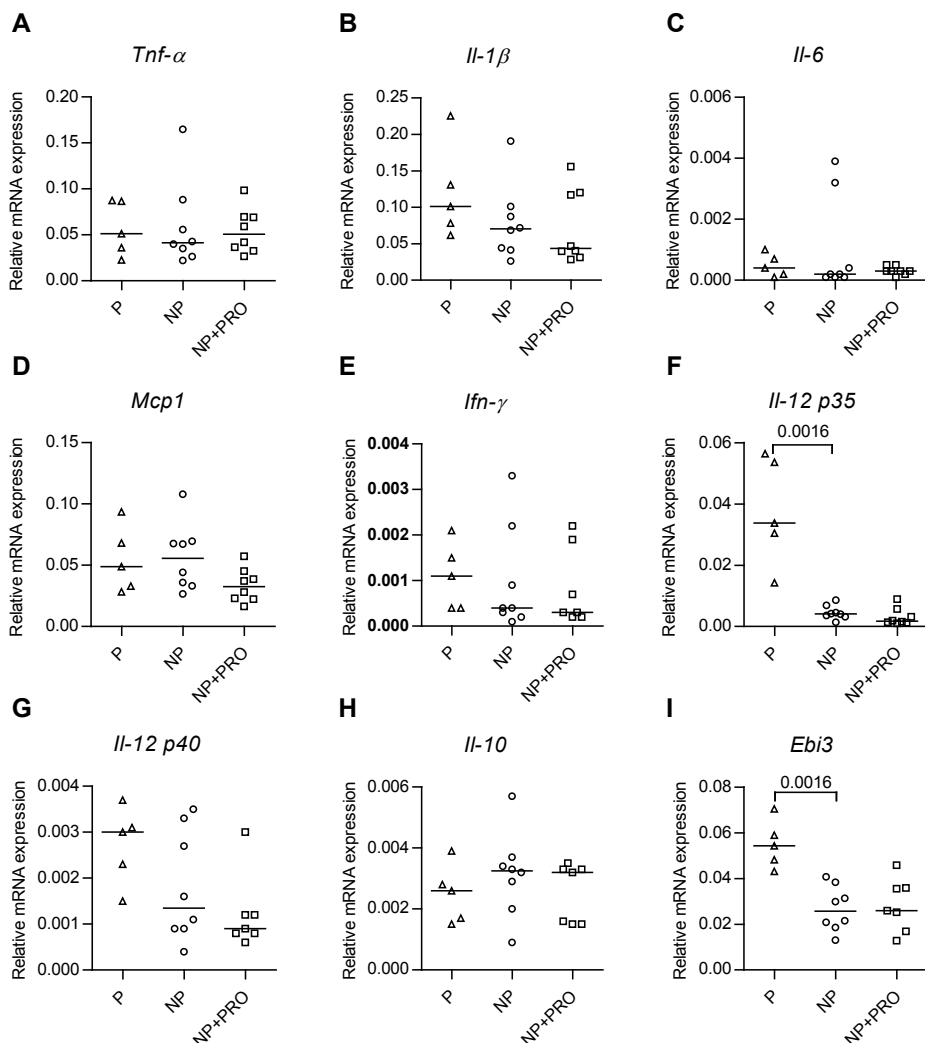


Figure 3. mRNA expression of (anti-)inflammatory cytokines in distal colon of *Muc2^{-/-}* mice in dietary subgroups

mRNA expression of inflammatory cytokines *Tnf-α* (A), *Il-1β* (B), *Il-6* (C), *Mcp-1* (D), *Ifn-γ* (E), and *Il-12 p35* (F) and *p40* (G) and anti-inflammatory cytokines *Il-10* (H) and *Ebi3* (I) in distal colonic tissue of *Muc2^{-/-}* mice that were fed a non-purified diet (NP), purified diet (P) or a non-purified diet supplemented with probiotics (NP+PRO). *Il-12 p35* and *Ebi3* mRNA expression were significantly increased in *Muc2^{-/-}* that were fed P-diet compared to the NP-diet. Gene expression levels were normalized for β -actin mRNA expression and depicted as median. Groups are depicted as Δ : *Muc2^{-/-}* mice that were fed the purified (P) diet, \circ : *Muc2^{-/-}* mice that were fed the non-purified (NP) diet, \square : *Muc2^{-/-}* mice that were fed the NP diet substituted with probiotics (NP+PRO)

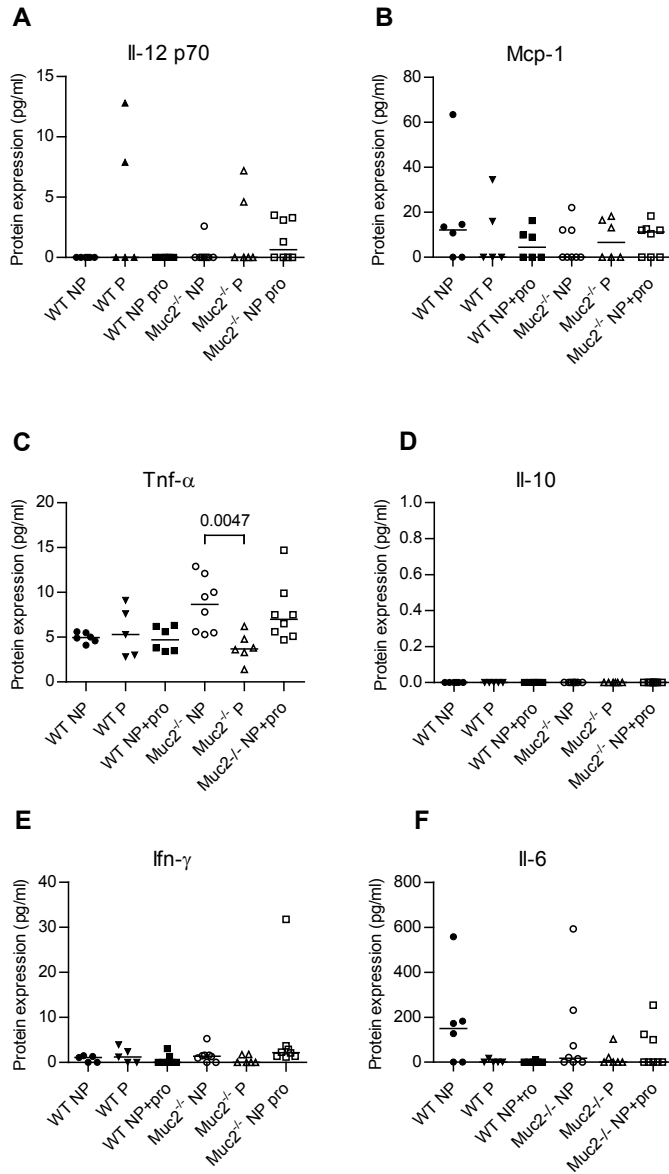


Figure 4. Protein expression of pro- and anti-inflammatory cytokines in serum of wild type and Muc2^{-/-} mice in dietary subgroups

Expression of serum cytokines Il-12 p70 (A), Mcp-1 (B), Tnf- α (C), Il-10 (D), Ifn- γ (E) and Il-6 (F) in ▼: WT mice that were fed purified (P) diet, △: Muc2^{-/-} mice that were fed the P diet, ●: WT that were fed the non-purified (NP) diet and ○: Muc2^{-/-} mice that were fed the NP diet, ■ WT mice that were fed the NP diet substituted with probiotics (NP+PRO) and □: Muc2^{-/-} mice that were fed the NP+PRO. Expression of the pro-inflammatory cytokine Tnf- α was significantly increased in serum of Muc2^{-/-} NP mice compared to Muc2^{-/-} P mice. Values are depicted as median.

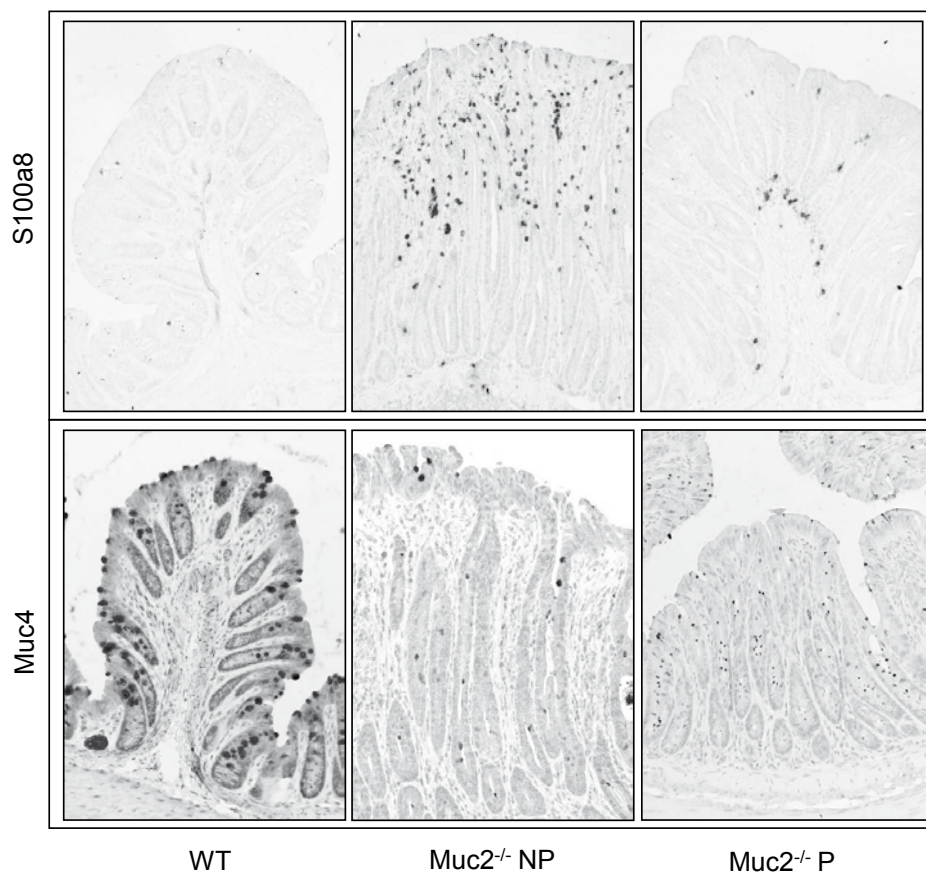


Figure 5. Expression and localization of S100a8 and Muc4 protein in Muc2^{-/-} mice. Expression of S100a8 (upper panels) and Muc4 (lower panels) is depicted in WT (left panel), Muc2^{-/-} mice that were fed the non-purified NP diet (middle panel) and Muc2^{-/-} mice that were fed the purified (P) diet (right panel). The tissue samples are representative for all mice in the studied groups. Note that the expression of S100a8 is increased in Muc2^{-/-} mice compared to WT mice. Moreover, Muc2^{-/-} NP showed increased amounts of S100a8-positive cells compared to Muc2^{-/-} P mice. For Muc4, expression was decreased in Muc2^{-/-} compared to WT mice and with a more pronounced decrease in Muc2^{-/-} NP mice compared to Muc2^{-/-} P mice.

DISCUSSION

The present study investigates the effect of two different diets and probiotic supplementation on colitis-severity in Muc2^{-/-} mice. We demonstrate that a purified diet decreases disease severity in Muc2^{-/-} mice and therefore the choice of diet plays a crucial role in this colitis model.

Beneficial effects of the purified diet reflected in increased body weight combined with decreased crypt length in Muc2^{-/-} P mice, indicating that the purified diet reduces

disease severity in Muc2^{-/-} mice. As bodyweight and crypt length in WT mice were not affected by the type of diet, the quality of the diet seems to be particularly important in case of disease, more specifically colitis in Muc2^{-/-} mice. Overall, digestibility of the purified diet seems to be more efficient compared to the non-purified diet, resulting in increased availability of nutrients needed for growth, as reflected in increased body weight in Muc2^{-/-} P mice.

Two major differences exist between the two diets used in this study, which might explain the observed difference in disease severity in Muc2^{-/-} mice. First, protein content in the NP diet mainly consists of plant proteins, whereas casein is the main protein source in the purified diet. Although protein composition does not influence the effectiveness of enteral nutrition in the treatment of active adult Crohn's disease²⁶, a beneficial effect of a casein-based diet in pediatric Crohn's disease has been proposed.^{8,27-28} Second, the amount of insoluble fiber is considerably higher in the NP diet. Bacterial fermentation of insoluble fiber in the proximal colon is less compared to soluble fiber, and thereby limits the amounts of short chain fatty acids (SCFAs) that are produced.²⁹⁻³⁰ The protective effect of butyrate, one of the major SCFAs, has been described by several authors, as reviewed by Hamer et al.³¹ Interestingly, butyrate has an anti-inflammatory effect, which is exerted by suppression of nuclear factor kappa B (NF-κB) activation.³² Colonic contents form a nutrient source for bacteria in the colon and therefore presumably lead to differences in the composition of the microbiota and SCFA production between the two dietary subgroups. Therefore, differences in intestinal inflammation between Muc2^{-/-} NP and Muc2^{-/-} P mice might be related to the amount of SCFAs, more specifically butyrate, that are produced. Finally, insoluble fiber has a more pronounced laxative effect compared to soluble fiber³⁰, consequently accelerating small bowel transit. This might increase symptoms of diarrhea that already exist in Muc2^{-/-} mice, regardless of the diet. To further elucidate the effect of specific proteins and the type of fibre on colitis severity in Muc2^{-/-} mice, diets that differ in their protein and fiber content need to be studied into further detail. However, from the current study it is clear that the diet needs to be thoroughly considered in the experimental design as it might significantly influence the disease model.

The mechanisms through which probiotics may exert their potential beneficial effects are still largely unknown. We demonstrate that probiotic supplementation leads to a decreased crypt length in Muc2^{-/-} mice. As probiotics can influence cytokine expression³³⁻³⁶ and we previously showed that *Tnf-α* and *IL-1β* are up-regulated in Muc2^{-/-} mice¹, we hypothesized that probiotic supplementation might restore the disbalanced cytokine profile in Muc2^{-/-} mice and thereby limit disease severity. However, although crypt length was decreased in Muc2^{-/-} NP+PRO mice compared to Muc2^{-/-} NP mice, the abundance of Cd3ε-positive T-cells as well as cytokine expression levels were not different between these mice. Our findings suggest that probiotics might directly influence epithelial

proliferation of the intestinal epithelial cells and thereby limit excessive proliferation as seen in *Muc2*^{-/-} mice that were fed the NP diet without probiotic supplementation. Yet, as probiotics did not restore the disbalance in cytokine expression levels in *Muc2*^{-/-} NP+PRO mice, disease severity is most likely not limited by the probiotics used in this study. This is in line with the fact that not all probiotic strains have an effect on cytokine expression, let alone have the same effect on the immune system. Interestingly, differing immunological effects have been reported even within the same species of bacteria.³⁷⁻³⁸

Several inflammation markers, namely the reduced influx of Cd3ε-positive cells, increased serum Tnf-α levels, and the limited mucosal expression of S100a8 and S100a9 proteins indicate that inflammation is significantly reduced in *Muc2*^{-/-} mice that were fed P diet compared to *Muc2*^{-/-} mice that were fed the NP diet. Interestingly, serum cytokine levels only showed significant increased Tnf-α levels in *Muc2*^{-/-} NP mice compared to *Muc2*^{-/-} P mice. Tnf-α mRNA levels in the distal colon of *Muc2*^{-/-} mice were not affected by the type of diet, neither by probiotic supplementation. All other serum cytokines were not affected. Therefore, systemic Tnf-α levels can be regarded as a general marker for colitis in *Muc2*^{-/-} mice.

Of all cytokines studied in the distal colon, only Il-12 related cytokines showed differences between the studied diets. The interleukin-12 cytokine family includes IL-12, IL-23, IL-27, and the recently identified IL-35.³⁹ All four are heterodimeric cytokines, composed of an α-chain (p19, p28, or p35) and a β-chain (p40 or Ebi3). IL-12 and IL-23 are highly expressed in the gut of mice and patients with inflammatory bowel diseases.⁴⁰⁻⁴¹ IL-12, which consists of a heterodimer of a p35 and a p40 subunit, is known as a pro-inflammatory cytokine, whereas IL-35, the heterodimer of p35 and Ebi3 is linked to regulatory T-cells and possesses immune suppressive capacities. As IL-12 p40 also showed a trend towards increased levels in *Muc2*^{-/-} mice that were fed the P-diet, together with significantly increased levels of IL-12 p35, might indicate increased pro-inflammatory IL-12 expression. However, *Muc2*^{-/-} P mice do not show increased colitis severity. On the contrary, *Muc2*^{-/-} mice fed the P diet showed a decrease in colitis severity compared to *Muc2*^{-/-} mice fed the NP diet. Given that Ebi3 is also significantly increased in *Muc2*^{-/-} mice fed the P-diet, the above described data are in favor of increased IL-35 production (i.e. heterodimer formation of Ebi3 and IL12p35). As IL-35 is known as an immune suppressive cytokine, increased IL-35 levels would also explain the decreased disease severity in *Muc2*^{-/-} mice that were fed the P-diet compared to *Muc2*^{-/-} mice that were fed the NP-diet. Yet, further studies are necessary to confirm whether the P diet indeed increases IL35 levels in *Muc2*^{-/-} mice.

Highest numbers of S100a8- and S100a9-positive cells were observed in *Muc2*^{-/-} NP mice (Fig. 5). Interestingly these mice also showed the highest disease severity as reflected by lowest body weights and highest increase in crypt lengthening (Fig. 1C). Therefore, the S100 proteins can be regarded as indicators for the degree of colonic

inflammation in Muc2^{-/-} mice.. In accordance with our findings, fecal calprotectin, the heterodimer of S100a8 and S100a9, is regarded as a marker for inflammation in the gastrointestinal tract, and has been used clinically to follow disease activity in IBD.⁴²⁻⁴³

Immunohistochemical staining for Muc4 revealed that abundance of Muc4-positive cells is decreased in Muc2^{-/-} NP mice compared to Muc2^{-/-} P mice. This finding corresponds with previous studies that show decreased numbers of Muc4-positive goblet cells in adult Muc2^{-/-} mice and decreased Muc4 protein expression in patients with CD.⁴⁴⁻⁴⁵ Interestingly, the areas with the highest abundance of S100a8-positive cells showed the lowest numbers of Muc4-positive cells. We recently showed that Muc4 protein is localized in the intestinal goblet cell⁴⁶, implying that Muc4 is not only a membrane bound mucin, but also a secretory mucin in the mouse intestine. Increased secretion of Muc4 in Muc2^{-/-} mice that were fed the NP diet might therefore explain the decreased number of Muc4-positive cells in these mice compared to Muc2^{-/-} mice fed the P diet. Speculating, increased secretion of Muc4 might be caused by a greater need for Muc4 secretion to compensate for Muc2-deficiency in Muc2^{-/-} NP mice. In Muc2^{-/-} P mice the need for this compensatory Muc4 secretion is less as the diet ameliorates colitis-symptoms, and therefore Muc4 protein remains stored in the goblet cell granules of these mice.

In summary, the type of diet significantly influences disease severity, as measured by differences in bodyweight and crypt lengths, in the Muc2^{-/-} colitis model. Secondly, supplementation of the NP diet with probiotics limited crypt lengthening in Muc2^{-/-} mice compared to Muc2^{-/-} mice fed the NP diet only. Compared to Muc2^{-/-} mice fed NP diet, Muc2^{-/-} mice fed the P diet showed a reduced influx of Cd3ε-positive cells that was accompanied by differences in Il-12 related cytokines. These data point to an immune suppressive effect of the P diet, most likely by means of increased Il-35 production. Moreover, a systemic increase of Tnf-α was seen in Muc2^{-/-} mice fed the NP diet, which was not seen in Muc2^{-/-} mice fed the P diet. Finally, mucosal inflammatory markers S100a8 and S100a9 and the epithelial damage marker Muc4 showed that histological signs of colitis are significantly increased in Muc2^{-/-} mice that were fed the NP diet compared to the P diet. The above described differences, namely decreased growth retardation, reduced crypt lengthening and decreased inflammation markers in Muc2^{-/-} P mice compared to Muc2^{-/-} NP mice might be explained by the type of protein and the type and amount of fibers in the diet. In conjunction, these data imply that feeding strategy in subjects with colitis might have considerable implications for disease severity.

ACKNOWLEDGEMENT

This work was supported by Danone Research (Friedrichsdorf, Germany).

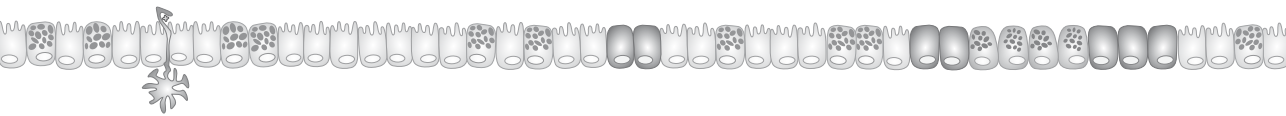
REFERENCES

1. Van der Sluis M, De Koning BA, De Bruijn AC, Velcich A, Meijerink JP, Van Goudoever JB, Buller HA, Dekker J, Van Seuningen I, Renes IB, Einerhand AW. Muc2-deficient mice spontaneously develop colitis, indicating that MUC2 is critical for colonic protection. *Gastroenterology* 2006;131:117-29.
2. Pullan RD, Thomas GA, Rhodes M, Newcombe RG, Williams GT, Allen A, Rhodes J. Thickness of adherent mucus gel on colonic mucosa in humans and its relevance to colitis. *Gut* 1994;35:353-9.
3. Tytgat KM, van der Wal JW, Einerhand AW, Buller HA, Dekker J. Quantitative analysis of MUC2 synthesis in ulcerative colitis. *Biochem Biophys Res Commun* 1996;224:397-405.
4. Jacobs LR, Huber PW. Regional distribution and alterations of lectin binding to colorectal mucin in mucosal biopsies from controls and subjects with inflammatory bowel diseases. *J Clin Invest* 1985;75:112-8.
5. Schaart MW, de Bruijn AC, Bouwman DM, de Krijger RR, van Goudoever JB, Tibboel D, Renes IB. Epithelial Functions of the Residual Bowel After Surgery for Necrotising Enterocolitis in Human Infants. *J Pediatr Gastroenterol Nutr* 2009.
6. Dziechciarz P, Horvath A, Shamir R, Szajewska H. Meta-analysis: enteral nutrition in active Crohn's disease in children. *Aliment Pharmacol Ther* 2007;26:795-806.
7. Heuschkel RB, Menache CC, Megerian JT, Baird AE. Enteral nutrition and corticosteroids in the treatment of acute Crohn's disease in children. *J Pediatr Gastroenterol Nutr* 2000;31:8-15.
8. Fell JM, Paintin M, Arnaud-Battandier F, Beattie RM, Hollis A, Kitching P, Donnet-Hughes A, MacDonald TT, Walker-Smith JA. Mucosal healing and a fall in mucosal pro-inflammatory cytokine mRNA induced by a specific oral polymeric diet in paediatric Crohn's disease. *Aliment Pharmacol Ther* 2000;14:281-9.
9. Bannerjee K, Camacho-Hubner C, Babinska K, Dryhurst KM, Edwards R, Savage MO, Sanderson IR, Croft NM. Anti-inflammatory and growth-stimulating effects precede nutritional restitution during enteral feeding in Crohn disease. *J Pediatr Gastroenterol Nutr* 2004;38:270-5.
10. de Jong NS, Leach ST, Day AS. Polymeric formula has direct anti-inflammatory effects on enterocytes in an in vitro model of intestinal inflammation. *Dig Dis Sci* 2007;52:2029-36.
11. Yamamoto T, Nakahigashi M, Saniabadi AR, Iwata T, Maruyama Y, Umegae S, Matsumoto K. Impacts of long-term enteral nutrition on clinical and endoscopic disease activities and mucosal cytokines during remission in patients with Crohn's disease: a prospective study. *Inflamm Bowel Dis* 2007;13:1493-501.
12. Guzy C, Schirbel A, Paclik D, Wiedenmann B, Dignass A, Sturm A. Enteral and parenteral nutrition distinctively modulate intestinal permeability and T cell function in vitro. *Eur J Nutr* 2009;48:12-21.
13. Leach ST, Mitchell HM, Eng WR, Zhang L, Day AS. Sustained modulation of intestinal bacteria by exclusive enteral nutrition used to treat children with Crohn's disease. *Aliment Pharmacol Ther* 2008;28:724-33.
14. Noerr B. Current controversies in the understanding of necrotizing enterocolitis. Part 1. *Adv Neonatal Care* 2003;3:107-20.
15. Schanler RJ, Lau C, Hurst NM, Smith EO. Randomized trial of donor human milk versus preterm formula as substitutes for mothers' own milk in the feeding of extremely premature infants. *Pediatrics* 2005;116:400-6.

16. Gibson GR, Roberfroid MB. Dietary modulation of the human colonic microbiota: introducing the concept of prebiotics. *J Nutr* 1995;125:1401-12.
17. Rolfe VE, Fortun PJ, Hawkey CJ, Bath-Hextall F. Probiotics for maintenance of remission in Crohn's disease. *Cochrane Database Syst Rev* 2006:CD004826.
18. Mallon P, McKay D, Kirk S, Gardiner K. Probiotics for induction of remission in ulcerative colitis. *Cochrane Database Syst Rev* 2007:CD005573.
19. Deshpande G, Rao S, Patole S, Bulsara M. Updated Meta-analysis of Probiotics for Preventing Necrotizing Enterocolitis in Preterm Neonates. *Pediatrics* 2010.
20. Roselli M, Finamore A, Nuccitelli S, Carnevali P, Brigidi P, Vitali B, Nobili F, Rami R, Garaguso I, Mengheri E. Prevention of TNBS-induced colitis by different *Lactobacillus* and *Bifidobacterium* strains is associated with an expansion of gammadeltaT and regulatory T cells of intestinal intraepithelial lymphocytes. *Inflamm Bowel Dis* 2009;15:1526-36.
21. Chen CC, Chiu CH, Lin TY, Shi HN, Walker WA. Effect of probiotics *Lactobacillus acidophilus* on *Citrobacter rodentium* colitis: the role of dendritic cells. *Pediatr Res* 2009;65:169-75.
22. Mahler M, Leiter EH. Genetic and environmental context determines the course of colitis developing in IL-10-deficient mice. *Inflamm Bowel Dis* 2002;8:347-55.
23. Velcich A, Yang W, Heyer J, Fragale A, Nicholas C, Viani S, Kucherlapati R, Lipkin M, Yang K, Augenlicht L. Colorectal cancer in mice genetically deficient in the mucin *Muc2*. *Science* 2002;295:1726-9.
24. Verburg M, Renes IB, Meijer HP, Taminiau JA, Buller HA, Einerhand AW, Dekker J. Selective sparing of goblet cells and paneth cells in the intestine of methotrexate-treated rats. *Am J Physiol Gastrointest Liver Physiol* 2000;279:G1037-47.
25. Jones M, Cordell JL, Beyers AD, Tse AG, Mason DY. Detection of T and B cells in many animal species using cross-reactive anti-peptide antibodies. *J Immunol* 1993;150:5429-35.
26. Zachos M, Tondeur M, Griffiths AM. Enteral nutritional therapy for inducing remission of Crohn's disease. *Cochrane Database Syst Rev* 2001:CD000542.
27. Jones S, Shannon H, Srivastava E, Haboubi N. A novel approach to a patient with Crohn disease and a high stoma output: a missed opportunity? *Scand J Gastroenterol* 2004;39:398-400.
28. Donnet-Hughes A, Duc N, Serrant P, Vidal K, Schiffrin EJ. Bioactive molecules in milk and their role in health and disease: the role of transforming growth factor-beta. *Immunol Cell Biol* 2000;78:74-9.
29. Floch MH, Narayan R. Diet in the irritable bowel syndrome. *J Clin Gastroenterol* 2002;35: S45-52.
30. Spiller RC. Pharmacology of dietary fibre. *Pharmacol Ther* 1994;62:407-27.
31. Hamer HM, Jonkers D, Venema K, Vanhoutvin S, Troost FJ, Brummer RJ. Review article: the role of butyrate on colonic function. *Aliment Pharmacol Ther* 2008;27:104-19.
32. Andoh A, Fujiyama Y, Hata K, Araki Y, Takaya H, Shimada M, Bamba T. Counter-regulatory effect of sodium butyrate on tumour necrosis factor-alpha (TNF-alpha)-induced complement C3 and factor B biosynthesis in human intestinal epithelial cells. *Clin Exp Immunol* 1999;118: 23-9.
33. Chen CC, Kong MS, Lai MW, Chao HC, Chang KW, Chen SY, Huang YC, Chiu CH, Li WC, Lin PY, Chen CJ, Li TY. Probiotics have clinical, microbiologic, and immunologic efficacy in acute infectious diarrhea. *Pediatr Infect Dis J* 2010;29:135-8.
34. Pagnini C, Saeed R, Bamias G, Arseneau KO, Pizarro TT, Cominelli F. Probiotics promote gut health through stimulation of epithelial innate immunity. *Proc Natl Acad Sci U S A* 2010;107: 454-9.

35. Foligne B, Nutton S, Grangette C, Dennin V, Goudercourt D, Poiret S, Dewulf J, Brassart D, Mercenier A, Pot B. Correlation between in vitro and in vivo immunomodulatory properties of lactic acid bacteria. *World J Gastroenterol* 2007;13:236-43.
36. He F, Morita H, Hashimoto H, Hosoda M, Kurisaki J, Ouwehand AC, Isolauri E, Benno Y, Salminen S. Intestinal Bifidobacterium species induce varying cytokine production. *J Allergy Clin Immunol* 2002;109:1035-6.
37. Medina M, Izquierdo E, Ennahar S, Sanz Y. Differential immunomodulatory properties of Bifidobacterium logum strains: relevance to probiotic selection and clinical applications. *Clin Exp Immunol* 2007;150:531-8.
38. Lopez P, Gueimonde M, Margolles A, Suarez A. Distinct Bifidobacterium strains drive different immune responses in vitro. *Int J Food Microbiol* 2010;138:157-65.
39. Collision LW, Workman CJ, Kuo TT, Boyd K, Wang Y, Vignali KM, Cross R, Sehý D, Blumberg RS, Vignali DA. The inhibitory cytokine IL-35 contributes to regulatory T-cell function. *Nature* 2007;450:566-9.
40. Monteleone G, Biancone L, Marasco R, Morrone G, Marasco O, Luzzza F, Pallone F. Interleukin 12 is expressed and actively released by Crohn's disease intestinal lamina propria mononuclear cells. *Gastroenterology* 1997;112:1169-78.
41. Parronchi P, Romagnani P, Annunziato F, Sampognaro S, Becchio A, Giannarini L, Maggi E, Pupilli C, Tonelli F, Romagnani S. Type 1 T-helper cell predominance and interleukin-12 expression in the gut of patients with Crohn's disease. *Am J Pathol* 1997;150:823-32.
42. Roseth AG, Aadland E, Jahnsen J, Raknerud N. Assessment of disease activity in ulcerative colitis by faecal calprotectin, a novel granulocyte marker protein. *Digestion* 1997;58:176-80.
43. Bunn SK, Bisset WM, Main MJ, Golden BE. Fecal calprotectin as a measure of disease activity in childhood inflammatory bowel disease. *J Pediatr Gastroenterol Nutr* 2001;32:171-7.
44. Buisine MP, Desreumaux P, Debailleul V, Gambiez L, Geboes K, Ectors N, Delescaut MP, Degand P, Aubert JP, Colombel JF, Porchet N. Abnormalities in mucin gene expression in Crohn's disease. *Inflamm Bowel Dis* 1999;5:24-32.
45. Buisine MP, Desreumaux P, Leteurtre E, Copin MC, Colombel JF, Porchet N, Aubert JP. Mucin gene expression in intestinal epithelial cells in Crohn's disease. *Gut* 2001;49:544-51.
46. Jonckheere N, Van Der Sluis M, Velghe A, Buisine MP, Suttmüller M, Ducourouble MP, Pigny P, Buller HA, Aubert JP, Einerhand AW, Van Seuningen I. Transcriptional activation of the murine Muc5ac mucin gene in epithelial cancer cells by TGF-beta/Smad4 signalling pathway is potentiated by Sp1. *Biochem J* 2004;377:797-808.

Chapter 9



Intestinal threonine uptake routes for mucin synthesis in preterm pigs and infants

Patrycja J. Puiman, **Nanda Burger-van Paassen**, Barbara Stoll, Adrianus C.J.M. de Bruijn, Kristien Dorst, Henk Schierbeek, Per T. Sangild, Günther Boehm, Ingrid B. Renes, Johannes B. van Goudoever

Manuscript in preparation



ABSTRACT

Mucin MUC2 is the major secretory mucin synthesized by goblet cells. We previously showed that systemic/ arterial threonine is rapidly incorporated into small intestinal MUC2 of preterm infants. However, it is unknown whether goblet cells are capable of using luminal threonine for MUC2 synthesis. We hypothesized that enteral threonine would preferentially be used over basolateral threonine for MUC2 synthesis, underlining the importance of enteral nutrition in the preterm neonate. We determined the preferential site of threonine absorption for MUC2 synthesis in preterm pigs (n=12) and preterm infants with ileostomies (n=5). We conducted a dual-isotope tracer infusion, allowing incorporation of both enteral and systemic threonine isotope tracers into collected MUC2. Threonine from both the basolateral and luminal side was used for MUC2 synthesis in preterm infants and preterm pigs. Preterm pigs showed higher MUC2 synthesis rates than the preterm infants recovering from intestinal disease and surgery. In preterm pigs, colostrum feeding (n=6) stimulated threonine uptake for MUC2 synthesis from the luminal vs. the basolateral side, and increased MUC2 fractional synthesis rate when compared to formula feeding (n=6) (177 ± 17 vs. $121 \pm 17\%/d$ respectively). First we concluded that goblet cells use of both luminal and basolateral threonine for synthesis of MUC2. Second, colostrum feeding stimulated MUC2 synthesis while increasing threonine absorption from the luminal side. Collectively, colostrum feeding of preterm pigs may enhance gut barrier function via stimulation of luminal threonine uptake for MUC2 synthesis.

Key words: preterm, neonate, formula, nutrition, mucin

INTRODUCTION

The neonatal gut is in need of threonine to synthesize mucins necessary for epithelial protection. The mucin MUC2 is the most predominant secretory mucin in the human intestinal tract synthesized by goblet cells.¹⁻³ The peptide backbone of MUC2 is particularly rich in threonine constituting ~30% of the total amino acids.⁴⁻⁸ Hence, it is not surprising that threonine availability impacts mucosal protein and mucin synthesis in pigs and rats.⁹⁻¹²

A diminished or disrupted mucus layer causes intestinal inflammation and mucosal eruption, facilitating bacterial translocation and, in combination with an immature immune system, renders the preterm infant at particular risk for the development of sepsis and necrotizing enterocolitis (NEC).¹³ Therefore, adequate threonine uptake by the mucin producing cells is pivotal for prevention of NEC. Intestinal mucosal cells are unique among body cells in that they are presented with substantial quantities of threonine from both the diet and the mesenteric arterial circulation. However, it is unknown whether goblet cells, known to be secretory cells, are able to use enteral substrates like enterocytes do, or whether they are dependent on basolateral absorption as site of mucin precursor uptake.

In preterm neonates, the splanchnic tissues extract 70-82% of dietary threonine.¹⁴ In infants pigs, the intestine is responsible for >70% of splanchnic first-pass metabolism and there is continuous removal of arterial amino acids by the portal-drained viscera which appear to be channeled towards mucosal constitutive protein synthesis.¹⁵⁻¹⁶ A recent study showed that arterial threonine is incorporated rapidly into small intestinal MUC2 of partially enteral fed preterm infants following bowel resection for NEC.¹⁷ However, this study could not determine whether there is a preference for luminal or arterial threonine for MUC2 synthesis. This is of importance for the preterm neonate at risk for NEC when enteral feeding is withheld or delayed. The lack of luminal nutrients, in particular threonine may decrease MUC2 synthesis and hence gut barrier function.

We hypothesized that enteral threonine would preferentially be used over arterial threonine for MUC2 synthesis by goblet cells, underlining the importance of enteral nutrition in the preterm neonate. We conducted a dual-isotope tracer infusion in preterm pigs and preterm infants, allowing incorporation of both enteral and systemic threonine isotope tracers into MUC2. To be able to compare porcine and human MUC2, our first aim was to isolate and identify porcine MUC2 and determine its homology to human MUC2. Our second aim was to determine the preferential site of threonine absorption for MUC2 synthesis in preterm pigs fed formula or colostrum, and in preterm infants with ileostomies.

MATERIALS AND METHODS

Materials

Stable isotopes of L-threonine (thr) [^{15}N]thr (98 atom%) and [$\text{U-}^{13}\text{C}$]thr (99.5 atom%) were purchased from Cambridge Isotope Laboratories, Andover, Massachusetts. All isotopes were tested and found sterile and pyrogen free.

Preterm pigs

Preterm pigs (Danish landrace X Yorkshire) were delivered via cesarean section at day 105 - 107 of gestation, as described in detail previously.¹⁸ Animal protocols and procedures were approved by the Danish National Committee on Animal Experimentation. Total parenteral nutrition (TPN) was administered for the first 2 days as described previously.¹⁸ After 48 h, TPN was discontinued and the pigs were assigned to receive either human milk formula (FORM, $n=6$) or bovine colostrum feeding (COL, $n=6$) via an orogastric tube ($15 \text{ ml} \cdot \text{kg}^{-1} \cdot 3 \text{ h}^{-1}$) for 2 days. The milk formula consisted of a mix of three different commercial formula's for human infants as described previously to meet protein and energy requirements.¹⁸ Bovine colostrum was derived from the first milking of Holstein-Friesian cows and irradiated ($1 \times \text{kGy}$) before use. To make the diets isocaloric, the colostrum was diluted with water in a 2:1 ratio. An aliquot of the diluted colostrum was assayed for protein content using Pierce assay (BCA, Protein Assay, Thermo scientific, Rockford, USA). The threonine concentration of both formula and colostrum were determined using gas chromatography-mass spectrometry. An aliquot of colostrum and formula was hydrolyzed for 24 h at 110°C in 6 mol/L HCl and dried (Speedvac Savant, Thermofisher, Breda, the Netherlands). Samples were then derivatized and analyzed using the same method as that for tissue samples (below).

Isotope infusion protocol. After completion of the feeding protocol piglets received a dual- isotope tracer infusion for 9 h. A primed ($25 \mu\text{mol} \cdot \text{kg}^{-1}$), continuous ($25 \mu\text{mol} \cdot \text{kg}^{-1} \cdot \text{h}^{-1}$) infusion of [$\text{U-}^{13}\text{C}$]thr was administered through the arterial catheter. Simultaneously, a primed ($25 \mu\text{mol} \cdot \text{kg}^{-1}$), hourly bolus ($25 \mu\text{mol} \cdot \text{kg}^{-1} \cdot \text{h}^{-1}$) of [^{15}N]thr was administered via the orogastric tube. During this protocol, piglets were switched to 1-h feeding intervals. Blood samples were taken at 0, 6, 8.5, and 9 h after start of the tracer infusion for mass spectrometry analyses. Blood samples were centrifuged immediately and the plasma fraction was stored at -80°C until further analysis. After the 9h-infusion protocol, piglets were euthanized with an overdose of pentobarbital (200 mg/kg iv; LIFE Faculty pharmacy, University of Copenhagen, Denmark).

Tissue collection. Immediately after animals were killed, the entire small intestine (SI) and colon were removed as described in detail previously.¹⁸ The small intestine length was divided into three segments, which were designated proximal, middle, and distal SI.

Tissue samples were frozen in liquid nitrogen and stored at -80°C . Mucosal scraping of the last 10 cm of the distal SI was frozen in liquid nitrogen for MUC2 analysis (below).

Preterm infants

The study was conducted at Erasmus MC-Sophia Children's Hospital (Rotterdam, the Netherlands) after approval from the Erasmus MC Institutional Review Board. Written informed consent was obtained from the parents. Infants who had a bowel resection in the neonatal period and received a temporary ileostomy during surgery were eligible for this study. Exclusion criterion for this study was cystic fibrosis. We included five infants in the study that underwent surgery for NEC ($n=2$), milk curd obstruction ($n=1$), midgut volvulus ($n=1$), and meconium ileus ($n=1$). Table 1 lists their main clinical characteristics.

Isotope infusion protocol. The study was performed when the infants were clinically stable, i.e. 24 ± 4 days following bowel resection, and received partial enteral nutrition. Then, a primed ($10.5 \mu\text{mol}\cdot\text{kg}^{-1}$), continuous 12-h infusion ($10.5 \mu\text{mol}\cdot\text{kg}^{-1}\cdot\text{h}^{-1}$) of [$U-^{13}\text{C}$]thr was administered intravenously. Simultaneously, a primed ($21 \mu\text{mol}\cdot\text{kg}^{-1}$), hourly bolus ($21 \mu\text{mol}\cdot\text{kg}^{-1}\cdot\text{h}^{-1}$) of [^{15}N]thr was administered via the nasogastric tube. At baseline, after 9 h, and 12 h of tracer administration, blood samples were collected by heel stick. Blood was centrifuged immediately and the plasma was stored at -80°C . Beginning at the start of the isotope infusion, ileostomy outflow fluid samples were collected at 3-h intervals for 36 h for MUC2 isolation and stored at -80°C .

Table 1. Demographics and enteral threonine intake of preterm infants

Patient	Sex	GA (wk)	BW (g)	AS (d)	AI (d)	Type of enteral feeding	Enteral intake ($\text{ml}\cdot\text{kg}^{-1}\cdot\text{h}^{-1}$)	Enteral threonine intake ($\mu\text{mol}\cdot\text{kg}^{-1}\cdot\text{h}^{-1}$)	Parenteral intake ($\text{ml}\cdot\text{kg}^{-1}\cdot\text{h}^{-1}$)	Parenteral threonine intake ($\mu\text{mol}\cdot\text{kg}^{-1}\cdot\text{h}^{-1}$)
1	F	34.6	2345	1	31	MM + NPI	2.2	10.1	1.0	31.5
2	M	27.9	1130	15	34	Nen 15.4%	3.8	31.9	0.5	16.0
3	M	25.6	865	22	40	Nen 16.5%	4.3	45.3	0.8	25.1
4	M	25.6	755	22	59	MM + BMF	4.4	33.6	0.5	15.8
5	F	33.0	1460	10	28	MM + BMF	4.6	35.3	0.4	12.4

GA gestational age; BW birth weight; AS age at surgery; AI age at isotope infusion; MM mother's milk; NPI1 nutrilon premium 1 13.5% (Nutricia, Zoetermeer, the Netherlands); Nen neonatal (Nutricia); BMF breast milk fortifier 4.2% (Nutricia). Parenteral intake: Primene 10% (Baxter, Utrecht, the Netherlands).

Mucin MUC2 isolation

MUC2 isolation was performed using a cesium chloride (CsCl) density gradient ultracentrifugation method combined with gravity gel filtration chromatography, as described in detail previously.^{3,17,19} Briefly, samples were homogenized and, after chemical reduction of the mucin disulfide bonds and carboxymethylation of the sulfhydryl groups, mucins were

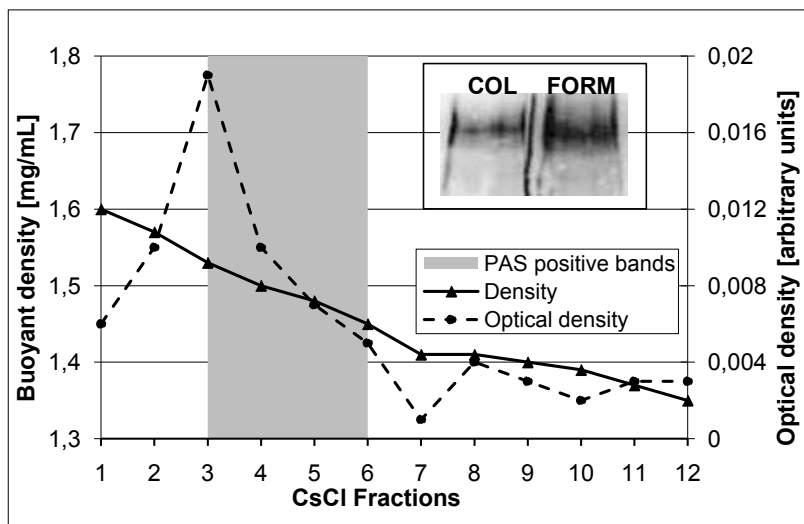


Figure 1. Isolation and determination of porcine Muc2 in intestinal tissue. Gray area represents periodic acid schiff²⁰ positive fractions 3-6 after ultracentrifugation. Closed line represents the buoyant density of the fractions. Staggered line represents the hexose content of the fractions. Western blot analysis shows positive bands for porcine MUC2 in colostrum (COL) and formula (FORM) fed piglets.

purified by equilibrium ultracentrifugation (Beckmann Coulter, 50.2 Ti rotor at 250,000 g for 72–88 h at 4°C) on a CsCl (Roche, Uppsala, Sweden) density gradient of 1.40 g/mL. CsCl-gradient fractions were collected, dialyzed, and analyzed for the presence of mucins. MUC2 containing fractions, i.e. fractions 3-6 identified by periodic acid schiff²⁰ positive bands after SDS-PAGE, had a buoyant density between 1.45 and 1.53 mg/mL. This corresponded to relatively high hexose levels in the MUC2 fractions as determined by hexose assay according to François et al.²¹ (Figure 1). MUC2 containing fractions were pooled, and further purified by gravity gel filtration chromatography using a Sepharose CL-2B column. MUC2 samples were then extensively dialyzed, analyzed for presence of MUC2 by Western blot, and stored freeze-dried at –20°C.

Porcine MUC2 DNA sequence analysis

To identify porcine MUC2 and further investigate its homology to human MUC2, we used reverse transcriptase-polymerase chain reaction (RT-PCR) and sequence analysis according to the method described previously.²² Total RNA was isolated from colon samples according to the manufacturer's protocol (RNeasy midi RNA-isolation, Qiagen) and transcribed into cDNA using reverse transcriptase. The final reaction condition was: 2.5 µM pdN6/20 nM oligodT (mix of random hexamers), 200 µM dNTP's, 1 U/µL RNAsin, 8 U/µL mMLV. The entire RT reaction was performed as follows: 45 min at 37°C, then 15 min at 42°C, and was stopped at 94°C (5 min). This was followed by a PCR-reaction in

Table 2. Human MUC2 primer sequences used for RT-PCR on mRNA isolated from pig colonic tissue.

Primers	Primer sequences
P133 - 149	5'- GTCTGCAGCACCTGGGG -3'
P697 - 713	5'- GAGTGTGAGAGGCTGCT -3'
P607 - 623	5'- GGGAACATGCAGAAGAT -3'
P1144 - 1160	5'- TGTGTCTGTAACGCTGG -3'

a total volume of 50 μ L using 5 μ LcDNA as template in combination with human MUC2 primers (Table 2). In one PCR- reaction primer P133-149 was used in combination with P697-713 and P607-623 was used with P1144-1160. Final PCR-reaction conditions were: 4mM $MgCl_2$, 200 μ M dNTP's, Taq DNA polymerase, and 0.3 pmol of each primer (forward and reverse). The PCR-reaction was carried out as follows: 5 min 95°C, and 30 cycles of 1 min 95°C, 1 min 55°C and 1 min 72°C. After the last cycle a 10 min extension step at 72°C followed. The resulting PCR-product was isolated after analysis on a 1.2% agarose gel using Wizard SV Gel and PCR Clean-up System (Promega). Then, BigDye terminator cycle sequencing was performed in a 3130xl Genetic analyzer (Applied Biosystems). Sequencing reactions were prepared as follows: 3-5 ng of PCR-product template, 3 pmol/ μ L primer, Ready Reaction Primix and BigDye Sequencing buffer. Amplification was over 25 cycles at 96°C for 10 seconds, 50°C for 5 seconds, and 60°C for 4 minutes. The amplification products were ethanol precipitated for 10-15 minutes at room temperature, centrifuged at maximum speed for 20 minutes, washed with 70% ethanol, and dried by opening the tubes to remove unincorporated dyes. Then pellets were dissolved in HiDi-formamide and run on the sequence analyzer.

Mass spectrometry

Threonine enrichment analyses

Plasma samples were prepared to determine threonine enrichment by GC-MS as described previously^{17,23} with some modifications. As internal standard [2,3,4,4,4-D₅, ¹⁵N]thr was used and an additional derivatization step was performed to block the free hydroxyl group of threonine by adding 20 μ L of pyridine and 50 μ L of acetic anhydride to the dried ethyl chloroformate derivatives. The samples were briefly shaken on a vortex mixer and left for 60 min at 60°C. After cooling down, the samples were dried under a gentle nitrogen flow at room temperature and resuspended in 50 μ L of ethyl acetate. Standard curves were prepared by mixing aqueous solutions of natural and labeled threonine for both enrichment and concentration determination. GC-MS analyses were performed in selective ion-monitoring mode (SIM) after electron impact ionization (EI) on a MSD 5975C Agilent GCMS (Agilent Technologies, Amstelveen, Netherlands). SIM was carried

out at m/z 146.1, 147.1, 149.1 and 152.1. Separation was achieved on a VF17MS (30m x 0.25mm i.d., 0.25 μ m film thickness) fused-silica capillary column (Varian, Middelburg, the Netherlands). Helium was used as a carrier gas at a constant flow of 1.2 mL/min. The column was held at 55°C for 1 min, and then programmed at 30°C/min to 160°C, 5°C/min to 200°C, and at 10°C/min to 300°C, with a 8-min hold. Threonine enrichment was expressed in mole percent excess (MPE).

Determination of intestinal intracellular free threonine

Intestinal tissues from the distal SI were homogenized with ice cold water in a 100 mg/mL concentration. The protein fraction was isolated as described previously.²³ Isotopic enrichment and concentration of [U-¹³C]thr and [15N]thr in the tissue amino acid free pool was determined by GC-MS analysis of the acetyl-ethoxycarbonyl-ethylester using EI with a MSD 5975C Agilent GCMS as described before for plasma samples.

Mucin MUC2 synthesis

Dried MUC2 samples were hydrolyzed by adding 1 mL of 6 mol/L HCl and incubating at 110° C for 20 h. Dried hydrolysates (Speedvac Savant, Thermofisher, Breda, the Netherlands) were dissolved in 0.2 mL MilliQ water and amino acids isolated by cation exchange separation as described for the blood amino acid fraction. Enrichment of [U-¹³C]thr in MUC2 isolates was determined using GCMS as described above.

Calculations and interpretation of threonine labeling

The FSR of MUC2 is expressed as percentage of the total MUC2-pool newly synthesized per day and calculated as follows¹⁷:

$$\text{FSR} = (\text{SL-E [U-}^{13}\text{C]thr}_{\text{MUC2}} / \text{E [U-}^{13}\text{C]thr}_{\text{Plasma/TF}}) * 24 \text{ h} * 100\%$$

where SL-E [U-¹³C]thr_{MUC2} is the slope of the linear hourly increase of E [U-¹³C]thr_{MUC2} where E [U-¹³C]thr_{MUC2} is the isotopic enrichment of [U-¹³C]thr incorporated into MUC2. In preterm pigs, SL-E [U-¹³C]thr_{MUC2} was determined from the slope of the increase of E [U-¹³C]thr_{MUC2} at the time of euthanasia. E [U-¹³C]thr_{MUC2} at baseline was assumed to be 0 MPE. [U-¹³C]thr enrichment of the intracellular tissue free (TF) amino acid pool (E [U-¹³C]thr_{TF}) was used as the precursor to calculate MUC2 FSR. For preterm infants, [U-¹³C]thr plasma enrichments (E [U-¹³C]thr_{Plasma}) were used as the precursor pool because of the absence of intestinal samples for obvious ethical reasons. Similarly, in the following equations, plasma and tissue free (TF) precursor pools will be depicted as E thr_{Plasma/TF} for neonates and piglets respectively.

In the fed state, the mucosal threonine pool can be derived from the diet, i.e. luminal uptake, or from the systemic supply, i.e. basolateral uptake. During an intragastric

[^{15}N]thr infusion, the input of the label is from the luminal side and, after transport by the enterocyte into the systemic pool, from the basolateral side. The infusion of intravenous [$\text{U-}^{13}\text{C}$]thr leads to uptake from the basolateral side. Thus, by the end of the dual-tracer infusion, there are two populations of labeled threonine molecules in MUC2: [$\text{U-}^{13}\text{C}$]thr directly from the basolateral side, and [^{15}N]thr derived from both the luminal and basolateral side. The enrichment of the [^{15}N]thr in MUC2 absorbed from the basolateral side ($E [^{15}\text{N}]thr_{\text{MUC2-BL}}$) can be calculated by using the percentage of the plasma or tissue free [$\text{U-}^{13}\text{C}$]thr incorporated into MUC2 as precursor pool:

$$E [^{15}\text{N}]thr_{\text{MUC2-BL}} = E [^{15}\text{N}]thr_{\text{Plasma/TF}} * (E [\text{U-}^{13}\text{C}]thr_{\text{MUC2}} / E [\text{U-}^{13}\text{C}]thr_{\text{Plasma/TF}})$$

where $E [^{15}\text{N}]thr_{\text{Plasma/TF}}$ is the enrichment of [^{15}N]thr in the plasma or tissue free (TF) pool, $E [\text{U-}^{13}\text{C}]thr_{\text{MUC2}}$ is the enrichment of the [$\text{U-}^{13}\text{C}$]thr in MUC2, and $E [\text{U-}^{13}\text{C}]thr_{\text{Plasma/TF}}$ is the enrichment of the [$\text{U-}^{13}\text{C}$]thr tracer in the plasma or the tissue free (TF) pool.

Then, the proportion of threonine expressed as % absorbed basolaterally into MUC2 can be calculated by:

$$\text{Basolateral THR absorption (\%)} = (E [^{15}\text{N}]thr_{\text{MUC2-BL}} / E [^{15}\text{N}]thr_{\text{Plasma/TF-BL}}) * 100\%$$

where $E [^{15}\text{N}]thr_{\text{TF-BL}}$ is the enrichment of the [^{15}N]thr tracer in the TF pool taken up from the basolateral side.

Following, the enrichment of the [^{15}N]thr in MUC2 absorbed from the luminal side ($E [^{15}\text{N}]thr_{\text{MUC2-LUM}}$) can be calculated by:

$$E [^{15}\text{N}]thr_{\text{MUC2-LUM}} = E [^{15}\text{N}]thr_{\text{MUC2}} - E [^{15}\text{N}]thr_{\text{MUC2-BL}}$$

where $E [^{15}\text{N}]thr_{\text{MUC2}}$ is the total enrichment of the [^{15}N]thr tracer, i.e. from both the luminal and basolateral side, in MUC2.

The proportion of threonine expressed as % absorbed luminally can then be calculated by:

$$\text{Luminal THR absorption (\%)} = (E [^{15}\text{N}]thr_{\text{MUC2-LUM}} / E [^{15}\text{N}]thr_{\text{DIET/TF-LUM}}) * 100\%$$

where the enrichment of the [^{15}N]thr tracer in the diet ($E [^{15}\text{N}]thr_{\text{DIET}}$) is used as a precursor in the infants, and the enrichment of the [^{15}N]thr tracer in the TF pool taken up from the luminal side is used as precursor for the piglets. From the rate of the dietary threonine intake of the patients during the isotope infusion and the rate of the intragastric [^{15}N]thr administration, $E [^{15}\text{N}]thr_{\text{DIET}}$ was calculated.

9

Statistics

Minitab statistical software (Minitab, State College, PA) was used for statistical analysis. Data were analyzed by one-way ANOVA-General Linear Model. Data are presented as the mean \pm SEM and $P < 0.05$ was considered statistically significant.

RESULTS

Porcine MUC2

Isolated pig MUC2 showed high similarity to MUC2 found in human preterm infants with respect to its buoyant density, molecular weight, PAS stainability, and hexose content.^{17,19} Specifically, pig MUC2 has a buoyant density between 1.45 and 1.53 mg/mL, has a relative high molecular weight, is visible with PAS on SDS-PAGE (not shown), and contained relatively high amounts of hexose (Figure 1). Recognition of the purified porcine MUC2 samples by western blotting with anti-HCM, i.e. an antibody specific for human MUC2²², suggested high homology between porcine and human MUC2 (Figure 1). Overlapping parts of pig *MUC2* cDNA were cloned by RT-PCR on pig ileal mRNA following the strategy as shown in Figure 2. Pig *MUC2* cDNA sequences were amplified, sequenced and combined to one fragment of 1028 bp, which showed 85% homology to human *MUC2* cDNA. This 1028 bp fragment was found to encode a fragment of 342 amino acids of the N-terminus of pig MUC2, which showed 81% homology to human MUC2 (Figure 3).

Preterm pigs

Body and organ weights

As shown in Table 3 there was no difference in birth weight between FORM and COL piglets. Weight gain was lower in FORM pigs compared to COL pigs. No difference was observed between FORM and COL pigs with respect to the length or wet mass weights of the small intestine. The percentage of mucosa was also not different between groups.

Table 3. Body and organ weights in preterm pigs fed formula or colostrum*

	COLOSTRUM	FORMULA	<i>P</i>
Birth weight, g	871 \pm 47.3	805 \pm 46.7	0.2
Final body weight, g	941 \pm 49.7	832 \pm 54.4	0.1
Weight gain, g·kg ⁻¹ ·d ⁻¹	20.0 \pm 1.7	8.4 \pm 6.2	0.2
Small intestinal length, cm/kg body wt	305 \pm 12.7	362 \pm 17.4	0.05
Small intestinal weight, g/kg body wt	29.8 \pm 0.8	32.5 \pm 1.8	0.3
Mucosa dry weight, %	69.5 \pm 2.8	67.5 \pm 4.7	0.4

*Values are presented as means \pm SEM; $n=6$ /group.

hMUC2: 133	<u>GTCTGCAGCA CCTGGGGCAA</u> CTTCCACTAC AAGACCTTCG ACGGGGACGT
pMUC2:	GTCTGCAGCA CCTGGGGC GA CTTCCACTAC AAGACCTTCG ACGGGGACGT
hMUC2: 183	CTTCCGCTTC CCCGGCCTCT GCGACTACAA CTTGCGCTCC GACTGCCGAG
pMUC2:	CTTCCGCTTC CC GGGCCTGT GCGACTACAA CTTGCGCTCC GACTGCCG GG
hMUC2: 233	GCTCCTACAA GGAATTTGCT GTGCACCTGA AGCGGGGTCC GGGCCAGGCT
pMUC2:	ACGCCTACAA GG AGTT CGCT GTGCACCTGA GACGGGGCCC CGCGGGCAGT
hMUC2: 283	GAGGCCCCCG CCGGGGTGGA GTCCATCCTG CTGACCATCA AGGATGACAC
pMUC2:	GGGGCCCCCT CCCAGGTCGA GT ACAT CCTG CTGAC GGT CA AGGATGACAC
hMUC2: 333	CATCTACCTC ACCCGCCACC TGGCTGTGCT TAACGGGGCC GTGGTCAGCA
pMUC2:	CATCTACCTC ACTCAGCAGC TGG TCGTG GT GAACGGGGCC ATGGTCAGCA
hMUC2: 383	CCCCGACTA CAGCCCCGGG CTGCTCATTG AGAAGAGCGA TGCCTACACC
pMUC2:	CCCCGACTA TAGCCC GGGG CTGCTCATTG AG AGGAGTGC CGTCTACACC
hMUC2: 433	AAAGTCTACT CCCGCGCCGG CCTCACCTCT ATGTGGAACC GGGAGGATGC
pMUC2:	AAGTCTATT CCC GA GTGG C TTGCTCTC GTGTGGAACA GAGAGGACTC
hMUC2: 483	ACTCATGCTG GAGCTGGACA CTAAGTTCCG GAACCAACACC TGTGGCCTCT
pMUC2:	GGTCATGCTG GAGCTGGACA GTAAGTTCCA GAACCA ACAG TGTGGCCTCT
hMUC2: 533	GCGGGGACTA CAACGGCCTG CAGAGCTATT CAGAATTCTT CTCTGACGGC
pMUC2:	GCG GA ACTA CAACGGCCTG CAG ACCTACT CAG AGTTCTT CT CGGAGGGC
hMUC2: 583	GTGCTCTTCA GTCCCTTGA GTTTGGGAAC ATGCAGAAGA TCAACAGGCC
pMUC2:	ATCCCTTCA G CCCC TTGA GT TCGGGAAC ATGCAGAAGA TCAAC AAGCC
hMUC2: 633	CGATGTGGTG TGTGAGGATC CCGAGGAGGA GGTGGCCCCC GCATCCTGCT
pMUC2:	CG AGGAGAAG TGT GACGACC CCGAGGAG GC ACAGGCCAAG CTGTCTCTGCT
hMUC2: 683	CCGAGCACCG CGCCAGTGT GAGAGGCTGC TGACCGCCGA GGCCTTCGCG
pMUC2:	CTGAGCACCG CGCCGAGT GC GAGAGGCTGC TGAC GGACGT GGCCTTCGAG
hMUC2: 733	GACTGTCAAG ACCTGTGTGCC GCTGGAGCCG TATCTGCGCG CCTGCCAGCA
pMUC2:	GACT GCCAGG GGCT GTGTGCC ACTGGAGCTG TACGTGCAGG CCT GCGTGCA
hMUC2: 783	GGACCGCTGC CGGTGCCCGG GCGGTGACAC CTGCGTCTGC AGCACCGTGG
pMUC2:	GGACCGCTGT CAGTGCCCGC AGGGCACCTC CTGCGTCTGC AGCAC GATCG
hMUC2: 833	CCGAGTTCTC CCGCCAGTGC TCCCACGCCG GCGGCCGGCC CGGGAATCGG
pMUC2:	CCGAGTTCTC CCGCCAGTGC TCCCACGCCG GTGG GCGGCC TGGGAATCGG
hMUC2: 883	AGGACCGCCA CGCTCTGCCC CAAGACCTGC CCCGGGAACC TGGTGTACCT
pMUC2:	AGGACCGCCA AGCTCTGCCC TAAGAGCTGC CCTGGGAACA TGGTTACCT
hMUC2: 933	GGAGAGCGGC TCGCCCTGCA TGGACACCTG CTCACACCTG GAGGTGAGCA
pMUC2:	GGAGAGC AGC TCGCCCT GCG TGGACACCTG CTC GCA CTG GAGGT CAGCA
hMUC2: 983	GCCTGTGCGA GGAGCACCGC ATGGACGGCT GTTTCTGCCC AGAAGGCACC
pMUC2:	GCCTGTGCGA G GAAC ACCGC ATGGATGGCT GTTTCTGCCC AGAAGGC ACT
hMUC2: 1033	GTATATGACG ACATCGGGGA CAGTGGCTGC GTTCTGTGA GCCAGTGCCA
pMUC2:	GTGTATGATG ACATCG CGGG CAG AGGCTGC ATCCCCGTGA GCCAGTGCTA
hMUC2: 1083	CTGCAGGCTG CACGGACACC TGTACACACC GGGCCAGGAG ATCACC AATG
pMUC2:	CTGCA AGCTG CACGGG CACC AGTATGCGCC CGGCCAGCAG GTCACCA ACA
hMUC2: 1133	<u>ACTGCGAGCA GTGTGTCTGT AACGCTGG</u>
pMUC2:	ACTGCGAGCA ATGTGTCTGT AACGCTGG

Figure 2. Part of the 5' cDNA sequence of porcine *MUC2*, and sequence comparison with human *MUC2*. The sequence of the 1028 bp-long 5' part of porcine *MUC2* (p*MUC2*) is aligned to the 5' sequence of human *MUC2* (h*MUC2*). The p*MUC2* sequence is for 85% identical to h*MUC2*. Mismatches are indicated in bold script in the p*MUC2* sequence. Underlined sequences correspond with sequences of primers designed on human *MUC2* cDNA sequences that were used to amplify porcine *MUC2* cDNA.

hMUC2: 36	VCSTWGNFHYKTFDGDVFRFPGLCDYNFASDCRGSYKEFAVHLKRPGQA
pMUC2:	VCSTWGD F HYKTFDGDVFRFPGLCDYNFASDCR DGY KEFAVHLRRPG GS
hMUC2: 86	EAPAGVESILLTIKDDTIYLTRHLAVLNGAVVSTPHYSPGLLIEKSDAYT
pMUC2:	GGPSQ VEYILLTVKDDTIYLT QQLV VVNGAMVSTPHYSPGLLIER SAVYT
hMUC2: 136	KVYSRAGLTLMWNRDALMLELDTKFRNHTCGLCGDYNGLQSYSEFLSDG
pMUC2:	KVYSRAGL ALV WNR EDSV MLELDTK FQ NHTCGLCGDYNGLQTYSEFL SEG
hMUC2: 186	VLFSPLFEGNMQKINQPDVVCEDPEEEVAPASCSEHRAECERLLTAEFA
pMUC2:	IPF SPLFEGNMQK INKPEEK DDPEE AQAKL SCSEHRAECERLLT DVAFE
hMUC2: 236	DCQDLVPLEPYLRACQQDRRCPCGGDTCVCSTVAEFSRQCSHAGGRPGNW
pMUC2:	DCQ GLV PLELY VQACV QDR CQCPQGT SCVCSIAEFSRQCSHAGGRPGNW
hMUC2: 286	RTATLCPKTCPGNLVYLESGPCMDTCSHLEVSSLCEEHRMDGCFCEP
pMUC2:	RTAK LCPK SCPG NM VYLESS SPC VDTC SHLEV SSLCEEHRMDGCFCEP
hMUC2: 336	VYDDIGDSGCVVSQCHCRLHGHLYTPGQEITNDCEQCVCNAG
pMUC2:	VYDD IAG RGCVVSQCH CKL HGH QYAPG QQVTNNCEQCVCNAG

Figure 3. Part of the N-terminal amino acid sequence of porcine MUC2, and sequence comparison with human MUC2. The sequence of the 342 amino acids-long N-terminal part of the porcine MUC2 (pMUC2) polypeptide fragment is aligned to the N-terminal sequence of human MUC2 (hMUC2). The pMUC2 sequence is for 81% identical to hMUC2. Mismatches are indicated in bold script in the pMUC2 sequence.

Threonine tracer kinetics

One pig in the FORM group was excluded from isotopic analyses because of infusion failure of the tracer. Enrichments of both [^{15}N]thr and [$\text{U-}^{13}\text{C}$]thr were measured in the plasma (steady state), in the intracellular free pool of the distal SI, and in purified MUC2 samples derived from the distal SI (Table 4). In FORM piglets, 60 ± 6.8 % of threonine in MUC2 was absorbed from the basolateral side and 40 ± 6.8 % was absorbed from the luminal side (Figure 4). In COL piglets, 41 ± 4.3 % of dietary threonine in MUC2 was absorbed from the basolateral side and 59 ± 4.3 % was absorbed from the luminal side (Figure 4). MUC2 FSR, representing the percentage of newly synthesized MUC2 per day

Table 4. Threonine kinetics in piglets fed colostrum or formula*

	COLOSTRUM	FORMULA
E [^{15}N]thr _{DIET} (MPE)	11.039	11.804
E [^{15}N]thr _{Plasma} (MPE)	5.9 ± 0.30	5.7 ± 0.53
E [U^{13}C]thr _{Plasma} (MPE)	13 ± 0.85	9.8 ± 0.97
E [^{15}N]thr _{TF} (MPE)	1.5 ± 0.10	5.2 ± 1.5
E [U^{13}C]thr _{TF} (MPE)	1.7 ± 0.07	3.9 ± 0.25
E [^{15}N]thr _{Muc2} (MPE)	1.2 ± 0.10	1.7 ± 0.46
E [U^{13}C]thr _{Muc2} (MPE)	1.1 ± 0.09	1.7 ± 0.24
Muc2 FSR** (%/d)	177 ± 17.1	121 ± 16.7

*Values are presented as means \pm SEM; COLOSTRUM $n=5$; FORMULA $n=6$.

**Muc2 FSR COLOSTRUM vs. FORMULA $P = 0.047$.

THR threonine; MPE mole percent excess; FSR fractional synthesis rate.

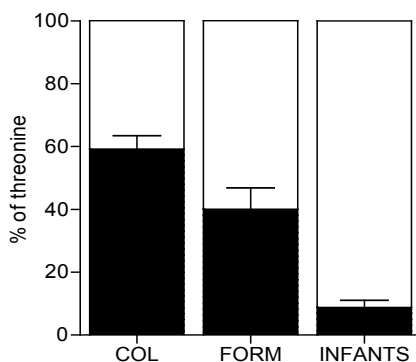


Figure 4. Percentage of luminal and basolateral threonine absorption for MUC2 synthesis in preterm pigs fed colostrum (COL) or formula (FORM) and preterm infants. Black bars represents luminal absorption of threonine and white bars remaining basolateral absorption of threonine incorporated into MUC2.

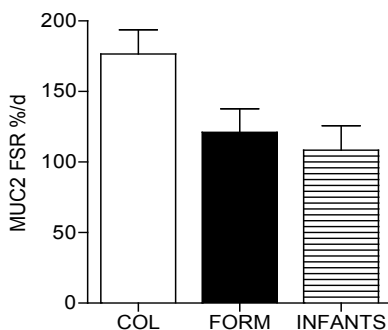


Figure 5. MUC2 FSR expressed as percentage of newly synthesized MUC2 per day in preterm pigs fed either colostrum (COL) or formula (FORM), and in preterm infants.

in the distal SI, was relatively high, and was lower in FORM pigs (121 ± 17 %/d) compared to COL pigs (177 ± 17 %/d) (Figure 5).

Preterm infants

Enrichments of both $[^{15}\text{N}]\text{thr}$ and $[\text{U-}^{13}\text{C}]\text{thr}$ were measured in the plasma at steady state and in purified MUC2 samples from the ileal outflow fluid (Table 5). In preterm infants, 91 % of the dietary threonine in MUC2 was absorbed from the basolateral side, whereas 9 % was absorbed from the luminal side (Figure 4). The mean MUC2 FSR in the ileum was 108 ± 17 %/d (Figure 5, Table 5).

Table 5. Threonine kinetics in preterm infants.

Patients	1	2	3	4	5
Enteral threonine intake ($\mu\text{mol}\cdot\text{kg}\cdot\text{h}^{-1}$)	10.1	31.9	45.3	33.6	35.3
E [15N]thr _{Diet} (MPE)	40.0	56.7	45.6	57.1	62.8
E [15N]thr _{Plasma} (MPE)	9.0	7.9	7.2	7.6	5.5
E [U ¹³ C]thr _{Plasma} (MPE)	3.8	4.2	3.1	3.3	3.1
E [15N]thr _{Muc2} (MPE)	7.9	5.1	4.1	3.3	4.2
E [U ¹³ C]thr _{Muc2} (MPE)	1.9	1.4	1.6	0.9	1.1
Muc2 FSR (%/d)	147	76	144	61	114

THR threonine; MPE mole percent excess; FSR fractional synthesis rate

DISCUSSION

Threonine is important for mucosal protein and mucin synthesis to provide epithelial protection. The preferential site of threonine uptake, i.e. basolateral or luminal, for mucin synthesis has implications for nutritional therapy in the preterm infant since disruption of the mucus layer increases the risk of NEC. We studied the preferential site of threonine absorption for MUC2 synthesis in partially enterally fed preterm infants and in colostrum or formula-fed preterm pigs. First, we showed by two independent techniques (Western blot and sequence analysis) that porcine MUC2 is expressed in the ileum, and that it is 81% homologous to human MUC2. Second, our results show that threonine from both the basolateral and luminal side is used for MUC2 synthesis in preterm pigs and infants. Under these conditions, luminal threonine absorption and MUC2 synthesis rate was higher in preterm pigs than in partially enterally fed preterm infants. Furthermore, colostrum feeding in preterm pigs stimulated threonine uptake from the luminal side, and increased MUC2 fractional synthesis rate compared to formula feeding.

In both preterm pigs and preterm infants, threonine was taken up for MUC2 synthesis from both the arterial and luminal side. Uptake of both systemically and enterally derived nutrients for synthesis of peptides such as glutathione has been described before.²⁴ However, mucin producing goblet cells are secretory cells and hence not designed for nutrient uptake. Amino acids in the small intestinal lumen are actively absorbed across the apical enterocyte membranes.²⁵ The major apical neutral amino acid transporter is B⁰AT1 and transports all neutral amino acids including threonine, albeit to a varying extent.²⁶ The apical ASCT2 transporter has a higher affinity for small neutral amino acids such as threonine.²⁶ However, it is unknown whether goblet cells exhibit these transporters on their apical membrane. Studies performed on human and murine tissues have shown that goblet cells do not exhibit the PEPT1 transporter responsible for peptide transport on their apical membrane.²⁷⁻²⁸ Based on all these data, it seems unlikely that goblet

cells transport amino acids via the apical membrane. Hence, the uptake of threonine coming directly from the luminal side has to come from inter- or paracellular trafficking between enterocytes and goblet cells. It is argued that paracellular transport becomes highly significant at high substrate concentration.²⁹ At the mucosal surface high amino acid concentrations are present due to local peptidases. However, future studies are warranted to elucidate the detailed mechanisms regulating uptake of threonine from the luminal side. Transporters 4F2/LAT2 and SNAT2 are responsible for basolateral uptake of neutral amino acids.²⁶ Interestingly, the transporter is upregulated by amino acid depletion and is likely to provide amino acids to intestinal epithelial cells, when recruiting few amino acids from the lumen.³⁰ Whether this takes place at the basolateral membrane of the goblet cells remains to be investigated.

Luminal threonine uptake, as a percentage of the enteral intake, and MUC2 synthesis in preterm infants was lower compared to that observed in preterm pigs. Preterm infants were only partially enterally fed, after receiving full TPN for some time after intestinal surgery, which might have impacted luminal threonine uptake. In piglets receiving TPN, the first pass splanchnic uptake is bypassed, and gut atrophy occurs that is likely to result in diminished gastro-intestinal requirements.³¹⁻³² This is consistent with the finding that whole body threonine requirements of neonatal piglets receiving TPN is considerably lower than that of piglets receiving an identical diet intragastrically.³³ Interestingly, decreased luminal threonine concentrations negatively affected mucin synthesis in piglets.¹⁰ Therefore, in preterm infants the lower luminal threonine uptake might have resulted in the reduced MUC2 synthesis rates observed. Consequently, it is possible that parenteral nutrition, by restricting the supply of enteral threonine, might severely restrict MUC2 synthesis, causing deterioration of gut barrier function. If so, it is possible that, under circumstances of TPN, the provision of threonine via the intestine might provide significant functional benefit to the preterm infant at risk for NEC.

Our finding that porcine MUC2 is highly homologous to human MUC2, provides the opportunity to study human MUC2 synthesis and regulation by nutritional factors in an animal model. Our preterm pig model shows that, besides the route of nutrition, type of enteral nutrition, i.e. colostrum or formula, impacts luminal threonine uptake for MUC2 synthesis. MUC2 synthesis rate was higher in colostrum fed piglets, and was accompanied by a higher luminal threonine uptake. Alternatively, luminal threonine concentrations are known to stimulate mucin synthesis but were in the same range for colostrum and formula fed piglets.¹⁰ Therefore, the mechanism for these effects might be indirectly regulated by colostrum growth factors and immunoglobulins stimulating mucosal growth, or directly by stimulation of intestinal metabolic pathways. Colostrum feeding in preterm pigs has shown to decrease NEC incidence by stimulation of gut maturation, nutrient absorption, and protection against colonization, in which adequate threonine supply and hence stimulation of MUC2 synthesis might play an important role.^{18,34}

The difference in luminal threonine uptake and MUC2 synthesis between colostrum and formula fed piglets, could not be observed between the preterm infants fed formula or their own mothers' milk. However, the sample size was limited and therefore there was a lack of power to detect an effect. Furthermore, patients were still recovering from intestinal disease and surgery, and were not on full enteral feeds, and hence might not resemble physiological MUC2 synthesis. However, the isotope infusion protocol had to be performed before removal of the (central) venous catheters required for the isotope infusion, according to our NICU guidelines when close to full enteral intake was reached.

The isotopic data from our experiments suggest that there is threonine uptake from both the luminal and basolateral side for MUC2 synthesis. Furthermore, both luminal threonine uptake and MUC2 synthesis seem to be influenced by the amount and type of enteral nutrition. Firstly, luminal threonine uptake and MUC2 synthesis was low in partially enterally fed preterm infants. Therefore, restriction of enteral threonine might diminish MUC2 synthesis, and might cause the deterioration of gut barrier function that occurs when nutrients are supplied solely by the parenteral route. Hence, provision of threonine via the intestine during TPN administration might provide significant functional benefit to the preterm infant at risk for NEC. Secondly, type of enteral feeding, i.e. colostrum feeding, enhances luminal threonine uptake and MUC2 synthesis when compared to formula feeding. Thus, the beneficial effect of human or own mother's milk on prevention of NEC in the preterm infant might not only reside in the direct effect of immune- and growth factors, but also indirectly by stimulation of nutrient uptake, and in this case luminal threonine uptake to enhance the MUC2 synthesis necessary for adequate gut barrier function.

FUNDING

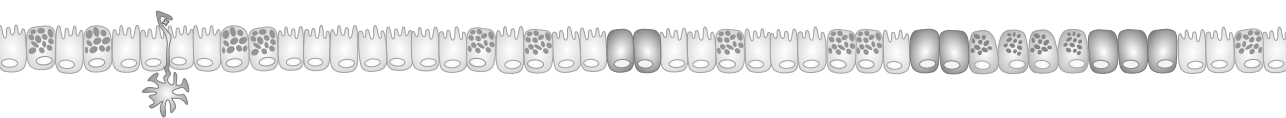
Partly supported by Danone Research. The study sponsor had no role in the study design, analysis of data, or writing of the manuscript.

REFERENCES

1. Specian RD, Oliver MG. Functional biology of intestinal goblet cells. *Am J Physiol* 1991;260: C183-93.
2. Van Klinken BJ, Tytgat KM, Buller HA, Einerhand AW, Dekker J. Biosynthesis of intestinal mucins: MUC1, MUC2, MUC3 and more. *Biochem Soc Trans* 1995;23:814-8.
3. Tytgat KM, Buller HA, Opdam FJ, Kim YS, Einerhand AW, Dekker J. Biosynthesis of human colonic mucin: Muc2 is the prominent secretory mucin. *Gastroenterology* 1994;107:1352-63.
4. Gum JR, Jr., Hicks JW, Toribara NW, Rothe EM, Lagace RE, Kim YS. The human MUC2 intestinal mucin has cysteine-rich subdomains located both upstream and downstream of its central repetitive region. *J Biol Chem* 1992;267:21375-83.
5. Lien KA, Sauer WC, Fenton M. Mucin output in ileal digesta of pigs fed a protein-free diet. *Z Ernährungswiss* 1997;36:182-90.
6. Mantle M, Allen A. Isolation and characterization of the native glycoprotein from pig small-intestinal mucus. *Biochem J* 1981;195:267-75.
7. Allen A, Hutton DA, Pearson JP. The MUC2 gene product: a human intestinal mucin. *Int J Biochem Cell Biol* 1998;30:797-801.
8. Toribara NW, Gum JR, Jr., Culhane PJ, Lagace RE, Hicks JW, Petersen GM, Kim YS. MUC-2 human small intestinal mucin gene structure. Repeated arrays and polymorphism. *J Clin Invest* 1991;88:1005-13.
9. Faure M, Mettraux C, Moennoz D, Godin JP, Vuichoud J, Rochat F, Breuille D, Obled C, Cortesys-Theulaz I. Specific amino acids increase mucin synthesis and microbiota in dextran sulfate sodium-treated rats. *J Nutr* 2006;136:1558-64.
10. Nichols NL, Bertolo RF. Luminal threonine concentration acutely affects intestinal mucosal protein and mucin synthesis in piglets. *J Nutr* 2008;138:1298-303.
11. Law GK, Bertolo RF, Adjiri-Awere A, Pencharz PB, Ball RO. Adequate oral threonine is critical for mucin production and gut function in neonatal piglets. *Am J Physiol Gastrointest Liver Physiol* 2007;292:G1293-301.
12. Faure M, Moennoz D, Montigon F, Mettraux C, Breuille D, Ballevre O. Dietary threonine restriction specifically reduces intestinal mucin synthesis in rats. *J Nutr* 2005;135:486-91.
13. Anand RJ, Leaphart CL, Mollen KP, Hackam DJ. The role of the intestinal barrier in the pathogenesis of necrotizing enterocolitis. *Shock* 2007;27:124-33.
14. van der Schoor SR, Wattimena DL, Huijman J, Vermes A, van Goudoever JB. The gut takes nearly all: threonine kinetics in infants. *Am J Clin Nutr* 2007;86:1132-8.
15. Stoll B, Burrin DG, Henry J, Jahoor F, Reeds PJ. Phenylalanine utilization by the gut and liver measured with intravenous and intragastric tracers in pigs. *Am J Physiol* 1997;273:G1208-17.
16. Stoll B, Burrin DG, Henry JF, Jahoor F, Reeds PJ. Dietary and systemic phenylalanine utilization for mucosal and hepatic constitutive protein synthesis in pigs. *Am J Physiol* 1999;276: G49-57.
17. Schaart MW, de Bruijn AC, Schierbeek H, Tibboel D, Renes IB, van Goudoever JB. Small intestinal MUC2 synthesis in human preterm infants. *Am J Physiol Gastrointest Liver Physiol* 2009;296:G1085-90.
18. Bjornvad CR, Thymann T, Deutz NE, Burrin DG, Jensen SK, Jensen BB, Molbak L, Boye M, Larsson LI, Schmidt M, Michaelsen KF, Sangild PT. Enteral feeding induces diet-dependent mucosal dysfunction, bacterial proliferation, and necrotizing enterocolitis in preterm pigs on parenteral nutrition. *Am J Physiol Gastrointest Liver Physiol* 2008;295:G1092-103.

19. Schaart MW, Schierbeek H, de Bruijn AC, Tibboel D, van Goudoever JB, Renes IB. A novel method to determine small intestinal barrier function in human neonates in vivo. *Gut* 2006; 55:1366-7.
20. Sharma R, Tepas JJ, 3rd, Hudak ML, Wludyka PS, Mollitt DL, Garrison RD, Bradshaw JA, Sharma M. Portal venous gas and surgical outcome of neonatal necrotizing enterocolitis. *J Pediatr Surg* 2005;40:371-6.
21. Francois C, Marshall RD, Neuberger A. Carbohydrates in protein. 4. The determination of mannose in hen's-egg albumin by radioisotope dilution. *Biochem J* 1962;83:335-41.
22. van Klinken BJ, Einerhand AW, Duits LA, Makkink MK, Tytgat KM, Renes IB, Verburg M, Buller HA, Dekker J. Gastrointestinal expression and partial cDNA cloning of murine Muc2. *Am J Physiol* 1999;276:G115-24.
23. Schaart MW, Schierbeek H, van der Schoor SR, Stoll B, Burrin DG, Reeds PJ, van Goudoever JB. Threonine utilization is high in the intestine of piglets. *J Nutr* 2005;135:765-70.
24. Reeds PJ, Burrin DG, Stoll B, Jahoor F, Wykes L, Henry J, Frazer ME. Enteral glutamate is the preferential source for mucosal glutathione synthesis in fed piglets. *Am J Physiol* 1997;273: E408-15.
25. Silk DB, Grimble GK, Rees RG. Protein digestion and amino acid and peptide absorption. *Proc Nutr Soc* 1985;44:63-72.
26. Broer S. Amino acid transport across mammalian intestinal and renal epithelia. *Physiol Rev* 2008;88:249-86.
27. Hussain I, Kellett L, Affleck J, Shepherd J, Boyd R. Expression and cellular distribution during development of the peptide transporter (PepT1) in the small intestinal epithelium of the rat. *Cell Tissue Res* 2002;307:139-42.
28. Groneberg DA, Doring F, Eynott PR, Fischer A, Daniel H. Intestinal peptide transport: ex vivo uptake studies and localization of peptide carrier PEPT1. *Am J Physiol Gastrointest Liver Physiol* 2001;281:G697-704.
29. Pappenheimer JR. On the coupling of membrane digestion with intestinal absorption of sugars and amino acids. *Am J Physiol* 1993;265:G409-17.
30. Franchi-Gazzola R, Visigalli R, Bussolati O, Dall'Asta V, Gazzola GC. Adaptive increase of amino acid transport system A requires ERK1/2 activation. *J Biol Chem* 1999;274:28922-8.
31. Shulman RJ. Effect of different total parenteral nutrition fuel mixes on small intestinal growth and differentiation in the infant miniature pig. *Gastroenterology* 1988;95:85-92.
32. Niinikoski H, Stoll B, Guan X, Kansagra K, Lambert BD, Stephens J, Hartmann B, Holst JJ, Burrin DG. Onset of small intestinal atrophy is associated with reduced intestinal blood flow in TPN-fed neonatal piglets. *J Nutr* 2004;134:1467-74.
33. Bertolo RF, Chen CZ, Law G, Pencharz PB, Ball RO. Threonine requirement of neonatal piglets receiving total parenteral nutrition is considerably lower than that of piglets receiving an identical diet intragastrically. *J Nutr* 1998;128:1752-9.
34. Sangild PT, Siggers RH, Schmidt M, Elnif J, Bjornvad CR, Thymann T, Grondahl ML, Hansen AK, Jensen SK, Boye M, Moelbak L, Buddington RK, Westrom BR, Holst JJ, Burrin DG. Diet- and colonization-dependent intestinal dysfunction predisposes to necrotizing enterocolitis in preterm pigs. *Gastroenterology* 2006;130:1776-92.

Chapter 10



General discussion



Necrotizing enterocolitis is a devastating disease that mainly affects premature neonates. Despite the recent advances of neonatal intensive care, NEC remains a major health concern in the intensive care nursery and an important cause of neonatal morbidity and mortality. Due to the increased number of very immature infants and the increased survival of very low birth weight (VLBW; birth weight <1500 g) infants, the incidence is likely to further increase in the future if no adequate prevention is found. Although prematurity, enteral feeding and bacterial colonization are known risk factors, the etiology of NEC is still largely unknown. Therapeutic options are limited to supportive care and surgical intervention and besides human milk feeding, no preventative strategies are available. As this disease has serious consequences on health care costs and quality of life, there is an urgent need for understanding the mechanisms through which this disease exerts its deleterious effects, which thereby might form targets for preventative and therapeutic intervention.

Therefore, the objective of this thesis was to study 1) intestinal epithelial defense mechanisms in early postnatal life in mice and human and 2) the effect of dietary interventions on intestinal epithelial barrier function *in vitro* and *in vivo*.

The major findings of this thesis will be discussed in the following section and we speculate on future perspectives to reach the final overall objective, namely the design of an effective treatment for NEC.

MAJOR FINDINGS

Innate defense during perinatal life

The early postnatal period is a time frame during which dramatic changes occur in the intestinal epithelium of *Muc2*^{-/-} mice. The first part of this thesis describes the effect of inflammation and/ or suckling-weaning transition on innate defense capacity in infants with severe NEC and *Muc2*^{-/-} mice.

Postnatal development of colitis in *Muc2*^{-/-} mice

It was previously demonstrated that *Muc2*^{-/-} mice display clinical and histological signs of colitis from the age of 5 weeks.¹ In **Chapter 2** we studied whether absence of *Muc2* already causes development of colitis in the early postnatal period, more specifically, before weaning of mother's milk. We hypothesized that lack of *Muc2* induces the development of colitis early after birth, which aggravates during the suckling-weaning transition. The dietary transition from mother's milk to solid food results in considerable changes in the intestinal microbiota in mice²⁻⁴ and humans.⁵ No signs of colitis were seen during fetal life. We demonstrate that the first evident signs of colitis, i.e. decreased body weight, increased crypt length and morphological alterations such as epithelial flattening and

superficial erosion were seen after weaning, which is indicative of a protective effect of mother's milk. Before weaning, increased expression of *Foxp3* mRNA, which is a marker for regulatory T-cells, was seen. Regulatory T cells (also named suppressor T cells) are a specialized subpopulation of T-cells that act to suppress activation of the immune system and thereby maintain immune system homeostasis. Moreover, expression of IL-10 was increased in *Muc2*^{-/-} mice compared to WT mice at the age of two weeks. Interleukin (IL)-10 maintains intestinal homeostasis by suppressing pro inflammatory cytokine production.⁶⁻⁸ IL-10-deficient (IL-10^{-/-}) mice spontaneously develop chronic colitis.⁹ Interestingly, mice that lack both *Muc2* and IL-10 develop colitis, which is more severe in every aspect compared to *Muc2*^{-/-} and IL-10^{-/-} mice¹⁰, indicating that the anti-inflammatory cytokine IL-10 can control epithelial damage in case of *Muc2* deficiency. Together, the increased expression of *Foxp3* and IL-10 in *Muc2*^{-/-} mice suggest that there is an immune suppressive response in *Muc2*^{-/-} mice before weaning.

After weaning, this regulatory capacity declines and pro-inflammatory responses become predominant resulting in a pro-inflammatory cytokine profile. Gene expression levels of Tgfβ1, a peptide with immune suppressive capacities by inhibiting the secretion and activity of cytokines including IFN-γ, TNF-α and various interleukins, were significantly increased in WT mice after weaning, whereas in *Muc2*^{-/-} mice expression of Tgfβ1 significantly decreased after weaning. Furthermore, at the age of 4 weeks, expression of Tgfβ1 was significantly lower in *Muc2*^{-/-} mice compared to WT mice, indicating that immune suppressive capacity declines after weaning in *Muc2*^{-/-} mice.

Mother's milk contains functional nutrients that help provide the microenvironment for gut protection and maturation.¹¹ Several components of breast milk can reduce the inflammatory response to stimuli in the newborn intestine, including transforming growth factor (TGF)-β, interleukin (IL)-10, erythropoietin, and lactoferrin. Moreover, the third largest component of human milk consists of human milk oligosaccharides of which several functions have been postulated.¹²⁻¹³ N-acetylglucosamine-containing oligosaccharides have been reported to act as prebiotics by promoting the growth of *Bifidobacterium bifidum*, thereby suppressing the growth of undesirable bacteria.¹⁴⁻¹⁶ This presumed effect of mother's milk of driving the intestinal microbiota towards a non-pathogenic environment, might partially explain the differences in intestinal Toll-like receptor expression and corresponding cytokine profiles as TLRs are differentially induced by Gram-positive and Gram-negative bacteria.¹⁷ Although *Muc2*-deficient mice seem predestined to develop colitis due to the absence of a protective mucus layer, mother's milk might decrease disease severity by increasing the anti-inflammatory response. Further studies with continued mother's milk feeding are required to evaluate the protective potential of mother's milk in *Muc2*^{-/-} mice.

In **Chapter 3**, gene array analysis and subsequent confirmation by quantitative PCR analysis revealed that genes involved in cell structure related pathways (focal adhesion,

regulation of the actin cytoskeleton, and adherens-, gap- and tight junctions) were significantly altered in 4-week-old Muc2^{-/-} mice. Although one could expect an upregulation of intestinal barrier function related genes to compensate for the loss of Muc2, Muc2^{-/-} mice showed a further decrease in epithelial barrier function as demonstrated by the altered expression of tight junction related genes. Furthermore, mRNA expression levels of genes regulating cell growth were significantly increased in 4-week-old Muc2^{-/-} mice compared to WT mice, which most likely explain the increased crypt length in Muc2^{-/-} from the age of 21 days onwards as was described in Chapter 2.

Immunological responses during suckling-weaning transition

Although there were no signs of colitis during early postnatal life, we observed an influx of CD3-positive T-cells in Muc2^{-/-} mice at the postnatal age of 1.5 days as described in **Chapter 2**. Strikingly, at the age of two weeks WT mice also showed an increased influx of CD3-positive T-cells, which disappeared again after weaning. In Muc2^{-/-} mice a further increase was seen. Although T-cells are generally related to inflammation, the influx of T-cells in WT mice most likely does not involve a pathological process. The mucosal immune system is directly exposed to the external environment and stimulated by antigens consisting of commensal and potentially pathogenic micro-organisms and food antigens. The intestinal epithelium provides an essential part of innate immunity, as it must control the access of potential antigens and pathogens by means of tight junctions, antimicrobial substances and trapping of bacteria and viruses in the mucus layer. Although the exact mechanism of mucosal tolerance needs to be clarified, it most likely involves either a state of unresponsiveness of T lymphocytes to antigenic stimulation, or induction of regulatory T cells that produce anti-inflammatory cytokines such as IL 10 and/or TGF- β .¹⁸ On the other hand, intestinal growth during weaning has been related to a state of physiological inflammation which is supported by several lines of evidence.¹⁹⁻²⁴ Therefore, the changes observed in WT mice during the suckling and weaning transition can be largely attributed to the development of mucosal tolerance and establishment of epithelial growth by means of a physiological inflammatory reaction. However, in Muc2^{-/-} mice, the influx of CD3-positive T-cells is regarded as the first sign of colitis development. Due to the lack of Muc2, there is no protective mucus layer. This results in a direct contact between the microbiota and the intestinal epithelium and presumably alters or stimulates bacterial-TLR interactions and the subsequent signaling cascade that leads to the production of inflammatory cytokines. Moreover, the composition of the microbiota is very likely to play a role in disease development in Muc2^{-/-} mice. As the large mucus glycoproteins form a food source for certain bacteria in normal WT mice²⁵⁻²⁷, the microbiota in Muc2^{-/-} mice lacking this food-source is most likely different from WT animals and lead to altered cytokine profiles.

Of all upregulated genes in *Muc2*^{-/-} mice, described in **Chapter 3**, the majority were primarily involved in immune responses related to antigen processing/presentation, B- and T-cell receptor signaling, leukocyte transendothelial migration, and Jak-STAT signaling. Specifically, *Muc2*^{-/-} mice expressed high mRNA levels of immunoglobulins, murine histocompatibility 2, cytokines (e.g. *Tnf-α* and *Il1β*) and chemokines. Moreover, several antimicrobial proteins like the regenerating genes *Reg3β* and *Reg3γ*, and angiogenin-4 (*Ang4*) showed altered expression levels and therefore, we focused our attention on these genes in **Chapter 4**. *Reg3β*, *Reg3γ*, and *Ang4* play an important role during bacterial colonization. More specifically, expression of *Reg3γ* (also called HIP/PAP in humans), is up-regulated in the small intestine and colon after bacterial reconstitution of germ-free mice²⁸⁻²⁹ and expression of angiogenin-4 (*Ang4*), the orthologue of human ANG, is induced upon colonization with *Bacteroides thetaiotaomicron*, an anaerobe Gram-negative microbe that belongs to the normal mouse and human microbiota.³⁰ Therefore, we aimed to study the effect of weaning and the consequences of *Muc2*-deficiency on the expression and localization of these innate defense molecules. Interestingly, expression levels of *Reg3β*, *Reg3γ*, and *Ang4* in the proximal colon were considerably higher compared to expression levels in the distal colon of WT and *Muc2*^{-/-} mice. An intrinsic program encoded in the epithelial cells is most likely responsible for the segmental expression of the studied innate defense molecules.³¹⁻³² However, the microbiota also seem to play an important role. First of all, bacterial counts are higher in the proximal colon, compared to the distal colon.³³ Moreover, marked differences exist in the spatial association between commensal bacteria and the different segments of murine colonic wall.³⁴ For example, the cecum and proximal colon are tightly filled with high concentrations of bacteria and bacteria are in direct contact with the bowel wall. More importantly, abundant bacteria within colonic crypts are a uniform characteristic of proximal large intestinal segments. On the other hand, in the distal colon and rectum, intra-luminal bacteria were prohibited from contact to the bowel wall, and no microorganisms are detected in the colonic crypt.³⁴⁻³⁵ Swidsinski et al. hypothesize that these differences replicate functional differences between colonic segments. The 'physiological' contact that takes place between bacteria and the proximal large intestinal wall may underlie the tolerance of the colonic epithelium towards commensal bacteria that characterize the healthy state. Moreover, it offers an attractive explanation as to why colitis very often originates in the distal colon, where the bacteria are separated from the mucosa and tolerance does not develop.³⁴ In the *Muc2*^{-/-} colitis model, signs of colitis were mainly seen in the distal colon. This finding is likely to be related to spatial differences in bacterial concentrations and differences in the localization of bacteria in the crypts. Due to an absent mucus layer, bacteria are allowed to come into closer contact to the intestinal epithelium. In the proximal colon, this situation resembles physiological status since close contact of the bacteria to epithelial cells in the crypts is also seen in WT mice. However, in the distal colon, an important

shift takes place that enables bacterial-epithelial interaction due to the absence of Muc2. Although tolerance exists in the proximal colon, the distal colon is not able to induce mechanisms that establish tolerance which finally leads to the development of colitis.

The expression of *Reg3γ* and *Ang4* is differentially regulated by distinct bacteria, e.g. one specific bacterial species is a potent inducer of gene expression, whereas another species is less potent or even decreases expression levels.^{28,30,36} Several studies have suggested that HIP/PAP, the human homologue of *Reg3γ*, could have an anti-inflammatory capacity.³⁷⁻³⁹ This is in agreement with its strong induction observed during the course of inflammatory diseases such as pancreatitis, Crohn's disease and ulcerative colitis, but also with our finding that expression levels of *Reg3β* and *Reg3γ* were consistently higher in *Muc2^{-/-}* mice compared to WT mice in both the proximal and distal colon. In concordance with Chapter 2, differences in gene expression are most likely driven by differences in the intestinal microbiota in *Muc2^{-/-}* mice compared to WT mice, together with increased bacterial-epithelial contact due to the absence of Muc2 as the major constituent of the intestinal mucus barrier but also as a food source for bacteria. As the induction of *Reg3γ*, *Ang4* and presumably *Reg3β* differs upon stimulation with certain bacteria, specific inhabitants of the microbiota might be responsible for disease development on one hand or prevention of disease on the other hand. Therefore, influencing the microbiota towards the generation of an anti-inflammatory stimulus by means of *Reg*-gene or *Ang4* expression, might be a promising preventative strategy in case of intestinal inflammatory disease such as IBD and NEC.

Although no evident signs of small intestinal inflammation are present in the *Muc2^{-/-}* colitis model, we demonstrated that small intestinal expression of *Reg3β* and *Reg3γ* is increased in *Muc2^{-/-}* mice compared to WT mice after weaning, again suggesting altered innate defense capacity due to the lack of Muc2 and presumably changes in the intestinal microbiota.

Surprisingly, not all the genes that have antibacterial properties were upregulated during colitis development in *Muc2^{-/-}* mice. On the contrary, *Ang4* gene and protein expression appeared to be down regulated. It is known that *Ang4* can be cytotoxic to endothelial cells.⁴⁰ Therefore, the down-regulation of *Ang4* expression in *Muc2^{-/-}* mice at the age of 4 weeks might be a mechanism to prevent further tissue damage to the distal colonic mucosa. Consequently, the effects of this innate defense gene seems to be a very delicate balance between beneficial and harmful effects.

Focusing on the localization of *Reg3β*, *Reg3γ*, and *Ang4* in the intestinal epithelium we showed that *Reg3β*, *Reg3γ* and *Ang4* are expressed in goblet cells, enterocytes and Paneth cells. Besides secreting *Relmβ*, which is suggested to have an immune effector function⁴¹⁻⁴³, goblet cells were until now not known to play a role in innate defense response via the secretion anti-bacterial proteins. With our studies we highlighted a new and important role for goblet cells in innate defense, namely the expression of innate defense molecules.

Paneth cell abundance and function in acute and regenerative NEC

Paneth cells play a significant role in the innate immune response. Although Paneth cell dysfunction in NEC has been suggested⁴⁴, little is known about Paneth cell abundance and function in preterm infants with NEC. Therefore, we studied Paneth cell presence, protein expression, and developmental changes in preterm infants with NEC compared to both preterm and term control patients who underwent resection for intestinal developmental defects or intestinal diseases other than NEC in **Chapter 5**. Paneth cells execute their functions by production of antimicrobial proteins/peptides like lysozyme⁴⁵⁻⁴⁶, secretory phospholipase-A2 (sPLA2)⁴⁷, and human α -defensins (HD5 and -6).⁴⁸⁻⁴⁹ We demonstrated low Paneth cell numbers with low HD5 mRNA levels during acute NEC and Paneth cell hyperplasia with increased HD5 mRNA expression during reanastomosis. Paneth cell numbers in preterm controls that underwent reanastomosis were also increased compared to the initial corrective surgery. Although inflammation is not the primary characteristic in the control patients, there seems to be an inflammatory component that plays an important role in the period between the initial surgery and the reanastomosis, which might be involved in Paneth cell hyperplasia and metaplasia in these patients. A novel and unexpected finding in our study is the occurrence of Paneth cell metaplasia in the colon during NEC-recovery. Although Paneth cell metaplasia has not been described in NEC until now, this phenomenon has been reported in adult IBD patients.⁵⁰ During recovery, we showed that lysozyme, trypsin, and sPLA2 were present in intestinal outflow fluid and that protein isolates from ileostomy outflow fluid inhibited growth of bacteria in vitro, suggesting that Paneth cells in preterm infants are not only present but also functional by secreting their antimicrobial products in order to augment epithelial defense. Although human milk contains lysozyme, there was no difference in the antibacterial capacity between ileostomy outflow fluid from infants receiving breast milk compared to infants receiving formula feeding. The protective effects of human milk with regard to NEC are mostly related to differences in bacterial colonization between human milk-fed and formula-fed preterm infants. However, the presence or absence of the intestinal microbiota does not seem to have a major influence on the production of defensins.⁵¹⁻⁵² Therefore, the protective effects of human milk by means of influencing the intestinal microbiota in the prevention of NEC does not seem to be related to increased protective capacity via defensins. However, as the intestinal microbiota of NEC patients is different from healthy term infants, further research is needed to answer this hypothesis.

In conclusion, part I of this thesis demonstrates that the transition from mother's milk to solid food in *Muc2*^{-/-} mice coincided with the development of colitis and differences in gene expression profiles which might indicate 1) a preventative effect of mother's milk and 2) a major role for the intestinal microbiota that is established during this period. Moreover, innate defense capacity was significantly altered during the development

and/ or regeneration of disease, i.e. colitis development in *Muc2*^{-/-} mice and necrotizing enterocolitis in premature infants.

Dietary modulation of innate defense: implications for therapeutic and preventative strategies.

Since it was demonstrated in part I of this thesis that the type of nutrition, i.e. mother's milk versus solid food, seems to play a key role in the development of colitis, the effect of dietary interventions on innate defense was studied in further detail in part II.

Effect of probiotics on intestinal epithelial barrier function

Probiotics are effective in the prevention of NEC in premature infants⁵³ and possibly also IBD.⁵⁴⁻⁵⁵ However, the exact mechanisms through which probiotics exert their beneficial effect are largely unknown. Probiotics are capable of influencing many of the components of epithelial barrier function. Several cellular and molecular mechanisms are suggested for probiotic regulation in IBD therapy as reviewed by Vanderpool and co-workers.⁵⁶ For example, probiotics block pathogenic bacterial effects by producing bactericidal substances and competing with pathogens and toxins for adherence to the intestinal epithelium. Moreover, probiotics regulate immune responses by enhancing the innate immunity and modulating pathogen-induced inflammation via Toll-like receptor-regulated signaling pathways. Finally, probiotics regulate intestinal epithelial homeostasis by promoting intestinal epithelial cell survival, enhancing barrier function, and stimulating protective responses. As the mucin MUC2 plays an important role in intestinal barrier function, we hypothesized that *Lactobacillus rhamnosus* GG (LGG) increases MUC2 synthesis. Indeed, we showed that stimulation of LS174T cells leads to dose dependent increase in MUC2 mRNA expression and activation of the *MUC2* promoter via the transcription factor AP-1 in **Chapter 6**. Interestingly, nonviable bacteria, although less potent, and LGG conditioned culture media (LGG-CM) also stimulated *MUC2* promoter activation. Short chain fatty acids (SCFAs) were, at least partly, responsible for the stimulatory effect LGG-CM. However, as nonviable bacteria also induced MUC2 synthesis, it is likely that different mechanisms are responsible for the observed effects. This is also supported by the fact that mutation of the AP-1 site on the *MUC2* promoter only leads to partial inhibition of *MUC2* promoter transactivation, indicating that other mechanisms must be present to explain the remaining promoter transactivation after mutation of the AP-1 promoter binding site. Moreover, van Baarlen et al. showed that expression profiles of human mucosa displayed striking differences in modulation of NF- κ B-dependent pathways, depending on the specific growth phase of the probiotic bacterium *L. plantarum*.⁵⁷ Interestingly, in contrast to Schlee et al. demonstrated that lactobacilli and a bacterial mixture strengthen intestinal barrier function through activation of the human beta defensin-2 promoter via binding of AP-1 as well as NF- κ B.⁵⁸

Although NF- κ B activation generally leads to an inflammatory response via production of pro-inflammatory cytokines, limited activation of the transcription factors NF- κ B and AP-1 may be favourable, as the activation below the inflammation threshold might render the immune system more alert against hostile confrontations. Increasing NF- κ B production in patients that already have increased NF- κ B activation due to inflammatory processes, might explain the ineffectiveness of probiotic treatment in patients with IBD. Finally, this might, at least partially, explain the differences between different probiotic strains, as it was shown that they have opposite effects on the NF- κ B system.⁵⁹⁻⁶¹ Therefore, a tight balance between pro-inflammatory and anti-inflammatory factors, together with probiotic characteristics such as growth phase and specific strains and host factors such as availability of nutrients in the intestinal lumen, make the unraveling of probiotic mechanisms extremely complex.

Although Chapter 6 clearly indicates that probiotics exert their effect via induction of MUC2 synthesis, we aimed to study the effect of probiotic supplementation in Muc2-deficient mice, in search for other mechanisms that might be involved in this matter. Therefore, we treated Muc2^{-/-} and WT mice with a probiotic mixture of two *Bifidobacteria* in **Chapter 8**. Although no differences were observed in clinical disease activity such as growth retardation and gross blood loss, probiotic supplementation led to a significant decrease in crypt length in Muc2^{-/-} mice. This difference could not be attributed to alterations in immune responses such as CD3-positive T-cells influx or cytokine expression levels.

In most definitions of probiotics, viability throughout the gastrointestinal tract is a requirement. However, in Chapter 6, we show that nonviable bacteria and LGG-conditioned media also increase MUC2 synthesis. Therefore, viability of probiotics does not seem to be a prerequisite for efficacy of probiotic treatment. This feature can be of utmost importance for the use of probiotics in clinical trials, since safety of probiotics remains an issue. The administration of nonviable probiotic bacteria or specific metabolic bacterial products seems promising in this respect. Further clinical evaluation of these substances is needed. Perhaps, the definition of probiotics as 'live' bacteria should be subject to further discussion.

Probiotics exert their beneficial effects via several mechanisms

As SCFA were identified as biological secretagogues in LGG-CM, we further studied the effect of SCFAs (butyrate, propionate and acetate) on epithelial cell morphology, proliferation, and MUC2 as marker for epithelial protection (**Chapter 7**). All studied SCFAs showed a dose dependent increase in MUC2 mRNA expression. Interestingly, butyrate at a concentration of 1 mM induced an increase in MUC2 mRNA levels, whereas MUC2 mRNA levels returned to basal levels after incubation with 5–15 mM butyrate. This is especially interesting as the amount of butyrate is significantly higher in formula

fed infants compared to human milk fed infants.⁶² The latter have a decreased risk for the development of NEC. We therefore speculate that low concentrations of butyrate could have a protective effect on intestinal barrier function by increasing mucin MUC2 production, whereas moderate to high concentrations may decrease intestinal barrier function by decreasing MUC2 production. This effect might partially explain the difference in incidence of NEC between the formula-fed and human milk-fed newborn infants. Manipulation of the SCFA profile can be established by influencing the composition of microbiota, for instance by treatment with prebiotics, probiotics and/or human milk. This approach seems to be promising in the treatment of IBD and NEC. Several studies demonstrated the beneficial effect of butyrate on MUC2 synthesis, however, data seem to be conflicting. These conflicting results might be explained by the strict dose-effect relation of butyrate, as we have demonstrated.⁶³⁻⁶⁴ Moreover, the production of SCFAs has also been related to intestinal diseases.⁶⁵⁻⁶⁹ Since the microbiota and concomitant SCFA profiles are dependent on a large variety of factors, influencing the intestinal SCFA profile towards a beneficial composition is very challenging. Future studies examining the effect of probiotics and/or prebiotics and human milk on intestinal microbiota and subsequent SCFA profiles in premature infants are needed in this respect. Moreover, the beneficial effect of probiotics can only partly be attributed to SCFA production as nonviable bacteria also increase MUC2 synthesis, and therefore, further studies are needed to reveal other mechanisms of probiotic treatment.

Finally, MUC2 promoter regulation by butyrate at 10–15 mM was associated with increased acetylation of histone H3 and H4 and methylation of H3 at the promoter site. Acetylation and methylation are both known as epigenetic phenomena. Epigenetics is defined as ‘the study of inherited changes in phenotype or gene expression caused by mechanisms other than changes in the underlying DNA sequence’ and one of the most extensively studied modulators of epigenetics is the diet.⁷⁰ A wide variety of health problems and related therapies have been attributed to epigenetics. Therefore, influencing these inheritable changes via dietary interventions seems to be a powerful therapeutic tool.

Importance of daily diet in the Muc2^{-/-} experimental animal model

In **Chapter 8**, we studied the effect of two different diets on colitis-severity in Muc2^{-/-} mice. We demonstrated that a purified diet decreased disease severity in Muc2^{-/-} mice as reflected in alterations in body weight, crypt length and a variety of inflammatory markers and therefore the choice of diet plays a crucial role in this colitis model.

Two major differences are present between the studied diets, namely the protein source which is plant proteins in the standard rodent diet versus semi-synthetic proteins in purified diet and the amount of insoluble fibers that is significantly higher in the standard rodent diet. As both fibers and proteins form a source for bacterial fermentation,

differences in short chain fatty acid distribution might explain the difference in disease severity between the studied diets. For example, butyrate has an anti-inflammatory effect that is exerted by suppression of nuclear factor kappa B (NF- κ B) activation.⁷¹⁻⁷² Bacterial fermentation might explain the predilection site for colitis symptoms in the distal colon compared to the proximal colon. In more proximal regions of the large intestine, fermentative substrates consist mainly of non-digestible carbohydrates, e.g. resistant starch. In the distal colon, carbohydrate availability is lower, leading to increased fermentation of protein and amino acids.⁷³ One recognizable characteristic of ulcerative colitis, but also colitis in the Muc2^{-/-} mouse model is its increased prevalence in the distal compared with proximal colon. Unlike bacterial metabolism of carbohydrates, amino acid fermentation results in potentially toxic metabolites, including ammonia, amines and some phenolic compounds.⁷⁴ Therefore, it is possible that protein/ modified protein metabolism in this region is inter-related with development of disease. This might explain the localization of colitis in the distal colon of Muc2^{-/-} mice, but also the increased colitis-severity in animals that were fed the standard rodent diet compared to the semi-synthetic diet. Reduced digestibility of the standard rodent compared to the semi-synthetic diet, might result in a higher amount of undigested proteins in the distal colon, leading to the production of toxic metabolites.

Colostrum stimulates uptake of luminal threonine used for intestinal mucin MUC2 synthesis

Threonine (THR) is an essential amino acid that is of particular interest to the neonatal gut for mucin synthesis necessary for epithelial protection. The peptide backbone of MUC2 is particularly rich in THR constituting ~30% of the total amino acids.⁷⁵⁻⁷⁹ Therefore, threonine availability impacts mucosal protein synthesis and mucin synthesis in pigs and rats.⁸⁰⁻⁸³ The preferential site of threonine uptake, i.e. basolateral or luminal, for mucin synthesis has implications for (par)enteral nutritional therapy in the preterm infant since disruption of the mucus layer increases the risk of NEC. We therefore studied the preferential site of threonine absorption for MUC2 synthesis in partially enterally fed preterm infants and in colostrum and formula fed preterm pigs in **Chapter 9**. Our results show that threonine from both the basolateral and luminal side are used for MUC2 synthesis in preterm pigs and infants. However, full enteral feeding in preterm pigs stimulated luminal THR uptake accompanied by higher MUC2 synthesis rates when compared to partially enterally fed preterm infants. Furthermore, colostrum feeding in preterm pigs stimulated THR uptake from the luminal side, and increased MUC2 fractional synthesis rate, compared to formula feeding.

In conclusion, part II of this thesis clearly shows that dietary interventions can increase intestinal epithelial barrier function and thereby form a promising target for the prevention of intestinal inflammatory diseases.

Future Perspectives

Since the *Muc2*^{-/-} mouse model was not designed as a pure NEC model, future modifications to the existing model might convert it into a genuine NEC model. This model would enable us to study the role of MUC2 in the development of NEC in further detail. As it is known that formula feeding increases the risk of NEC development in premature neonates compared to human milk feeding, the effect of the neonatal diet on NEC development and the mechanisms that are involved in this should be investigated in further detail. Moreover, colonizing the animals with a bacterial preparation with species that are known to predominate in NEC, in particular *Gammaproteobacteria*⁸⁴, might further mimic the development in NEC in the *Muc2*^{-/-} mouse model.

Although the role of the microbiota in colitis development seems evident, the microbiota of *Muc2*^{-/-} mice has not been characterized yet. Additional studies will be needed to examine the microbiota itself, but also the effect of dietary interventions on the microbiota and the effect of specific bacterial species on colitis development. Currently, a mouse intestinal tract Chip is available, enabling us to study the microbiota in *Muc2*^{-/-} mice. Generation of germ-free mice and bacterial colonization of these mice with specific bacteria such as a 'NEC-like' dominated by *Gammaproteobacteria*, will increase our knowledge about the role of specific bacteria and mechanisms of disease development.

Intestinal bacteria use the glycosyl-chains of mucins as a nutrient source. As mentioned previously, mucins play a key role in the intestine as they form a physical barrier on top of the intestinal epithelium. The fetal intestine seems to contain immature mucins reflecting in low variability of mucin structures, i.e. oligosaccharide structures and glycosylation pattern compared to the adult intestine.⁸⁵ Moreover, fetal mucins only show slight variation in the expression level of certain glycans in contrast to adults. This suggests that region-specific glycosylation of intestinal mucins is acquired after birth, most likely depending on environmental factors such as nutrition and bacterial colonization. Furthermore, differences in sulfation and sialylation of acidic mucins were observed 4 days after birth in conventionally reared chicks again implicating a role for postnatal bacterial colonization of the intestine.⁸⁶ As immature mucins might limit intestinal barrier function in premature neonates, the expression and post-translational modifications of mucins in the premature intestine form an interesting topic for future research.

Besides specific gene expression as described in the previous paragraph, gene expression profiling in premature infants with and without NEC could contribute to our knowledge concerning the disease processes that are involved in NEC and de develop-

ment of the intestine in premature infants compared to term infants. These issues are currently under investigation within our research group.

A recent meta-analysis of randomized, controlled trials indicates that probiotic treatment results in a lower mortality and a decreased incidence of NEC in preterm (<34 weeks' gestation) VLBW neonates.⁵³ The dramatic effect sizes, tight confidence intervals, extremely low P-values, and overall evidence indicate that additional placebo controlled trials are unnecessary if a suitable probiotic product is available. Although probiotic sepsis has been reported in immunocompromised hosts and neonates⁸⁷⁻⁸⁹, it is reassuring to know that no significant adverse events, especially probiotic sepsis, have been reported in any of the trials included in the meta-analysis by Deshpande et al. and others.

Up to date, reports concerning adverse effects of probiotics are sparse and mainly concern case reports.⁹⁰⁻⁹⁷ Caution is especially warranted in severely ill patients, demonstrated in a study with adult patients suffering from acute pancreatitis.⁹⁰ Although this study examined a different patient group, the results warrant us to be extremely careful with the use of probiotics in premature infants. However, it is exactly this specific group of patients, i.e. premature infants and immune compromised patients, which form a group of interest for studying the effects of probiotics. The use of viable probiotics requires careful surveillance for probiotic sepsis, development of antibiotic resistance and altered immune responses in the long-term.⁹⁸ The administration of nonviable probiotic bacteria or specific metabolic bacterial products seems promising in this respect. However, further clinical evaluation of these substances is needed. Considering the abovementioned evidence for effectiveness of probiotic treatment, probiotics as a routine therapy for preterm neonates should be seriously advocated. Although additional placebo-controlled trials are not warranted according to the authors, the best suitable probiotic strain or combination of strains, associated dosage, duration and method of administration are still to be investigated. A recent study suggests that one-dose supplementation might be effective which might have serious implications on safety and practical issues.⁹⁹ The best approach to answer all open questions would be a randomized multi-centre trial in which different preparations, dosages, dosing intervals and strains or combinations of strains are compared. Moreover, extra attention needs to be paid to infants with a birth weight <1000g as this is the sole subgroup in which true evidence for effectiveness of probiotic preventative treatment is lacking.

In the seventies it was already acknowledged that infants fed human milk have a lower risk of developing NEC¹⁰⁰ together with an improved neurodevelopmental outcome.¹⁰¹⁻¹⁰² The mechanism of these effects of human milk is poorly understood. Most likely there is not one single factor but rather a synergism between the large variety of bioactive substances found in human milk and nutrients in human milk.¹⁰³ Although the quality of preterm infant formula has improved dramatically, up till now no infant formula has been designed that exerts all benefits of human milk. Although mothers are strongly

recommended to feed their children with expressed breast milk, only 25% of the infants receive own mother's milk at discharge from the neonatal intensive care unit. In the near future, a donor human milk bank will be implemented in the Netherlands as a multicenter open randomized intervention study to assess whether feeding VLBW infants with human milk based diet (own mother's milk or donor milk) results in a better outcome compared to an exclusively bovine milk based diet or a mixed diet. Moreover, this study will enable us to examine a broad range of biological markers that might play a role in NEC development that could serve as disease markers in the future.


As mothers' milk seems to possess protective effects against the development of colitis in *Muc2^{-/-}* mice, future experiments with prolonged human milk feeding or early administration of formula feeding would give us valuable information. Further studies on the exact bioactive substances in human milk would further increase our knowledge on the possibilities of mimicking these qualities in formula feeding.

Although a reduction of NEC-prevalence is expected in the group that will be fed exclusively with human milk, NEC will not be completely abolished. Therefore, the addition of probiotics to human milk in VLBW infants might further decrease NEC incidence and should be considered in this study. Especially in human donor milk this might be a valuable addition as probiotics that naturally occur in human milk¹⁰⁴, but also other compounds, are partly lost during the pasteurization process.

In this thesis, cell culture models and the *Muc2^{-/-}* mouse model were used to study several innate defense mechanisms. Although these models are invaluable, the findings of these studies still need to be translated to the human individual. Gene expression analysis of tissues samples from term and preterm infants with diseases such as NEC and congenital diseases of the intestinal tract is ongoing and will increase our knowledge. Moreover, it might direct our future research.

Concluding remarks

In this thesis we studied the development of colitis during the suckling-weaning transition phase and the effect of dietary interventions on innate defense. First of all, the *Muc2^{-/-}* mouse model was used to study colitis development during perinatal life and during suckling-weaning transition. In this period there is a major change in the diet, i.e. mothers' milk versus solid pelleted food. Moreover, bacterial colonization is established during this time frame, which makes this model a powerful tool to study innate defense responses during colitis development. Innate defense in NEC patients was studied in biopsies from premature infants that underwent surgery for severe NEC. We focused our attention on the expression of antimicrobial peptides during acute and regenerative NEC. Moreover, the effect of the diet, i.e. human milk feeding versus formula feeding on innate defense capacity was studied by measuring Paneth cell products in ileostomy outflow fluid and subsequently determining the antimicrobial capacity. Furthermore, we



studied the effect of the probiotic *Lactobacillus rhamnosus* GG and SCFAs on MUC2 synthesis in a goblet-cell like cell culture model and we elaborated on the mechanisms that are responsible for this effect. Finally, we studied the effect of two different diets and probiotic supplementation on disease severity in Muc2^{-/-} mice indicating that the choice of diet is crucial in the Muc2^{-/-} colitis-model and most likely also other disease models.

With this work, we gained insight into mechanisms involved in intestinal inflammatory diseases. Moreover, we increased the knowledge concerning the effects of dietary interventions on the development of intestinal inflammation and innate defense capacity in a susceptible host. Hopefully this will contribute the development and implementation of therapeutic strategies for diseases such as IBD and NEC.

REFERENCES

1. Van der Sluis M, De Koning BA, De Bruijn AC, Velcich A, Meijerink JP, Van Goudoever JB, Buller HA, Dekker J, Van Seuningen I, Renes IB, Einerhand AW. Muc2-deficient mice spontaneously develop colitis, indicating that MUC2 is critical for colonic protection. *Gastroenterology* 2006;131:117-29.
2. Davis CP, McAllister JS, Savage DC. Microbial colonization of the intestinal epithelium in suckling mice. *Infect Immun* 1973;7:666-72.
3. Inoue R, Otsuka M, Ushida K. Development of intestinal microbiota in mice and its possible interaction with the evolution of luminal IgA in the intestine. *Exp Anim* 2005;54:437-45.
4. Mackie RI, Sghir A, Gaskins HR. Developmental microbial ecology of the neonatal gastrointestinal tract. *Am J Clin Nutr* 1999;69:1035S-1045S.
5. Morelli L. Postnatal development of intestinal microflora as influenced by infant nutrition. *J Nutr* 2008;138:1791S-1795S.
6. Bouma G, Strober W. The immunological and genetic basis of inflammatory bowel disease. *Nat Rev Immunol* 2003;3:521-33.
7. Fiocchi C. Inflammatory bowel disease: etiology and pathogenesis. *Gastroenterology* 1998;115:182-205.
8. Strober W, Fuss IJ, Blumberg RS. The immunology of mucosal models of inflammation. *Annu Rev Immunol* 2002;20:495-549.
9. Kuhn R, Lohler J, Rennick D, Rajewsky K, Muller W. Interleukin-10-deficient mice develop chronic enterocolitis. *Cell* 1993;75:263-74.
10. van der Sluis M, Bouma J, Vincent A, Velcich A, Carraway KL, Buller HA, Einerhand AW, van Goudoever JB, Van Seuningen I, Renes IB. Combined defects in epithelial and immunoregulatory factors exacerbate the pathogenesis of inflammation: mucin 2-interleukin 10-deficient mice. *Lab Invest* 2008;88:634-42.
11. Walker A. Breast milk as the gold standard for protective nutrients. *J Pediatr* 2010;156:S3-7.
12. Donovan SM. Human milk oligosaccharides - the plot thickens. *Br J Nutr* 2009;101:1267-9.
13. Bode L. Human milk oligosaccharides: prebiotics and beyond. *Nutr Rev* 2009;67 Suppl 2: S183-91.
14. Gyorgy P, Norris RF, Rose CS. Bifidus factor. I. A variant of *Lactobacillus bifidus* requiring a special growth factor. *Arch Biochem Biophys* 1954;48:193-201.
15. Gauhe A, Gyorgy P, Hoover JR, Kuhn R, Rose CS, Ruelius HW, Zilliken F. Bifidus factor. IV. Preparations obtained from human milk. *Arch Biochem Biophys* 1954;48:214-24.
16. Coppa GV, Zampini L, Galeazzi T, Gabrielli O. Prebiotics in human milk: a review. *Dig Liver Dis* 2006;38 Suppl 2:S291-4.
17. Takeuchi O, Hoshino K, Kawai T, Sanjo H, Takada H, Ogawa T, Takeda K, Akira S. Differential roles of TLR2 and TLR4 in recognition of gram-negative and gram-positive bacterial cell wall components. *Immunity* 1999;11:443-51.
18. Mowat AM, Parker LA, Beacock-Sharp H, Millington OR, Chirido F. Oral tolerance: overview and historical perspectives. *Ann N Y Acad Sci* 2004;1029:1-8.
19. Cummins AG, Eglinton BA, Gonzalez A, Robertson DM. Immune activation during infancy in healthy humans. *J Clin Immunol* 1994;14:107-15.
20. Thompson FM, Catto-Smith AG, Moore D, Davidson G, Cummins AG. Epithelial growth of the small intestine in human infants. *J Pediatr Gastroenterol Nutr* 1998;26:506-12.

21. Cummins AG, Steele TW, LaBrooy JT, Shearman DJ. Maturation of the rat small intestine at weaning: changes in epithelial cell kinetics, bacterial flora, and mucosal immune activity. *Gut* 1988;29:1672-9.
22. Thompson FM, Mayrhofer G, Cummins AG. Dependence of epithelial growth of the small intestine on T-cell activation during weaning in the rat. *Gastroenterology* 1996;111:37-44.
23. Masjedi M, Tivey DR, Thompson FM, Cummins AG. Activation of the gut-associated lymphoid tissue with expression of interleukin-2 receptors that peaks during weaning in the rat. *J Pediatr Gastroenterol Nutr* 1999;29:556-62.
24. Schaeffer C, Diab-Assef M, Plateroti M, Laurent-Huck F, Reimund JM, Keding M, Foltzer-Jourdaine C. Cytokine gene expression during postnatal small intestinal development: regulation by glucocorticoids. *Gut* 2000;47:192-8.
25. Sonnenburg JL, Angenent LT, Gordon JI. Getting a grip on things: how do communities of bacterial symbionts become established in our intestine? *Nat Immunol* 2004;5:569-73.
26. Derrien M, Vaughan EE, Plugge CM, de Vos WM. *Akkermansia muciniphila* gen. nov., sp. nov., a human intestinal mucin-degrading bacterium. *Int J Syst Evol Microbiol* 2004;54:1469-76.
27. Martens EC, Chiang HC, Gordon JI. Mucosal glycan foraging enhances fitness and transmission of a saccharolytic human gut bacterial symbiont. *Cell Host Microbe* 2008;4:447-57.
28. Cash HL, Whitham CV, Behrendt CL, Hooper LV. Symbiotic bacteria direct expression of an intestinal bactericidal lectin. *Science* 2006;313:1126-30.
29. Ogawa H, Fukushima K, Naito H, Funayama Y, Unno M, Takahashi K, Kitayama T, Matsuno S, Ohtani H, Takasawa S, Okamoto H, Sasaki I. Increased expression of HIP/PAP and regenerating gene III in human inflammatory bowel disease and a murine bacterial reconstitution model. *Inflamm Bowel Dis* 2003;9:162-70.
30. Hooper LV, Stappenbeck TS, Hong CV, Gordon JI. Angiogenins: a new class of microbicidal proteins involved in innate immunity. *Nat Immunol* 2003;4:269-73.
31. Jobin C, Behrns KE, Brenner DA. Molecular and cellular biology of the small intestine. *Curr Opin Gastroenterol* 1999;15:103-7.
32. Walters JR, Howard A, Rumble HE, Prathalingam SR, Shaw-Smith CJ, Legon S. Differences in expression of homeobox transcription factors in proximal and distal human small intestine. *Gastroenterology* 1997;113:472-7.
33. Sarma-Rupavtarm RB, Ge Z, Schauer DB, Fox JG, Polz MF. Spatial distribution and stability of the eight microbial species of the altered schaedler flora in the mouse gastrointestinal tract. *Appl Environ Microbiol* 2004;70:2791-800.
34. Swidsinski A, Loening-Baucke V, Lochs H, Hale LP. Spatial organization of bacterial flora in normal and inflamed intestine: a fluorescence in situ hybridization study in mice. *World J Gastroenterol* 2005;11:1131-40.
35. Johansson ME, Phillipson M, Petersson J, Velcich A, Holm L, Hansson GC. The inner of the two Muc2 mucin-dependent mucus layers in colon is devoid of bacteria. *Proc Natl Acad Sci U S A* 2008;105:15064-9.
36. Sonnenburg JL, Chen CT, Gordon JI. Genomic and metabolic studies of the impact of probiotics on a model gut symbiont and host. *PLoS Biol* 2006;4:e413.
37. Heller A, Fiedler F, Schmeck J, Luck V, Iovanna JL, Koch T. Pancreatitis-associated protein protects the lung from leukocyte-induced injury. *Anesthesiology* 1999;91:1408-14.
38. Vasseur S, Folch-Puy E, Hlouschek V, Garcia S, Fiedler F, Lerch MM, Dagorn JC, Closa D, Iovanna JL. p8 improves pancreatic response to acute pancreatitis by enhancing the expres-

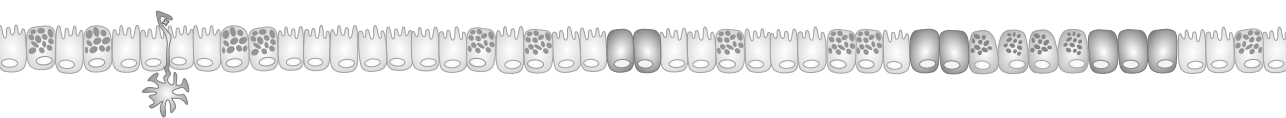
- sion of the anti-inflammatory protein pancreatitis-associated protein I. *J Biol Chem* 2004; 279:7199-207.
39. Zhang H, Kandil E, Lin YY, Levi G, Zenilman ME. Targeted inhibition of gene expression of pancreatitis-associated proteins exacerbates the severity of acute pancreatitis in rats. *Scand J Gastroenterol* 2004;39:870-81.
 40. Saxena SK, Rybak SM, Davey RT, Jr, Youle RJ, Ackerman EJ. Angiogenin is a cytotoxic, tRNA-specific ribonuclease in the RNase A superfamily. *J Biol Chem* 1992;267:21982-6.
 41. Artis D, Wang ML, Keilbaugh SA, He W, Brenes M, Swain GP, Knight PA, Donaldson DD, Lazar MA, Miller HR, Schad GA, Scott P, Wu GD. RELMbeta/FIZZ2 is a goblet cell-specific immune-effector molecule in the gastrointestinal tract. *Proc Natl Acad Sci U S A* 2004;101: 13596-600.
 42. Krimi RB, Kotelevets L, Dubuquoy L, Plaisancie P, Walker F, Lehy T, Desreumaux P, Van Seuninghen I, Chastre E, Forgue-Lafitte ME, Marie JC. Resistin-like molecule beta regulates intestinal mucous secretion and curtails TNBS-induced colitis in mice. *Inflamm Bowel Dis* 2008;14:931-41.
 43. Steppan CM, Brown EJ, Wright CM, Bhat S, Banerjee RR, Dai CY, Enders GH, Silberg DG, Wen X, Wu GD, Lazar MA. A family of tissue-specific resistin-like molecules. *Proc Natl Acad Sci U S A* 2001;98:502-6.
 44. Coutinho HB, da Mota HC, Coutinho VB, Robalinho TI, Furtado AF, Walker E, King G, Mahida YR, Sewell HF, Wakelin D. Absence of lysozyme (muramidase) in the intestinal Paneth cells of newborn infants with necrotising enterocolitis. *J Clin Pathol* 1998;51:512-4.
 45. Erlandsen SL, Parsons JA, Taylor TD. Ultrastructural immunocytochemical localization of lysozyme in the Paneth cells of man. *J Histochem Cytochem* 1974;22:401-13.
 46. Klockars M, Reitamo S. Tissue distribution of lysozyme in man. *J Histochem Cytochem* 1975; 23:932-40.
 47. Kiyohara H, Egami H, Shibata Y, Murata K, Ohshima S, Ogawa M. Light microscopic immunohistochemical analysis of the distribution of group II phospholipase A2 in human digestive organs. *J Histochem Cytochem* 1992;40:1659-64.
 48. Jones DE, Bevins CL. Paneth cells of the human small intestine express an antimicrobial peptide gene. *J Biol Chem* 1992;267:23216-25.
 49. Jones DE, Bevins CL. Defensin-6 mRNA in human Paneth cells: implications for antimicrobial peptides in host defense of the human bowel. *FEBS Lett* 1993;315:187-92.
 50. Tanaka M, Saito H, Kusumi T, Fukuda S, Shimoyama T, Sasaki Y, Suto K, Munakata A, Kudo H. Spatial distribution and histogenesis of colorectal Paneth cell metaplasia in idiopathic inflammatory bowel disease. *J Gastroenterol Hepatol* 2001;16:1353-9.
 51. Putsep K, Axelsson LG, Boman A, Midtvedt T, Normark S, Boman HG, Andersson M. Germ-free and colonized mice generate the same products from enteric prodefensins. *J Biol Chem* 2000;275:40478-82.
 52. Karlsson J, Putsep K, Chu H, Kays RJ, Bevins CL, Andersson M. Regional variations in Paneth cell antimicrobial peptide expression along the mouse intestinal tract. *BMC Immunol* 2008; 9:37.
 53. Deshpande G, Rao S, Patole S, Bulsara M. Updated meta-analysis of probiotics for preventing necrotizing enterocolitis in preterm neonates. *Pediatrics* 2010;125:921-30.
 54. Butterworth AD, Thomas AG, Akobeng AK. Probiotics for induction of remission in Crohn's disease. *Cochrane Database Syst Rev* 2008;CD006634.

55. Mallon P, McKay D, Kirk S, Gardiner K. Probiotics for induction of remission in ulcerative colitis. *Cochrane Database Syst Rev* 2007;CD005573.
56. Vanderpool HY. Surgeons as mirrors of common life: a novel inquiry into the ethics of surgery. *Tex Heart Inst J* 2009;36:449-50.
57. van Baarlen P, Troost FJ, van Hemert S, van der Meer C, de Vos WM, de Groot PJ, Hooiveld GJ, Brummer RJ, Kleerebezem M. Differential NF-kappaB pathways induction by *Lactobacillus plantarum* in the duodenum of healthy humans correlating with immune tolerance. *Proc Natl Acad Sci U S A* 2009;106:2371-6.
58. Schlee M, Harder J, Koten B, Stange EF, Wehkamp J, Fellermann K. Probiotic lactobacilli and VSL#3 induce enterocyte beta-defensin 2. *Clin Exp Immunol* 2008;151:528-35.
59. Kim YG, Ohta T, Takahashi T, Kushiro A, Nomoto K, Yokokura T, Okada N, Danbara H. Probiotic *Lactobacillus casei* activates innate immunity via NF-kappaB and p38 MAP kinase signaling pathways. *Microbes Infect* 2006;8:994-1005.
60. Ruiz PA, Hoffmann M, Szczesny S, Blaut M, Haller D. Innate mechanisms for *Bifidobacterium lactis* to activate transient pro-inflammatory host responses in intestinal epithelial cells after the colonization of germ-free rats. *Immunology* 2005;115:441-50.
61. Petrof EO, Kojima K, Ropeleski MJ, Musch MW, Tao Y, De Simone C, Chang EB. Probiotics inhibit nuclear factor-kappaB and induce heat shock proteins in colonic epithelial cells through proteasome inhibition. *Gastroenterology* 2004;127:1474-87.
62. Knol J, Scholtens P, Kafka C, Steenbakkers J, Gro S, Helm K, Klarczyk M, Schopfer H, Bockler HM, Wells J. Colon microflora in infants fed formula with galacto- and fructo-oligosaccharides: more like breast-fed infants. *J Pediatr Gastroenterol Nutr* 2005;40:36-42.
63. Hamer HM, Jonkers DM, Vanhoutvin SA, Troost FJ, Rijkers G, de Bruine A, Bast A, Venema K, Brummer RJ. Effect of butyrate enemas on inflammation and antioxidant status in the colonic mucosa of patients with ulcerative colitis in remission. *Clin Nutr* 2010.
64. Hamer HM, Jonkers D, Venema K, Vanhoutvin S, Troost FJ, Brummer RJ. Review article: the role of butyrate on colonic function. *Aliment Pharmacol Ther* 2008;27:104-19.
65. Lin J, Nafday SM, Chauvin SN, Magid MS, Pabbatireddy S, Holzman IR, Babyatsky MW. Variable effects of short chain fatty acids and lactic acid in inducing intestinal mucosal injury in newborn rats. *J Pediatr Gastroenterol Nutr* 2002;35:545-50.
66. Nafday SM, Green RS, Chauvin SN, Holzman IR, Magid MS, Lin J. Vitamin A supplementation ameliorates butyric acid-induced intestinal mucosal injury in newborn rats. *J Perinat Med* 2002;30:121-7.
67. MacPherson BR, Pfeiffer CJ. Experimental production of diffuse colitis in rats. *Digestion* 1978;17:135-50.
68. Kim HS, Berstad A. Experimental colitis in animal models. *Scand J Gastroenterol* 1992;27:529-37.
69. Di Lorenzo M, Bass J, Krantis A. An intraluminal model of necrotizing enterocolitis in the developing neonatal piglet. *J Pediatr Surg* 1995;30:1138-42.
70. Cooney CA, Dave AA, Wolff GL. Maternal methyl supplements in mice affect epigenetic variation and DNA methylation of offspring. *J Nutr* 2002;132:2393S-2400S.
71. Andoh A, Fujiyama Y, Hata K, Araki Y, Takaya H, Shimada M, Bamba T. Counter-regulatory effect of sodium butyrate on tumour necrosis factor-alpha (TNF-alpha)-induced complement C3 and factor B biosynthesis in human intestinal epithelial cells. *Clin Exp Immunol* 1999;118:23-9.

72. Place RF, Noonan EJ, Giardina C. HDAC inhibition prevents NF-kappa B activation by suppressing proteasome activity: down-regulation of proteasome subunit expression stabilizes I kappa B alpha. *Biochem Pharmacol* 2005;70:394-406.
73. Macfarlane GT, Gibson GR, Cummings JH. Comparison of fermentation reactions in different regions of the human colon. *J Appl Bacteriol* 1992;72:57-64.
74. Macfarlane GT, Cummings JH, Allison C. Protein degradation by human intestinal bacteria. *J Gen Microbiol* 1986;132:1647-56.
75. Gum JR, Jr., Hicks JW, Toribara NW, Rothe EM, Lagace RE, Kim YS. The human MUC2 intestinal mucin has cysteine-rich subdomains located both upstream and downstream of its central repetitive region. *J Biol Chem* 1992;267:21375-83.
76. Lien KA, Sauer WC, Fenton M. Mucin output in ileal digesta of pigs fed a protein-free diet. *Z Ernährungswiss* 1997;36:182-90.
77. Mantle M, Allen A. Isolation and characterization of the native glycoprotein from pig small-intestinal mucus. *Biochem J* 1981;195:267-75.
78. Allen A, Hutton DA, Pearson JP. The MUC2 gene product: a human intestinal mucin. *Int J Biochem Cell Biol* 1998;30:797-801.
79. Toribara NW, Gum JR, Jr., Culhane PJ, Lagace RE, Hicks JW, Petersen GM, Kim YS. MUC-2 human small intestinal mucin gene structure. Repeated arrays and polymorphism. *J Clin Invest* 1991;88:1005-13.
80. Faure M, Mettraux C, Moennoz D, Godin JP, Vuichoud J, Rochat F, Breuille D, Obled C, Corthesy-Theulaz I. Specific amino acids increase mucin synthesis and microbiota in dextran sulfate sodium-treated rats. *J Nutr* 2006;136:1558-64.
81. Nichols NL, Bertolo RF. Luminal threonine concentration acutely affects intestinal mucosal protein and mucin synthesis in piglets. *J Nutr* 2008;138:1298-303.
82. Law GK, Bertolo RF, Adjiri-Awere A, Pencharz PB, Ball RO. Adequate oral threonine is critical for mucin production and gut function in neonatal piglets. *Am J Physiol Gastrointest Liver Physiol* 2007;292:G1293-301.
83. Faure M, Moennoz D, Montigon F, Mettraux C, Breuille D, Ballevre O. Dietary threonine restriction specifically reduces intestinal mucin synthesis in rats. *J Nutr* 2005;135:486-91.
84. Wang Y, Hoenig JD, Malin KJ, Qamar S, Petrof EO, Sun J, Antonopoulos DA, Chang EB, Claud EC. 16S rRNA gene-based analysis of fecal microbiota from preterm infants with and without necrotizing enterocolitis. *ISME J* 2009;3:944-54.
85. Robbe-Masselot C, Maes E, Rousset M, Michalski JC, Capon C. Glycosylation of human fetal mucins: a similar repertoire of O-glycans along the intestinal tract. *Glycoconj J* 2009;26:397-413.
86. Forder RE, Howarth GS, Tivey DR, Hughes RJ. Bacterial modulation of small intestinal goblet cells and mucin composition during early posthatch development of poultry. *Poult Sci* 2007;86:2396-403.
87. Thompson C, McCarter YS, Krause PJ, Herson VC. *Lactobacillus acidophilus* sepsis in a neonate. *J Perinatol* 2001;21:258-60.
88. Broughton RA, Gruber WC, Haffar AA, Baker CJ. Neonatal meningitis due to *Lactobacillus*. *Pediatr Infect Dis* 1983;2:382-4.
89. Perapoch J, Planes AM, Querol A, Lopez V, Martinez-Bendayan I, Tormo R, Fernandez F, Peguero G, Salcedo S. Fungemia with *Saccharomyces cerevisiae* in two newborns, only one of whom had been treated with ultra-levura. *Eur J Clin Microbiol Infect Dis* 2000;19:468-70.

90. Besselink MG, van Santvoort HC, Buskens E, Boermeester MA, van Goor H, Timmerman HM, Nieuwenhuijs VB, Bollen TL, van Ramshorst B, Witteman BJ, Rosman C, Ploeg RJ, Brink MA, Schaapherder AF, Dejong CH, Wahab PJ, van Laarhoven CJ, van der Harst E, van Eijk CH, Cuesta MA, Akkermans LM, Gooszen HG, Dutch Acute Pancreatitis Study G. Probiotic prophylaxis in predicted severe acute pancreatitis: a randomised, double-blind, placebo-controlled trial. *Lancet* 2008;371:651-9.
91. Chomarat M, Espinouse D. *Lactobacillus rhamnosus* septicemia in patients with prolonged aplasia receiving ceftazidime-vancomycin. *Eur J Clin Microbiol Infect Dis* 1991;10:44.
92. Griffiths JK, Daly JS, Dodge RA. Two cases of endocarditis due to *Lactobacillus* species: antimicrobial susceptibility, review, and discussion of therapy. *Clin Infect Dis* 1992;15:250-5.
93. Kalima P, Masterton RG, Roddie PH, Thomas AE. *Lactobacillus rhamnosus* infection in a child following bone marrow transplant. *J Infect* 1996;32:165-7.
94. Land MH, Rouster-Stevens K, Woods CR, Cannon ML, Cnota J, Shetty AK. *Lactobacillus* sepsis associated with probiotic therapy. *Pediatrics* 2005;115:178-81.
95. Patel R, Cockerill FR, Porayko MK, Osmon DR, Ilstrup DM, Keating MR. *Lactobacillemia* in liver transplant patients. *Clin Infect Dis* 1994;18:207-12.
96. Rahman M. Chest infection caused by *Lactobacillus casei* ss *rhamnosus*. *Br Med J (Clin Res Ed)* 1982;284:471-2.
97. Salminen MK, Tynkkynen S, Rautelin H, Saxelin M, Vaara M, Ruutu P, Sarna S, Valtonen V, Jarvinen A. *Lactobacillus* bacteremia during a rapid increase in probiotic use of *Lactobacillus rhamnosus* GG in Finland. *Clin Infect Dis* 2002;35:1155-60.
98. Ammor MS, Florez AB, van Hoek AH, de Los Reyes-Gavilan CG, Aarts HJ, Margolles A, Mayo B. Molecular characterization of intrinsic and acquired antibiotic resistance in lactic acid bacteria and bifidobacteria. *J Mol Microbiol Biotechnol* 2008;14:6-15.
99. Richard MG, O'Connor PM, David R, Gene D, Anthony RC, Paul RR, Catherine S. Prolonged faecal excretion following a single dose of probiotic in low birth weight infants. *Acta Paediatr* 2010.
100. Kliegman RM, Pittard WB, Fanaroff AA. Necrotizing enterocolitis in neonates fed human milk. *J Pediatr* 1979;95:450-3.
101. Lucas A, Morley R, Cole TJ, Lister G, Leeson-Payne C. Breast milk and subsequent intelligence quotient in children born preterm. *Lancet* 1992;339:261-4.
102. Lucas A, Morley R, Cole TJ. Randomised trial of early diet in preterm babies and later intelligence quotient. *BMJ* 1998;317:1481-7.
103. Newburg DS, Walker WA. Protection of the neonate by the innate immune system of developing gut and of human milk. *Pediatr Res* 2007;61:2-8.
104. Martin R, Langa S, Reviriego C, Jimenez E, Marin ML, Xaus J, Fernandez L, Rodriguez JM. Human milk is a source of lactic acid bacteria for the infant gut. *J Pediatr* 2003;143:754-8.

Chapter 11



Samenvatting



Necrotiserende enterocolitis (NEC) is een ernstige darmziekte die met name voorkomt bij prematuur geboren neonaten. Ondanks de recente vooruitgang in de zorg voor prematuur geboren neonaten, veroorzaakt NEC een aanzienlijke morbiditeit en mortaliteit. Vanwege het toegenomen aantal zeer immature pasgeborenen en de toegenomen overlevingskansen van pasgeborenen met een zeer laag geboortegewicht (de zogenaemde very low birth weight infants met een geboortegewicht lager dan 1500g; VLBW), zal de NEC incidentie verder stijgen als er geen adequate preventieve therapie gevonden wordt.

Prematuriteit, voeding via het maag-darmkanaal en bacteriële kolonisatie zijn bekende risico factoren voor het ontwikkelen van NEC. Echter, de exacte etiologie is nog grotendeels onbekend. De therapeutische opties zijn beperkt tot ondersteunde therapie en chirurgische interventie en naast borstvoeding bestaat er tot op heden geen preventieve therapie.

Aangezien deze ziekte aanzienlijke consequenties heeft voor gezondheidszorg kosten en kwaliteit van leven, is er een dringende behoefte aan een beter begrip van de mechanismen waardoor de ernstige schade veroorzaakt wordt, hetgeen uiteindelijk mogelijk kan leiden tot preventieve en therapeutische interventies.

Dit proefschrift is ingedeeld in twee delen waarbij epitheliale afweermechanismen in de darmen gedurende het vroege postnatale leven in muizen en mensen worden beschreven in deel 1 en het effect van dieet interventies op darmbarrierefunctie *in vitro* and *in vivo* worden beschreven in deel 2.

De belangrijkste bevindingen van dit proefschrift worden samengevat in dit hoofdstuk.

In **Hoofdstuk 2**, werd de ontwikkeling van colitis in Muc2 knockout (Muc2^{-/-}) muizen gedurende de perinatale periode en de transitie van moedermelk naar vast voedsel (vanaf nu 'spenen' genoemd) bestudeerd. Het mucine Muc2 is de structurele component van de mucuslaag in het colon. Uit eerdere studies is bekend dat afwezigheid van Muc2 chronische colitis veroorzaakt in Muc2^{-/-} muizen. De ontwikkeling van colitis gedurende het foetale en/ of vroeg postnatale leven was tot heden nog niet onderzocht. In dit hoofdstuk wordt beschreven dat Muc2^{-/-} muizen in utero geen tekenen van colitis vertoonden. De eerste subtiele tekenen van colitis, namelijk influx van Cd3-positieve T-cellen, werden gezien op de postnatale leeftijd van 1.5 dag in het distale colon. In wildtype muizen (WT) werd een verhoogde influx van T-cellen gezien op de postnatale leeftijd van 14 dagen, hetgeen naar alle waarschijnlijkheid veroorzaakt wordt door een fysiologische ontstekingsreactie. Na spenen, op de leeftijd van 21 dagen, nam het aantal Cd3-positieve T-cellen af in WT muizen. In tegenstelling tot WT muizen, was er in Muc2^{-/-} muizen sprake

van een toename van het aantal Cd3-positieve T-cellen. In *Muc2^{-/-}* muizen was er voor spenen reeds sprake van een krachtige immuun-respons, waarbij pro-inflammatoire cytokines in balans gehouden werden door anti-inflammatoire cytokines en immuunsuppressieve factoren. Er was daarbij geen uitgesproken dominantie van een van de specifieke T helper (th) cellen Th1, Th2 of Th17. Na spenen, op de leeftijd van 28 dagen, was de expressie van *Foxp3*, *Il-12 p35*, *Tgfb1*, and *Tnf-a* significant verlaagd in *Muc2^{-/-}* muizen vergeleken met de expressie voor spenen, terwijl *Il-10* gen-expressie behouden bleef. Hierdoor lijkt de Th2 immuunrespons op deze leeftijd een prominente rol te spelen. Vanaf de leeftijd van 21 dagen werden er milde morfologische verschijnselen van colitis gezien, zich uitend in toegenomen crypt lengte en toegenomen influx van CD3-positieve T-cellen. Ernstige colitis-verschijnselen, zoals verdere toename van cryptlengte, persisterende aanwezigheid van toegenomen aantallen Cd3-positieve T-cellen, epitheliale afvlakking en oppervlakkige erosie van het epitheel, werden waargenomen vanaf de leeftijd van 28 dagen. Met behulp van kwantitatieve RT-PCR (qRT-PCR) werd aangetoond dat expressie profielen van de Toll-like receptoren (TLr) Tlr2, Tlr4 en Tlr9 en goblet-cel specifieke eiwit-expressie beïnvloed worden door spenen en correleren met de toename van de ernst van colitis verschijnselen in *Muc2^{-/-}* muizen.

In **Hoofdstuk 3** werden genexpressie profielen bestudeerd met behulp van microarrays om genen en biologische reacties te identificeren die een rol spelen bij de ontwikkeling van colitis in *Muc2^{-/-}* muizen. Een groot deel van genen die sterk verhoogd tot expressie kwamen in *Muc2^{-/-}* muizen op de leeftijd van 2 en 4 weken, waren betrokken bij immuunresponsen die gerelateerd zijn aan antigeenverwerking en -presentatie, B-cel en T-cel receptor signaling, leucocyte transendotheel migratie en Jak-STAT signaling. Met name de mRNA expressie van immuunglobulines, murine histocompatibility-2, pro-inflammatoire cytokines en antimicrobiële eiwitten was sterk verhoogd in *Muc2^{-/-}* muizen. Daarnaast was de expressie van genen die betrokken zijn bij celstructuur gerelateerde pathways significant verschillend van WT muizen op de leeftijd van 4 weken. Vooral het tight-junction geassocieerde gen claudin-10 kwam verhoogd tot expressie, terwijl claudin-1 en claudin-5 juist verlaagd tot expressie werden gebracht. Bovendien vertoonden 4 weken oude *Muc2^{-/-}* muizen een verhoogde expressie van genen die celgroei reguleren, tezamen met verhoogde cryptlengte en verhoogde epitheliale proliferatie. Hieruit kan geconcludeerd worden dat afwezigheid van Muc2 leidt tot een actieve immuun-respons in 2 en 4 weken oude *Muc2^{-/-}* muizen. Tevens vertoonden 4 weken oude *Muc2^{-/-}* muizen een vermindering van epitheliale barrière functie en een verhoging van epitheliale proliferatie zoals aangetoond door respectievelijk veranderde expressie van tight junction gerelateerde genen en verhoogde expressie van genen die celgroei stimuleren. Met behulp van deze data werd aangetoond worden dat er verschillende fasen van colitis ontwikkeling zijn in *Muc2^{-/-}* muizen.

In Hoofdstuk 3 werd reeds aangetoond dat de expressie van antimicrobiële eiwitten zoals de zogenoemde regenerating genes *Reg3β* and *Reg3γ*, en angiogenin-4 (*Ang4*) verhoogd tot expressie komen in 2 en 4 weken oude *Muc2^{-/-}* muizen. In **Hoofdstuk 4** werden deze genen daarom in verder detail bestudeerd. Hierbij was het doel om de gevolgen van *Muc2*-deficiëntie op de expressie van de anti-bacteriële eiwitten *Reg3β*, *Reg3γ* en *Ang4* in de darmen te bestuderen. De afwezigheid van *Muc2* veroorzaakte een sterk verhoogde expressie van *Reg3β* en *Reg3γ* mRNA in de dunne darm en het colon. De expressie van *Reg3β*, *Reg3γ* en *Ang4* mRNA in de dunne darm en het proximale colon was verhoogd ten opzichte van het distale colon. Daarnaast was de expressie van *Reg3β*, *Reg3γ* en *Ang4* mRNA verlaagd op de leeftijd van 4 weken ten opzichte van 2 weken in het distale colon van *Muc2^{-/-}* muizen. Dit is met name interessant omdat morfologische tekenen van colitis met name in het distale colon gezien worden. Met behulp van *in situ* hybridisatie en immunohistochemie werd aangetoond dat *Reg3β*, *Reg3γ* en *Ang4* tot expressie gebracht worden in Paneth cellen in de dunne darm en enterocyten en goblet cellen in zowel dunne darm als colon. Met name de expressie van antimicrobiële eiwitten in goblet cellen benadrukt een nieuwe en belangrijke rol voor goblet cellen in de aangeboren afweer van de darmen. Tezamen suggereren deze data dat *Reg3* eiwitten en/ of *Ang4* darmontsteking/ darmschade beperken.

Paneth cellen produceren antimicrobiële eiwitten die een belangrijk onderdeel vormen van de afweer in de darmen, in het bijzonder de zogenoemde aangeboren afweer of 'innate defense'. In **Hoofdstuk 5** worden de aanwezigheid van Paneth cellen, de expressie van antimicrobiële eiwitten en ontwikkelingsgerelateerde veranderingen hierin bestudeerd in premature neonaten met NEC. Tevens wordt de aanwezigheid en antimicrobiële activiteit van Paneth cel producten in stomavloeistof van NEC patiënten gemeten. Darmweefsel van NEC patiënten en premature en à terme controle patiënten met een aangeboren of verworven darmafwijking zoals atresie, malrotatie en gastroschisis, werd verzameld gedurende chirurgische resectie van darmweefsel en gedurende reanastomose van het stoma na herstel van de acute ziekteperiode. Gedurende de acute fase van NEC was het aantal Paneth cellen in de dunne darm verminderd ten opzichte van premature controle patiënten. Na herstel van NEC werd er Paneth cel hyperplasie aangetoond in de dunne darm, hetgeen bevestigd werd door een toegenomen expressie van HD5 mRNA in het ileum. In het colon was er sprake van metaplasie, aangezien er Paneth cellen aangetoond werden, waar deze bij gezonde individuen alleen aanwezig zijn in de dunne darm. In stomavloeistof konden Paneth cel eiwitten worden aangetoond die groei van bacteriën remden. De inductie van Paneth cel hyperplasie en metaplasia gedurende de herstelfase van NEC is suggestief voor een toegenomen capaciteit van het innate defense system in reactie op uitgestelde ontsteking. Dit bevestigt het belang van Paneth cellen in innate defense en suggereert

dat toegenomen eiwit expressie en secretie van Paneth-cell producten bijdraagt aan de genezing van NEC.

Aan het gebruik van probiotica worden verschillende positieve effecten toegeschreven. Echter, het exacte werkingsmechanisme is nog grotendeels onbekend. Derhalve wordt in **Hoofdstuk 6** het effect van het probioticum *Lactobacillus rhamnosus* GG (LGGs) op MUC2 synthese in LS174T cellen, een humane goblet cel-achtige cellijn, beschreven. LS174T cellen werden behandeld met levende LGGs, geïnactiveerde LGGs of LGGs cultuurmedium (CM) waarin LGGs overnacht gekweekt werden (LGG-geconditioneerd CM, LGG-CM). Behandeling van LS174T cellen met LGG resulteerde in een dosisafhankelijke toename van de hoeveelheid MUC2 mRNA en MUC2 promotor transactivatie. Levende LGGs induceerden een sterkere toename in MUC2 expressie en MUC2 promotor transactivatie vergeleken met geïnactiveerde LGGs. Stimulatie van LS174T cellen met LGG-CM veroorzaakte eveneens een toename in de hoeveelheid MUC2 mRNA en MUC2 promotor transactivatie. Het gegeven dat zowel levende als geïnactiveerde bacteriën een krachtig stimulerend effect hebben op MUC2 synthese is met name interessant voor het gebruik van probiotica in klinische studies, aangezien veiligheid van probiotica behandeling een terugkerend probleem is. Geïnactiveerde bacteriën of metabole eindproducten van bacteriële fermentatie zijn wellicht veelbelovend in dit opzicht. De definitie van probiotica als 'levende bacteriën' staat in dit licht ter discussie.

Op zoek naar de biologisch actieve stof die verantwoordelijk is voor de inductie van MUC2, werden LS174T cellen gestimuleerd met LGG-CM en dat van tevoren blootgesteld was aan verschillende biochemische behandelingen, namelijk hitte behandeling, DNase behandeling en behandeling met proteasen (proteïnase K, trypsine en papaïne). Geen van de biochemische behandelingen had effect op de hoeveelheid MUC2 mRNA. Ook werd er geen verlies van MUC2 promotor transactivatie gezien. Een en ander impliceert dat bacterieel DNA en gesecreteerde eiwitten niet als de biologisch actieve stoffen aangemerkt kunnen worden.

Korte keten vertzuren, de zogenoemde short chain fatty acids (SCFAs) worden met name in de dikke darm gevormd door bacteriële fermentatie van onverteerde koolhydraten. SCFAs, in het bijzonder butyraat, propionaat en acetaat, zijn de voornaamste anionen in het lumen van de dikke darm. Stimulatie van LS174T cellen met korte keten vetzuren, de zogenoemde short chain fatty acids (SCFA) zoals die gemeten werden in LGG-CM veroorzaakte een toegenomen MUC2 promotor transactivatie. Daarbij bleek een combinatie van de verschillende SCFAs effectiever vergeleken met de individuele SCFAs, hetgeen een synergistisch effect impliceert.

In **Hoofdstuk 7** wordt het effect van SCFAs op mucine synthese in verder detail bestudeerd. Hierbij werd aangetoond dat stimulatie van LS174T cellen met een lage

concentratie butyraat (1 mM) mucine synthese stimuleert, terwijl gematigde tot hoge concentraties (5-15 mM) de hoeveelheid MUC2 mRNA juist terug laten keren naar basale waarden. Het laatste is vooral interessant in het licht van de butyraat concentratie in ontlasting van pasgeborenen, waarbij in pasgeborenen die flesvoeding krijgen een hogere butyraat concentratie gemeten wordt dan bij kinderen die moedermelk krijgen. Propionaat en acetaat induceerden ook de synthese van MUC2. Echter, bij concentraties van 5-15 mM bleef de hoeveelheid MUC2 mRNA gelijk.

Vervolgens werden de mechanisme die het butyraat gemedieerde effect op MUC2 synthese reguleren bestudeerd. SCFA-gevoelige regio's en *cis*-elementen in de MUC2 promoter werden geïdentificeerd met behulp van transfectie assays en gel-shift assays. Hierbij werd een actief AP-1 (c-Fos/c-Jun) *cis*-element ter hoogte van -818/-808 gevonden die het stimulerende effect van butyraat veroorzaakt. Het effect van butyraat op epigenetische veranderingen werd bestudeerd met behulp van chromatine immuunprecipitatie assays, waarbij MUC2 regulatie door hoge concentraties butyraat geassocieerd was met toegenomen acetylatie van histon H3 en H4 en methylatie van H3 op de MUC2 promoter.

In eerdere experimenten van van der Sluis et al. en Velcich et al. werd duidelijk dat het fenotype van de *Muc2*^{-/-} muis variabel is. Aanvankelijk werd dit gewijd aan de genetische achtergrond van het muismodel. Echter, dit kon de zeer wisselende fenotypes niet geheel verklaren. Vanuit humane studies is bekend dat voeding een belangrijke rol speelt in de ontwikkeling van NEC en de behandeling van IBD. In **Hoofdstuk 8** werd daartoe het effect van twee verschillende diëten en het effect van probiotica substitutie op de ernst van colitis-verschijnselen in *Muc2*^{-/-} muizen bestudeerd. *Muc2*^{-/-} muizen en WT muizen kregen na spenen een semi-synthetisch dieet (AIN-93G), een niet-synthetisch dieet (standaard knaagdierenvoer) of een niet synthetisch dieet gesupplementeerd met probiotica (*Bifidobacterium breve* en *Bifidobacterium animalis subsp. lactis* in eindconcentratie van 1x10⁹CFU/dier/dag) of controle (maltodextrine) gedurende 5 weken. De diëten verschillen met name in de hoeveelheid vezels, waarbij het semi-synthetische dieet 60% minder vezels bevat vergeleken met het niet-synthetische dieet. Daarnaast bestaat het semi-synthetische dieet voornamelijk uit caseïne eiwit en het niet-synthetische dieet uit planteiwit. Het type dieet veroorzaakte geen significante verschillen in lichaamsgewicht, crypt lengte of influx van immuuncellen in WT muizen. Echter, in *Muc2*^{-/-} muizen resulteerde het semi-synthetische dieet in verminderde ziekte-ernst, zich uitend in een hoger lichaamsgewicht en afgenomen cryptlengte, vergeleken met het niet-synthetische dieet. De laatstgenoemde groep vormt een intermediaire groep tussen de gezonde WT muizen en de *Muc2*^{-/-} muizen met ernstige colitis-verschijnselen die het niet-synthetische dieet kregen. In *Muc2*^{-/-} muizen die gesuppleerd werden met probiotica, werd een reductie van de cryptlengte gezien, vergeleken met de dieren die het controle mengsel

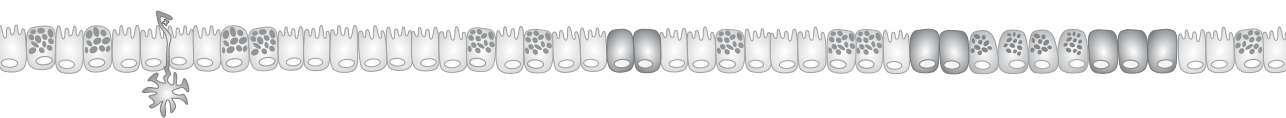
222

kregen. Echter, er werden na probiotica toediening geen verschillen gezien in klinische verschijnselen zoals lichaamsgewicht, macroscopisch bloedverlies of diarree. Tenslotte vertoonden *Muc2*^{-/-} muizen die het semi-synthetische dieet kregen een verminderde influx van S100a8 en S100a9 (waarvan de dimeer calprotectin genoemd wordt; een maat voor ontsteking in de darmen) en CD3 positieve T-cellen als marker voor ontsteking, vergeleken met *Muc2*^{-/-} muizen die het niet-synthetische dieet of het niet-synthetische dieet gesuppleerd met probiotica kregen, hetgeen eveneens wijst op een verminderde ziekte-activiteit in *Muc2*^{-/-} dieren die het semi-synthetische dieet kregen. De bevindingen van dit hoofdstuk benadrukken het belang van de dieet-keuze in dierexperimenten, aangezien het ziektemodel aanzienlijk beïnvloed kan worden door het dieet.

Hoofdstuk 9

MUC2 is het voornaamste secretoire mucine in menselijke darm en wordt gesynthetiseerd door goblet cellen. Het eiwit Muc2 in de darm wordt gekenmerkt door tandem repeats van de aminozuren threonine, proline en serine. De grote hoeveelheden threonine die worden ingebouwd in eiwitten van de darm kunnen de Muc2 synthese in de gobletcellen van de darm weerspiegelen. In eerdere studies werd reeds aangetoond dat systemische/arteriële snel geïncorporeerd wordt in MUC2 in de dunne darm van prematuur geboren neonaten. Echter, tot op heden was onbekend of goblet cellen in staat zijn om threonine vanuit de luminale zijde van de darm op te nemen voor MUC2 synthese. In deze studie werd de voorkeursplaats voor absorptie van threonine voor MUC2 synthese in preterme biggen en preterme neonaten met een ileostomie bestudeerd met behulp van de infusie van twee stabiele isotopen. Zowel threonine van de basolaterale zijde als de luminale zijde werd gebruikt voor MUC2 synthese in preterme neonaten en biggen. In preterme biggen werden hogere synthesesnelheden van MUC2 gezien vergeleken met preterme neonaten in de herstelfase van darmziekte en bijbehorende chirurgische interventie. Colostrum stimuleert de opname van threonine voor MUC2 synthese vanuit de luminale zijde ten opzichte van de basolaterale zijde en een toegenomen fractionele synthesesnelheid van MUC2 vergeleken met kunstvoeding. Hieruit kan geconcludeerd worden dat goblet cellen threonine zowel vanuit de luminale zijde als vanuit de basolaterale zijde van de goblet cel gebruiken voor MUC2 synthese. Daarnaast stimuleert colostrum de synthese van MUC2 en de opname van threonine vanuit de luminale zijde.

Dankwoord



'Guts' wordt in verschillende woordenboeken vertaald als:

Guts (the ~)

Moed (de ~ (m)), lef (de ~ (m)), durf (de ~ (m)), gewaagdheid (de ~ (v)), buiken (de ~), dikke pensen (znw.), spekbuike (de ~), ingewanden (de ~), darmen (de ~).

Het is dus duidelijk: zonder moed, lef, durf, gewaagdheid en darmen geen proefschrift! Voor de totstandkoming van dit proefschrift waren de 'guts' van een aantal mensen een eerste en continue vereiste. Graag wil ik een aantal mensen in het bijzonder bedanken.

Mijn promotoren, Prof.dr. J.B. van Goudoever en Prof.dr. G. Boehm. Beste Hans, na mijn periode als AGNIO heb je me de mogelijkheid gegeven om promotieonderzoek te doen binnen de neonatologie. Het onderzoek is voor mij steeds een grote uitdaging geweest en op momenten dat ik beren op de weg zag, wist jij me altijd snel weer te overtuigen van het feit dat 'alles wel goed kwam'. Dear Prof. Boehm, I thank you for the scientific discussions and for critically reviewing my abstracts and papers. Your experience in the field of infant nutrition is impressive.

Mijn co-promotor, dr. I.B. Renes. Beste Ingrid, de afgelopen jaren mocht ik bij jou in het Laboratorium Kindergeneeskunde werken binnen de neonatologie onderzoeksgroep. Als dokter heb ik veel kunnen leren van de oneindige mogelijkheden binnen het lab.

De leden van de kleine promotiecommissie: Prof.dr. D. Tibboel, Prof.dr. E.E.S. Nieuwenhuis en Prof.dr. E.H.H.M. Rings dank ik voor het beoordelen van het manuscript.

Uiteraard zou dit boekje nooit tot stand gekomen zijn zonder de hulp en medewerking van alle patiënten, ouders, verpleegkundigen en zorgassistenten op de IC Neonatologie. Ik wil jullie hiervoor hartelijk danken. Voor de verpleegkundigen een extra woord van dank. Ik heb altijd met heel veel plezier op de afdeling gewerkt en heb me door jullie erg gesteund gevoeld tijdens mijn gehele periode in het Sophia.

Mijn paranimfen Maria en pa. Lieve Maria, jij weet als geen ander hoe ik mijn onderzoeksperiode doorlopen heb. Eerst als directe collega, later helaas vanaf de zijlijn. Ik heb je altijd erg gewaardeerd als collega en ben blij dat we onze collegialiteit hebben ingeruild voor een fijne vriendschap. Lieve pap, ik hoefde niet lang na te denken om jou als paranimf te kiezen. Je bent mijn maatje en ik waardeer jouw interesse in mijn carrièreontwikkelingen en promotieonderzoek enorm. Na de spannende tijden in het begin van dit jaar, ben ik erg blij dat je er op deze bijzondere dag bent om mij te steunen. Ik kan me geen beter duo voorstellen.

Janneke, je bent op de meeste van de hoofdstukken in dit proefschrift co-auteur. Ik heb de afgelopen jaren veel van jou geleerd en heb je inzet voor alle experimenten en je zorgzaamheid, die gepaard ging met veel koppen koffie en thee tot het afwassen van mijn stapels afwas, ontzettend gewaardeerd. Ik wens jou veel succes in je verdere carrière als research analist en veel geluk samen met Arjan.

De rest van de Neonatologie-groep: Ad en Anita: dank voor alle experimenten die jullie voor mijn proefschrift gedaan hebben. Nicolas, I enjoyed the time that you worked here as a student. Sometimes, 'la vie est comme une poubelle', but the rest of the time it's a lot of fun! Peng, Jiaping and Laura, you gave our group an international character which I appreciated. En natuurlijk Patrycja. Wat was het fijn om een collega-dokter in het lab te hebben. Samen hebben we met vallen en opstaan heel veel geleerd en zijn we klaar voor de volgende stap: de opleiding tot kinderarts.

Dear Isabelle and Audrey. Thank you very much for the valuable cooperation on the SCFA-work and all the rest.

Lieve Daniëlla, ik wil je graag bedanken voor alles wat je voor me gedaan hebt. Ik kon altijd bij jou terecht om dingen te regelen, afspraken te maken en vooral ook om even te kletsen. Ik wens je heel veel plezier en suc-6 in Amsterdam!

Alle stafleden en nurse practitioners van de IC Neonatologie in het Sophia, in het bijzonder André, George, Monique Williams en Ilke wil ik heel hartelijk bedanken voor alle support de afgelopen jaren. Ik mis jullie.

Mijn onderzoekstijd zou nooit zo leuk en gezellig zijn geweest zonder alle collega onderzoekers. Hester en Denise: ik heb een tuintje in mijn hart voor jullie! Dank voor alle Doppio-tjes en 'werkoverleg-sessies'. Ik mis jullie en verheug me op jullie promoties. Marie-Chantal, jij hebt het NEC-stokje grotendeels overgenomen. Ik wens je veel succes met jouw onderzoek en verdere carrière in de (kinder)chirurgie. Sk2210: fijn dat ik af en toe even bij jullie binnen mocht lopen. Ineke, bedankt voor al je hulp bij de METC-toetsingen. Ik wens jou en natuurlijk Willemijn heel veel succes met de moedermelkbank. Het massaspectrometrielab: bedankt voor jullie gastvrijheid in de afgelopen jaren. Toch nog 1 hoofdstuk over stabiele isotopen in mijn boekje!

Alle onderzoekers die ik onmogelijk allemaal op kan noemen: SUPER BEDANKT!

Inmiddels ben ik 'verhuisd' van Rotterdam naar Amersfoort, alwaar ik een begin mag maken aan mijn opleiding tot kinderarts. Ik dank mijn nieuwe collega's van het Meander MC voor de steun tijdens de laatste loodjes van dit proefschrift en hoop dat we nog veel gezellige en leerzame momenten zullen hebben.

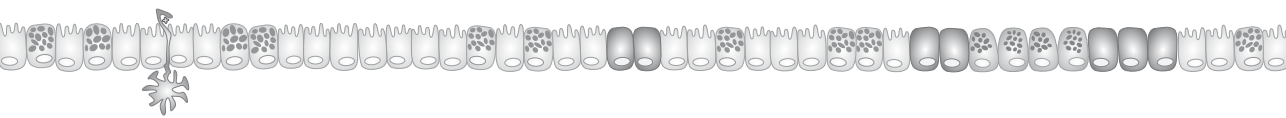
Buiten het werk waren er gelukkig mensen die weinig of niets met de kindergeneeskunde of wetenschappelijk onderzoek te maken hebben en dat was heerlijk. Vooral Tamara en Mariska wil ik bedanken voor de broodnodige afleiding, maar ook voor het inspringen als ik weer eens in Rotterdam moest zijn. Ward, bedankt voor het ontwerpen van het figuur in de introductie en de omslag van mijn boekje. Het was erg leuk om jou een 'spoedcursusje darmepitheel' te geven en het resultaat is prachtig!

Er staan al genoeg stellingen op het lijstje voorin dit proefschrift, maar deze wil ik graag aan mijn dankwoord toevoegen: 'You can only understand how much your parents love you when you become a parent yourself'. Lieve pa en ma, ik wil jullie bedanken voor de liefde en het grenzeloze vertrouwen waar jullie mij altijd mee hebben omringd. Maar vooral wil ik jullie bedanken voor de hartverwarmende liefde die jullie Thijs geven. De band tussen grootouders en kleinkinderen is uniek en ik vind het bijzonder dat we dit samen mogen meemaken. Zonder de enorme hulp en steun en de warme thuisbasis die jullie hebben gecreëerd, hadden we het de afgelopen drukke jaren niet gered.

And last, but surely not least: mijn mannen, René en Thijs Floris. Wat is het heerlijk om na een dag hard werken weer lekker bij jullie thuis te komen. We zullen elkaar de komende tijd nog veel moeten missen, maar vergeet niet dat jullie altijd in mijn gedachten zijn.

Nanda

Portfolio



PHD PORTFOLIO SUMMARY

Summary of PhD training and teaching activities

Name PhD student N. Burger-van Paassen
 Erasmus MC Department Laboratory of Pediatrics, division Neonatology

PhD period April 2005- July 2010
 Promoters Prof.dr. J.B. van Goudoever
 Prof.dr. G. Boehm
 Co-promoter/Supervisor dr. I.B. Renes

1. PhD training

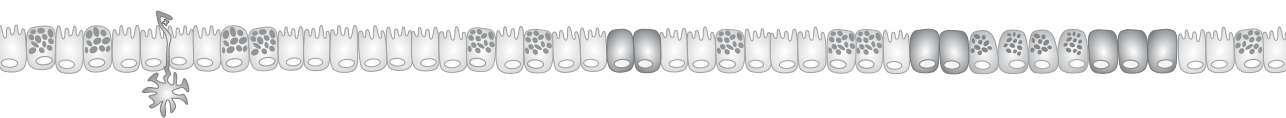
	Year	Workload (ECTS)
General Academic Skills		
Course on Laboratory Animal Science, Artikel 9	2006	3.0
Organization Neo-retraite Thorn	2008	1.0
Opvang van het acuut zieke kind (APLS)	2008	0.5
Member AIO-committee Laboratory Pediatrics	2008-2009	2.0
Basiscursus Regelgeving en Organisatie voor klinisch Onderzoekers (BROK)	2009	1.0
Sollicitatietraining Stern Loopbaanadvies	2009	1.4
(Inter)national conferences		
Digestive Diseases week, Washington DC, United States	2007	1.0
Poster: <i>Paneth cell alterations in necrotizing enterocolitis and intestinal innate defense</i>		
48th Annual Meeting of the European Society for Paediatric Research, Prague, Czech republic	2007	1.5
Oral: <i>Paneth cell alterations in necrotizing enterocolitis and intestinal innate defense</i>		
Poster: <i>The effect of short chain fatty acids on mucin MUC2 synthesis: implications for epithelial protection?</i>		
Nederlands Kindergeneeskunde Congres 2008, Veldhoven, the Netherlands	2007	1.0
Poster: <i>SNAP-II score voorspelt mortaliteit en ECMO-behoefte bij pasgeborenen met congenitale hernia diafragmatica</i>		
Pediatric Academic Society, Annual meeting, Honolulu, Hawaii	2008	1.5
Oral: <i>Mucin Muc2 deficiency and intestinal inflammation during postnatal development and suckling-weaning transition in mice</i>		
Poster: <i>The effect of short chain fatty acids on mucin MUC2 synthesis: role in pathogenesis and treatment of necrotizing enterocolitis?</i>		

Federation of American Societies for Experimental Biology New Orleans, United States Oral: <i>Innate defense responses in Muc2 deficient mice: an important role for goblet cells</i> Oral: <i>Regulation of the intestinal mucin MUC2 expression by short chain fatty acids: implications for epithelial protection</i>	2009	1.5
Nederlandse Vereniging Gastroenterologie (NVGE), voorjaarsvergadering, Veldhoven, the Netherlands Poster: <i>Innate defense responses in Muc2 deficient mice: an important role for goblet cells</i> Poster: <i>Role of probiotics on intestinal barrier function: effect of Lactobacillus GG on mucin MUC2 expression</i> Poster: <i>The regulation of the intestinal mucin MUC2 expression by short chain fatty acids: implications for epithelial protection</i>	2009	1.5
Nederlandse Vereniging Gastroenterologie (NVGE), voorjaarsvergadering, Veldhoven, the Netherlands Oral: <i>Development of colitis in Muc2-deficient mice: diet matters!</i>	2010	1.0
Pediatric Academic Society, Annual meeting, Vancouver, Canada Poster: <i>Dietary effects on the development of colitis in Muc2-deficient mice: diet matters!</i>	2010	1.0
Seminars and workshops		
Gut microbiota in health and disease, 2 nd international workshop, Amsterdam, the Netherlands	2007	1.0
Summer School, European Society Pediatric Gastroenterology Hepatology and Nutrition (ESPGHAN)	2007	1.0
Interklinische avond	2006-2009	0.5
PhD day Erasmus MC	2007	
Onderzoeksdag Kindergeneeskunde	2006-2009	0.5

2. Teaching activities

	Year	Workload (ECTS)
Supervision Nicolas Le Polles, student AgroParisTech, 6 months internship	2009	1.0
Supervision Nelleke Bleijenberg, scholier VWO, profielwerkstuk	2010	0.5
Introduction of Pediatric Residents starting Intensive Care Neonatology training period	2005-2009	5.0

Appendix



CHAPTER 2

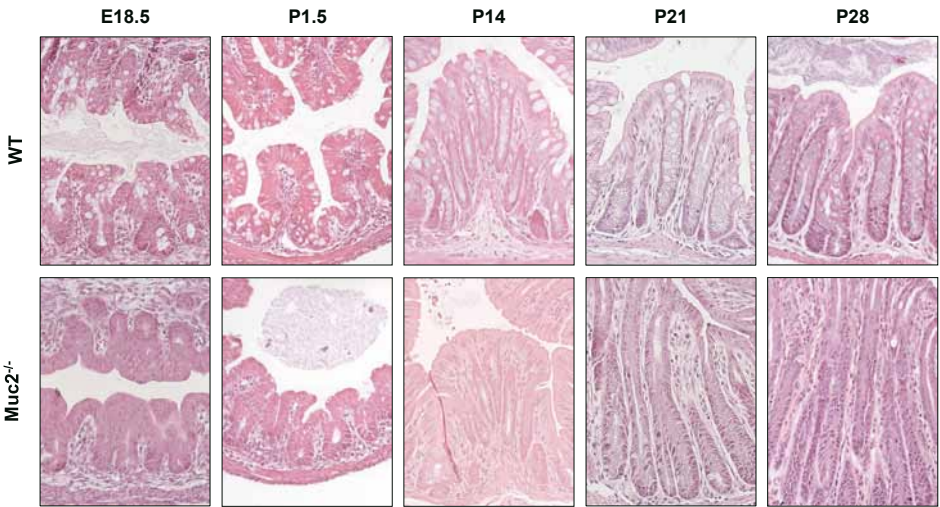


Figure 2. Colonic morphology of WT and Muc2^{-/-} mice

Morphology of the distal colon in WT (upper panels) and Muc2^{-/-} (lower panels) mice by hematoxylin and eosin staining. Representative sections of the distal colon are depicted at E18.5, P1.5, P14, P21 and P28. The tissue samples are representative of all mice in the studied groups. Note, no evident signs of inflammation or epithelial damage were seen at E18.5, P1.5 and P14. After weaning, at P28, the first signs of colitis (i.e. epithelial flattening and superficial erosion were seen).

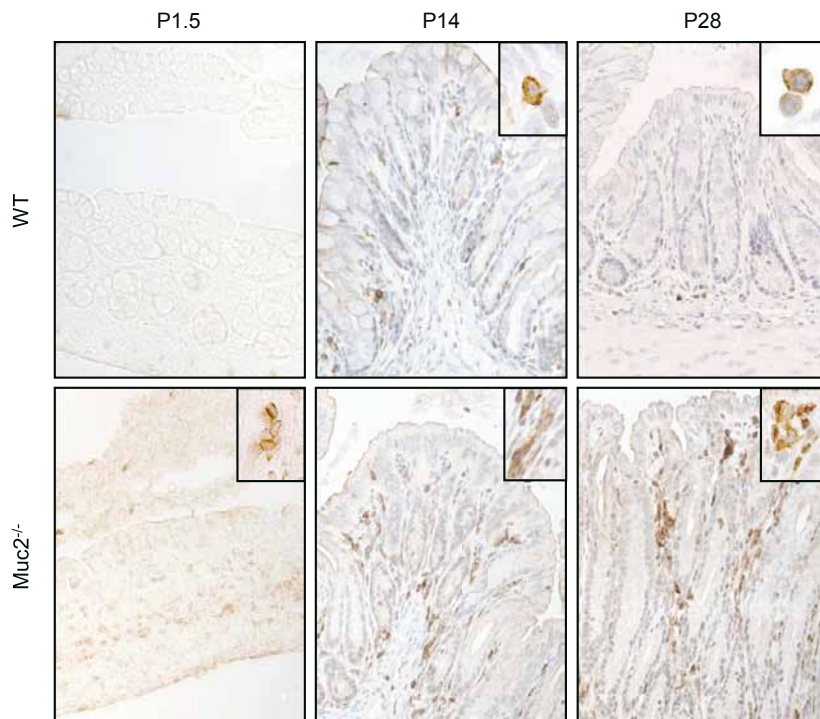


Figure 4. The amount of Cd3-positive T-cells is increased in Muc2^{-/-} mice before and after weaning. Infiltration of T-cells determined by Cd3 immunohistochemistry on distal colon sections at different ages (P1.5, P14 and P28). Inserted pictures show higher magnification to point out individual Cd3-positive T-cells. The tissue samples are representative of all mice in the studied groups. Note, the influx of Cd3-positive T-cells, was increased in WT as well as Muc2^{-/-} mice before weaning. Weaning from mother’s milk resulted in exacerbation of colitis in Muc2^{-/-} mice, but not WT mice.

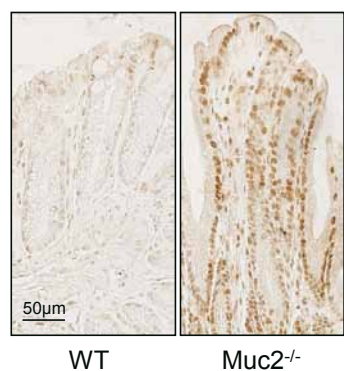


Figure 8. Expression of Irf3 protein in distal colon of WT and Muc2^{-/-} mice. Expression and localization of IRF3 in distal colon of WT (left panel) and Muc2^{-/-} mice (right panel) at P28 was studied by immunohistochemistry. In WT mice Irf3 expression is confined to the nuclei of the epithelial cells of the surface epithelium, whereas in Muc2^{-/-} mice, nuclear Irf3 staining is seen in the epithelial cells along the entire crypts and the surface epithelium. Tissue samples are representative of all mice in the studied groups.

CHAPTER 3

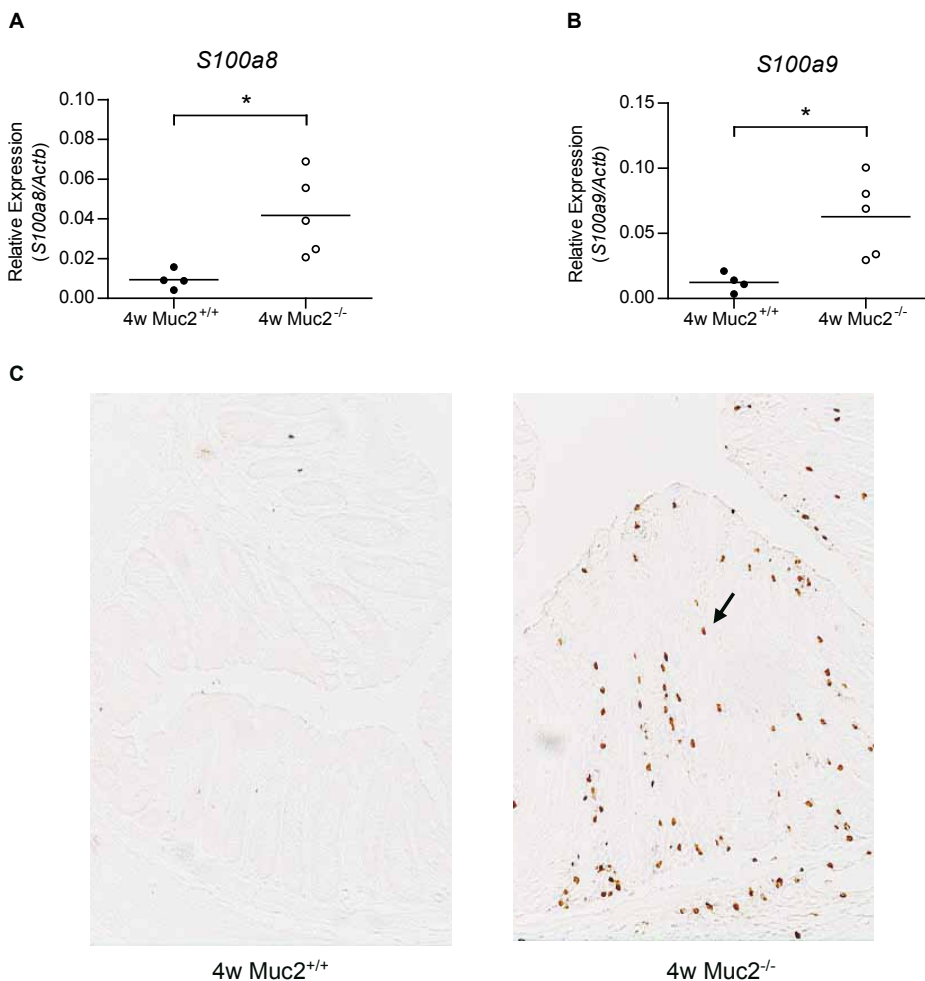


Figure 4. Expression of S100 proteins is up-regulated in distal colon of *Muc2*^{-/-} mice. Expression of *S100a8* (A) and *S100a9* (B) in distal colon of 4-week-old *Muc2*^{+/+} and *Muc2*^{-/-} mice was quantified with qRT-PCR. (C) Representative sections presenting S100a8 localization in the distal colon of 4-week-old *Muc2*^{+/+} and *Muc2*^{-/-} mice, detected with anti-S100a8 antibody. The arrow indicates the positive stained cells.

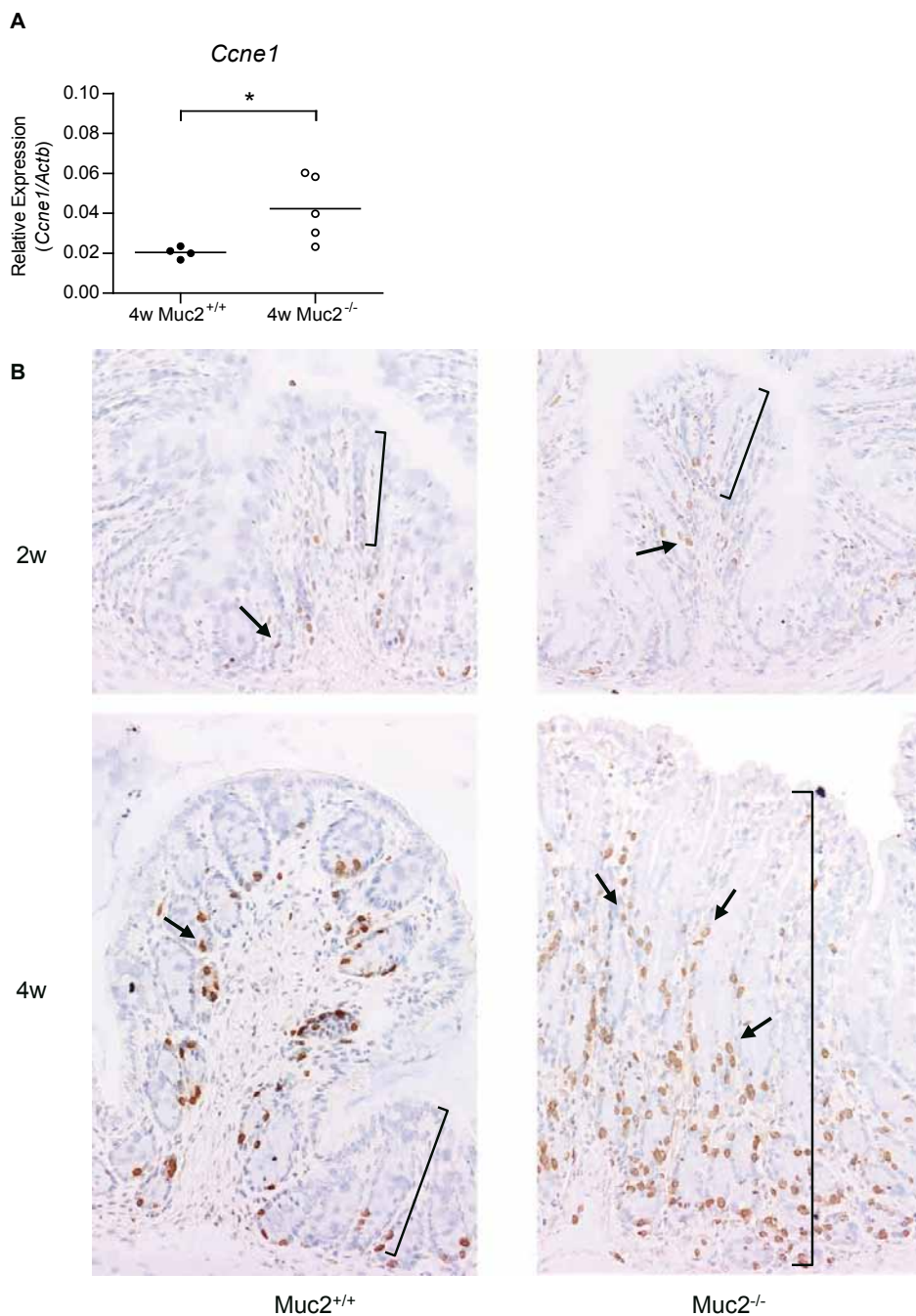


Figure 6. Increased proliferation in the distal colon of *Muc2*^{-/-} mice.
 (A) Expression of *Ccne1* in distal colon of 4-week-old *Muc2*^{+/+} and *Muc2*^{-/-} mice was quantified with qRT-PCR. (B) Representative BrdU stained sections of distal colon of 2- and 4-week-old *Muc2*^{+/+} and *Muc2*^{-/-} mice. The arrow indicates the positive stained cells, and the square bracket shows the crypt region.

CHAPTER 4

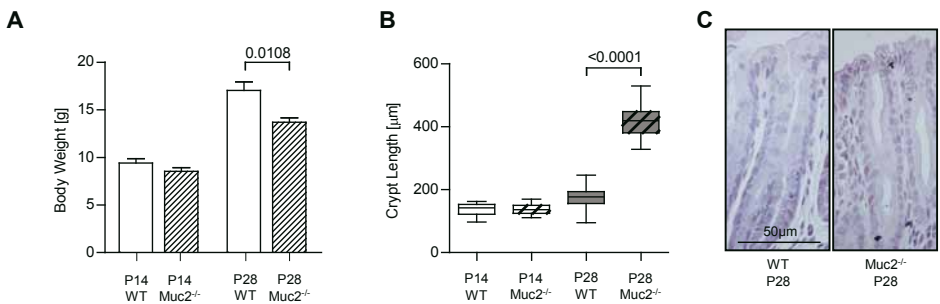


Figure 1. Clinical Symptoms and intestinal morphology (A) Body weight of WT and Muc2^{-/-} mice are depicted at P14 and P28. Body weight was significantly lower in Muc2^{-/-} compared to WT mice at P28. (B) Crypt lengths of WT and Muc2^{-/-} mice at P14 and P28 in distal colonic tissue sections. Values are depicted as box-and-whisker diagrams (maximum value, upper quartile, median, lower quartile and minimal value respectively). (C) Hematoxylin and eosin staining in WT and Muc2^{-/-} mice at P28 are displayed.

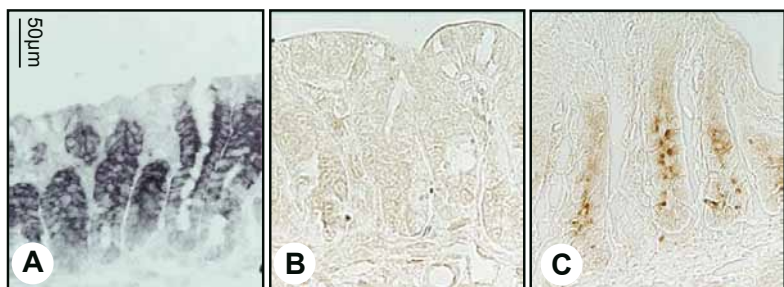


Figure 5. Localization of *Reg3β* mRNA and *Reg3γ* protein in the proximal colon. Localization of *Reg3β* mRNA in Muc2^{-/-} by ISH (A), and localization of *Reg3γ* protein by immunohistochemistry in (B) WT and (C) Muc2^{-/-} mice at P28.

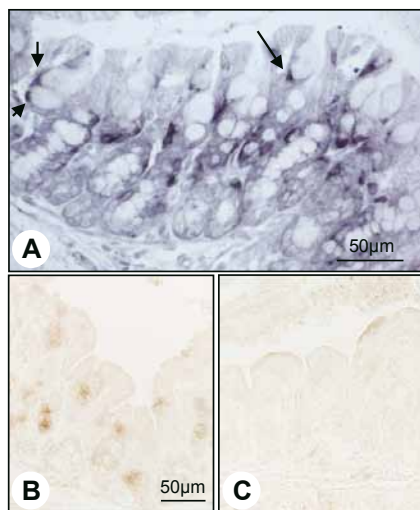


Figure 6. Localization of *Ang4* mRNA and *Ang4* protein in the proximal colon
Localization of *Ang4* mRNA in *Muc2*^{-/-} mice by ISH (A) (arrows depict *Ang4* mRNA at the basolateral side of goblet cells), and localization of *Ang4* protein by immunohistochemistry in (B) WT and (C) *Muc2*^{-/-} mice at P28.

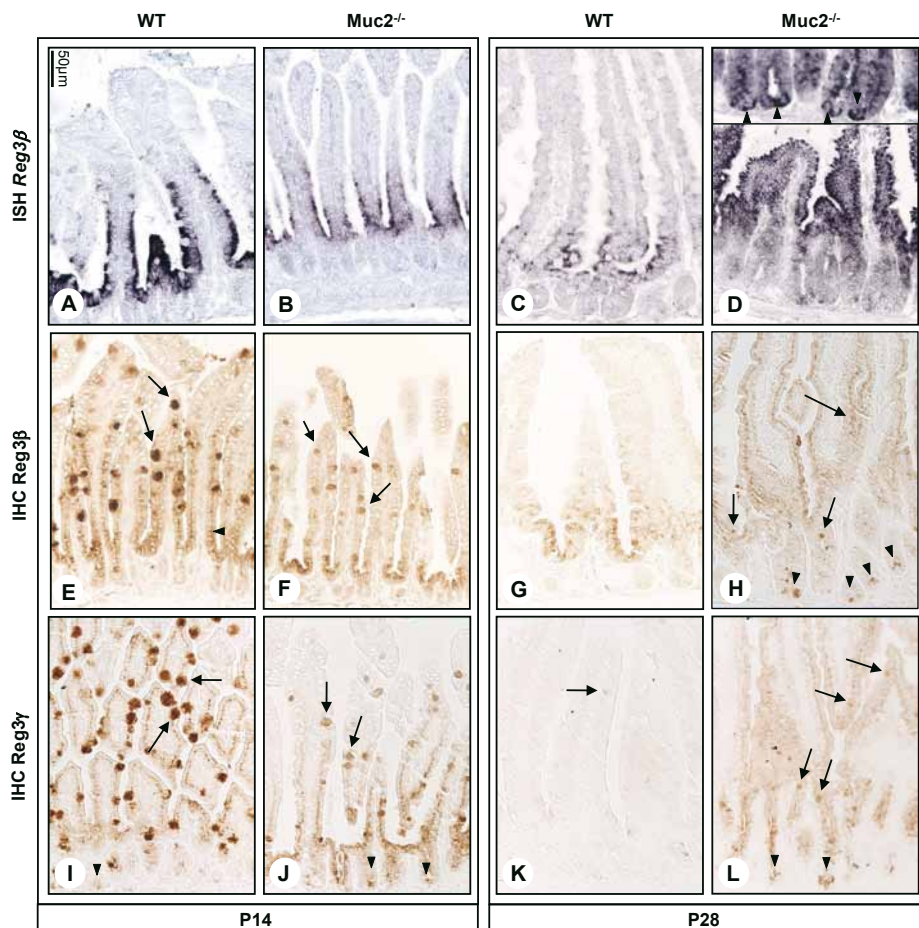


Figure 7. Localization of *Reg3β* mRNA and *Reg3β* and *Reg3γ* protein in the small intestine. ISH for *Reg3β* mRNA in WT and *Muc2*^{-/-} mice at P14 (A,B) and P28 (C,D)(arrowheads in zoom in indicate *Reg3β*-positive Paneth cell in *Muc2*^{-/-} at P28). Immunohistochemical staining for *Reg3β* in WT and *Muc2*^{-/-} mice at P14 (E,F) (arrowhead indicates Golgi-staining in enterocytes in WT at P14) and P28 (G,H)(arrows indicate *Reg3γ*-positive goblet cells in WT and *Muc2*^{-/-} mice at P14, arrowheads indicate *Reg3β*-positive Paneth cells in *Muc2*^{-/-} at P28). Immunohistochemical staining for *Reg3γ* is depicted in the lower panel in WT and *Muc2*^{-/-} mice at P14 (I,J)(arrows indicate *Reg3γ*-positive goblet cells, arrowheads indicate *Reg3γ*-positive Paneth cells) and P28 (K,L)(arrows indicate *Reg3γ*-positive goblet cells, arrowheads indicate *Reg3γ*-positive Paneth cells).

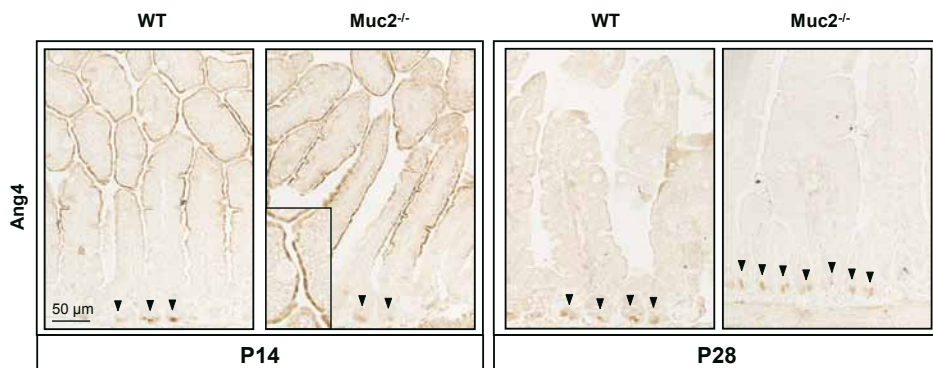


Figure 8. Localization of Ang4 protein in the small intestine
Localization of Ang4 protein in small intestine of WT and *Muc2*^{-/-} mice at P14 (left panel) and P28 (right panel)(arrowheads indicate Ang4-positive Paneth cells).

CHAPTER 5

ILEUM

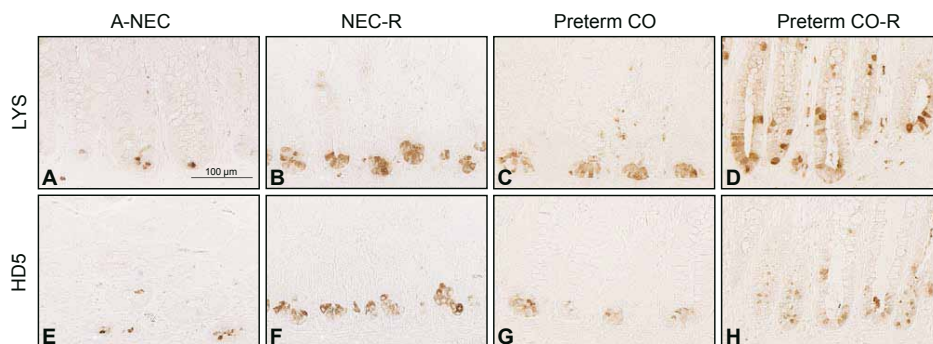


Figure 2. Immunohistochemistry for lysozyme- (LYS) (A-D) and HD5-positive (E-H) Paneth cells in ileal tissue from NEC patients and Preterm CO. (A, E) A-NEC; (B, F) NEC-R; (C, G) Preterm CO; (D, H) Preterm CO-R. Images are representative of 19 A-NEC, 21 NEC-R, 9 Preterm CO, and 6 Preterm CO-R specimens derived from the ileum.

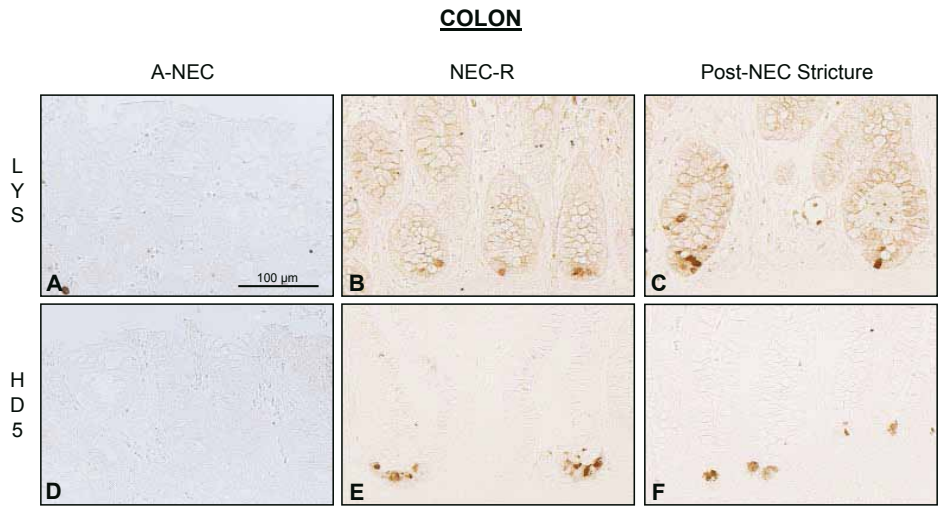


Figure 4. Representative immunohistochemistry for lysozyme (LYS; A-C) and HD5 (D-F) in metaplastic Paneth cells in colonic tissue from NEC patients. (A, D) A-NEC. (B, E) NEC-R. (C, F) Post-NEC Stricture. Images are representative of 10 A-NEC, 11 NEC-R, and 5 Post-NEC Stricture specimens.

CHAPTER 6

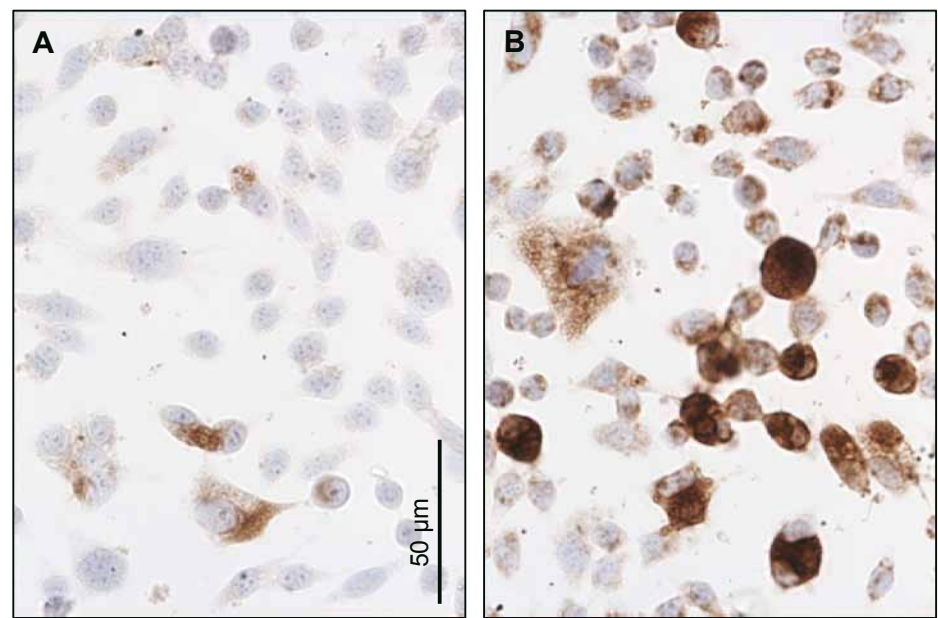


Figure 2. LGG increases MUC2 protein expression
 LS174 T cells were stimulated with 10⁶ viable LGG. Nonstimulated LS174T cells (A) are compared with LS174T cells stimulated with viable LGG (B).

CHAPTER 7

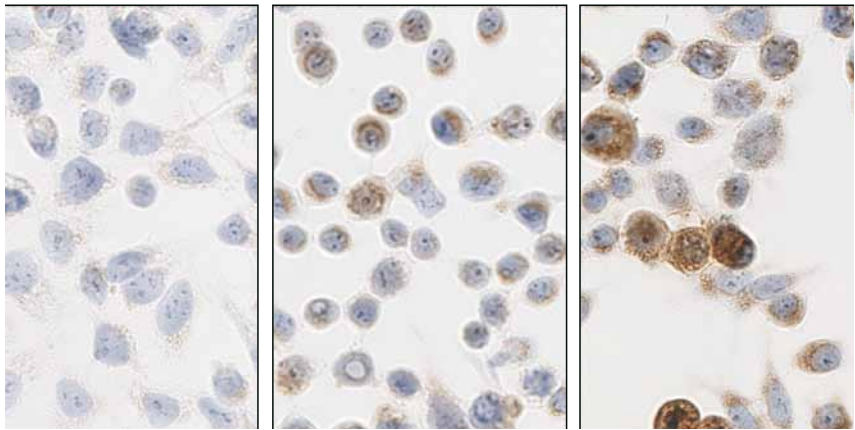


Figure 3. Effect of butyrate on MUC2 protein expression
MUC2 apomucin expression by immunocytochemistry in non-stimulated (0 mM) and butyrate (1 and 2 mM) stimulated LS174T cells. (Magnification x40)

CHAPTER 8

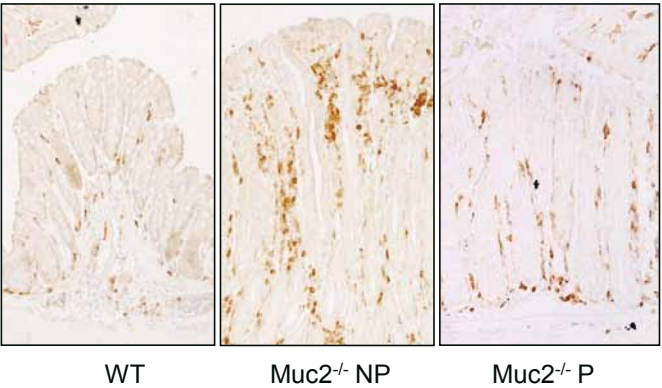


Figure 2. Influx of Cd3ε-positive T-cells
The extent of inflammation in the distal colon was assessed by immunohistochemistry for Cd3ε. Representative stained tissue samples for all groups are shown. Normal WT mice hardly show any Cd3ε-positive T-cells (left panel), whereas *Muc2*^{-/-} mice that were fed the non-purified (NP) diet show an increased amount of Cd3ε-positive T-cells that are localized along the complete crypt length, but also cluster together at the luminal side of the epithelium (middle panel). *Muc2*^{-/-} mice that were fed the purified (P) diet showed a decreased amount of Cd3ε-positive T-cells compared to *Muc2*^{-/-} NP mice, that was still increased compared to WT mice (right panel). Crypt lengthening in *Muc2*^{-/-} mice, as quantified in Fig. 2B, is evident when WT are compared with *Muc2*^{-/-} NP or *Muc2*^{-/-} P mice.

Nanda Burger-van Paassen was born on April 17th in Naaldwijk, the Netherlands. She passed her secondary school exam (VWO) at the Interconfessioneel Westland College in Naaldwijk in 1996. In the same year she started studying HBO-verpleegkunde at the Hogeschool Rotterdam en Omstreken. In 1998 she started her medical training at the Faculty of Medicine at the University of Leiden. In 2002 she participated in a project investigating the effect of nonsteroidal anti-inflammatory drugs on cognitive behavior in children with juvenile idiopathic arthritis at the department of pediatric rheumatology, Leiden University Medical Centre, Willem-Alexander Kind en Jeugd centrum. After obtaining her medical degree in 2004, she worked as a resident at the Intensive Care department of Pediatric Surgery (head: Prof. dr. Tibboel) and the Neonatal Intensive Care Unit (head: Prof. dr. J.B. van Goudoever) at the Sophia Children's hospital in Rotterdam. In 2006 she started working as a research fellow at the department of Neonatology of the Erasmus MC – Sophia Children's hospital in Rotterdam (supervised by Prof. dr. J.B. van Goudoever, Prof. dr. G. Boehm and dr. I.B. Renes) working on the research presented in this thesis. She combined her research job with clinical activities as a resident at the Neonatal Intensive Care Unit. In July 2010 she started her clinical pediatric residency in training (AIOs) at the Meander Medisch Centrum in Amersfoort (head: Dr. P.H.G. Hogeman) as part of her training at the University Medical Centre Utrecht – Wilhelmina Children's hospital in Utrecht (heads: Prof. dr. E.E.S. Nieuwenhuijs and Dr. J. Frenkel). She is married to René Michel Burger and together they have a son named Thijs Floris.

ISBN 978-90-8559-130-6